Mathematical Problems in Engineering

Mathematical Foundation of Probabilistic Preference Theory and Applications in Engineering

Lead Guest Editor: Zeshui Xu
Guest Editors: Huchang Liao and Janusz Kacprzyk

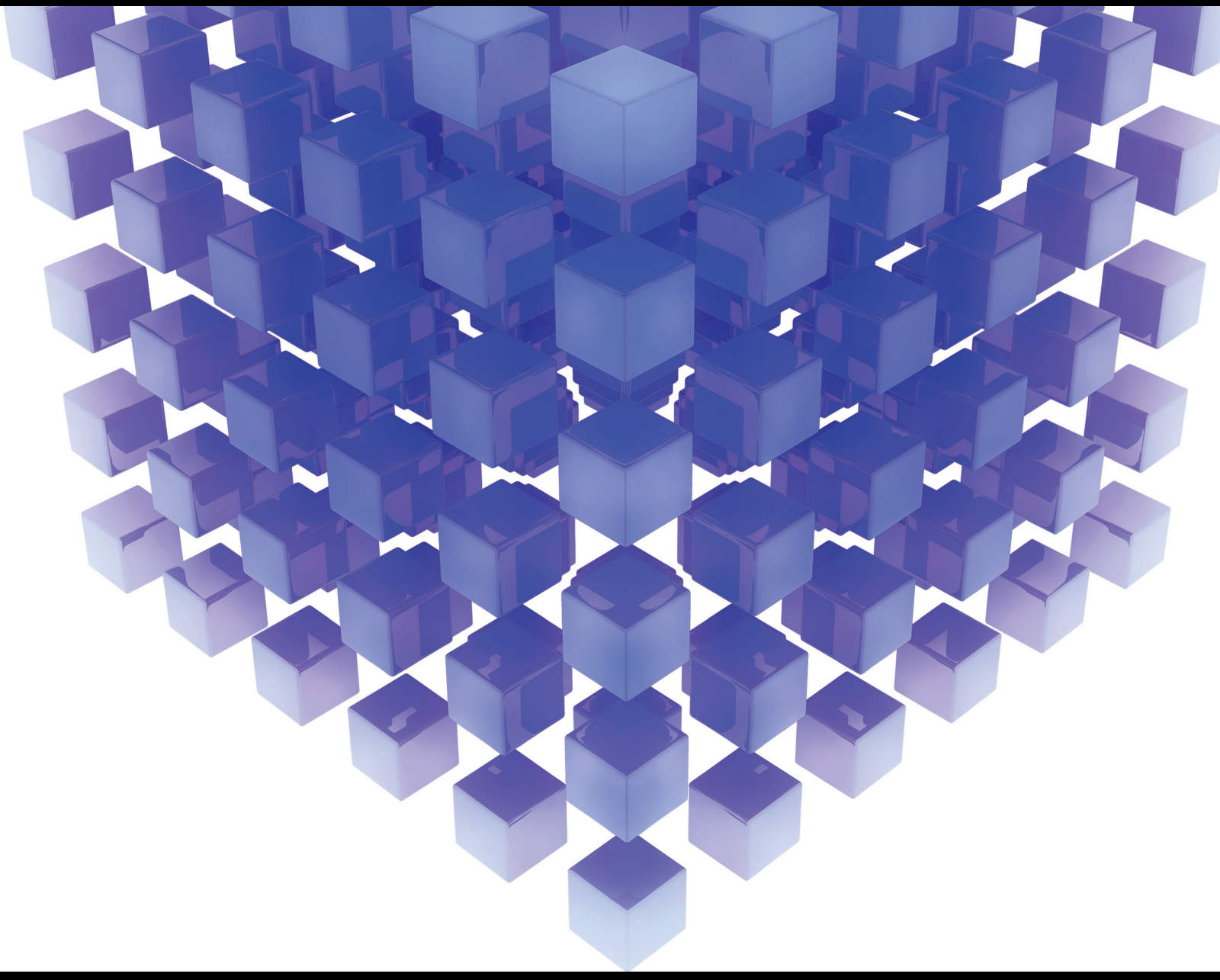

Mathematical Foundation of Probabilistic Preference Theory and Applications in Engineering

Mathematical Problems in Engineering

Mathematical Foundation of Probabilistic Preference Theory and Applications in Engineering

Lead Guest Editor: Zeshui Xu
Guest Editors: Huchang Liao and Janusz Kacprzyk

Chief Editor

Academic Editors

Contents

Hindawi
Mathematical Problems in Engineering
Volume 2021, Article ID 7459239, 12 pages
https://doi.org/10.1155/2021/7459239

Research Article

Search Path Planning Algorithm Based on the Probability of Containment Model

Jia Ren,[1] **Kun Liu**,[1] **Yani Cui**,[1] **and Wencai Du**[2]

[1]*School of Information and Communication Engineering, Hainan University, Haikou 570228, China*
[2]*Institute of Data Science, City University of Macau, Taipa, Macau, China*

Correspondence should be addressed to Yani Cui; cyn0213@163.com

Received 22 August 2020; Revised 22 December 2020; Accepted 6 January 2021; Published 28 January 2021

Academic Editor: Zeshui Xu

The location of distress object in the maritime search area is difficult to determine, which has brought great difficulties to the search path planning. Aiming at this problem, a search path planning algorithm based on the probability of containment (POC) model for a distress object is proposed. This algorithm divides the area to be searched into several subareas by grid method and dynamically evaluates the POC of the distress object in each subarea using the Monte Carlo random particle method to build the POC model. On this basis, the POC is dynamically updated by employing the Bayes criterion within the constraint of the time window. Then, the sum of the POC of the object in the subareas is regarded as the weight of the search path. And the proposed algorithm dynamically executes the search path planning according to the maximum path weight. In comparison with the parallel line search path planning algorithm given in the "International Aeronautical and Maritime Search and Rescue Manual," the simulation results show that the search path planning algorithm based on the POC model of the distress object can effectively improve the search efficiency and the probability of search success of the distress object.

1. Introduction

Search and rescue of maritime distress target is a high-risk, difficult, time-sensitive, and professional task, and it is also the only way to search and rescue survivors [1]. Its essence is to predict the drift trajectory of the distress target, estimate the search area accurately, plan the search path reasonably, and deploy the search platform for rapid search and rescue based on the characteristic information of the sea condition, the distress target, and the last known location information in the incident area [2, 3]. However, due to the influence of many factors, such as marine meteorology, hydrological environment, and geometric characteristics of distress target, the drift trajectory of distress target in the sea area is extremely uncertain, which greatly increases the difficulty of accurately estimating the search area [4, 5]. The traditional search area estimation method is mainly based on the final known location of the distress target and the sea conditions of the incident area. The drift trajectory of the distress target is estimated through expert experience, and the search area scope is determined by this method. However, it is difficult to fully consider the potential relationship between many factors affecting the drift process of the target in distress by expert experience alone, and the accuracy is low, which affects the success rate of search and rescue. For this reason, the researchers used statistical and stochastic theory frameworks to express the drift model of the distress target and used machine learning method to estimate the drift trajectory [6–8]. In [8], a statistical model of the drift path of the distress target is constructed according to the meteorological data of the incident sea area to obtain the search area. According to the drift model based on the random particle method proposed by Allen A A and Breivik Ø, field experiments were carried out in the Tyrrhenian Sea and Sicily Strait, respectively, to verify the accuracy of the drift model to predict the search area under different parameters. Besides being related to the meteorological and hydrological environment, the geometric characteristics of the distress target should be considered further [9]. Brushett et al. [10] carried out field tests in the accident-prone waters of the

Pacific Ocean to complete the determination of the downwind and crosswind drift coefficients of three small vessels of different sizes for determining the search area. In [11], based on the information such as the debris location obtained during the search, a drift inverse model was established to predict the base position of the distress target, so as to predict the search area. The abovementioned references, while using meteorological and hydrological data in the incident area, also fully consider the geometric characteristics of the distress target and have reference significance for the construction of the drift path prediction model of the distress target. However, due to the uncertainty of time and space, the whole search area cannot be completely searched by the deployed search platform in a limited time window. If the target is drifting out of the predicted search area, the search mission will fail. Therefore, efficient search path planning becomes an effective way to improve the success rate of search and rescue after the search area is determined [12, 13].

Maritime search path planning is essentially a problem of coverage path planning (CPP) [14, 15]. The traditional method is to use parallel line method, extended square method, and other regular search paths in the search area for full coverage search. However, this kind of regular search path assumes that the location of distress target in search area follows equal probability distribution, and the search platform must carry out full coverage search, which will not only cause the waste of search time but also reduce the success rate of search and rescue. Yu et al. [16] used Bayes criterion to calculate the probability distribution map of the location of the distress target in the search area, and the search path planning was completed by genetic simulated annealing algorithm. But the algorithm does not consider that the probability distribution map of the distress target position will change dynamically with time. The paper [17] regarded the search path planning task as a multiconstrained objective optimization problem based on fully considering the dynamic update of the probability distribution map of the distress target location, and the improved particle swarm optimization algorithm was used to realize the dynamic planning of the search path. However, the update of the search area using the above algorithm is based on the full coverage, that is, only after completing the full coverage search of the search area or reaching the next search time, the search area is updated, which may face the invalid search and rescue caused by the drift of the distress target out of the search area.

Aiming at the above problems, this paper proposes a search path planning algorithm (search path planning algorithm based on the probability of containment of distress target, POC-SPPA) based on the probability of distress target inclusion. Firstly, the algorithm uses Monte Carlo random particle method to simulate the drift motion of the distress target and realize the evaluation of the search area. Secondly, the target inclusion probability of each subsearch area is evaluated using the number of particles after the grid processing of the search area; thus, the target inclusion probability model can be constructed, and then the dynamic update of the probability of containment (POC) model according to Bayes criterion is realized. Finally, the search path planning is transformed into the maximum weight path planning problem with POC as the model weights, and the dynamic programming of the search path is realized under the constraints of the search time window.

The rest of the paper is organized as follows. Section 2 introduces the task scenario and problem description. The POC model of the distress target is formulated in Section 3. Section 4 proposes a search path planning algorithm based on the POC model of distress targets. Simulation results and analysis are shown in Section 5. Section 6 draws the conclusions of the work.

2. Task Scenario Description

2.1. Problem Description. The probability of success (POS) of a distress target in maritime search-rescue is determined jointly by POC of the distress target within the search area and the probability of detection (POD) of the distress target:

$$p_S = p_C \times p_D, \tag{1}$$

where p_S, p_C, and p_D refer to POS, POC, and POD of the distress target, respectively. POC is the probability that the distress target exists in the search area, which is closely related to the accurate evaluation of the search area. POD of distress target refers to the probability of successful discovery by the search platform assuming that the distress target already exists within the detection range of the search platform. It is related to sea condition, geometric characteristics of distress target, search mode of search platform, sweep width, and so on. Considering visual searching, when the distance between the search platform and the target is less than 0.1n mile, the value of p_D will be close to 1 and the POS of the distress target is mainly related to the POC. At the same time, the maritime search and rescue mission has the characteristics of strong timeliness, and reasonable search path planning is also the main factor affecting the POS. Therefore, in order to improve the success rate of search and rescue, the following issues need to be addressed:

(1) The POC model of the distress target in the search area should be constructed so as to accurately evaluate the drift trajectory of the distress target and improve the prediction accuracy of the search area

2. Grid processing for the search area is used to realize the dynamic evaluation of the POC of distress target in each search subarea, and on this basis, the search path planning is carried out to improve the efficiency of search and rescue.

2.2. Process of Maritime Search and Rescue for Distress Targets at Sea. According to the above problem description, the process of maritime search and rescue for distress targets is shown in Figure 1.

(1) In the event of a maritime accident, the ship in distress sends messages (including the time, place, and characteristics of the distress target) to the Maritime Search and Rescue Centre through satellite

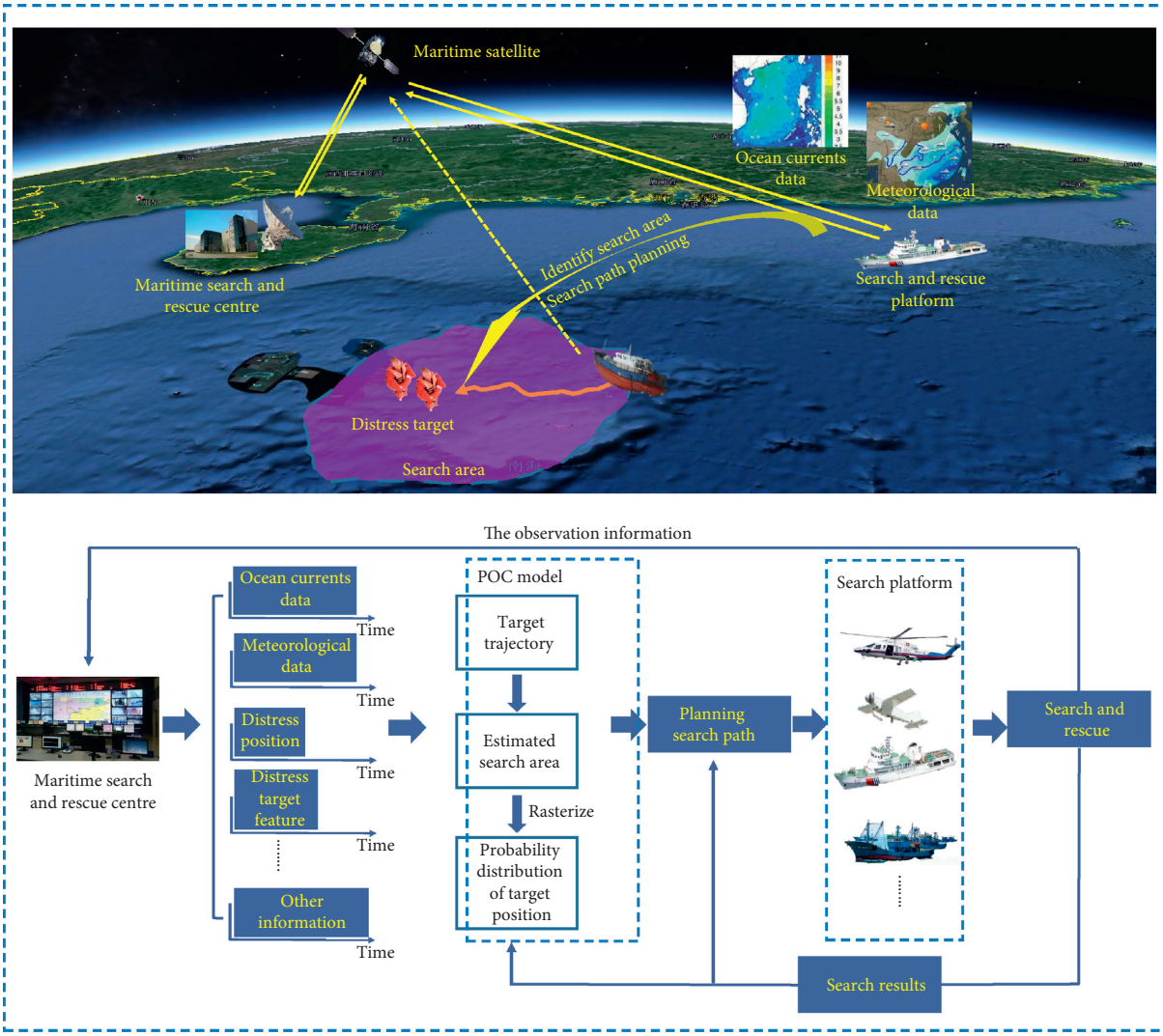

Figure 1: Process of maritime search and rescue for distress targets.

telephones on board, land networks, medium and high frequency (MF/HF), and very high frequency (VHF) systems.

(2) After receiving the distress information, the Maritime Search and Rescue Centre first retrieves the ocean currents and meteorological data of the incident area, in order to complete the study of search task according to the distress target characteristics, and then constructs the distress target POC model to estimate the distress target drift trajectory and search area, as well as determines the search platform type. Finally, the search task instruction and all relevant information are issued to the search platform (including distress target information, ocean currents and meteorological information, sea condition, estimated drift trajectory, and search area,).

(3) The search platform receives mission instructions to prepare for the search. At the same time, the search platform divides the search area into small meshes according to the relevant information sent by the Maritime Search and Rescue Centre and the effective detection range of the carrying equipment to further determine the probability distribution of the location of the target in distress in the search area.

(4) According to the probability distribution of the location of the distress target, the search platform carries out the search path planning and starts the search and rescue mission. During the execution of the mission, the search platform will interact with the Maritime Search and Rescue Centre in real time and continuously update the probability distribution of the location of the target in distress in the search area according to the search progress, so as to dynamically adjust the search path.

3. Construction of POC Model of Distress Target

3.1. Drift Prediction Model of Target in Distress. Accurate prediction of drift trajectory of distress target is a prerequisite for establishing the POC model. The drift motion of

the target in distress is the result of the combined action of total current, sea surface wind pressure difference, wave, and other factors. When the size of the distress target is less than 30 m, the wave has little effect on the drift motion and the effect of the wave on drift motion can be ignored [18, 19]. At this point, the drift motion of the target in distress is mainly affected by the total current and wind pressure difference. Hence, its drift dynamics model is shown as follows:

$$\begin{aligned}&\frac{1}{2}(C_dS\rho)_W\left|\mathbf{V}_W-\mathbf{V}_T\right|(\mathbf{V}_W-\mathbf{V}_T)\\&\quad=\frac{1}{2}(C_dS\rho)_C\left|\mathbf{V}_T-\mathbf{V}_C\right|(\mathbf{V}_T-\mathbf{V}_C),\end{aligned}\tag{2}$$

where $\mathbf{V}_W$, $\mathbf{V}_C$, and $\mathbf{V}_T$ refer to the wind pressure differential velocity on the sea surface, the total current velocity under the sea surface, and the drift velocity of the target in distress, respectively; C_d is the drag force coefficient; S denotes the cross-sectional area; ρ_W and ρ_C, respectively, denote the density of air and sea water. Assuming that the total current and wind pressure difference are independent of each other and follow the Gaussian distribution, $\mathbf{V}_T$ satisfies equation (3).

Letting $((C_dS\rho)_W/(C_dS\rho)_C)=\lambda^2$ and taking the absolute value of the expression in equation (2), we can get

$$\lambda\left|\mathbf{V}_W-\mathbf{V}_T\right|=\left|\mathbf{V}_T-\mathbf{V}_C\right|.\tag{3}$$

According to equation (4), equation (2) can be rewritten as

$$\lambda(\mathbf{V}_W-\mathbf{V}_T)=(\mathbf{V}_T-\mathbf{V}_C).\tag{4}$$

Thus, the drift velocity of the distress target without considering the wave forces can be defined as

$$\mathbf{V}_T=\frac{1}{1+\lambda}\mathbf{V}_C+\frac{\lambda}{1+\lambda}\mathbf{V}_W=f\mathbf{V}_C+(1-f)\mathbf{V}_W,\tag{5}$$

where

$$f=\frac{1}{1+\lambda}=\frac{1}{1+\sqrt{((C_dS\rho)_W/(C_dS\rho)_C)}}.\tag{6}$$

Equation (5) indicates that $\mathbf{V}_T$ can be regarded as a weighted average of $\mathbf{V}_C$ and $\mathbf{V}_W$, and thus, the mean and variance satisfy

$$\begin{aligned}E[\mathbf{V}_T]&=f\cdot E[\mathbf{V}_C]+(1-f)\cdot E[\mathbf{V}_W],\\\mathrm{Var}[\mathbf{V}_T]&=f^2\cdot\mathrm{Var}[\mathbf{V}_C]+(1-f)^2\cdot\mathrm{Var}[\mathbf{V}_W].\end{aligned}\tag{7}$$

According to the above analysis, the total current and wind pressure difference are determined, that is, the drift velocity of the distress target can be obtained and then the drift trajectory of the distress target can be obtained as well. Because of the high randomness of total current and wind pressure difference in the drift process, the influence factors are complex and changeable, there is space-time uncertainty, and some influence factors have strong coupling between them, so they cannot be analysed positively. Therefore, the drift trajectory of the distress target can only be predicted by probability theory [6]. For this purpose, this paper uses the Monte Carlo stochastic particle method to simulate the drift motion of the distress target, and on this basis, the POC model of the distress target is constructed.

3.2. POC Model of the Distress Target. If the POC model of the distress target is constructed using the Monte Carlo random particle method, the distress target is abstracted as N particles, and assuming that the motion between the particles is independent of each other and has all the drift characteristics of the distress target, the probability distribution of the particle after a period of time represents the probability distribution of the distress target at sea after drifting in the same period of time.

Let us mark the drift velocity and position of N particles as $\mathbf{V}_N$ and $\mathbf{L}_N$. $\mathbf{V}_N=[\mathbf{v}_1,\ldots,\mathbf{v}_n,\ldots,\mathbf{v}_N]^{\mathrm{T}}$, $\mathbf{L}_N=[\mathbf{l}_1,\ldots,\mathbf{l}_n,\ldots,\mathbf{l}_N]^T$, and $\mathbf{v}_n$ and $\mathbf{l}_n=[\ln g_n, lat_n]$ represent the drift velocity and position of n particles, respectively. The initialization of particles is placed at the last known position of the distress target, and the drift velocity $\mathbf{V}_N^t$ of the particle at time t is randomly simulated according to equations (5)–(7). On this basis, according to the position of the particle $\mathbf{L}_N^{t-1}$ at time $t-1$, the position of the particle $\mathbf{L}_N^t$ at time t can be obtained. At this point, the smallest rectangular region G^t containing all particles is the search region, that is, the rectangle G^t has $(\min(lng_n^t), \min(lat_n^t))$, $(\min(lng_n^t), \max(lat_n^t))$, $(\max(lng_n^t), \min(lat_n^t))$, $(\max(lng_n^t), \max(la\,t_n^t))$, and $(n\in\{1,2,\ldots,N\})$ as vertical.

In order to obtain the probability distribution of the location of the distress target in the search area G^t, this paper uses the grid method to divide the search area G^t into $L_i^t\times L_j^t$ square search subareas $g_{(i,j)}^t$ with d as the length of each side, where $i\in\{1,2,\ldots,L_i^t\}$ and $j\in\{1,2,\ldots,L_j^t\}$. The POC of the distress target $p_{C(i,j)}^t$ corresponding to the search subarea $g_{(i,j)}^t$ is as follows:

$$p_{C(i,j)}^t=\frac{N_{g_{(i,j)}^t}}{N}.\tag{8}$$

In this formula, $N_{g_{(i,j)}^t}$ refers to the number of particles which are searched at time t in the subarea $g_{(i,j)}^t$. According to each search subarea $p_{C(i,j)}^t$, we can obtain the POC model of the distress target at time t, including the search area G^t and its corresponding POC matrix $\mathbf{P}_C^t=\left\{p_{C(i,j)}^t\right\}$.

Because the location of the distress target will change greatly over time, the POC model of the distress target presents the characteristics of time sensitivity. As a result, based on the search task planned by the POC model of the distress target at time t, the search platform needs complete searching in the search area G^t within the time window $(t,t+T)$, where T is the search time window and its value is related to the drift velocity of the distress target $\mathbf{V}_T$ and the length of the search subarea d. When the search time exceeds the search time window T and the search platform has not found the distress target, it is necessary to update the POC matrix of the search area G^t according to Bayes criterion. The updated POC matrix is recorded as $\mathbf{P}_C^t$. On this basis, the number of particles in each search subarea is updated, and

the position of the particles is reinitialized. Then, the POC model at time $t+T$ is established, so as to realize the adaptive update of the POC model. Due to the update of the POC of the distress target $p^t_{C(i,j)}$ corresponding to the search subarea $g^t_{(i,j)}$ is not only related to itself but also related to the probability of detection of the distress target $p^t_{D(i,j)}$, the general updated formula of the POC matrix is shown in equation (9), and the updated formula of the number of particles in each search subarea is shown in equation (10).

$$p^{t'}_{C(i,tj)} = \begin{cases} \dfrac{p^t_{C(i,j)} \cdot \left(1 - p^t_{D(i,j)}\right)}{\left(1 - p^t_{C(i,j)}\right) + p^t_{C(i,j)} \cdot \left(1 - p^t_{D(i,j)}\right)}, & g^t_{(i,j)} \text{ has been searched}, \\ \dfrac{p_{t(i,j)}}{\left(1 - \sum_{g^t_{(i,j)} \in Z^t_{\text{selected}}} p^t_{C(i,j)}\right) + \sum_{g^t_{(i,j)} \in Z^t_{\text{selected}}} \left(p^t_{C(i,j)} \cdot \left(1 - p^t_{D(i,j)}\right)\right)}, & g^t_{(i,j)} \text{ is not searched}, \end{cases} \tag{9}$$

$$N'_{g^t_{(i,j)}} = N \cdot p^{t'}_{C(i,j)}, \tag{10}$$

where $p^{t'}_{C(i,j)}$ represents the POC of distress targets corresponding to the updated search subarea $g^t_{(i,j)}$; $p^t_{D(i,j)}$ represents the POD of the search platform corresponding to the search subarea $g^t_{(i,j)}$; Z^t_{selected} represents the search path at time t; $N'_{g^t_{(i,j)}}$ represents the number of particles corresponding to the search subarea $g^t_{(i,j)}$.

Note that equation (9) is the general updated formula for the POC of distress target in each search subarea, and in Section 2.1, when explaining equation (1), we point out that if taking visual searching, the distance between the search platform and the distress target is less than 0.1 n mile, the value of p_D will be close to 1, and the POS of the distress target is mainly related to the POC. Therefore, this paper mainly solves the POC problem, and when we update the POC of the distress target in each search subarea according to equation (9), the value of $p^t_{D(i,j)}$ is 1.

4. Search Path Planning Algorithm Based on the POC Model of Distress Targets

4.1. Description of Search Path Planning Algorithm Based on the POC Model of Distress Targets. Because the POC model of the distress targets is time sensitive, the search path planning needs to be carried out within the constraints of the time window T. At the same time, in order to improve the success rate of search and rescue, the planned search path must cover the area where the POC is as high as possible and give the priority to the search subarea with high probability. Therefore, based on the constructed POC model of distress targets, the POC is taken as the weight of each search subarea, and the sum of the POC of all search subareas is regarded as the weight of the search path. Then, the search path planning is transformed into the maximum weight path planning problem based on the POC model of distress target, so as to build the search path planning model which can be expressed as follows:

$$Z^t_{\text{selected}} = \arg\max_{Z^t_r \in Z^t_{R_m}} \left(\sum_{q=1}^{m} \gamma^{m-1} p^t_{C\left(i_{rq}, j_{rq}\right)} \right), \tag{11}$$

where the specified path step is represented as m, that is, the number of search subareas that can be searched by the search platform in the time window T, whose expression is shown in equation (12); Z^t_{selected} represents the search planning path at time t; $Z^t_{R_m}$ represents the collection of all optional search paths at time t; Z^t_r represents one of the search paths in $Z^t_{R_m}$; $p^t_{C(i_{rq},j_{rq})}$ refers to the POC of the distress targets corresponding to the search subarea $g^t_{(i_{rq},j_{rq})}$ covered by the search path Z^t_r; and $\gamma \in (0,1)$ represents the discount factor.

Assuming that the search platform travels at a constant speed V_{ss} and can turn in four directions $s\,(s=4)$, that is, up, down, left, and right, the number of searchable subareas m within the time window T is fixed and satisfies

$$m = \lfloor \frac{V_{ss} \cdot T}{d} \rfloor. \tag{12}$$

After the modeling of the search path planning problem is completed, the dynamic programming algorithm is used to obtain the best search path Z^t_{selected}. The main idea of solving the path planning problem by using dynamic programming algorithm is that, in the process of search path planning, after calculating the weights of search path with the same starting point and end point, only the search path with the maximum sum of weights is retained, and others are deleted. Besides, the weights are only calculated once for repeated path points in the same search path.

An example is given to illustrate the process of solving the search path planning problem based on the POC model of distress target by using dynamic programming algorithm, as shown in Figure 2. Figure 2(a) represents the POC model of the distress target, that is, the search area is divided into 5×5 search subareas by grid method, and the number within each search subarea represents the corresponding POC. Assuming that the search platform is located in the search subarea $g_{(2,2)}$, that is, the search path to be planned starts with the search subarea $g_{(2,2)}$, the search path step m that needs to be planned in the time window T and discount factor $\gamma = 0.98$. Figure 2(b) presents the first two steps. In Figure 2, the possible path points are placed in the circles, the

0.0000	0.0000	0.0034	0.0707	0.0000
0.0299	0.0474	0.0858	0.0750	0.0037
0.0342	0.0889	0.1026	0.0802	0.0412
0.0050	0.0711	0.0826	0.0818	0.0423
0.0000	0.0105	0.0202	0.0185	0.0050

(a)

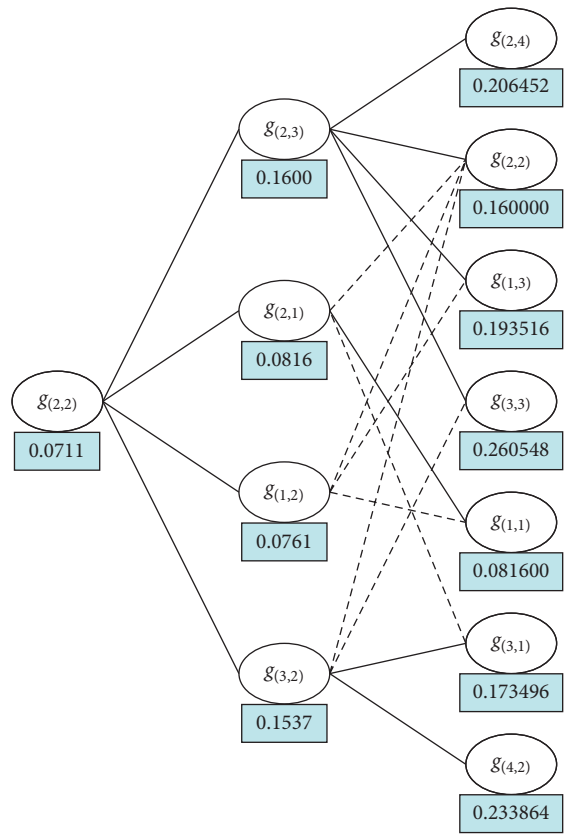

(b)

Figure 2: Calculating process of the search path planning model based on the POC model. (a) the POC model of distress target. (b) the path planning process of the first two step.

number in each box represents the sum of the current weights of the path, the solid line denotes the existing path, and the dotted line stands for the deleted path.

Firstly, the search path planning of step 1 is carried out. The search platform is currently located in the search subarea $g_{(2,2)}$ and can be turned up, down, left, and right, so the first set Z_{P_1} of path points is optional, that is, $\{g_{(2,3)}, g_{(2,1)}, g_{(1,2)}, g_{(3,2)}\}$ and all the alternative search path sets Z_{R_1} are $\{\{g_{(2,2)}, g_{(2,3)}\}, \{g_{(2,2)}, g_{(2,1)}\}, \{g_{(2,2)}, g_{(1,2)}\}, \{g_{(2,2)}, g_{(3,2)}\}\}$. Because there is no duplicate path point in all the optional search paths, the set including the corresponding path weights is $\{0.0711 + 0.0889, 0.0711 + 0.0101, 0.0711 + 0.0050, 0.0711 + 0.0826\}$, that is, $\{0.1600, 0.0816, 0.0761, 0.1537\}$. Because there is no search path with the same starting and ending points in all the optional search paths, it is unnecessary to do the deletion of the optional path and directly plan the next step size.

Secondly, the search platform takes the first optional path point as the starting point for the second step of the search path planning. At this time, the optional path point set Z_{P_2} is $\{g_{(2,4)}, g_{(2,2)}, g_{(1,3)}, g_{(3,3)}, g_{(1,1)}, g_{(3,1)}, g_{(4,2)}\}$ and all the optional search path sets Z_{R_2} are $\{\{g_{(2,2)}, g_{(2,3)}, g_{(2,4)}\}, \{g_{(2,2)}, g_{(2,3)}, g_{(2,2)}\}, \{g_{(2,2)}, g_{(2,3)}, g_{(1,3)}\}, \{g_{(2,2)}, g_{(2,3)}, g_{(3,3)}\}, \{g_{(2,2)}, g_{(2,1)}, g_{(2,2)}\}, \{g_{(2,2)}, g_{(2,1)}, g_{(1,1)}\}, \{g_{(2,2)}, g_{(2,1)}, g_{(3,1)}\}, \{g_{(2,2)}, g_{(1,2)}, g_{(2,2)}\}, \{g_{(2,2)}, g_{(1,2)}, g_{(1,3)}\}, \{g_{(2,2)}, g_{(1,2)}, g_{(1,1)}\}, \{g_{(2,2)}, g_{(3,2)}, g_{(2,2)}\}, \{g_{(2,2)}, g_{(3,2)}, g_{(3,3)}\}, \{g_{(2,2)}, g_{(3,2)}, g_{(3,1)}\}, \{g_{(2,2)}, g_{(3,2)}, g_{(4,2)}\}\}$. Among all the optional search path sets Z_{R_2}, some search paths contain duplicate path points whose weights can only be calculated once. For example, the search path contains duplicate path point $\{g_{(2,2)}, g_{(2,3)}, g_{(2,2)}\}$. Therefore, the sum of the weights of this search path is $0.0711 + 0.0889 + 0.98 \times 0 = 0.1600$. According to this method, the sum of the weights corresponding to all optional search paths can be calculated as {0.206452, 0.160000, 0.193516, 0.260548, 0.081600, 0.081600, 0.101396, 0.109616, 0.076100, 0.076100, 0.254248, 0.173496, 0.153700, 0.233864}. At the same time, because there are five groups of search paths with the same starting point and end point in all the optional search path sets, which are $\{\{g_{(2,2)}, g_{(2,3)}, g_{(2,2)}\}, \{g_{(2,2)}, g_{(2,1)}, g_{(2,2)}\}, \{g_{(2,2)}, g_{(1,2)}, g_{(2,2)}\}, \{g_{(2,2)}, g_{(3,2)}, g_{(2,2)}\}\}$, $\{\{g_{(2,2)}, g_{(2,3)}, g_{(1,3)}\}, \{g_{(2,2)}, g_{(1,2)}, g_{(1,3)}\}\}$, $\{\{g_{(2,2)}, g_{(2,3)}, g_{(3,3)}\}, \{g_{(2,2)}, g_{(3,2)}, g_{(3,3)}\}\}$, $\{\{g_{(2,2)}, g_{(2,1)}, g_{(1,1)}\}, \{g_{(2,2)}, g_{(1,2)}, g_{(1,1)}\}\}$, $\{\{g_{(2,2)}, g_{(2,1)}, g_{(3,1)}\}, \{g_{(2,2)}, g_{(3,2)}, g_{(3,1)}\}\}$, respectively, we need to delete the optional path according to the sum of the path weights, and only the search path with the maximum sum of the weights is retained, which are $\{g_{(2,2)}, g_{(2,3)}, g_{(2,2)}\}$, $\{g_{(2,2)}, g_{(2,3)}, g_{(1,3)}\}$, $\{g_{(2,2)}, g_{(2,3)}, g_{(3,3)}\}$,

$\{g_{(2,2)}, g_{(2,1)}, g_{(1,1)}\}$, $\{g_{(2,2)}, g_{(3,2)}, g_{(3,1)}\}$. At this point, the sets of all the alternative paths Z_{R_2} are $\{\{g_{(2,2)}, g_{(2,3)}, g_{(2,4)}\}, \{g_{(2,2)}, g_{(2,3)}, g_{(2,2)}\}, \{g_{(2,2)}, g_{(2,3)}, g_{(1,3)}\}, \{g_{(2,2)}, g_{(2,3)}, g_{(3,3)}\}, \{g_{(2,2)}, g_{(2,1)}, g_{(1,1)}\}, \{g_{(2,2)}, g_{(3,2)}, g_{(3,1)}\}, \{g_{(2,2)}, g_{(3,2)}, g_{(4,2)}\}\}$, and the sum of the corresponding path weights is {0.206452, 0.160000, 0.193516, 0.260548, 0.081600, 0.173496, 0.233864}.

Then, the search platform takes the second step optional path point as the starting point and carries on the third step size plan, which has the same processes as the second step. The planning will not stop until it completes m steps, and the set Z_{R_m} containing all the optional path planning is obtained. Finally, the path with the largest weight will be chosen, that is, Z_{selected}.

4.2. Implementation of Search Path Planning Algorithm Based on the POC Model of Distress Targets. According to the above description and calculation process of solving search path planning problem by dynamic programming algorithm, the search path planning algorithm based on the POC model of distress target is mainly realized by the following seven steps:

Step 1: it uses the Monte Carlo random particle method and the grid method to obtain the POC model of distress target at time t, that is, the search area G^t and its corresponding POC matrix $\mathbf{P}_C^t = \left\{p_{C(i,j)}^t\right\}$.

Step 2: the search platform calculates the required path step m in the current time window T according to equation (12).

Step 3: the search platform takes the current optional path point as the starting point and uses the dynamic programming algorithm to carry out the kth step search path planning. According to the directions that the search platform can choose, we obtain the selected path point set $Z_{P_k}^t$ and all the optional search path sets $Z_{R_k}^t$.

Step 4: the sum of the weights of each search path in all the optional search path sets $Z_{R_k}^t$ is computed according to equation (11). In the process of the calculation, it is necessary to judge whether there are repeated path points in the search path, and if so, the weights of repeated path points can only be calculated once.

Step 5: it determines whether there is a search path with the same starting and ending points in the set $Z_{R_k}^t$ including all the optional search paths, and if so, the optional path is deleted according to the sum of the path weights. For the search path with the same starting point and end point, only the search path with the maximum sum of weights is retained, and then the updated set $Z_{R_k}^t$ containing optional search paths is obtained.

Step 6: it determines whether k is greater than m, that is, whether the search platform completes the search path planning within the step size m and returns Step 3 if it is not satisfied; otherwise, the iteration terminates, and in all the optional search paths, the search path with the maximum sum of the path weights is selected according to equation (11), which is the best search path Z_{selected}^t.

Step 7: it determines whether the search platform finds a distress target, and if the target is found, the search task ends; otherwise, it determines whether the search time exceeds the search time window T, and if not, the platform continues to perform the search task according to the currently planned search path. Otherwise, the POC model of the distress target is updated according to equations (9) and (10) and returns Step 2 to replan the search path. Then, the search platform performs the search task according to the reprogrammed search path.

5. Simulation and Analysis

5.1. Simulation Assumptions and Parameter Setting. Based on the search and rescue work of people in distress in Qiongzhou Strait as the simulation scene, we conduct the following experiments to study the effectiveness of the POC-SPPA algorithm. The parameters are set as follows:

(1) Assume that the person in distress falls into the water, and its location is (110°30′36″E, 20°13′48″N), 20 nmile east and 10 nmile north of the Maritime Search and Rescue Centre

(2) At the time of the incident, the total current of the Qiongzhou Strait was from west to east, $V_C = 1$ kn, and the direction of the wind pressure difference was southwest, $V_W = 15$ kn

(3) After receiving a search mission, the search platform will travel from the Search and Rescue Centre to search, the speed is $V_{ss} = 15$ kn, and the scan radius is $sw = 0.1$ nmile

(4) In order to ensure that the probability of detection p_D of the distress target in the search area is close to 1, the side length of the search subarea is set at $d = 0.14$ nmile

(5) Simulation particles $N = 50000$ and time window $T = 0.9$ h.

5.2. Establishment and Updating of the POC Model of Distress Target. Monte Carlo random particle method and grid method are used to compute the update of the POC of the distress target. A coordinate system is established with the drowning position of the person in distress as the origin. The constructed POC model of the distress target is shown in Figure 3. Figures 3(a) and 3(b) represent the POC model at time t and time $t + T$, respectively. Each square in Figure 3 represents the search subarea $g_{(i,j)}$. The different colors in the square indicate the varying values of the POC, $p_{C(i,j)}$, corresponding to the search subarea $g_{(i,j)}$.

From Figure 3, it can be seen that compared with the POC model of distress target at time t, the POC model at time $t + T$ is updated, that is, the search area and the POC of the distress target have changed. At time t, within the constraint of the search time window T, the platform starts to execute the search task according to the current planning

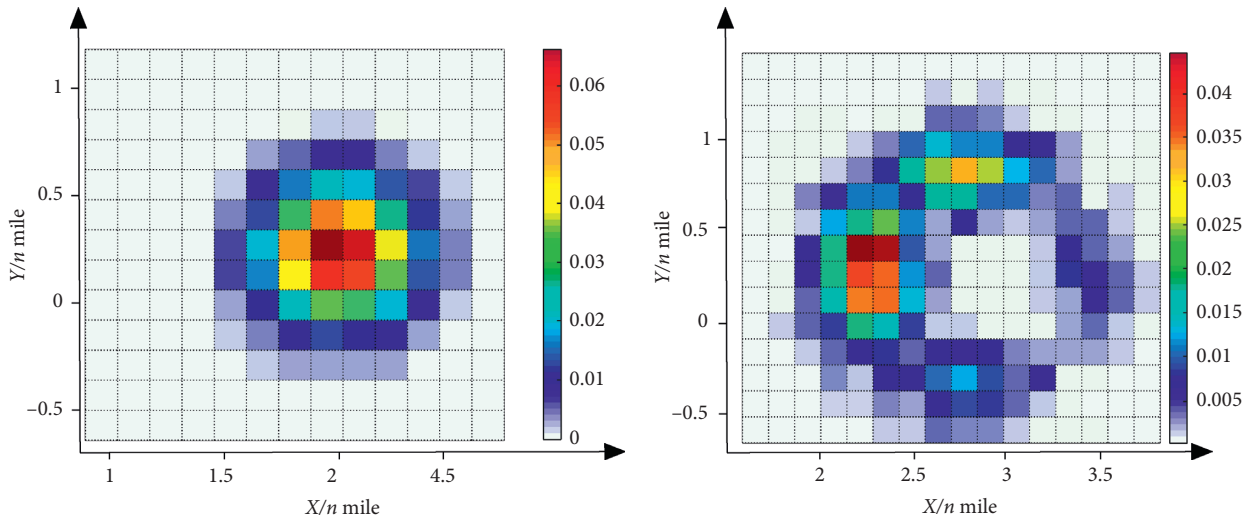

Figure 3: Construction and update of the POC model: (a) POC model at time t. (b) POC model at time $t + T$.

path. When the search time exceeds the time window T, since the platform fails to find the distress target, the POC in the search area is adaptively updated using Bayes criterion, and thus the POC in the area has been already searched. And then, the POC model can be updated at time $t + T$ by resimulating the drift motion of the distress target so as to realize the adaptive update of the POC matrix. Furthermore, because the drift motion of the target in distress is the result of the combined action of total current, sea surface wind pressure difference, wave, and other factors, the location uncertainty of the distress target increases as the time goes by, making the search area larger as shown in Figure 3(b).

5.3. Comparison of Search Path Planning Algorithms

5.3.1. Validation of POC-SPPA. Firstly, the parallel line search path planning algorithm (PL-SPPA) [14, 20], specified in the International Aeronautical and Maritime Search and Rescue Manual, is used as a comparison algorithm to verify the effectiveness of the POC-SPPA.

PL-SPPA takes a corner of the search area as the search starting point, and the search path is parallel to the boundary of the search area. The distance between the first search path and the boundary of the search area closest to the search starting point is 1/2 of the search line spacing, that is, a scan radius. And the subsequent search paths remain parallel to each other and are separated by a search line spacing.

Under the simulation conditions and parameters set in Section 5.1, the drift motion of the distress target is simulated by Monte Carlo random particle method. And based on this, search path planning is carried out by using two different algorithms, including POC-SPPA and PL-SPPA. The simulation results are shown in Figures 4 and 5, where the red lines represent the simulated drift trajectory of the distress target, the blue lines stand for the search path planned by POC-SPPA, and the green lines represent the search path planned by PL-SPPA. Figure 4 shows the search path planned by the two algorithms from alarm to time t_1.

Figures 5(a) and 5(b) represent the search path planned by the two algorithms in time period (t_1, t_2), respectively. On the basis of the POC model of the distress target, POC-SPPA carries on the search path planning according to the POC of each search subarea. However, PL-SPPA holds that the distress target follows the equal probability distribution in the search area, and the regular search path planning is carried out according to the full coverage search.

Figures 5(c) and 5(d) represent the location of the distress target and the search platform at time t_2 $(t_2 = t_1 + T)$ using the above two methods. We can see from Figure 5(c) that POC-SPPA fully considers the time-sensitive characteristics of the search task under the constraints of the time window, and the POC model of the distress target is dynamically updated, so that the distress target is still in the search area, and the search path is replanned on this basis. PL-SPPA does not consider the time window constraint and the dynamic update of search area. It performs the search task according to the estimated search area and search path at time T. Hence, the distress target has drifted out of the search area, as shown in Figure 5(d).

Figures 5(e) and 5(f) represent the search path planned by the two algorithms in time period (t_2, t_3) employing two methods, respectively. POC-SPPA gives the priority to the search subarea with higher probability and successfully finds the distress target at time t_3, while PL-SPPA can only update the search area at the next search time $t + 1$ $(t_2 < t + 1 < t_3)$ and still cannot find the distress target at time t_3.

In order to compare the search effect of the two algorithms in different marine environments, the search success rate and the average search time are taken as the evaluation metrics, and the simulation results are shown in Table 1. As a result, POC-SPPA can effectively improve the search success rate and search speed, especially in the harsh marine

Figure 4: Results of POC-SPPA and PL-SPPA in time period $(0, t_1)$.

environment, where the drift speed and uncertainty of the target are high. POC-SPPA maintains a high search success rate since it is able to dynamically update within the constraint of the time window, while PL-SPPA can hardly find the target because it has to carry out full coverage search and the update speed is slow.

5.3.2. Effectiveness Verification of Updating the POC Matrix Based on Bayes Criterion. On the basis of verifying the effectiveness of POC-SPPA with PL-SPPA, it is further compared with the search path planning algorithm based on the static probability of distress target containment (SPOC-SPPA) to verify the necessity and effectiveness of dynamic update of the POC model based on Bayes criterion in the POC-SPPA.

SPOC-SPPA means that, under the time window constraint, the dynamic update of the POC matrix and the dynamic evaluation of the search area do not use Bayes criterion, but only use Monte Carlo random particle method to simulate the drift trajectory of the distress target according to the initial distress position of the distress target and then replan the search path.

From the above analysis of the simulation results shown in Figure 5, it can be seen that, in the time period (t_1, t_3), POC-SPPA updates the POC model based on the Bayes criterion at time $t_2\,(t_2 = t_1 + T)$ according to equation (9), ensuring that the distress target is still in the estimated search area. In order to fully and effectively illustrate the effectiveness of updating the POC model based on the Bayes criterion, on the basis of the experimental data obtained from the simulation experiment using POC-SPPA in Section 5.3.1, we use SPOC-SPPA to simulate the search and rescue process of the search platform in time period $[t_2, t_3)$. The simulation results are shown in Figure 6, where the red lines represent the simulated drift trajectory of the distress target, the magenta lines stand for the search path planned by SPOC-SPPA, and red "$*$" and magenta "$*$" represent the location of the distress target and the search platform, respectively.

Since SPOC-SPPA also takes into account the time-sensitive characteristics of the search task, it also updates the POC model at time $t_2\,(t_2 = t_1 + T)$. The updated POC model is shown in Figure 6(a). From it, we can see that SPOC-SPPA fully considers the time-sensitive characteristics of the search task, and the POC model of the distress target is dynamically updated under the time window constraint so that the distress target is still in the updated search area. However, when SPOC-SPPA updates the POC model, it only simulates the drift motion of the distress target relied on the initial distress position of the target and the marine environment data information in time period $(0, t_2)$ and does not consider the influence of the search platform execution of search and rescue task on the POC of the distress target in the search area, that is, it does not consider the correlation between the POC model at the updated time before and after, which makes the POC of the distress target in the searched area in time period (t_1, t_2) still relatively high. Unlike SPOC-SPPA, when POC-SPPA algorithm updates the POC model, it uses the POC model at time t_1 as prior information, obtains the posterior information of the probability area of the distress target appearance at time $t_2\,(t_2 = t_1 + T)$ by using the probability propagation characteristic of Bayes criterion, and realizes the probability propagation of the distress target position in the time window before and after, which makes the distress target located in the search area with relatively high probability, as shown in Figure 5(c).

Figure 6(b) represents the search path planned by SPOC-SPPA in time period (t_2, t_3). From it, we can observe that although SPOC-SPPA also gives the priority to the search subarea with higher probability, the correlation between the POC model at the updated time before and after is not considered in the update of the POC model, which leads to the search task in time period (t_2, t_3) has nothing to do with the search results in time period $(0, t_2]$. Namely, the current search tasks a brand new search task. The search platform researched the distress target according to the planned search path (indicated by blue lines in Figure 6(b)), resulting in failure to find the distress target at time t_3. And at this time, the search platform based on the POC-SPPA successfully finds the distress target, as shown in Figure 5(e).

From the above simulation experiments, it can be seen that the POC model update mechanism based on Bayes criterion fully considers the influence of the search platform execution of search and rescue task on the POC of the

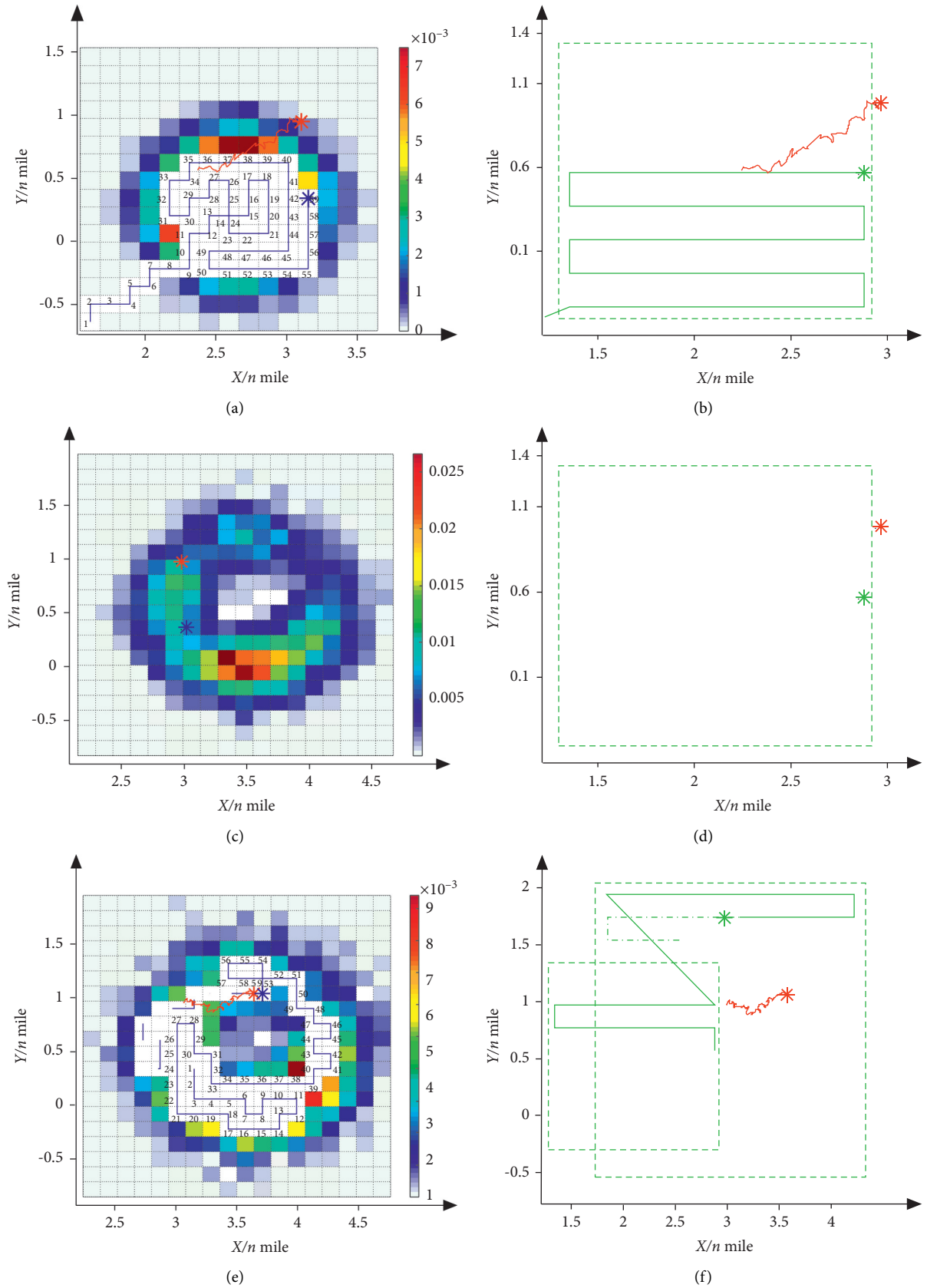

Figure 5: Results of POC-SPPA and PL-SPPA in time period (t_1, t_3). (a) Search path in time period (t_1, t_2) (POC-SPPA). (b) Search path in time period (t_1, t_2) (PL-SPPA). (c) Distress target and search platform location. (d) Distress target and search platform location at time t_2 (POC-SPPA) and at time t_2 (PL-SPPA). (e) Search path in time period (t_2, t_3) (POC-SPPA). (f) Search path in time period (t_2, t_3) (PL-SPPA).

Table 1: Comparison of search results of two search path planning algorithms in different marine environments.

Serial number	V_C (kn)	V_W (kn)	Search success rate (%)		Average search time (h)	
			POC-SPPA	PL-SPPA	POC-SPPA	PL-SPPA
1	1	15	97.9	80.1	2.94	4.18
2	1.5	20	90.0	51.6	4.15	7.02
3	2	25	85.6	24.3	4.84	9.60
4	2.5	30	73.4	18.4	6.05	10.20

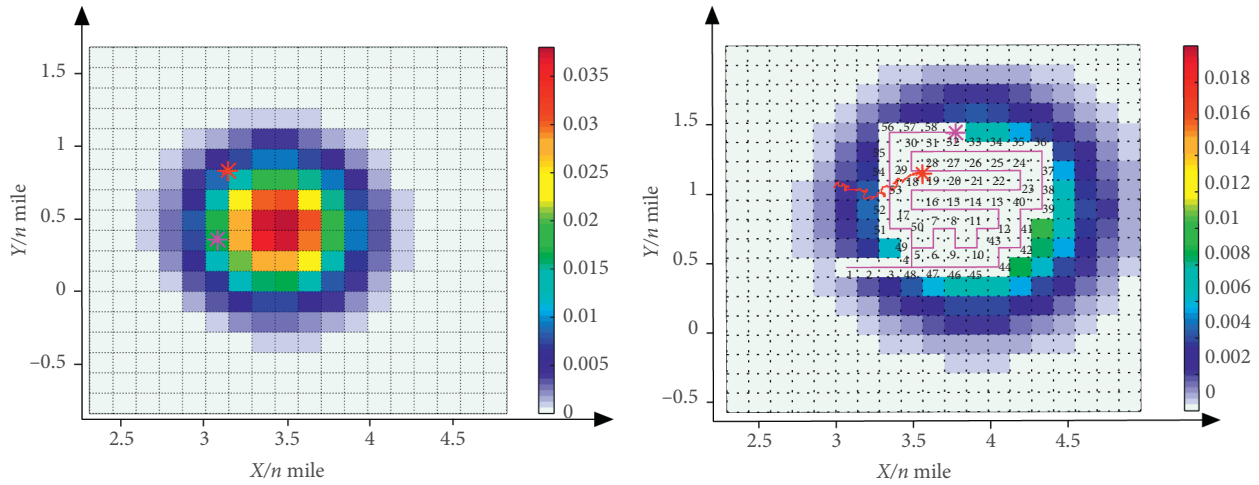

Figure 6: Results of SPOC-SPPA in time period $[t_2, t_3)$. (a) The updated POC model at time t_2. (b) Search path in time period (t_2, t_3).

distress target in the search area and realizes the probability propagation of the distress target position in the time window before and after by using the probability propagation characteristic of Bayes criterion. This makes it possible to make full use of the existing search result information during the entire search process to provide positive feedback information for subsequent searches, effectively improving the accuracy and precision of the search area estimation, thereby increasing the search and rescue success rate.

6. Conclusions

A search path planning algorithm (POC-SPPA) based on the POC model of the distress target is proposed in this paper to solve the path planning problem in the search and rescue process of a distress target at sea. The algorithm uses Monte Carlo random particle method to simulate the drift motion of the distress target and realizes the evaluation of the search area. On this basis, grid processing is employed for the search area. POC-SPPA evaluates the POC of each subsearch area target through the number of particles to construct the POC model of the distress target and realizes the dynamic update of the POC model according to Bayes criterion under the time window constraint. Besides, the sum of the POC of distress target in the search subarea is used as the weight of the search path so that the search path planning is transformed into the maximum weight path planning problem based on the POC model, and the dynamic programming algorithm is used to complete the search path planning. The simulation results show that the proposed algorithm can realize the dynamic prediction of search area and improve the speed and success rate of search and rescue for maritime distress target.

Data Availability

No data were used to support this study.

Conflicts of Interest

The authors declare that there are no conflicts of interest regarding the publication of this paper.

Acknowledgments

This research was funded by the Hainan Provincial Natural Science Foundation of China (619MS030), National Natural Science Foundation of China and Macau Science and Technology Development Joint Fund (61961160706 and 0066/2019/AFJ), the program of and the Scientific Research Foundation of Hainan University (KYQD(ZR)1859), and the International S&T Cooperation Projects of China (2015DFR10510).

References

[1] X. Zhou, L. Cheng, K. Min et al., "A framework for assessing the capability of maritime search and rescue in the south China sea," *International Journal of Disaster Risk Reduction*, vol. 47, p. 101568, 2020.

[2] M. Karatas, N. Razi, and M. M. Gunal, "An ILP and simulation model to optimize search and rescue helicopter operations," *Journal of the Operational Research Society*, vol. 68, no. 11, pp. 1335–1351, 2017.

[3] N. Yong-Wook and K. Yong-Hyuk, "Prediction of drifter trajectory using evolutionary computation," *Discrete Dynamics in Nature and Society*, vol. 2018, Article ID 6848745, 15 pages, 2018.

[4] X. Zhou, L. Cheng, F. Zhang et al., "Integrating island spatial information and integer optimization for locating maritime search and rescue bases: a case study in the south China sea," *ISPRS International Journal of Geo-Information*, vol. 8, no. 2, p. 88, 2019.

[5] N. M. Dinnbier, Y. Thueux, A. Savvaris, and A. Tsourdos, "Target detection using Gaussian mixture models and fourier transforms for UAV maritime search and rescue," in *Proceedings of the 2017 International Conference on Unmanned Aircraft Systems (ICUAS)*, pp. 1418–1424, IEEE, Miami, FL, USA, June 2017.

[6] D. Agbissoh OTOTE, B. Li, B. Ai et al., "A decision-making algorithm for maritime search and rescue plan," *Sustainability*, vol. 11, no. 7, p. 2084, 2019.

[7] A. Shabani, B. Asgarian, S. A. Gharebaghi, M. A. Salido, and A. Giret, "A new optimization algorithm based on search and rescue operations," *Mathematical Problems in Engineering*, vol. 2019, Article ID 2482543, 23 pages, 2019.

[8] J. Zhang, Â. P. Teixeira, C. Guedes Soares, and X. Yan, "Probabilistic modelling of the drifting trajectory of an object under the effect of wind and current for maritime search and rescue," *Ocean Engineering*, vol. 129, pp. 253–264, 2017.

[9] A. D. Maio, M. V. Martin, and R. Sorgente, "Evaluation of the search and rescue LEEWAY model in the Tyrrhenian Sea: a new point of view," *Natural Hazards and Earth System Sciences*, vol. 16, pp. 1979–1997, 2016.

[10] B. A. Brushett, A. A. Allen, V. C. Futch, B. A. King, and C. J. Lemckert, "Determining the leeway drift characteristics of tropical Pacific island craft," *Applied Ocean Research*, vol. 44, pp. 92–101, 2014.

[11] H. Guo, Z. Jiang, and H. Zhang, "Determing confidence region for maritime search and rescue operation model," *Journal of Residuals Science and Technology*, vol. 13, pp. 156.1–156, 2016.

[12] Y. Yi, W. Si-cai, and N. Ying, "Optimal algorithm of searching route for large amphibious aircraft," *Journal of Jilin University (engineering and Technology Edition)*, vol. 13, no. 4, pp. 156.1–156, 2019.

[13] G. Xia, Z. Han, B. Zhao, C. Liu, and X. Wang, "Global path planning for unmanned surface vehicle based on improved quantum ant colony algorithm," *Mathematical Problems in Engineering*, vol. 2019, Article ID 2902170, 10 pages, 2019.

[14] Y. H. DU, L. N. XING, and Y. G. CHEN, "Strategies of maritime cooperative searching and path optimization using multiple platforms," *Control and Decision*, vol. 35, no. 1, pp. 147–154, 2020.

[15] D. Mu, G. Wang, Y. Fan, Y. Bai, and Y. Zhao, "Fuzzy-based optimal adaptive line-of-sight path following for underactuated unmanned surface vehicle with uncertainties and time-varying disturbances," *Mathematical Problems in Engineering*, vol. 2018, Article ID 7512606, 10 pages, 2018.

[16] P. Yu, J. Wang, Z.-T. Liu, and H.-R. Bian, "Modeling of point search area and rescue path for maritime air crash," in *Proceedings of the 2015 34th Chinese Control Conference (CCC)*, pp. 2786–2791, IEEE, Hangzhou, China, July 2015.

[17] J. LYU and H. Zhao, "Factorial-based particle swarm optimization and its application to maritime moving target search," *Control and Decision*, vol. 33, pp. 1983–1989, 2018.

[18] Q. Lu, Y. Xu, Y. Chen, R. Huang, and L. Chen, "Enhancing state space search for planning by Monte-Carlo random walk exploration," in *Proceedings of the International Conference on Intelligent Data Engineering and Automated Learning*, pp. 37–45, Springer, Yangzhou, China, November 2016.

[19] K. Zhu, L. Mu, D. S. Wang et al., "Advance maritime search and rescue decision support techniques," *Journal of Applied Oceanography*, vol. 38, no. 3, pp. 440–449, 2019.

[20] L. Z. Tan, P. Tan, and B. Wang, "Computing method of aerial searching's sweep width at sea," *Ship Electronic Engineering*, vol. 39, no. 6, pp. 146–150+175, 2019.

Hindawi
Mathematical Problems in Engineering
Volume 2020, Article ID 5649525, 10 pages
https://doi.org/10.1155/2020/5649525

Research Article

A Novel IVPLTS Decision Method Based on Regret Theory and Cobweb Area Model

Peng Li and Huanhuan Peng

College of Economics and Management, Jiangsu University of Science and Technology, Zhenjiang, Jiangsu 212003, China

Correspondence should be addressed to Peng Li; jellyok@126.com

Received 28 May 2020; Revised 6 July 2020; Accepted 27 November 2020; Published 9 December 2020

Academic Editor: Zeshui Xu

For the multiple criteria decision-making (MCDM) problem with interval-valued probabilistic linguistic information, we propose a novel method considering the regret theory and cobweb area model. We first propose a new score function, which can be used to compare different interval-valued probabilistic linguistic term sets (IVPLTSs) and transform the IVPLTSs into crisp numbers. Some properties of the score function are verified. Then, we utilize the regret theory to obtain the perceived utilities of decision makers (DMs), which can reflect the DMs' bounded rationality. Furthermore, we use the cobweb area model to aggregate decision information. Finally, a real case of evaluating nursing homes is used to illustrate the effectiveness and features of our method.

1. Introduction

Multiple criteria decision-making (MCDM) widely exists in all aspects of human life. In the real decision environment, due to the complexity of decision-making problems and the limited personal knowledge of decision makers (DMs), it is difficult for DMs to express their preference information with crisp values. In 1975, Zadeh [1] first proposed the concept of fuzzy linguistic approach, advocating the use of natural linguistic instead of crisp numbers to express qualitative evaluation information in MCDM problems. Then, Rodriguez et al. [2] developed the fuzzy linguistic information and proposed the definition of hesitant fuzzy linguistic term set (HFLTS). HFLTS can express the hesitance of DMs but cannot reflect the importance of the linguistic terms. To cope with this issue, Pang et al. [3] proposed the definition of probabilistic linguistic term sets (PLTSs). Since the concept of PLTS was proposed, there had been a large amount of studies about PLTS, such as operational rules for PLTSs [3, 4], outranking methods [5], and preference relation of PLTSs [6].

Based on the PLTS, Bai et al. [7] further proposed the interval-valued probabilistic linguistic term set (IVPLTS) and developed some comparison rules, operation rules, and aggregation operator. Yu et al. [8] proposed a new possibility degree method for uncertain probabilistic linguistic term set (UPLTS). Zhang et al. [9] considered probability distribution and interval-valued hesitant fuzzy set and proposed the definition of probabilistic interval-valued hesitant fuzzy set (P-IVHFS). Jin et al. [10] proposed the basic operation rules and aggregation operators of uncertain probabilistic linguistic term set (UPLTS) and extended the traditional TOPSIS method to the UPLTS environment. Krishankumar et al. [11] proposed interval-valued probabilistic linguistic simple weighted geometry (IVPLSWG) to aggregate preference information of decision makers and extended the VIKOR method to the decision environment of IVPLTS.

For the aspect of behavior theory, extensive studies have been conducted. Liu and Li [12] applied prospect theory to the decision environment of probabilistic linguistic and proposed a multiobjective optimization method of MULTIMOORA based on prospect theory. Gu et al. [13] proposed a multiattribute decision-making framework based on prospect theory in probabilistic linguistic environment. Wang et al. [14] constructed a novel risk priority model for failure mode and effects analysis (FMEA). Qin [15] proposed a capital asset pricing model based on regret theory to explore the impact of regret aversion on capital pricing. Bai

and Sarkis [16] proposed a new hybrid group decision-making method combining hesitant fuzzy set and regret theory for the evaluation and selection of block chain technology.

Interval-valued probabilistic linguistic term set (IVPLTS) is further improved on the basis of PLTS and can solve the problem of uncertain probability. In view of the strong applicability and advantages of IVPLTS, we extend the decision framework of IVPLTS. However, there are few studies of behavior theory in interval-valued probabilistic linguistic environment. It is necessary to consider the research of decision-makers' limited rationality. Regret theory is simpler than prospect theory [17]. Furthermore, long-term care for elders has been a serious problem in China. A rational method of evaluating nursing homes is necessary. Score function is a kind of effective tool to defuzzy probabilistic linguistic information, which can make the decision process simple. A suitable score function should be flexible and can reflect preference of DM. Therefore, in this paper, we will propose a novel decision-making method for IVPLTSs based on regret theory and apply the method to the problem of selecting nursing homes for a hospital. The main contributions of our method can be concluded as follows:

(1) We propose a new score function for IVPLTSs containing risk parameter and preference parameter of DMs. DMs can flexibly choose the two parameters according their risk attitudes and preferences and compare different IVPLTSs.

(2) We present a novel decision-making method for IVPLTSs using regret theory and cobweb area model, which can effectively reflect the bounded rationality of DMs and relieve the problem that some extremely large or small values exert too much influence on the final decision result.

The remainder of our paper is shown as follows. Section 2 reviews some basic definition and operational rules of IVPLTSs and regret theory. In Section 3, a novel score function for IVPLTSs is presented. Section 4 puts forward a novel decision method based on regret theory and cobweb area model. Section 5 applies our proposed method to a real case study and compares with the traditional TOPSIS method to illustrate the effectiveness and traits of our method. Section 6 makes a summary of our method and presents the future research scope.

2. Preliminaries

2.1. Interval-Valued Probabilistic Linguistic Term Set. In our real life, DMs usually use linguistic information to express their opinions rather than crisp numbers. For example, we can use "good" or "poor" to describe the quality of a car. The definition of linguistic term set (LTS) can be shown as follows.

Definition 1 (see [18]). Let τ be a positive integer, a symmetrical LTS can be defined as $S = \{s_\alpha | \alpha = -\tau, \ldots, -1, 0, 1, \ldots, \tau\}$, where s_α is called linguistic term.

The basic operational rules for LTSs can be concluded as follows [18].

Definition 2 (see [18]). Let s_{α_1} and s_{α_2} be two linguistic terms and λ be a positive number; then, the following rules hold:

(1) $s_{\alpha_1} \oplus s_{\alpha_2} = s_{\alpha_1+\alpha_2}$

(2) $s_{\alpha_1} \otimes s_{\alpha_2} = s_{\alpha_1 \times \alpha_2}$

(3) $\lambda s_{\alpha_1} = s_{\lambda\alpha_1}$

(4) $(s_{\alpha_1})^\lambda = s_{\alpha_1^\lambda}$

Pang et al. [3] proposed the definition of probabilistic linguistic term set (PLTS) as follows.

Definition 3 (see [3]). Let $S = \{S_t | = -\tau, \ldots, -1, 0, 1, \ldots, \tau\}$ be a LTS, a PLTS on S can be defined as $L(p) = \{L^{(k)}(p^{(k)}) | L^{(k)} \in S, p^{(k)} \geq 0, k = 1, 2, \ldots, \#L(p), \sum_{k=1}^{\#L(p)} p^{(k)}\}$, where $L^{(k)}(p^{(k)})$ is the linguistic term $L^{(k)}$ with respect to probability $p^{(k)}$ and $\#L(p)$ is the number of different LTSs in $L(p)$.

Bai et al. [7] extend the PLTS to interval-valued probabilistic linguistic term set (IVPLTS) as follows.

Definition 4 (see [7]). Let $S = \{S_t | t = -\tau, \ldots, -1, 0, 1, \ldots, \tau\}$ be a LTS, and an IVPLTS on S can be defined as

$$\widetilde{L}(p) = \left\{ L^k\left[\gamma_k^L, \gamma_k^U\right] | L^k \in S, \quad 0 \leq \gamma_k^L \leq \gamma_k^U \leq 1, k = 1, 2, \ldots, \#\widetilde{L}(p) \right\}, \tag{1}$$

where $L^k[\gamma_k^L, \gamma_k^U]$ is the linguistic term $L^{(k)}$ with respect to interval-valued probability $[\gamma_k^L, \gamma_k^U]$ with $\sum_{k=1}^{\#L(p)} \gamma_k^U \leq 1$.

The basic operational rules for IVPLTSs can be seen as follows.

Definition 5 (see [7]). Let $S = \{s_\alpha | \alpha = -\tau, \ldots, -1, 0, 1, \ldots, \tau\}$ be a LTS, $\widetilde{L}_1(p) = \{L_1^k[\gamma_{1k}^L, \gamma_{1k}^U]\}$ and $\widetilde{L}_2(p) = \{L_2^k[\gamma_{2k}^L, \gamma_{2k}^U]\}$ be two IVPLTSs on S, ξ be a positive number, $\eta_1^{(i)} \in g(\widetilde{L}_1(p)), \eta_2^{(j)} \in g(\widetilde{L}_2(p))$, $i = 1, 2, \ldots, \#\widetilde{L}_1(p)$, $j = 1, 2, \ldots, \#\widetilde{L}_2(p)$, and g: $[-\tau, \tau] \longrightarrow [0, 1]$ be an equivalent transformation function; then, the following rules hold:

(1) $\widetilde{L}_1(p) \oplus \widetilde{L}_2(p) = g^{-1}(\{(\eta_1^{(i)} + \eta_2^{(j)} - \eta_1^{(i)}\eta_2^{(j)}) \quad [\gamma_{1i}^L \cdot \gamma_{2j}^L, \gamma_{1i}^U \cdot \gamma_{2j}^U]\})$

(2) $\xi\widetilde{L}_1(p) = g^{-1}(\{(1 - (1 - \eta^{(i)})^\xi)[\gamma_{1i}^L, \gamma_{1i}^U]\})$

Bai et al. [7] proposed a normalization method to guarantee the ranges of probabilities in a standard interval [0, 1].

Let $\widetilde{L}(p) = \{L^k[\gamma_k^L, \gamma_k^U]\}$ be an IVPLTS; then, $\widetilde{L}(p)$ can be transformed to a standard IVPLTS $\bar{L}(p) = \left\{ L^k[\bar{\gamma}_k^L, t\bar{\gamma}_k^U] \right\}$ as follows:

$$\bar{\gamma}_k^L = \frac{\gamma_k^L}{\sqrt{\sum_{k=1}^{\#\widetilde{L}(p)} \left(\gamma_k^L\right)^2 + \left(\gamma_k^U\right)^2}}, \quad (2)$$

$$\bar{\gamma}_k^U = \frac{\gamma_k^U}{\sqrt{\sum_{k=1}^{\#\widetilde{L}(p)} \left(\gamma_k^L\right)^2 + \left(\gamma_k^U\right)^2}}. \quad (3)$$

For convenience narration, we still use $\widetilde{L}(p) = \{L^k[\gamma_k^L, \gamma_k^U]\}$ as standard IVPLTS.

Jin et al. [10] proposed a distance measure as follows.

Definition 6 (see [10]). Let $\widetilde{L}_1(p) = \{L_1^k[\gamma_{1k}^L, \gamma_{1k}^U], k = 1, 2, \ldots, \#\widetilde{L}_1(p)\}$ and $\widetilde{L}_2(p) = \{L_2^k[\gamma_{2k}^L, \gamma_{2k}^U], k = 1, 2, \ldots, \#\widetilde{L}_2(p)\}$ be two IVPLTSs, and then the distance between $\widetilde{L}_1(p)$ and $\widetilde{L}_2(p)$ can be defined as

$$d\left(\widetilde{L}_1(p), \widetilde{L}_2(p)\right) = \frac{\sum_{k=1}^{\#\widetilde{L}_1(p)} (1/2)\left(\left|\gamma_{1k}^L \times r_1^k - \gamma_{2k}^L \times r_2^k\right| + \left|\gamma_{1k}^U \times r_1^k - \gamma_{2k}^U \times r_2^k\right|\right)}{\#\widetilde{L}_1(p)}, \quad (4)$$

where r_1^k and r_2^k are the subscripts of L_1^k and L_2^k, respectively.

2.2. Regret Theory. Owing to the uncertain information, time pressure, and analysis capacity of DMs, in some cases, DMs usually have the feature of bounded rationality. Regret theory [17, 19, 20] is a powerful tool to deal with this situation.

Given two alternatives x_1 and x_2, the perceived utility of DM for choosing x_1 can be computed as follows.

$$U(x_1) = v(x_1) + R(v(x_1) - v(x_2)), \quad (5)$$

where $v(\cdot)$ is a utility function satisfying $v'(\cdot) > 0$ and $v''(\cdot) < 0$ and $R(\cdot)$ is a regret/rejoice function satisfying $R'(\cdot) > 0$, $R''(\cdot) < 0$, and $R(0) = 0$.

Zhang et al. [17] extended the RT theory from two alternatives to multiple ones.

Let $x_1, x_2, \ldots, x_m$ be m alternatives and $x^* = \max\{x_i | it = n1, 2q, h \ldots, xm\}$, and then perceived utility for x_i can be obtained as

$$U_i = v(x_i) + R(v(x_i) - v(x*)). \quad (6)$$

3. A New Score Function for IVPLTS

To compare different IVPLTSs, score function is a very useful tool. Pang et al. [3] proposed a score function for PLTS. Li and Wei [4] put forward a new score function based on D-S evidence theory. However, the research on score function for IVPLTS is infrequent. Therefore, we will propose a score function for IVPLTS.

Definition 7. Let $S = \{S_t | t = -\tau, \ldots, -1, 0, 1, \ldots, \tau\}$ be a LTS and $\widetilde{L}(p) = \{L^k[\gamma_k^L, \gamma_k^U]\}$ be an IVPLTS on S; then, the score function for $\widetilde{L}(p)$ can be defined as

$$Q(\widetilde{L}(p)) = \sum_{k=1}^{\#\widetilde{L}(p)} \left(\frac{\gamma_k^L \beta + \gamma_k^U (1-\beta)}{2}\right)\left(\frac{\tau + r^k}{2\tau}\right)^\theta, \quad (7)$$

where r^k is the subscript of L^k, $\beta \in [0, 1]$ is a risk parameter, and $\theta > 0$ is a preference parameter.

Note: the two parameters β and θ can be obtained by decision makers according to their risk preferences. If the decision maker is risk-seeking, the two parameters can be set relatively large values. Conversely, if the decision maker is risk evading, they can be set relative small values.

Theorem 1. *Let $\widetilde{L}(p)$ be a standard IVPLTS; then, score function $Q(\widetilde{L}(p))$ satisfies $0 \le Q(\widetilde{L}(p)) \le \#(\widetilde{L}(p))$.*

Proof. Because $\widetilde{L}(p)$ is a standard IVPLTS, we can easily obtain that $[\gamma_k^L, \gamma_k^U] \subset [0, 1]$ and $\sum_{k=1}^{\#\widetilde{L}(p)} \gamma_k^L \le \sum_{k=1}^{\#\widetilde{L}(p)} \gamma_k^U \le 1$. Because $\beta \in [0, 1]$, we have $\gamma_k^L \le (\gamma_k^L \beta + \gamma_k^U (1-\beta)/2) \le \gamma_k^U$. Then, we can draw a conclusion that $0 \le \sum_{k=1}^{\#\widetilde{L}(p)} ((\gamma_k^L \beta + \gamma_k^U (1-\beta)/2)) \le \#\widetilde{L}(p)$. Because $-\tau \le r^k \le \tau$, we can obtain $0 \le (\tau + r^k/2\tau) \le 1$. Owing to $\theta > 0$, we have $0 \le (\tau + r^k/2\tau)^\theta \le 1$. Therefore, we can obtain $0 \le \sum_{k=1}^{\#\widetilde{L}(p)} (\gamma_k^L \beta + \gamma_k^U (1-\beta)/2)((\tau + r^k)/2\tau)^\theta \le \#\widetilde{L}(p)$. □

Theorem 2. *For a fixed θ ($\theta > 0$), the score function $Q(\widetilde{L}(p))$ for $\widetilde{L}(p)$ is a decreasing function of parameter β ($\beta > 0$).*

Proof. Let $0 < \beta_1 \le \beta_2$, and we can obtain $\gamma_k^L \beta_1 + \gamma_k^U (1-\beta_1) = \gamma_k^U + (\gamma_k^L - \gamma_k^U)\beta_1$ and $\gamma_k^L \beta_2 + \gamma_k^U (1-\beta_2) = \gamma_k^U + (\gamma_k^L - \gamma_k^U)\beta_2$. Because $\gamma_k^L - \gamma_k^U \le 0$, then we have $(\gamma_k^L \beta_1 + \gamma_k^U (1-\beta_1)/2) \ge (\gamma_k^L \beta_2 + \gamma_k^U (1-\beta_2)/2)$. Because $0 \le (\tau + r^k/2\tau)^\theta \le 1$ and $\theta > 0$, we can obtain

$$\sum_{k=1}^{\#\widetilde{L}(p)} \left(\frac{\gamma_k^L \beta_1 + \gamma_k^U (1-\beta_1)}{2}\right)\left(\frac{\tau + r^k}{2\tau}\right)^\theta \ge \sum_{k=1}^{\#\widetilde{L}(p)} \left(\frac{\gamma_k^L \beta_2 + \gamma_k^U (1-\beta_2)}{2}\right)\left(\frac{\tau + r^k}{2\tau}\right)^\theta. \quad (8)$$

□

Theorem 3. *For a fixed β $(0 \le \beta \le 1)$, the score function $Q(\widetilde{L}(p))$ for $\widetilde{L}(p)$ is a decreasing function of parameter θ $(0 \le \theta \le 1)$.*

Proof. Assume that $0 \le \theta_1 \le \theta_2 \le 1$. Because $0 \le (\tau + r^k/2\tau) \le 1$, we can easily obtain $0 \le (\tau + r^k/2\tau)^{\theta_2} \le (\tau + r^k/2\tau)^{\theta_1} \le 1$. Because $0 \le \beta \le 1$, we can obtain $0 \le (\gamma_k^L \beta + \gamma_k^U (1-\beta)/2) \le 1$ and

$$\sum_{k=1}^{\#\widetilde{L}(p)} \left(\frac{\gamma_k^L \beta + \gamma_k^U (1-\beta)}{2}\right)\left(\frac{\tau + r^k}{2\tau}\right)^{\theta_1} \ge \sum_{k=1}^{\#\widetilde{L}(p)} \left(\frac{\gamma_k^L \beta + \gamma_k^U (1-\beta)}{2}\right)\left(\frac{\tau + r^k}{2\tau}\right)^{\theta_2}. \tag{9}$$

□

Example 1. Let $S = \{s_{-3}, s_{-2}, s_{-1}, s_0, s_1, s_2, s_3\}$ be a LTS and $\widetilde{L}(p) = \{s_0[0.3, 0.5], s_1[0.2, 0.3], s_2[0.35, 0.6]\}$ be an IVPLTS on S. Then, we can normalize $\widetilde{L}(p)$ as $\bar{L}(p) = \{s_0[0.31, 0.51], s_1[0.20, 0.31], s_2[0.36, 0.61]\}$ and obtain the score function as $Q(\bar{L}(P)) = 0.28$.

4. A Novel IVPLTS Decision Method Based on Regret Theory and Cobweb Area Model

4.1. Description of Decision-Making Problem. Given a decision-making problem, let $A = \{A_1, A_2, \ldots, A_m\}$ be an alternative set, $C = \{C_1, C_2, \ldots, C_n\}$ be a criterion set, and $W = (w_1, w_2, \ldots, w_n)$ be the criteria weights for criteria $C_1, C_2, \ldots, C_n$ satisfying $0 \le w_j \le 1$, $(j = 1, 2, \ldots, n)$, $\sum_{j=1}^{n} w_j = 1$. DMs propose a decision matrix $X = (x_{ij})_{m\times n}$, where x_{ij} is a IVPLTS and indicates the value of alternative A_i $(i = 1, 2, \ldots, m)$ in terms of C_j $(j = 1, 2, \ldots, n)$.

4.2. Obtaining the Criteria Weights Based on Maximizing Deviation Method. According to decision matrix $X = (x_{ij})_{m\times n}$, we normalize X to $Y = (y_{ij})_{m\times n}$ based on equations (2) and (3). Based on equation (4), the deviation between alternative A_i and other alternatives with respect to criterion C_j can be computed as

$$d_{ij}(w) = \sum_{l=1}^{m} d\left(y_{ij}, y_{lj}\right). \tag{10}$$

Then, the deviation between all the alternatives and other ones with respect to criterion C_j can be computed as

$$d_j(w) = \sum_{i=1}^{m}\sum_{l=1}^{m} d\left(y_{ij}, y_{lj}\right). \tag{11}$$

We establish a mathematical programming to obtain the criteria weights:

$$\begin{cases} \max d(w) = \sum_{j=1}^{n}\sum_{i=1}^{m}\sum_{l\neq i} w_j d\left(y_{ij}, y_{lj}\right), w_j \ge 0, j = 1, 2, \ldots, n, \quad \sum_{j=1}^{n} w_j^2 = 1. \end{cases} \tag{12}$$

By solving (12), we can use the Lagrange function:

$$L(w, \lambda) = \sum_{j=1}^{n}\sum_{i=1}^{m}\sum_{l\neq i} w_j d\left(y_{ij}, y_{lj}\right) + \frac{\lambda}{2}\left(\sum_{j=1}^{n} w_j^2 - 1\right), \tag{13}$$

where λ is the Lagrange parameter.

Then, we use the following equations to obtain the criteria weights $w = (w_1, w_2, \ldots, w_n)$:

$$\begin{cases} \dfrac{\partial L(w,\lambda)}{\partial w_j} = \sum_{i=1}^{m}\sum_{l\neq i} d\left(y_{ij}, y_{lj}\right) + \lambda w_j = 0, \\ j = 1, 2, \ldots, n, \dfrac{\partial L(w,\lambda)}{\partial \lambda} = \sum_{j=1}^{n} w_j^2 - 1 = 0. \end{cases} \tag{14}$$

Then, we can obtain the criteria weights $w = (w_1, w_2, \ldots, w_n)$ as follows:

$$w_j = \frac{\sum_{i=1}^{m}\sum_{l=1}^{m} d\left(y_{ij}, y_{lj}\right)}{\sum_{j=1}^{n}\sum_{i=1}^{m}\sum_{l=1}^{m} d\left(y_{ij}, y_{lj}\right)}. \tag{15}$$

4.3. Computing Perceived Utility Based on Regret Theory. Based on equation (7), we can transform the standard IVPLTS decision matrix $Y = (y_{ij})_{m\times n}$ into a score function matrix $Z = (z_{ij})_{m\times n}$.

Let $z^* = (z_1^*, z_2^*, \ldots, z_n^*)$ be the reference points under the criteria $C_1, C_2, \ldots, C_n$, where $z_j^* = \max_i\{z_{ij}\}$ $(j = 1, 2, \ldots, n)$. In this paper, based on references [19, 21, 22], we choose utility function $v(x) = x^\alpha$, where α is the risk aversion coefficient of the DMs satisfying $0 < \alpha < 1$. The smaller α, the greater risk aversion of DMs. And regret/rejoice function $R(\Delta v) = 1 - \exp(-\delta \Delta v)$, where δ is the regret aversion coefficient of the DMs satisfying $\delta > 0$. The larger δ, the larger regret aversion.

The graph for utility function $v(x) = x^\alpha$ with different α can be seen in Figure 1.

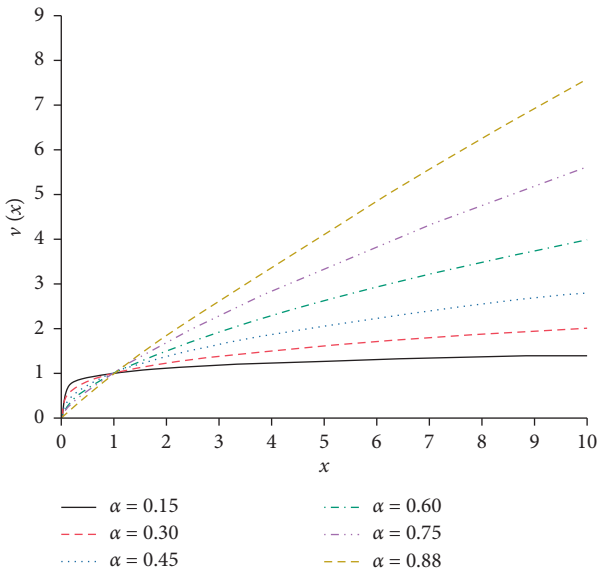

Figure 1: Graph for utility function with different α.

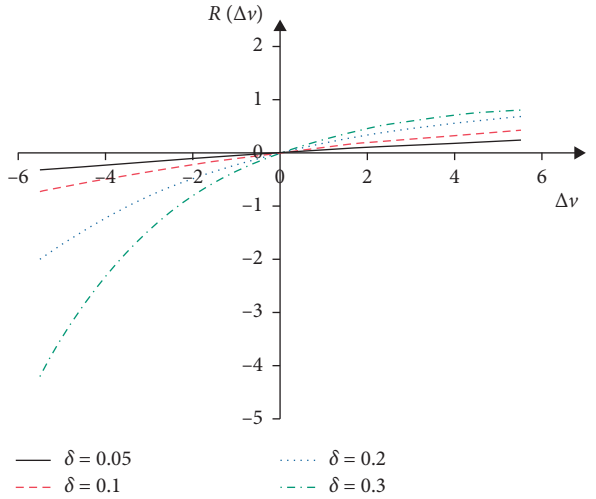

Figure 2: Graph for regret/rejoice function with different δ.

The graph for regret/rejoice function $R(\Delta v) = 1 - \exp(-\delta\Delta v)$ with different δ can be seen in Figure 2.

Then, we can compute the perceived utility for z_{ij} as

$$U(z_{ij}) = v(z_{ij}) + R(v(z_{ij}) - v(z_j^*)). \quad (16)$$

In this paper, equation (16) can be transform to

$$U(z_{ij}) = (z_{ij})^{\alpha} + 1 - \exp\left(-\delta \cdot \left|(z_{ij})^{\alpha} - (z_j^*)^{\alpha}\right|\right). \quad (17)$$

4.4. Aggregating Information Using Cobweb Area Model. Traditional method on aggregating information mainly focuses on the linear weighting model. In fact, in some cases, some extremely large or small values may make a very big impact on the final decision results [23]. To cope with this issue, we use the cobweb area model to aggregate information. The advantage of the cobweb area model lies in the fact that it uses the area of the values in different criteria and can reduce the influence of some extremely large or small values, which can partly solve the problem of malicious manipulation from some decision makers. The limitation of the cobweb area model is relatively massive calculation in the decision process.

The main idea of cobweb area model can be seen in Figure 3.

The main process of the cobweb area model is shown as follows:

(1) Determine the angles between the criteria $C_1, C_2, \ldots, C_n$ as $\xi_1 = \xi_2 = \cdots = \xi_n = 360^{\circ}/n$.

(2) Compute the endpoint $s_{ij} = w_j U(z_{ij})$ for alternative A_i under the criterion $C_j (j = 1, 2, \ldots, n)$.

(3) Compute the cobweb area for alternative A_i as

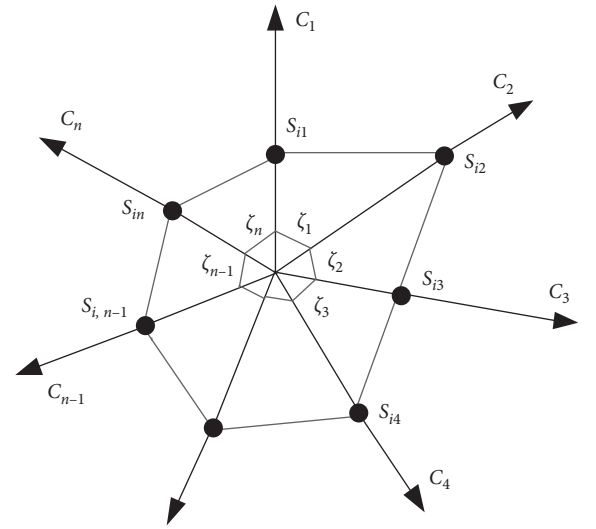

Figure 3: Main idea of the cobweb area model.

$$E_i = \frac{1}{2} \times s_{i1} \times s_{i2} \times \sin\frac{360^{\circ}}{n} + \frac{1}{2} \times s_{i2} \times s_{i3} \times \sin\frac{360^{\circ}}{n} + \cdots + \frac{1}{2} \times s_{in} \times s_{i1} \times \sin\frac{360^{\circ}}{n}. \quad (18)$$

(4) Rank the alternatives based on cobweb area. If $E_i > E_k$, then $A_i > A_k$.

Based on the above analysis, we can conclude the main decision steps as follows:

Step 1: based on decision matrix $X = (x_{ij})_{m\times n}$, normalize X to $Y = (y_{ij})_{m\times n}$ based on equations (2) and (3)

Step 2: according to equation (15), compute the criteria weights $W = (w_1, w_2, \ldots, w_n)$

Step 3: based on equation (7), we can transform the standard IVPLTS decision matrix $Y = (y_{ij})_{m\times n}$ into a score function matrix $Z = (z_{ij})_{m\times n}$

Step 4: compute the perceived utility $U(z_{ij})$ based on equation (17)

Step 5: compute the cobweb area E_i for alternative A_i $(i = 1, 2, \ldots, m)$ based on equation (18)

Step 6: rank the alternatives based on the value of cobweb area E_i $(i = 1, 2, \ldots, m)$

5. Case Study

With the development of medical level in China, the life expectancy of people has increased, and China has entered the aging society. By the end of 2017, there were more than 240,000,000 elders (60 years old or over) in China. Long-term care for elders became a serious social problem. An effective way to deal with this problem is the combination of medical treatment and endowment. A comprehensive Grade 3A hospital wants to cooperate with a nursing home based on the government policy. After preliminary screening, there are four nursing homes (alternatives) A_1, A_2, A_3, A_4 shortlisted. Some experts from hospitals, government, and nursing homes evaluate the four alternatives according to four factors (criteria) C_1 (service level), C_2 (business performance), C_3 (hardware facilities), and C_4 (management level). The experts use the LTS:

$$S = \{s_{-3}: \text{extremely poor}, s_{-2}: \text{very poor}, s_{-1}: \text{poor}, s_0: \text{medium}, s_1: \text{good}, s_2: \text{very good}, s_3: \text{extremely good}\}, \quad (19)$$

to express their opinions.

The experts give their opinions and propose a decision matrix X as Table 1.

For example, the linguistic assessment of A_1 is with respect to C_1 and the experts evaluate the probability of s_{-1} as 0.5–0.7 and the probability of s_0 as 0.2–0.4.

5.1. Decision Process

Step 1: based on equations (2) and (3), we can transform the decision matrix X to normalized matrix Y, as shown in Table 2.

Step 2: according to equation (15), we can obtain the criteria weights:

$$\begin{aligned} w_1 &= 0.289, \\ w_2 &= 0.254, \\ w_3 &= 0.182, \\ w_4 &= 0.275. \end{aligned} \quad (20)$$

Step 3: based on equation (7) and matrix Y, we can obtain the score function matrix Z, as shown in Table 3 $(\beta = 0.5, \theta = 1)$.

Step 4: based on equation (17), we can obtain the values of perceived utility $U(z_{ij})$, as shown in Table 4 $(\alpha = 0.88$ and $\delta = 0.3$, see [21]).

Step 5: based on equation (18), we can compute the cobweb area E_i for alternative A_i $(i = 1, 2, \ldots, 4)$ as follows:

$$\begin{aligned} E_1 = {} & \frac{1}{2} \times 0.289 \times 0.34 \times 0.99 \times 1 + \frac{1}{2} \times 0.254 \times 0.99 \times 1.21 \\ & \times 1 + \frac{1}{2} \times 0.182 \times 0.1.21 \times 0.93 \times 1 + \frac{1}{2} \times 0.275 \times 0.93 \\ & \times 0.34 \times 1 = 0.356. \end{aligned} \quad (21)$$

Similarly, we can obtain $E_2 = 1.044, E_3 = 0.882$, and $E_4 = 1.593$.

Step 6: the ranking result is $A_4 > A_2 > A_3 > A_1$.

Based on the selection of the above shortlisted nursing homes constructed in this paper, the ranking result is $A_4 > A_2 > A_3 > A_1$. In this case, the parameters can be selected by the decision maker according to their preferences. When the decision maker is optimistic about the decision problem, we can select $0.5 < \beta \leq 1$. When the decision maker is eclectic, we can select $\beta = 0.5$. When the decision maker is pessimistic, we can select $0 \leq \beta < 0.5$. The parameter θ reflects the preference of value judgment. If the decision maker is radical, we can select $\theta > 1$. Similarly, we can select $0 < \theta \leq 1$ if the decision maker is conservative. According to the values of the criteria weight, it can be seen that C_1 (service level) is the most important criterion. So, managers should focus on improving service levels.

5.2. Comparative Analysis. In this section, we will compare our method with the TOPSIS method for IVPLTS proposed by [10] and the VIKOR method proposed by [11].

5.2.1. Comparison with the TOPSIS Method. The main decision process of the method proposed by [10] can be concluded as the following decision steps:

(1) Determine the positive ideal solution PIS $Y^* = (y_1^*, y_2^*, \ldots, y_n^*)$ and negative ideal solution NIS $Y^- = (y_1^-, y_2^-, \ldots, y_n^-)$

(2) Compute the deviation degree between every alternative A_i and PIS $Y^* = (y_1^*, y_2^*, \ldots, y_n^*)$ as $d_i^+ = d(A_i, Y^*)$

(3) Compute the deviation degree between every alternative A_i and NIS $Y^- = (y_1^-, y_2^-, \ldots, y_n^-)$ as $d_i^- = d(A_i, Y^-)$

(4) Compute the closeness coefficient $\mathrm{CI}(A_i) = (d_i^-/\max_i\{d_i^-\}) - (d_i^+/\min_i\{d_i^+\})$

Table 1: Decision matrix X proposed by experts.

	C_1	C_2	C_3	C_4
A_1	$\{s_{-1}[0.5, 0.7], s_0[0.2, 0.4],\}$	$\{s_1[0.3, 0.6], s_2[0.2, 0.3],\}$	$\{s_1[0.5, 0.6], s_2[0.2, 0.5],\}$	$\{s_{-1}[0.4, 0.6], s_0[0.4, 0.7],\}$
A_2	$\{s_0[0.48, 0.7], s_1[0.55, 0.8],\}$	$\{s_1[0.5, 0.8], s_2[0.3, 0.5],\}$	$\{s_2[0.5, 0.7], s_3[0.3, 0.4],\}$	$\{s_1[0.35, 0.5], s_2[0.4, 0.55],\}$
A_3	$\{s_{-1}[0.45, 0.6], s_0[0.55, 0.7],\}$	$\{s_2[0.5, 0.6], s_3[0.4, 0.6],\}$	$\{s_2[0.6, 0.9], s_3[0.2, 0.4],\}$	$\{s_0[0.3, 0.6], s_1[0.6, 0.7],\}$
A_4	$\{s_1[0.3, 0.6], s_2[0.5, 0.8],\}$	$\{s_0[0.4, 0.55], s_1[0.55, 0.7],\}$	$\{s_2[0.3, 0.6], s_3[0.2, 0.5],\}$	$\{s_1[0.4, 0.5], s_2[0.5, 0.6].\}$

Table 2: Normalized decision matrix Y.

	C_1	C_2	C_3	C_4
A_1	$\{s_{-1}[0.52, 0.72], s_0[0.21, 0.41],\}$	$\{s_1[0.39, 0.79], s_2[0.26, 0.39],\}$	$\{s_1[0.53, 0.63], s_2[0.21, 0.53],\}$	$\{s_{-1}[0.37, 0.55], s_0[0.37, 0.65],\}$
A_2	$\{s_0[0.37, 0.54], s_1[0.43, 0.62],\}$	$\{s_1[0.45, 0.72], s_2[0.27, 0.45],\}$	$\{s_2[0.50, 0.70], s_3[0.30, 0.40],\}$	$\{s_1[0.38, 0.55], s_2[0.44, 0.60],\}$
A_3	$\{s_{-1}[0.39, 0.52], s_0[0.47, 0.60],\}$	$\{s_2[0.47, 0.56], s_3[0.38, 0.56],\}$	$\{s_2[0.51, 0.77], s_3[0.17, 0.34],\}$	$\{s_0[0.26, 0.53], s_1[0.53, 0.61],\}$
A_4	$\{s_1[0.26, 0.52], s_2[0.43, 0.69],\}$	$\{s_0[0.36, 0.49], s_1[0.49, 0.63],\}$	$\{s_2[0.35, 0.70], s_3[0.23, 0.58],\}$	$\{s_1[0.40, 0.50], s_2[0.50, 0.59].\}$

Table 3: Score function matrix Z.

	C_1	C_2	C_3	C_4
A_1	0.74	1.28	1.44	1.20
A_2	1.63	1.41	1.64	2.02
A_3	1.27	2.18	1.19	1.77
A_4	2.16	1.74	1.88	2.10

Table 4: Values of perceived utility.

	C_1	C_2	C_3	C_4
A_1	0.34	0.99	1.26	0.93
A_2	1.40	1.14	1.48	1.83
A_3	0.99	1.98	0.98	1.57
A_4	1.97	1.51	1.75	1.92

(5) Rank the alternatives according to CI (A_i)

We use the TOPSIS method proposed by [10] to solve our decision problem.

(1) We can obtain the PIS and NIS, as shown in Table 5.

(2) We can obtain the deviation degrees between every alternative A_i $(i = 1, 2, 3, 4)$ and PIS $Y^* = (y_1^*, y_2^*, \ldots, y_4^*)$ as

$$\begin{aligned} d_1^+ &= 0.821, \\ d_2^+ &= 0.349, \\ d_3^+ &= 0.479, \\ d_4^+ &= 0.240, \\ \min_{1\le i\le m} d_i^+ &= 0.240. \end{aligned} \tag{22}$$

(3) The deviation degree between every alternative A_i and NIS $Y^- = (y_1^-, y_2^-, \ldots, y_4^-)$ can be obtained as

$$\begin{aligned} d_1^- &= 0.069, \\ d_2^- &= 0.485, \\ d_3^- &= 0.318, \\ d_4^- &= 0.732, \\ \max_{1\le i\le m} d_i^- &= 0.732. \end{aligned} \tag{23}$$

(4) We can compute the closeness coefficient as

$$\begin{aligned} \mathrm{CI}(x_1) &= -2.421, \\ \mathrm{CI}(x_2) &= -0.455, \\ \mathrm{CI}(x_3) &= -0.992, \\ \mathrm{CI}(x_4) &= 0. \end{aligned} \tag{24}$$

Table 5: PIS and NIS for decision matrix Y.

	C_1	C_2	C_3	C_4
PIS	$\{s_1[0.26, 0.52],\ s_2[0.43, 0.69],\}$	$\{s_2[0.47, 0.56],\ s_3[0.38, 0.56],\}$	$\{s_2[0.35, 0.70],\ s_3[0.23, 0.58],\}$	$\{s_1[0.40, 0.50],\ s_2[0.50, 0.59],\}$
NIS	$\{s_{-1}[0.52, 0.72],\ s_0[0.21, 0.41],\}$	$\{s_1[0.39, 0.79],\ s_2[0.26, 0.39],\}$	$\{s_2[0.51, 0.77],\ s_3[0.17, 0.34],\}$	$\{s_{-1}[0.37, 0.55],\ s_0[0.37, 0.65].\}$

(5) The ranking result is $A_4 > A_2 > A_3 > A_1$.

5.2.2. Comparison with the VIKOR Method. To further verify our method, IVPLTS-based VIKOR proposed by [11] is taken for comparison with our method. The main decision process of the method can be concluded as the following decision steps:

(1) Determine the positive ideal solution (PIS) and negative ideal solution (NIS):

$$\begin{aligned}\tilde{L}^{*}(p) &= \max_{j\in\text{benefit}}\left(\frac{\left(r_{ij}^{k}\gamma_k^{L}+r_{ij}^{k}\gamma_k^{U}\right)}{2}\right),\\ &\text{or } \min_{j\in\text{cost}}\left(\frac{\left(r_{ij}^{k}\gamma_k^{L}+r_{ij}^{k}\gamma_k^{U}\right)}{2}\right),\\ \tilde{L}^{-}(p) &= \min_{j\in\text{benefit}}\left(\frac{\left(r_{ij}^{k}\gamma_k^{L}+r_{ij}^{k}\gamma_k^{U}\right)}{2}\right),\\ &\text{or } \max_{j\in\text{cost}}\left(\frac{\left(r_{ij}^{k}\gamma_k^{L}+r_{ij}^{k}\gamma_k^{U}\right)}{2}\right).\end{aligned} \tag{25}$$

(2) Compute the group utility (S) and individual regret (R) of every alternative by using the following equations:

$$S^{l}=\left(\sum_{j\in\text{benefit}} w_j\left(\frac{d\left(\tilde{L}\left(\gamma_k^{U}\right),\tilde{L}^{*}(p)\right)}{d\left(\tilde{L}^{*}(p),\tilde{L}^{-}(p)\right)}\right)+\sum_{j\in\text{cost}} w_j\left(\frac{d\left(\tilde{L}\left(\gamma_k^{L}\right),\tilde{L}^{*}(p)\right)}{d\left(\tilde{L}^{*}(p),\tilde{L}^{-}(p)\right)}\right)\right), \tag{26}$$

$$S^{u}=\left(\sum_{j\in\text{benefit}} w_j\left(\frac{d\left(\tilde{L}\left(\gamma_k^{L}\right),\tilde{L}^{*}(p)\right)}{d\left(\tilde{L}^{*}(p),\tilde{L}^{-}(p)\right)}\right)+\sum_{j\in\text{cost}} w_j\left(\frac{d\left(\tilde{L}\left(\gamma_k^{U}\right),\tilde{L}^{*}(p)\right)}{d\left(\tilde{L}^{*}(p),\tilde{L}^{-}(p)\right)}\right)\right), \tag{27}$$

$$R^{l}=\max\left(w_j\left(\frac{d\left(\tilde{L}\left(\gamma_k^{U}\right),\tilde{L}^{*}(p)\right)}{d\left(\tilde{L}^{*}(p),\tilde{L}^{-}(p)\right)}\right),w_j\left(\frac{d\left(\tilde{L}\left(\gamma_k^{L}\right),\tilde{L}^{*}(p)\right)}{d\left(\tilde{L}^{*}(p),\tilde{L}^{-}(p)\right)}\right)\right), \tag{28}$$

$$R^{u}=\max\left(w_j\left(\frac{d\left(\tilde{L}\left(\gamma_k^{L}\right),\tilde{L}^{*}(p)\right)}{d\left(\tilde{L}^{*}(p),\tilde{L}^{-}(p)\right)}\right),w_j\left(\frac{d\left(\tilde{L}\left(\gamma_k^{U}\right),\tilde{L}^{*}(p)\right)}{d\left(\tilde{L}^{*}(p),\tilde{L}^{-}(p)\right)}\right)\right). \tag{29}$$

(3) Compute the merit function (Q) for alternatives, respectively, by using the following equations:

$$Q^{l}=v\left(\frac{S^{l}-S^{*}}{S^{-}-S^{*}}\right)+(1-v)\left(\frac{R^{l}-R^{*}}{R^{-}-R^{*}}\right), \tag{30}$$

$$Q^{u}=v\left(\frac{S^{u}-S^{*}}{S^{-}-S^{*}}\right)+(1-v)\left(\frac{R^{u}-R^{*}}{R^{-}-R^{*}}\right), \tag{31}$$

where $[Q^l, Q^u]$ is the interval range of merit function, $v \in [0, 1]$ represents the strategy of the decision makers and $v \in [0, 1]$, $S^* = \min(S^l)$, $R^* = \min(R^l)$, $S^- = \max(S^u)$, and $R^- = \max(R^u)$.

(4) Determine the final merit function (Q) by calculating the mean of Q^l and Q^u. If $Q_i > Q_k$, then $A_i < A_k$.

We use the VIKOR method proposed by [11] to solve our decision problem and draw the ranking results in Table 6.

It is obvious that the decision results between our method and the one proposed by [10] are coincident. And it is different between our method and the one proposed by [11] in most cases. When $v = 0.9$ and $v = 1$, the results of the two methods are the same. Compared with the methods proposed by [10, 11], our method has the following traits:

(1) We use the regret theory to solve the decision problem, which will reflect the DMs' bounded rationality and make the decision result reasonable.

(2) We utilize the cobweb area model to aggregate decision information rather than traditional linear weighting method, which will overcome the problem

Table 6: Ranking results for the IVPLTS-VIKOR method.

v	Merit function (Q)				
	A_1	A_2	A_3	A_4	Ranking order
0.1	0.9055	0.1779	0.7991	0.5858	$A_2 > A_4 > A_3 > A_1$
0.2	0.8699	0.1668	0.7292	0.5235	$A_2 > A_4 > A_3 > A_1$
0.3	0.8342	0.1557	0.6593	0.4612	$A_2 > A_4 > A_3 > A_1$
0.4	0.7986	0.1447	0.5894	0.3990	$A_2 > A_4 > A_3 > A_1$
0.5	0.7630	0.1336	0.5195	0.3367	$A_2 > A_4 > A_3 > A_1$
0.6	0.7274	0.1226	0.4496	0.2744	$A_2 > A_4 > A_3 > A_1$
0.7	0.6918	0.1115	0.3797	0.2122	$A_2 > A_4 > A_3 > A_1$
0.8	0.6561	0.1005	0.3098	0.1499	$A_2 > A_4 > A_3 > A_1$
0.9	0.6205	0.0894	0.2399	0.0876	$A_4 > A_2 > A_3 > A_1$
1	0.5849	0.0784	0.1700	0.0254	$A_4 > A_2 > A_3 > A_1$

that some extremely large or small values may intensely influence the final decision results.

6. Conclusions

In this paper, we put forward a new decision method for IVPLTS based on regret theory. First, we propose a new score function for IVPLTS to transform the IVPLTSs into crisp numbers. We verify three mathematical properties of the score function, and we can see that the score function has great flexibility by adjusting the two parameters. Then, we use the regret theory to obtain the DMs' perceived utilities. Furthermore, we propose a cobweb area model to aggregate decision information to alleviate the problem that some extremely large or small values may exert an influence in final decision result. Finally, we apply our method to a real case of evaluating nursing homes and compare our method with the traditional TOPSIS method and VIKOR method. The comparative analysis illustrates the effectiveness and traits of our method.

Future research mainly focuses on multiple stages decision-making method for IVPLTSs.

Data Availability

All the data used to support the study are available from the corresponding author upon request.

Conflicts of Interest

The authors have no conflicts of interest.

Acknowledgments

This research was funded by Humanities and Social Science Fund of Ministry of Education of China, Grant no. 19YJA630039.

References

[1] L. A. Zadeh, "The concept of a linguistic variable and its application to approximate reasoning-I," *Information Sciences*, vol. 8, no. 3, pp. 199–249, 1975.

[2] R. M. Rodriguez, L. Martinez, and F. Herrera, "Hesitant fuzzy linguistic term sets for decision making," *IEEE Transactions on Fuzzy Systems*, vol. 20, no. 1, pp. 109–119, 2012.

[3] Q. Pang, H. Wang, and Z. Xu, "Probabilistic linguistic term sets in multi-attribute group decision making," *Information Sciences*, vol. 369, pp. 128–143, 2016.

[4] P. Li and C. P. Wei, "An emergency decision-making method based on D-S evidence theory for probabilistic linguistic term sets," *International Journal of Disaster Risk Reduction*, vol. 37, 2019.

[5] X. Yu, H. Chen, and Z. Ji, "Combination of probabilistic linguistic term sets and promethee to evaluate meteorological disaster risk: case study of Southeastern China," *Sustainability*, vol. 11, no. 5, p. 1405, 2019.

[6] Y. Zhang, Z. Xu, H. Wang, and H. Liao, "Consistency-based risk assessment with probabilistic linguistic preference relation," *Applied Soft Computing*, vol. 49, pp. 817–833, 2016.

[7] C. Bai, R. Zhang, S. Shen, C. Huang, and X. Fan, "Interval-valued probabilistic linguistic term sets in multi-criteria group decision making," *International Journal of Intelligent Systems*, vol. 33, no. 6, pp. 1301–1321, 2018.

[8] W. Yu, H. Zhang, and B. Li, "Comparison and operators based on uncertain probabilistic linguistic term set," *Journal of Intelligent & Fuzzy Systems*, vol. 36, no. 6, pp. 6359–6379, 2019.

[9] S. Zhang, Z. Xu, and H. Wu, "Fusions and preference relations based on probabilistic interval-valued hesitant fuzzy information in group decision making," *Soft Computing*, vol. 23, no. 17, pp. 8291–8306, 2019.

[10] C. Jin, H. Wang, and Z. Xu, "Uncertain probabilistic linguistic term sets in group decision making," *International Journal of Fuzzy Systems*, vol. 21, no. 4, pp. 1241–1258, 2019.

[11] R. Krishankumar, A. R. Mishra, K. S. Ravichandran et al., "A group decision framework for renewable energy source selection under interval-valued probabilistic linguistic term set," *Energies*, vol. 13, no. 4, 2020.

[12] P. Liu and Y. Li, "An extended MULTIMOORA method for probabilistic linguistic multi-criteria group decision-making based on prospect theory," *Computers & Industrial Engineering*, vol. 136, pp. 528–545, 2019.

[13] J. Gu, Y. Zheng, X. L. Tian, and Z. S. Xu, "A decision-making framework based on prospect theory with probabilistic linguistic term sets," *Journal of the Operational Research Society*, vol. 4, pp. 1–10, 2020.

[14] L. Wang, Y. P. Hu, H. C. Liu, and H. Shi, "A linguistic risk prioritization approach for failure mode and effects analysis: a case study of medical product development," *Quality and Reliability Engineering International*, vol. 35, no. 6, pp. 1735–1752, 2019.

[15] J. Qin, "Regret-based capital asset pricing model," *Journal of Banking & Finance*, vol. 114, 2020.

[16] C. Bai and J. Sarkis, "A supply chain transparency and sustainability technology appraisal model for blockchain technology," *International Journal of Production Research*, vol. 58, no. 7, pp. 2142–2162, 2020.

[17] S. Zhang, J. Zhu, X. Liu, and Y. Chen, "Regret theory-based group decision-making with multidimensional preference and incomplete weight information," *Information Fusion*, vol. 31, pp. 1–13, 2016.

[18] Z. Xu, "Deviation measures of linguistic preference relations in group decision making," *Omega*, vol. 33, no. 3, pp. 249–254, 2005.

[19] D. E. Bell, "Regret in decision making under uncertainty," *Operations Research*, vol. 30, no. 5, pp. 961–981, 1982.

[20] G. Loomes and R. Sugden, "Regret theory: an alternative theory of rational choice under uncertainty," *The Economic Journal*, vol. 92, no. 368, pp. 805–824, 1982.

[21] A. Tversky and D. Kahneman, "Advances in prospect theory: cumulative representation of uncertainty," *Journal of Risk and Uncertainty*, vol. 5, no. 4, pp. 297–323, 1992.
[22] C. G. Chorus, "Regret theory-based route choices and traffic equilibria," *Transportmetrica*, vol. 8, no. 4, pp. 291–305, 2010.
[23] P. Li and C. P. Wei, "A novel grey target decision method based on a cobweb area model for standard interval grey numbers," *Journal of Grey System*, vol. 31, no. 3, pp. 29–44, 2019.

Hindawi
Mathematical Problems in Engineering
Volume 2020, Article ID 6672088, 11 pages
https://doi.org/10.1155/2020/6672088

Research Article

Optimal Ordering Policy for Supply Option Contract with Spot Market

Xinru Hou,[1] Xinsheng Xu,[2] and Haibin Chen [1]

[1]*School of Management Science, Qufu Normal University, Rizhao, Shandong, China*
[2]*College of Science, Binzhou University, Binzhou, Shandong, China*

Correspondence should be addressed to Haibin Chen; chenhaibin508@qfnu.edu.cn

Received 19 October 2020; Revised 19 November 2020; Accepted 23 November 2020; Published 9 December 2020

Academic Editor: Zeshui Xu

This paper considers the procurement mechanism with two supply channels, namely, an option contract purchase and a spot market. For the mechanism, under the stochastic demand and the stochastic spot price, we consider the portfolio procurement with the spot trading liquidity and the option speculation respectively. To maximize the buyer's profit, we establish two optimal portfolio procurement strategy models for those two scenarios. Based on the buyer's cost-benefit analysis, we present a solution method to each model and provide an optimal ordering policy to the buyer. By the obtained results, we analyze the role of the spot trading liquidity and option speculation in a buyer's expected profit. Some numerical experiments are presented to show the validity of the formulated models.

1. Introduction

As an important supplement to the e-commerce, the spot market with the stochastic spot price plays an important role in commodity trading. For instance, in China, there are more than 200 spot markets providing spot trading of bulk commodities, and up to 60% of iron ore is purchased from the spot market [1]. In the United States, about 30% of memory chip and 60% of meat packing are purchased from the spot market [2], see e.g., [3] for a comprehensive review on spot market.

Although the spot market provides a flexible channel for trading of commodities, the stochastic of spot price and the liquidity of spot trading make the spot market unreliable. Compared with the spot market, supply contract, i.e., long-time contract or option contract, can guarantee the stability of the supply to buyer. Nevertheless, the supply contract has the risk caused by demand uncertainty. As a consequence, the portfolio procurement strategy which combines the supply contract and spot market is generated to cope with the stochastic demand and the stochastic spot price. It is reported that the Hewlett-Packard (HP) engaged the portfolio procurement with the option contract and spot market to meet the demand, and its portfolio procurement had saved HP over $425 million from 2000 to 2006 [4].

As for the research of the portfolio procurement with spot market, there are mainly two streams, one is on the long-time contract with spot market and the other is on the option contract with spot market. For the first stream, Peleg and Lee [5] compared three procurement strategies based on the buyer's expected cost minimization: a long-term strategy; a short-term strategy based on spot market; and a portfolio procurement strategy of the both. Chen and Liu [6] compared two procurement strategies: single long-term contract and the portfolio procurement with the long-term and the spot market and showed that the portfolio procurement can generate a higher buyer's profit than the single long-term contract. Goel and Gutierrez [7] considered the portfolio procurement and distribution policies for a firm and indicated that the portfolio procurement leads to significant reductions in inventory-related costs. Lee et al. [8] considered the portfolio procurement with the significant demand and spot price volatility and showed that the profit is higher for the spot market than for the long-time contract. Chen et al. [9] considered the portfolio procurement with a stochastic inventory, wherein prices follow a Markov

process. Adilov [10] considered the portfolio procurement from the perspective of the supplier. Inderfurth et al. [11] considered the multiperiod portfolio procurement with the short-term procurement of the spot market and the capacity reservation of the long-time contract, and so on [12–17].

For the second stream, Fu et al. [18] showed that the portfolio procurement strategy is superior to the single option contract or the spot market procurement strategy. Pei et al. [19] considered the portfolio procurement with volume discounts and volume premia and provided links between production and spot market characteristics, contract design, and efficiency. Zhao et al. [20] considered a two-stage portfolio procurement with the demand information updating. Merzifonluoglu [21, 22] studied the portfolio procurement with a special case that the demand obeys normal distribution. Luo and Chen [23] considered a single-period supplier-manufacturer portfolio procurement where the supplier is with a stochastic yield. Lee et al. [24] considered a multisupplier portfolio procurement with capacity constraints. Wan and Chen [25] considered the multiperiod and dual-sourcing replenishment portfolio procurement, and so on [26–31].

The above research assumes that the spot market is only used as a one-way trading channel for the buyer to buy purchase. Nevertheless, in practice, the buyer's exceeded products can be sold in the spot market to make speculation revenue. In addition, the spot market is imperfect because of the spot trading liquidity. In this paper, under the stochastic demand and the stochastic spot price, we, respectively, consider the spot market with the spot trading liquidity and with the option speculation. For this setting, to maximize the buyer's profit, we construct two optimal portfolio procurement strategy models. By analyzing the buyer's cost-benefit, we obtain a solution method for each model and provide an optimal ordering policy to the buyer. The role of the spot trading liquidity and option speculation in buyer's expected profit is analyzed, and the cost threshold and option pricing formula are obtained, which provide a decision basis for the buyer.

The remainder of this paper is organized as follows. In Sections 2 and 3, we, respectively, consider the portfolio procurement strategy model with the spot trading liquidity, and the portfolio procurement strategy model with the option speculation. Numerical experiments are presented in Section 4 to illustrate the validity of our research. Some conclusions are drawn in the last section.

2. The Portfolio Procurement with the Spot Trading Liquidity

In this section, under the stochastic demand and the stochastic spot price, we consider the portfolio procurement with the spot trading liquidity, that is, the buyer orders by the option contract and the spot market with the spot trading liquidity. For the concerned procurement system, we present the running pattern of it: before the selling season arrives, the buyer signs an option ordering quantity q units with the supplier by prepaying an option purchase price b for each unit based on the estimated stochastic demand during the selling season, and when the selling season comes, we assume that the realized demand and spot price can be determined. Then, the buyer can purchase any units up to the option level q by paying an option execution price e for each unit. In this sense, if the spot price in the spot market is higher than the option execution price, then the buyer will execute the options, and if the realized demand exceeds the option level q, the buyer will purchase the products from the spot market and vice versa. It is supposed that the spot capacity is Q_s. Besides, there is a spot trading liquidity $\gamma \in [0, 1]$, which defines the percentage of the products that can be traded for all the products in the spot market, i.e., the buyer can purchase the products no more than γQ_s from the spot market. If the realized market demand exceeds the sum of the option level and spot capacity, there will be a shortage penalty s for each lost sale. For this system, to maximize the buyer's profit, the buyer should make an optimal portfolio procurement strategy. To this end, we need some notations which are listed in Table 1.

The assumptions on the concerned model are as follows.

Assumption 1

(a) The sum of the option purchase price and option execution price is lower than the sum of the retail price and shortage price, i.e., $b + e \le r + s$

(b) The spot price is lower than the sum of the retail price and shortage price, i.e., $p \le r + s$

(c) The demand of the items during the selling season obeys the distribution with probability density function $f_1(x)$ and distribution function $F_1(x)$

(d) The spot price of the items during the selling season obeys the distribution with probability density function $f_2(y)$ and distribution function $F_2(y)$, and its expected value is $\overline{p}$

For convenience, we use $\Pi_1^o(q, D)$ to denote the profit from the option contract, and $\Pi_1^s(q, D, p)$ to denote the profit from the spot market and the shortage penalty for lost sales. According to the assumptions and the principle of the buyer's profit maximization, we can formulate the optimal portfolio procurement strategy model as the following optimization problem:

$$\max_q \Pi_1 = \Pi_1^o(q, D) + \Pi_1^s(q, D, p). \tag{1}$$

For the concerned model, if the buyer does not execute the options during the selling season, he/she will lose the option purchase price per unit, and when the selling season comes, the stochastic demand and the stochastic spot price can be determined. So, one of the following three cases will happen:

Case 1. $0 \le D < q + \gamma Q_s$ and $p > e$. In this case, the buyer will first execute the options of $\min(q, D)$ units by paying an option execution price e for each unit, and then the exceeded demand $(D - q)_+$ will be purchased at the spot price p for each unit from the spot market. Under this case, we have

Table 1: Notations.

Notation	Description
r	Retail price
b	Option purchase price
e	Option execution price
s	Shortage cost
Q_s	The maximum capacity of the spot market
γ	The spot trading liquidity
D	The stochastic demand
p	The stochastic spot price
q	Option ordering quantity
$E[\Pi_1(\cdot)]$	Expected profit with the spot trading liquidity
$E[\Pi_2(\cdot)]$	Expected profit with the option speculation

$\Pi_1^o(q,D) = -bq + (r-e)\min(q,D)$, and $\Pi_1^s(q,D,p) = (r-p)(D-q)_+$.

Case 2. $0 \le D < q + \gamma Q_s$ and $p \le e$. In this case, the buyer will first purchase $\min(\gamma Q_s, D)$ units from the spot market, and then the exceeded demand $(D - \gamma Q_s)_+$ will be satisfied through options. Under this case, we have $\Pi_1^o(q,D) = -bq + (r-e)(D-\gamma Q_s)_+$, and $\Pi_1^s(q,D,p) = (r-p)\min(\gamma Q_s, D)$.

Case 3. $D \ge q + \gamma Q_s$. In this case, regardless of $p > e$ or $p \le e$, the buyer will execute the options of q units and purchase γQ_s units from the spot market and pay the shortage penalty s for each lost sale. Under this case, we have $\Pi_1^o(q,D) = (r-e-b)q$, and $\Pi_1^s(q,D,p) = (r-p)\gamma Q_s - s(D-q-\gamma Q_s)$.

From the analysis above, we can see that the buyer's profit for option ordering quantity q is

$$\Pi_1(q) = -bq + \begin{cases} (r-e)\min(q,D) + (r-p)(D-q)_+, & 0 \le D < q+\gamma Q_s,\ p > e, \\ (r-e)(D-\gamma Q_s)_+ + (r-p)\min(\gamma Q_s, D), & 0 \le D < q+\gamma Q_s,\ p \le e, \\ (r-e)q + (r-p)\gamma Q_s - s(D-q-\gamma Q_s), & D \ge q+\gamma Q_s. \end{cases} \tag{2}$$

Considering the stochastic of the demand and the spot price, to solve problem (1), we compute the expectation of the buyer's profit. From this, the buyer's expected profit for ordering quantity q in the option contract is

$$\begin{aligned} E[\Pi_1(q)] = {} & -bq \\ & + \int_e^{r+s} (r-e) f_2(y)\mathrm{d}y \int_0^q x f_1(x)\mathrm{d}x + \int_e^{r+s} (r-e) f_2(y)\mathrm{d}y \int_q^{q+\gamma Q_s} q f_1(x)\mathrm{d}x \\ & + \int_e^{r+s} (r-y) f_2(y)\mathrm{d}y \int_q^{q+\gamma Q_s} (x-q) f_1(x)\mathrm{d}x \\ & + \int_0^e (r-y) f_2(y)\mathrm{d}y \int_0^{\gamma Q_s} x f_1(x)\mathrm{d}x + \int_0^e (r-y) f_2(y)\mathrm{d}y \int_{\gamma Q_s}^{q+\gamma Q_s} \gamma Q_s f_1(x)\mathrm{d}x \\ & + \int_0^e (r-e) f_2(y)\mathrm{d}y \int_{\gamma Q_s}^{q+\gamma Q_s} (x-\gamma Q_s) f_1(x)\mathrm{d}x \\ & + (r-e)\int_{q+\gamma Q_s}^{\infty} q f_1(x)\mathrm{d}x + (r-\overline{p})\int_{q+\gamma Q_s}^{\infty} \gamma Q_s f_1(x)\mathrm{d}x - s\int_{q+\gamma Q_s}^{\infty} (x-q-\gamma Q_s) f_1(x)\mathrm{d}x. \end{aligned} \tag{3}$$

The first term in the right-hand side is the cost of purchasing the options of q units before the selling season, the second to the fourth items represent the retail revenue of the buyer for the case that $0 \le D < q + \gamma Q_s$ and $p > e$, the fifth to the seventh items represent the retail revenue of the buyer for the case that $0 \le D < q + \gamma Q_s$ and $p \le e$, and the last three items represent the retail revenue and shortage cost of the buyer for the case that $D \ge q + \gamma Q_s$.

By maximizing the buyer's profit, we can obtain the optimal ordering policy.

Theorem 1. *The optimal option ordering quantity q_1^* to maximize the buyer's expected profit $E[\Pi_1(q)]$ satisfies*

$$r - e - b + s - [F_1(q_1^* + \gamma Q_s) - F_1(q_1^*)] \int_e^{r+s} F_2(y)\mathrm{d}y - F_1(q_1^*)(r + s - e) = 0. \tag{4}$$

Proof. For (3), it can be readily computed that

$$\begin{aligned} \frac{\partial E[\Pi_1(q)]}{\partial q} &= r - e - b + s - [F_1(q + \gamma Q_s) - F_1(q)] \int_e^{r+s} F_2(y)\mathrm{d}y - F_1(q)(r + s - e), \\ \frac{\partial^2 E[\Pi_1(q)]}{\partial q^2} &= -[f_1(q + \gamma Q_s) - f_1(q)] \int_e^{r+s} F_2(y)\mathrm{d}y - f_1(q)(r + s - e) \le 0, \end{aligned} \tag{5}$$

which implies $E[\Pi_1(q)]$ is concave in q. From the first-order optimality condition, we conclude that $E[\Pi_1(q)]$ achieves its maximum when q_1^* satisfies

$$r - e - b + s - [F_1(q_1^* + \gamma Q_s) - F_1(q_1^*)] \int_e^{r+s} F_2(y)\mathrm{d}y - F_1(q_1^*)(r + s - e) = 0. \tag{6}$$

□

For the optimal option ordering quantity given in the above conclusion, we have the following properties.

Corollary 1. *The buyer's optimal option ordering quantity q_1^* is increasing w.r.t. the retail price r and the shortage cost s.*

Proof. From (4), we can obtain that

$$\begin{aligned} \frac{\partial q_1^*}{\partial r} &= \frac{1 - F_1(q_1^* + \gamma Q_s)}{[f_1(q_1^* + \gamma Q_s) - f_1(q_1^*)] \int_e^{r+s} F_2(y)dy + f_1(q_1^*)(r + s - e)} \ge 0, \\ \frac{\partial q_1^*}{\partial s} &= \frac{1 - F_1(q_1^* + \gamma Q_s)}{[f_1(q_1^* + \gamma Q_s) - f_1(q_1^*)] \int_e^{r+s} F_2(y)dy + f_1(q_1^*)(r + s - e)} \ge 0, \end{aligned} \tag{7}$$

which implies q_1^* is increasing w.r.t. the retail price and shortage cost. □

From the conclusion, when retail price r increases, the buyer will have a larger retail revenue and underpurchasing loss; when the shortage cost s increases, the buyer will have a larger underpurchasing loss. From this, to reduce the underpurchasing loss, the buyer will order more options. In addition, when the retail price r or shortage cost s increases, the option purchase price b is relatively low. At this time, the buyer will order more options, and when the selling season comes, the buyer will choose a favorable purchase channel according to the spot price and option execution price. This increases the advantages of the option contract. So, when the retail price r or shortage cost s increases, the buyer should order more options.

Corollary 2. *The buyer's optimal option ordering quantity q_1^* is decreasing w.r.t. the option purchase price b, the option execution price e, and the spot trading liquidity γ.*

Proof. From (4), we can obtain that

$$\begin{aligned} \frac{\partial q_1^*}{\partial b} &= \frac{-1}{[f_1(q_1^* + \gamma Q_s) - f_1(q_1^*)] \int_e^{r+s} F_2(y)\mathrm{d}y + f_1(q_1^*)(r + s - e)} \le 0, \\ \frac{\partial q_1^*}{\partial e} &= \frac{-1 + [F_1(q_1^* + \gamma Q_s) - F_1(q_1^*)]F_2(e) + F_1(q_1^*)}{[f_1(q_1^* + \gamma Q_s) - f_1(q_1^*)] \int_e^{r+s} F_2(y)\mathrm{d}y + f_1(q_1^*)(r + s - e)}, \\ &\le \frac{F_1(q_1^* + \gamma Q_s) - 1}{[f_1(q_1^* + \gamma Q_s) - f_1(q_1^*)] \int_e^{r+s} F_2(y)\mathrm{d}y + f_1(q_1^*)(r + s - e)} \le 0, \\ \frac{\partial q_1^*}{\partial \gamma} &= \frac{-Q_s f_1(q_1^* + \gamma Q_s) \int_e^{r+s} F_2(y)\mathrm{d}y}{[f_1(q_1^* + \gamma Q_s) - f_1(q_1^*)] \int_e^{r+s} F_2(y)\mathrm{d}y + f_1(q_1^*)(r + s - e)} \le 0, \end{aligned} \tag{8}$$

which implies the assertion holds. □

From the conclusion, we can see that when the option purchase price b or option execution price e increases, the buyer will have a larger overpurchasing loss and a lower retail revenue. From this, to reduce the overpurchasing loss, the buyer will order fewer options. When the spot trading liquidity γ increases, the buyer will purchase more products from the spot market and order fewer options to reduce the over-ordering cost.

To gain more insights, we study the effect of the spot trading liquidity γ on the buyer's maximum expected profit $E[\Pi_1(q_1^*)]$.

Corollary 3. *The buyer's maximum expected profit $E[\Pi_1(q_1^*)]$ is increasing w.r.t. the spot trading liquidity γ.*

Proof. From (3) and (4), we can obtain that

$$\frac{\partial E[\Pi_1(q_1^*)]}{\partial \gamma} = Q_s[F_1(q_1^* + \gamma Q_s) - F_1(\gamma Q_s)]\int_0^e (e-y)f_2(y)dy + (r-\overline{p}+s)Q_s[1-F_1(q_1^*+\gamma Q_s)] \geq 0, \tag{9}$$

which implies the assertion holds.

From the conclusion, we can see that if there is a larger spot trading liquidity, the buyer can purchase more products from the spot market. In addition, the buyer's optimal option ordering quantity q_1^* is decreasing w.r.t. the spot trading liquidity γ. That is to say, the increase of γ helps the buyer increase the retail revenue and reduce the over-ordering loss. So, the buyer's maximum expected profit $E[\Pi_1(q_1^*)]$ is increasing w.r.t. the spot trading liquidity.

3. The Portfolio Procurement with the Option Speculation

For the portfolio procurement with the option speculation, when the demand is satisfied, the buyer's exceeded options can be sold in the spot market to make speculation revenue. Therefore, in this section, we incorporate the option speculation into the portfolio procurement in Section 2 under the stochastic demand and the stochastic spot price. We suppose that the option ordering quantity with option speculation is q_2. For convenience, we use $\Pi_2^o(q_2, D)$ to denote the profit from the option contract, and $\Pi_2^s(q_2, D, p)$ to denote the profit from the spot market and the shortage penalty for lost sales. Under the option speculation, according to the principle of the buyer's profit maximization, we can formulate the optimal portfolio procurement strategy model as the following optimization problem:

$$\max_{q_2} \Pi_2 = \Pi_2^o(q_2, D) + \Pi_2^s(q_2, D, p). \tag{10}$$

For the concerned model, when the selling season comes, the stochastic demand and the stochastic spot price can be determined. So, one of the following three cases will happen:

Case 1. $0 \leq D < q_2 + \gamma Q_s$, and $p > e$. In this case, the buyer will first execute the options of q_2 units. If the demand cannot be met, namely, $q_2 \leq D < q_2 + \gamma Q_s$, the exceeded demand $D - q_2$ will be satisfied through the spot market, and if the demand is met, namely, $0 \leq D < q_2$, the exceeded options of $q_2 - D$ units will be sold in the spot market at the spot price p for each unit. That is to say, only when $0 \leq D < q_2$ and $p > e$, the option speculation will occur and make speculation revenue. Under this case, we have $\Pi_2^o(q_2, D) = -bq_2 + (r-e)\min(q_2, D) + (p-e)(q_2 - D)_+$ and $\Pi_2^s(q_2, D, p) = (r-p)(D-q_2)_+$. The other two cases are the same as those in Section 2, which are omitted.

From the analysis above, we can see that the buyer's profit for option ordering quantity q_2 is

$$\Pi_2(q_2) = -bq_2 + \begin{cases} (r-e)\min(q_2, D) + (p-e)(q_2-D)_+ + (r-p)(D-q_2)_+, & D < q_2 + \gamma Q_s, p > e, \\ (r-e)(D-\gamma Q_s,)_+ + (r-p)\min(\gamma Q_s, D), & D < q_2 + \gamma Q_s, p \leq e, \\ (r-e)q_2 + (r-p)\gamma Q_s - s(D - q_2 - \gamma Q_s), & D \geq q_2 + \gamma Q_s. \end{cases} \tag{11}$$

Since the demand and the spot price are stochastic, to solve problem (10), we compute the expectation of the buy's profit. From this, the buyer's expected profit for ordering quantity q_2 in the option contract is given as

$$
\begin{aligned}
E[\Pi_2(q_2)] = {} & -bq_2 \\
& + \int_e^{r+s} (r-e) f_2(y)\mathrm{d}y \int_0^{q_2} x f_1(x)\mathrm{d}x + \int_e^{r+s} (r-e) f_2(y)\mathrm{d}y \int_{q_2}^{q_2+\gamma Q_s} q_2 f_1(x)\mathrm{d}x \\
& + \int_e^{r+s} (r-y) f_2(y)\mathrm{d}y \int_{q_2}^{q_2+\gamma Q_s} (x-q_2) f_1(x)\mathrm{d}x \\
& + \int_e^{r+s} (y-e) f_2(y)\mathrm{d}y \int_0^{q_2} (q_2-x) f_1(x)\mathrm{d}x \\
& + \int_0^{e} (r-y) f_2(y)\mathrm{d}y \int_0^{\gamma Q_s} x f_1(x)\mathrm{d}x + \int_0^{e} (r-y) f_2(y)\mathrm{d}y \int_{\gamma Q_s}^{q_2+\gamma Q_s} \gamma Q_s f_1(x)\mathrm{d}x \\
& + \int_0^{e} (r-e) f_2(y)\mathrm{d}y \int_{\gamma Q_s}^{q_2+\gamma Q_s} (x-\gamma Q_s) f_1(x)\mathrm{d}x \\
& + (r-e) \int_{q_2+\gamma Q_s}^{\infty} q_2 f_1(x)\mathrm{d}x + (r-\overline{p}) \int_{q_2+\gamma Q_s}^{\infty} \gamma Q_s f_1(x)\mathrm{d}x - s \int_{q_2+\gamma Q_s}^{\infty} (x-q_2-\gamma Q_s) f_1(x)\mathrm{d}x.
\end{aligned}
\tag{12}
$$

The first term in the right-hand side is the cost of purchasing the options of q_2 units before the selling season, the second to the fourth items represent retail revenue of the buyer for the case that $0 \le D < q_2 + \gamma Q_s$ and $p > e$, the fifth item is the speculation revenue from the exceeded options, the sixth to the eighth items represent the retail revenue of the buyer for the case that $0 \le D < q_2 + \gamma Q_s$ and $p \le e$, and the last three items represent the retail revenue and shortage cost of the buyer for the case that $D \ge q_2 + \gamma Q_s$.

By maximizing the buyer's profit, we can obtain an optimal ordering policy to the buyer.

Theorem 2. *The optimal option ordering quantity q_2^* with the option speculation to maximize the buyer's expected profit $E[\Pi_2(q_2)]$ satisfies*

$$
r - e - b + s - F_1(q_2^* + \gamma Q_s) \int_e^{r+s} F_2(y)dy = 0. \tag{13}
$$

Proof. For (12), it can be readily computed that

$$
\begin{aligned}
\frac{\partial E[\Pi_2(q_2)]}{\partial q_2} &= r - e - b + s - F_1(q_2 + \gamma Q_s) \int_e^{r+s} F_2(y)\mathrm{d}y, \\
\frac{\partial^2 E[\Pi_2(q_2)]}{\partial q_2^2} &= -f_1(q_2 + \gamma Q_s) \int_e^{r+s} F_2(y)\mathrm{d}y \le 0,
\end{aligned}
\tag{14}
$$

which implies $E[\Pi_2(q_2)]$ is concave in q_2. From the first-order optimality condition, we conclude that $E[\Pi_2(q_2)]$ achieves its maximum when q_2^* satisfies

$$
r - e - b + s - F_1(q_2^* + \gamma Q_s) \int_e^{r+s} F_2(y)\mathrm{d}y = 0. \tag{15}
$$

□

Theorems 1 and 2 give the optimal option ordering quantity without and with the option speculation when the spot trading liquidity γ is considered, respectively. If we let $\gamma = 0$, the optimal option ordering quantity without the option speculation, i.e., the optimal option ordering quantity with the spot trading liquidity, reduces to the optimal option

ordering quantity in the traditional newsvendor problem. Similar to Corollaries 1 and 2, we have the same results on the optimal option ordering quantity q_2^* w.r.t. the retail price r, the shortage cost s, the option purchase price b, the option execution price e, and the spot trading liquidity γ, which are omitted herein. Similar to Corollary 3, we have the buyer's maximum expected profit $E[\Pi_2(q_2^*)]$ with option speculation is increasing w.r.t. the spot trading liquidity γ, which is omitted herein.

Theorem 3. *The optimal option ordering quantity with the option speculation is larger than that with the spot trading liquidity, i.e., $q_2^* \geq q_1^*$.*

Proof. From $\int_e^{r+s}(y-e)\mathrm{d}F_2(y) = r+s-e-\int_e^{r+s}F_2(y)\mathrm{d}y$ and (4), we can obtain that

$$F_1(q_1^*+\gamma Q_s)\int_e^{r+s}F_2(y)\mathrm{d}y + F_1(q_1^*)\int_e^{r+s}(y-e)\mathrm{d}F_2(y) = r-e-b+s. \tag{16}$$

From (13), we can obtain that

$$F_1(q_2^*+\gamma Q_s)\int_e^{r+s}F_2(y)dy = r-e-b+s, \tag{17}$$

and then

$$F_1(q_1^*+\gamma Q_s)\int_e^{r+s}F_2(y)\mathrm{d}y + F_1(q_1^*)\int_e^{r+s}(y-e)\mathrm{d}F_2(y) = F_1(q_2^*+\gamma Q_s)\int_e^{r+s}F_2(y)\mathrm{d}y. \tag{18}$$

Since $F_1(q_1^*)\int_e^{r+s}(y-e)\mathrm{d}F_2(y) \geq 0$, we have $F_1(q_2^*+\gamma Q_s) \geq F_1(q_1^*+\gamma Q_s)$. Besides, the distribution function of the demand $F_1(\cdot)$ is an increasing function, and then it is obvious that $q_2^* \geq q_1^*$.

Since the optimal option ordering quantity with the option speculation is larger than that with the spot trading liquidity, a question then is how the option speculation can influence the expected profit of the buyer. We have the following result to address this issue.

Theorem 4. *Define*

$$\begin{aligned} Z = &\int_e^{r+s}(y-e)\mathrm{d}F_2(y)\int_0^{q_1^*}F(x)\mathrm{d}x_1 \\ &-\int_e^{r+s}(r+s-y)\mathrm{d}F_2(y)\int_{q_1^*+\gamma Q_s}^{q_2^*+\gamma Q_s}F_1(x)\mathrm{d}x \\ &-\int_0^{e}(r+s-e)\mathrm{d}F_2(y)\int_{q_1^*+\gamma Q_s}^{q_2^*+\gamma Q_s}F(x)\mathrm{d}x_1 \end{aligned} \tag{19}$$

when $e+b<r+s+(Z/(q_2^*-q_1^*))$, and the buyer's maximum expected profit with the spot trading liquidity is lower than that with the option speculation, i.e., $E[\Pi_1(q_1^*)] < E[\Pi_2(q_2^*)]$.

When $e+b>r+s+(Z/(q_2^*-q_1^*))$, the buyer's maximum expected profit with the spot trading liquidity is larger than that with the option speculation, i.e., $E[\Pi_1(q_1^*)] > E[\Pi_2(q_2^*)]$.

Proof. For (3) and (12), it can be readily computed that

$$\begin{aligned} &E[\Pi_2(q_2^*)] - E[\Pi_1(q_1^*)] \\ &= (r-e-b+s)(q_2^*-q_1^*) + \int_e^{r+s}(y-e)\mathrm{d}F_2(y)\int_0^{q_1^*}F_1(x)\mathrm{d}x \\ &\quad -\int_e^{r+s}(r+s-y)\mathrm{d}F_2(y)\int_{q_1^*+\gamma Q_s}^{q_2^*+\gamma Q_s}F_1(x)\mathrm{d}x - \int_0^{e}(r+s-e)\mathrm{d}F_2(y)\int_{q_1^*+\gamma Q_s}^{q_2^*+\gamma Q_s}F_1(x)\mathrm{d}x. \end{aligned} \tag{20}$$

To simplify, define

$$Z = \int_e^{r+s} (y-e)\mathrm{d}F_2(y) \int_0^{q_1^*} F_1(x)\mathrm{d}x - \int_e^{r+s} (r+s-y)\mathrm{d}F_2(y) \int_{q_1^*+\gamma Q_s}^{q_2^*+\gamma Q_s} F_1(x)\mathrm{d}x - \int_0^{e} (r+s-e)\mathrm{d}F_2(y) \int_{q_1^*+\gamma Q_s}^{q_2^*+\gamma Q_s} F(x)\mathrm{d}x_1, \tag{21}$$

and then

$$E[\Pi_2(q_2^*)] - E[\Pi_1(q_1^*)] = (r-e-b+s)(q_2^*-q_1^*) + Z. \tag{22}$$

When $e+b<r+s+(Z/(q_2^*-q_1^*))$, it follows $E[\Pi_1(q_1^*)] < E[\Pi_2(q_2^*)]$.

When $e+b>r+s+(Z/(q_2^*-q_1^*))$, it follows $E[\Pi_1(q_1^*)] > E[\Pi_2(q_2^*)]$.

When $e+b=r+s+(Z/(q_2^*-q_1^*))$, it follows $E[\Pi_1(q_1^*)] = E[\Pi_2(q_2^*)]$.

From the conclusion, we can see that option speculation is unreliable, and the buyer cannot rely excessively on option speculation. When $e+b>r+s+(Z/(q_2^*-q_1^*))$, the sum of the option purchase price and option execution price is too high, and the buyer is unlikely to profit from the option speculation. Hence, the buyer should order options without considering the option speculation. To sum up, if $0<e+b<r+s+(Z/(q_2^*-q_1^*))$, the buyer should consider option speculation to maximize the expected profit. If $r+s+(Z/(q_2^*-q_1^*))<e+b\le r+s$, the buyer should not consider the option speculation, namely, only consider the spot trading liquidity to maximize the expected profit. If $e+b=r+s+(Z/(q_2^*-q_1^*))$, the buyer will have the same maximum expected profit no matter whether the option speculation is considered or not, i.e., $E[\Pi_1(q_1^*)] = E[\Pi_2(q_2^*)]$.

Corollary 4. *If the buyer and the supplier sign the option purchase price $b=\overline{p}-E[\min(e,p)]$, the buyer's maximum expected profit with the spot trading liquidity is lower than that with the option speculation, i.e., $E[\Pi_1(q_1^*)] \le E[\Pi_2(q_2^*)]$.*

Proof. For (3) and (12), it can be readily computed that

$$\begin{aligned} E[\Pi_2(q_2^*)] - E[\Pi_1(q_1^*)] &= (r-e-b+s)(q_2^*-q_1^*) + \int_e^{r+s} (y-e)\mathrm{d}F_2(y) \int_0^{q_1^*} F_1(x)\mathrm{d}x \\ &\quad - \int_e^{r+s} (r+s-y)\mathrm{d}F_2(y) \int_{q_1^*+\gamma Q_s}^{q_2^*+\gamma Q_s} F_1(x)\mathrm{d}x - \int_0^{e} (r+s-e)\mathrm{d}F_2(y) \int_{q_1^*+\gamma Q_s}^{q_2^*+\gamma Q_s} F_1(x)\mathrm{d}x \\ &\ge (r-e-b+s)(q_2^*-q_1^*) + \int_e^{r+s} (y-e)\mathrm{d}F_2(y) \int_0^{q_1^*} F_1(x)\mathrm{d}x \\ &\quad - \int_e^{r+s} (r+s-y)\mathrm{d}F_2(y) \int_{q_1^*+\gamma Q_s}^{q_2^*+\gamma Q_s} \mathrm{d}x - \int_0^{e} (r+s-e)\mathrm{d}F_2(y) \int_{q_1^*+\gamma Q_s}^{q_2^*+\gamma Q_s} \mathrm{d}x \\ &= \left(\int_e^{r+s} (y-e)\mathrm{d}F_2(y) - b \right)(q_2^*-q_1^*) + \int_e^{r+s} (y-e)\mathrm{d}F_2(y) \int_0^{q_1^*} F_1(x)\mathrm{d}x. \end{aligned} \tag{23}$$

From $b=\overline{p}-E[\min(e,p)] = \int_e^{r+s}(y-e)\mathrm{d}F_2(y)$, we can obtain that

$$E[\Pi_2(q_2^*)] - E[\Pi_1(q_1^*)] \ge \int_e^{r+s} (y-e)\mathrm{d}F_2(y) \int_0^{q_1^*} F_1(x)\mathrm{d}x \ge 0. \tag{24}$$

From the conclusion, we can see that if the buyer and the supplier sign the option purchase price $b=\overline{p}-E[\min(e,p)]$, the buyer should consider the option speculation to maximize the expected profit. The option pricing formula $b=\overline{p}-E[\min(e,p)]$ ensures that the option purchase price is neither too high nor too low, which is a fair price for both the buyer and the supplier [32, 33]. □

4. Numerical Results

In this section, we provide some numerical examples to illustrate the validity of our research.

Example 1. Suppose that the demand D subjects to the uniform distribution $U[0,1000]$, and the spot price p subjects to the uniform distribution $U[6,r+s]$. For the given parameters, we solve the optimal option purchase quantities q_1^* and q_2^* and give sensitivity analysis on different parameters.

For $s=2, \gamma=0.5, Q_s=400, e=9,$ and $b=1.5,$ we compute the optimal option purchase quantities q_1^* and q_2^* with different retail price $r\in[11,13]$ in Figure 1, which shows that both the optimal option ordering quantities q_1^* and q_2^* are increasing w.r.t. the retail price r. It is also verified that the optimal option ordering quantity q_2^* is larger than q_1^* under different retail price r.

For $r=12, \gamma=0.5, Q_s=400, e=9,$ and $b=1.5,$ we compute the optimal option ordering quantities q_1^* and q_2^* with different shortage cost $s\in[1,3]$ in Figure 2. Figure 2 shows that both the optimal option ordering quantities q_1^* and q_2^* are increasing w.r.t. the shortage cost s. It is also

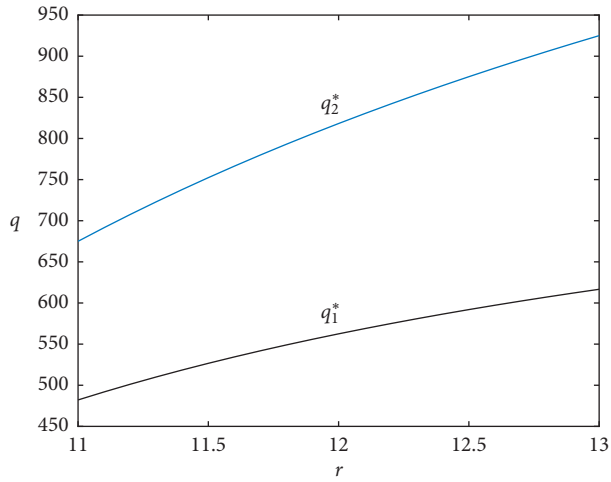

Figure 1: Optimal option ordering quantities q_1^* and q_2^* with different retail price r.

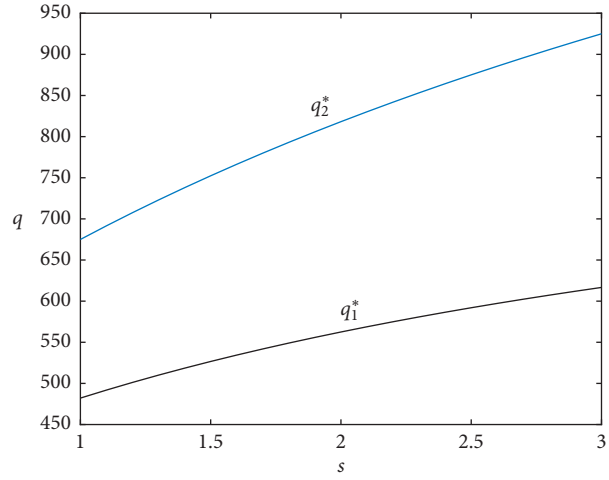

Figure 2: Optimal option ordering quantities q_1^* and q_2^* with different shortage cost s.

verified that the optimal option ordering quantity q_2^* is larger than q_1^* under different shortage cost.

For $r = 12, \gamma = 0.5, Q_s = 400, e = 9$, and $s = 2$, we compute the optimal option ordering quantities q_1^* and q_2^* with different option purchase price $b \in [0.5, 2.5]$ in Figure 3. Figure 3 shows that both the optimal option ordering quantities q_1^* and q_2^* are decreasing w.r.t. the option purchase price b. It is also verified that the optimal option ordering quantity q_2^* is larger than q_1^* under different option purchase price b.

For $r = 12, \gamma = 0.5, Q_s = 400, b = 1.5$, and $s = 2$, we compute the optimal option ordering quantities q_1^* and q_2^* with different option execution price $e \in [8, 10]$ in Figure 4. Figure 4 shows that both the optimal option ordering quantities q_1^* and q_2^* are decreasing w.r.t. the option execution price e. It is also verified that the optimal option ordering quantity q_2^* is larger than q_1^* under different option execution price e.

For $r = 12, e = 9, Q_s = 400, b = 1.5$, and $s = 2$, we compute the optimal option ordering quantities q_1^* and q_2^* with different spot trading liquidity $\gamma \in [0, 1]$ in Figure 5. Figure 5 shows that both the optimal option ordering quantities q_1^* and q_2^* are decreasing w.r.t. the spot trading liquidity γ. It is also verified that the optimal option ordering quantity q_2^* is larger than q_1^* under different spot trading liquidity γ. The red line indicates the optimal option ordering quantity in the traditional newsvendor problem, where $\gamma = 0$.

For $r = 12, e = 9, Q_s = 400, b = 1.5$, and $s = 2$, we compute the expected profit utilities $E[\prod_1(q_1^*)]$ and $E[\prod_2(q_2^*)]$ with different spot trading liquidity $\gamma \in [0, 1]$ in Figure 6. Figure 6 shows that both the expected profit utilities $E[\Pi_1(q_1^*)]$ and $E[\Pi_2(q_2^*)]$ are increasing w.r.t. the spot

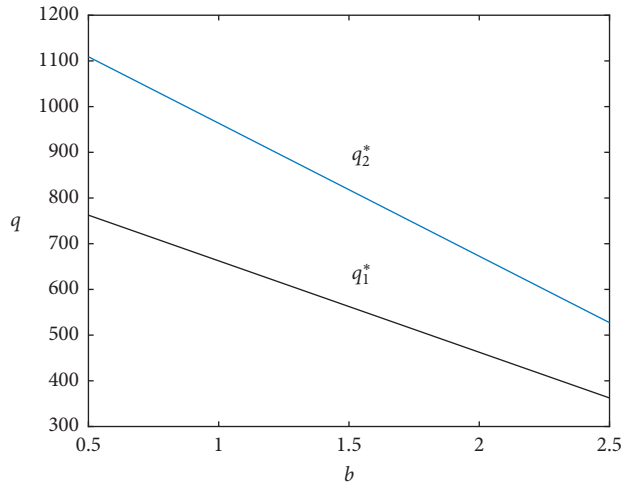

Figure 3: Optimal option ordering quantities q_1^* and q_2^* with different option purchase price b.

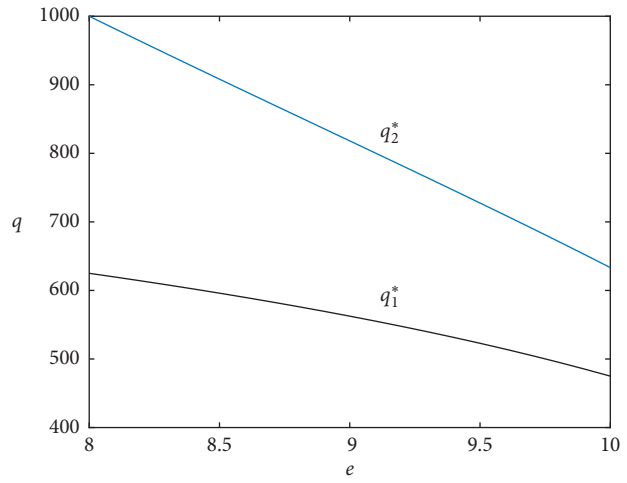

Figure 4: Optimal option ordering quantities q_1^* and q_2^* with different option execution price e.

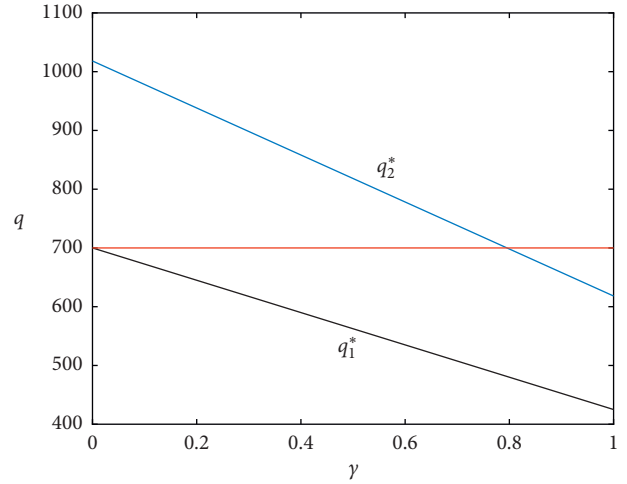

Figure 5: Optimal option ordering quantities q_1^* and q_2^* with different spot trading liquidity γ.

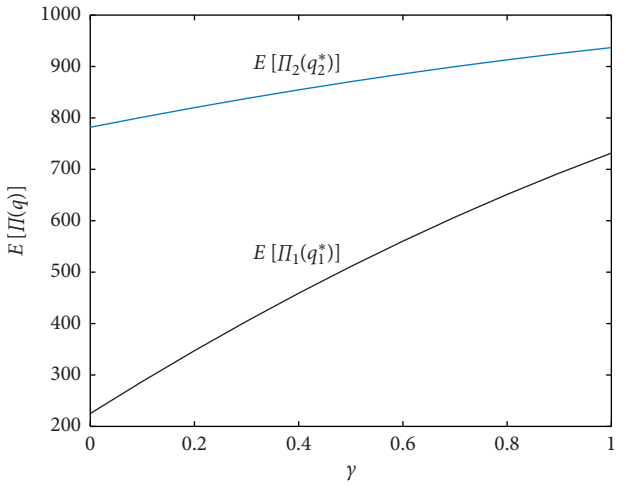

Figure 6: Expected profit utilities $E[\prod_1(q_1^*)]$ and $E[\prod_2(q_2^*)]$ with different spot trading liquidity γ.

trading liquidity γ. It is also verified that when $e + b < r + s + (Z/(q_2^* - q_1^*))$, the maximum expected profit without the option speculation is lower than that with the option speculation under different spot trading liquidity γ.

5. Conclusions

This paper investigated the portfolio procurement with the spot trading liquidity or the option speculation under the stochastic demand and the stochastic spot price. For these scenarios, two optimal portfolio procurement strategy models were established to maximize the buyer's profit, respectively. Based on the buyer's cost-benefit analysis, a global optimizing solution method for each model was obtained. Then, the role of the spot trading liquidity and option speculation in buyer's expected profit was analyzed. Furthermore, the cost threshold and option pricing formula were obtained, which provided a decision basis for the buyer. Numerical experiments were carried out to illustrate the validity of our research.

By using the mathematical foundation of probability, our research is quite generic and is essentially applicable to other industrial sectors with multiple sourcing and perishable products. In that sense, our research enriches the portfolio procurement literature in a broader context. Some extensions of our research are as follows. One possible extension is to consider the portfolio of a long-term contract and an option contract under a spot market. Another possible extension is to incorporate risk preference of the buyer into this study, which is a more interesting issue.

Data Availability

The data used to support the findings of this study are available from the corresponding author upon request.

Conflicts of Interest

The authors declare that there are no conflicts of interests regarding the publication of this paper.

Authors' Contributions

Each author equally contributed to this paper and read and approved the final manuscript.

Acknowledgments

This project was supported by the National Natural Science Foundation of China (12071250 and 12071249).

References

[1] J. Xu, G. Feng, W. Jiang, and S. Wang, "Optimal procurement of long-term contracts in the presence of imperfect spot market," *Omega*, vol. 52, pp. 42–52, 2015.

[2] R. W. Seifert, U. W. Thonemann, and W. H. Hausman, "Optimal procurement strategies for online spot markets," *European Journal of Operational Research*, vol. 152, no. 3, pp. 781–799, 2004.

[3] Ç. Haksöz and S. Seshadri, "Supply chain operations in the presence of a spot market: a review with discussion," *Journal of the Operational Research Society*, vol. 58, no. 11, pp. 1412–1429, 2007.

[4] V. Nagali, J. Hwang, D. Sanghera et al., "Procurement risk management (PRM) at hewlett-packard company," *Interfaces*, vol. 38, no. 1, pp. 51–60, 2008.

[5] B. Peleg and H. Lee, "Short-term *E*-procurement strategies versus long-term contracts," *Production and Operations Management*, vol. 11, no. 4, pp. 458–479, 2002.

[6] S.-L. Chen and C.-L. Liu, "Procurement strategies in the presence of the spot market-an analytical framework," *Production Planning & Control*, vol. 18, no. 4, pp. 297–309, 2007.

[7] A. Goel and G. J. Gutierrez, "Multiechelon procurement and distribution policies for traded commodities," *Management Science*, vol. 57, no. 12, pp. 2228–2244, 2011.

[8] C. K. M. Lee, D. Lin, and R. Pasari, "Strategic procurement from forward contract and spot market," *Industrial Management & Data Systems*, vol. 114, no. 5, pp. 778–796, 2014.

[9] Y. Chen, W. Xue, and J. Yang, "Technical note-optimal inventory policy in the presence of a long-term supplier and a spot market," *Operations Research*, vol. 61, no. 1, pp. 88–97, 2013.

[10] N. Adilov, "Strategic use of forward contracts and capacity constraints," *International Journal of Industrial Organization*, vol. 30, no. 2, pp. 164–173, 2012.

[11] K. Inderfurth, P. Kelle, and R. Kleber, "Dual sourcing using capacity reservation and spot market: optimal procurement policy and heuristic parameter determination," *European Journal of Operational Research*, vol. 225, no. 2, pp. 298–309, 2013.

[12] X. Gou, Z. Xu, and F. Herrera, "Consensus reaching process for large-scale group decision making with double hierarchy hesitant fuzzy linguistic preference relations," *Knowledge-Based Systems*, vol. 157, pp. 20–33, 2018.

[13] H. Liao, X. Mi, and Z. Xu, "A survey of decision-making methods with probabilistic linguistic information: bibliometrics, preliminaries, methodologies, applications and future directions," *Fuzzy Optimization and Decision Making*, vol. 19, no. 1, pp. 81–134, 2020.

[14] C. Wang, H. Chen, Y. Wang, and G. Zhou, "On copositiveness identification of partially symmetric rectangular tensors," *Journal of Computational and Applied Mathematics*, vol. 372, Article ID 112678, 2020.

[15] W. Wang, H. Chen, and Y. Wang, "A new C-eigenvalue interval for piezoelectric-type tensors," *Applied Mathematics Letters*, vol. 100, p. 106035, 2020.

[16] Y. Wang, X. Sun, and F. Meng, "On the conditional and partial trade credit policy with capital constraints: a Stackelberg model," *Applied Mathematical Modelling*, vol. 40, no. 1, pp. 1–18, 2016.

[17] Y. Wang, W. Xing, W. Xing, and H. Gao, "Optimal ordering policy for inventory mechanism with a stochastic short-term price discount," *Journal of Industrial & Management Optimization*, vol. 16, no. 3, pp. 1187–1202, 2020.

[18] Q. Fu, C.-Y. Lee, and C.-P. Teo, "Procurement management using option contracts: random spot price and the portfolio effect," *IIE Transactions*, vol. 42, no. 11, pp. 793–811, 2010.

[19] P. P.-E. Pei, D. Simchi-Levi, and T. I. Tunca, "Sourcing flexibility, spot trading, and procurement contract structure," *Operations Research*, vol. 59, no. 3, pp. 578–601, 2011.

[20] Y. Zhao, T.-M. Choi, T. C. E. Cheng, and S. Wang, "Supply option contracts with spot market and demand information updating," *European Journal of Operational Research*, vol. 266, no. 3, pp. 1062–1071, 2018.

[21] Y. Merzifonluoglu, "Risk averse supply portfolio selection with supply, demand and spot market volatility," *Omega*, vol. 57, pp. 40–53, 2015.

[22] Y. Merzifonluoglu, "Integrated demand and procurement portfolio management with spot market volatility and option contracts," *European Journal of Operational Research*, vol. 258, no. 1, pp. 181–192, 2017.

[23] J. Luo and X. Chen, "Risk hedging via option contracts in a random yield supply chain," *Annals of Operations Research*, vol. 257, no. 1-2, pp. 697–719, 2017.

[24] C.-Y. Lee, X. Li, and Y. Xie, "Procurement risk management using capacitated option contracts with fixed ordering costs," *IIE Transactions*, vol. 45, no. 8, pp. 845–864, 2013.

[25] N. Wan and X. Chen, "Multi-period dual-sourcing replenishment problem with option contracts and a spot market," *Industrial Management & Data Systems*, vol. 118, no. 4, pp. 782–805, 2018.

[26] E. Anderson, B. Chen, and L. Shao, "Supplier competition with option contracts for discrete blocks of capacity," *Operations Research*, vol. 65, no. 4, pp. 952–967, 2017.

[27] H. Chen, Y. Wang, and G. Zhou, "High-order sum-of-squares structured tensors: theory and applications," *Frontiers of Mathematics in China*, vol. 15, no. 2, pp. 255–284, 2020.

[28] M. Dong and H. Chen, "Geometry of the copositive tensor cone and its dual," *Asia-Pacific Journal of Operational Research*, vol. 37, no. 4, Article ID 2040008, 2020.

[29] X. Gou, H. Liao, Z. Xu, R. Min, and F. Herrera, "Group decision making with double hierarchy hesitant fuzzy linguistic preference relations: consistency based measures, index and repairing algorithms and decision model," *Information Sciences*, vol. 489, pp. 93–112, 2019.

[30] J. Namdar, X. Li, R. Sawhney, and N. Pradhan, "Supply chain resilience for single and multiple sourcing in the presence of disruption risks," *International Journal of Production Research*, vol. 56, no. 6, pp. 2339–2360, 2018.

[31] Z. Xu and X. Gou, "An overview of interval-valued intuitionistic fuzzy information aggregations and applications," *Granular Computing*, vol. 2, no. 1, pp. 13–39, 2017.

[32] P. Aggarwal and R. Ganeshan, "Using risk-management tools on B2Bs: an exploratory investigation," *International Journal of Production Economics*, vol. 108, no. 1-2, pp. 2–7, 2007.

[33] R. Ganeshan, T. Boone, and P. Aggarwal, "Optimal procurement portfolios when using B2Bs: a model and analysis," *International Journal of Production Economics*, vol. 118, no. 1, pp. 146–151, 2009.

Hindawi
Mathematical Problems in Engineering
Volume 2020, Article ID 5436507, 13 pages
https://doi.org/10.1155/2020/5436507

Research Article

Action Strategy Analysis in Probabilistic Preference Movement-Based Three-Way Decision

Chunmao Jiang and Shubao Zhao

School of Computer Science and Information Engineering, Harbin Normal University, Harbin 150025, Heilongjiang Province, China

Correspondence should be addressed to Shubao Zhao; machinelearner@126.com

Received 22 July 2020; Revised 3 November 2020; Accepted 6 November 2020; Published 9 December 2020

Academic Editor: Zeshui Xu

The trisecting-acting-outcome model is a methodology of "thinking in threes," which is the main idea of the three-way decision (3WD). It consists of three components: trisecting, acting, and outcome evaluation. A strategy selection method in a movement-based three-way decision (M-3WD) has been proposed in previous work. However, conflicting information widely existing in the information system has not yet been given sufficient consideration. The conflicting information brings massive noisy strategies when mining action strategies in three regions. This paper proposed a novel three-way decision model for action strategy set, which can analyze and classify strategies by introducing credibility and coverage. The model can remove noisy strategies and choose strategies more suitable for the need of decision makers. To evaluate and select an optimal action strategy, we analyze the probabilistic preference in a movement-based three-way decision. The approach determines the probability of movement by using the evidence theory (D-S) theory. The optimal action strategy is selected by analyzing the difference between the ideal movement and the actual movement, the lower the difference, the better the strategy. We give an example of medical decision-making to illustrate the effectiveness of the proposed method.

1. Introduction

Three-way decision [1] is an effective way of solving complex problems, whose core idea can be formulated as a three-step process within trisecting-acting-outcome (TAO) [2]. The trisecting is to divide a whole into three regions that are disjoint or weakly joint. The acting is to devise action strategies to process objects in the three regions. The outcome evaluation is to evaluate the effectiveness of the action strategy. The movement-based three-way decision [3] aims to mine actionable rules in three regions and transfer objects from the unfavorable region to the favorable region. We use an example of medical-making to illustrate the main ideas of the TAO model. In medical decision-making, one typically divides a set of suspected patients into three groups: suspected patients who have the disease, suspected patients who do not have the disease, and suspected patients who still need a further examination. According to the diagnosis result, the doctor may take some actions to turn the suspected patients who have the disease into disease-free, check the suspected patients who still need a further examination whether having the disease, and retain the suspected patients who do not have the disease. At last, the doctor develops new treatment protocols by evaluating the effects of treatment and medical examination.

Since the three-way decision was putting forward, it has expanded from a special three-way decision to a general three-way decision [4]. There are many studies on theories, such as three-way classification [5, 6], three-way clustering [7–12], three-way concept analysis [13, 14], three-way conflict analysis [15, 16], three-way game theory [17, 18], three-way support systems [19], three-way granular computing [20, 21], and three-way multiple attribute decision [22, 23]. Yao [2, 24] systematically studied the main ideas of three-way decision and the granular computing model based on three-way decision. Qi and Wei [25] combined formal

concept analysis with three-way decision and put forward three-way concept analysis theory. Yu [26] introduced three-way decision into clustering analysis and proposed three-way clustering approach. Wang and Yao [27] applied contraction and expansion in mathematical morphology to the three-way decision and proposed a three-way clustering algorithm based on mathematical morphology. In terms of application, three-way decision shows its unique superiority in image recognition [28, 29], mail filtering [30], medical decision-making [19], stream computing [31], recommendation system [32], and cloud computing [33].

Researchers have long focused on constructing a trisection from a whole [5, 6, 34]. Research on acting and outcome evaluation is still in its infancy. Gao and Yao [3] proposed a movement-based three-way decision model by mining actionable rules in three regions. Jiang and Yao [35, 36] proposed three-way decision models for quantity movement and probability movement. The corresponding outcome evaluation methods are also proposed.

In real life, the database usually stores a lot of inconsistent information [37], which is caused by missing values, duplicate, and errors. It is difficult to avoid even after many rounds of data processing. Inconsistent information refers to the data in an information system, whose condition attributes are the same but derive different decision results. In a movement-based three-way decision, the decision maker usually has a particular preference for different regions. The preference relationship will prompt the decision maker to construct action strategies in three regions. Objects will be moved from the unfavorable region to the favorable region according to the preference of decision-makers. The existence of conflicting information makes it inevitable to mine many inconsistent rules. The action strategy generated by inconsistent rules may induce multiple different decision results so that the movement-based three-way decision usually exhibits the characteristics of probability movement [35]. Determining the probability of movement and selecting an optimal action strategy are urgent problems that need to be solved.

This paper constructs a three-way decision model for strategy set by introducing the concepts of credibility and coverage [38]. The model can remove noisy strategies in the strategy set. To evaluate and select an optimal action strategy, we analyze the probabilistic preference in a movement-based three-way decision. The D-S theory determines the probability of movement. The optimal action strategy can be selected by analyzing the difference between the ideal movement and the actual movement, the lower the difference, the better the strategy.

The remainder of this paper is organized as follows. Section 2 reviews the TAO model of three-way decision and introduces the approach of constructing an action strategy. Section 3 analyses the uncertainty of the action strategy through an example of medical decision-making. Then, we propose a novel three-way decision model for the action strategy set. Section 4 analyses the probabilistic preference in M-3WD. The D-S theory is used to determine the probability of movement. The optimal action strategy is selected by analyzing the difference between the ideal movement and the actual movement. Section 5 illustrates the effectiveness of the proposed method with an example of medical decision-making. Section 6 gives a summary and planning for future work.

2. Preliminaries

In this section, we review the TAO model of three-way decision and the movement-based three-way decision.

2.1. TAO of Three-Way Decision. "Thinking in threes" [2, 39] is a kind of granular computing thought consistent with human cognition. After the summary and refinement by Yao [1, 24, 40], the three-way decision theory is formed. The TAO model of the three-way decision is given in Figure 1. The trisecting function, denoted by solid lines with arrows, is to divide a whole into three pairwise disjoint or weakly joint regions P_1, P_2, and P_3. The function, denoted by dashed lines, is mining actionable rules in three regions. The function of acting, denoted by dashed lines with arrows, is to devise action strategies for three regions. The three regions before acting are represented by P_1, P_2, and P_3. The new three regions after acting are represented by P_1', P_2', and P_3'. The outcome evaluation is to measure the effect of the trisection and action strategy.

The most fundamental issue of the three-way decision is how to construct a trisection from a whole with reasonable interpretations. Researchers have constructed three regions based on rough sets [40–43], fuzzy sets [34], shadowed sets [44, 45], intuitionistic fuzzy sets [46, 47], vague sets [48] and soft sets [49]. A three-way decision model with an ordered relationship is defined as follows.

Definition 1. Suppose that OB is a finite nonempty set of objects. E: OB $\longrightarrow$ $(L, <)$ is an evaluation function on set OB. For $x \in$ OB, $E(x)$ is an evaluation function value of x. Given a pair of thresholds $(\alpha, \beta) \in V \times V$ with $\beta \leq \alpha$, we trisect OB into three pairwise disjoint regions:

$$\begin{aligned} P_1 &= \{x \in \mathrm{OB} | E(x) \geq \alpha\}, \\ P_2 &= \{x \in \mathrm{OB} | \beta < E(x) < \alpha\}, \\ P_3 &= \{x \in \mathrm{OB} | E(x) \leq \beta\}. \end{aligned} \tag{1}$$

The three regions satisfy the following two conditions:

(1) $P_1 \cup P_2 \cup P_3 = \mathrm{OB}$

(2) $P_1 \cap P_2 = \Phi, P_1 \cap P_3 = \Phi, P_2 \cap P_3 = \Phi$

The P_1 region consists of objects with evaluation function value $E(x)$ greater than or equal to α. The P_3 region consists of objects with evaluation function value $E(X)$ less than or equal to β. The P_2 region consists of objects with evaluation function value $E(x)$ between the two thresholds.

The acting aims to design an appropriate action strategy to process three regions, according to trisection. An efficient action strategy can make decision maker increase benefits or reduce costs. The decision maker hopes to adopt an appropriate action strategy to move the object from unfavorable to the favorable region.

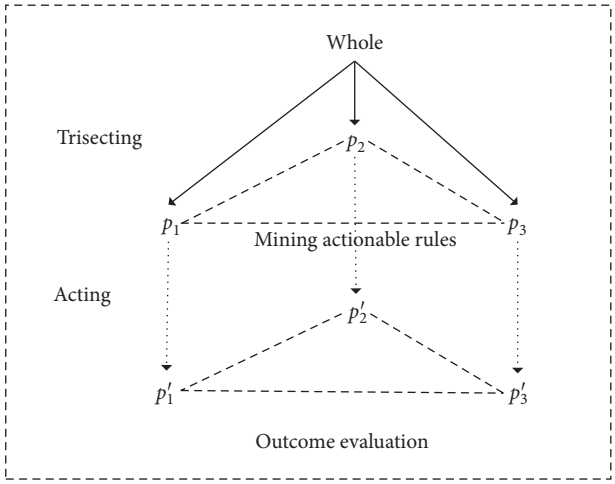

Figure 1: TAO model of trisecting-acting-outcome.

The outcome evaluation is to evaluate the effect of trisecting and acting. We can construct an evaluation function to evaluate the quality of trisecting:

$$Q\left(\pi_{(\alpha,\beta)}\right) = w_{P_1}Q(P_1) + w_{P_2}Q(P_2) + w_{P_3}Q(P_3), \tag{2}$$

where $Q(\pi_{(\alpha,\beta)})$ denotes the quality of trisection by a pair of threshold (α, β), $Q(P_i)$, $i = 1, 2, 3$, denotes the qualities or utilities of each regions, and w_{P_i}, $i = 1, 2, 3$, denotes the weights of each regions. For acting, we can construct an evaluation function to evaluate the effect of action strategy:

$$Q(\pi'|\pi) = Q(\pi') - Q(\pi), \tag{3}$$

where $Q(\pi)$ and $Q(\pi')$ denote the qualities or utilities of original three regions and new three regions.

2.2. Movement-Based Three-Way Decision. Gao and Yao [3] proposed a movement-based three-way decision by introducing actionable rules into the three-way decision. The actionable rules first proposed by Ras [50, 51]. It means that a user can mine actionable rules and moving objects to generate benefits. The movement-based three-way decision aims to mine action strategy in three regions and move objects from unfavorable regions to the favorable region.

Definition 2 (see [3]). Suppose that $[x]$ and $[y]$ are equivalence classes in different regions. We can get two decision rules:

$$\begin{aligned} r_{[x]}&: \left[\bigwedge_{s\in A_s} s = f_s(x)\right] \wedge \left[\bigwedge_{f\in A_f} f = f_f(x)\right] \Rightarrow d = f_d(x), \\ r_{[y]}&: \left[\bigwedge_{s\in A_s} s = f_s(y)\right] \wedge \left[\bigwedge_{f\in A_f} f = f_f(y)\right] \Rightarrow d = f_d(y), \end{aligned} \tag{4}$$

where $r_{[.]}, \in \{x, y\}$, is decision rule, A_s is a set of stable attributes, $f_s(\cdot)$ is the value of attribute s, A_f is a set of flexible attributes, $f_f(\cdot)$ is the value of attribute f, and $f_d(\cdot)$ is the value of decision attribute d.

Definition 3 (see [3]). Suppose that $[x]$ and $[y]$ are equivalence classes in different regions, where $[x]$ is the equivalence class that needs to be moved and $[y]$ is the target equivalence class. If a user wants to move the object from one region to another, we can design an appropriate action strategy, that is,

$$\begin{aligned} r_{[x]} \rightsquigarrow r_{[y]}&: \left[\bigwedge_{f\in A_f} f_f(x) \rightsquigarrow f_f(y)\right] \Rightarrow f_d(x) \rightsquigarrow f_d(y), \\ &\text{subject to } \left[\bigwedge_{s\in A_s} f_s(x) = f_s(y)\right], \end{aligned} \tag{5}$$

where $r_{[x]} \rightsquigarrow r_{[y]}$ is actionable rules from $[x]$ to $[y]$, $\wedge_{s\in A_s} f_s(x) = f_s(y)$ means that $[x]$ and $[y]$ have the same value of stable attributes, and $\wedge_{f\in A_f} f_f(x) \rightsquigarrow f_f(y)$ means that the value of flexible attributes f is changed from $f_f(x)$ to $f_f(y)$.

3. Three-Way Decision for Action Strategy Set

This section illustrates conflicting information through an example of medical decision-making and constructs the corresponding three-way decision model.

3.1. A Motivational Example. In real life, an information system often has much inconsistent information. The inconsistent information leads to a large number of inconsistent rules when mining actionable rules. It is not helpful to the decision maker and may even mislead them into choosing the wrong action strategy. The following example of medical decision-making illustrates conflicting information and the impact on the movement-based three-way decision.

Table 1 is a medical-decision information table. There are 20 suspected patients and six symptoms or attributes. All condition attributes had been discretized. The values of some attributes are grouped and reassigned as follows. Age is categorized into three groups, i.e., 0–20, 20–60, and 60+; they are reassigned to value 1 to 3, respectively. Sex is categorized as female and male; they are reassigned to value 1 and 0. Cholesterol is categorized into three groups, i.e., 0–199, 200–239, and 240+; they are reassigned to value 1 to 3, respectively. Blood pressure is categorized into three groups, i.e., 0–89, 90–139, and 140+; they are reassigned to value 1 to 3, respectively. Blood sugar is categorized into three groups, i.e., 0–3.9, 4.0–7.8, and 7.9+; they are reassigned to value 1 to 3, respectively. Among them, cholesterol, blood pressure, and blood sugar are abbreviated as chol, pb, and bs. Age and sex are stable attributes, and others are flexible attributes. The symbol "+" stands for suspected patients who have the disease. The symbol "–" stands for suspected patients who have not the disease. The symbol "?" stands for suspected patients who need a further examination.

All objects are divided into following 8 equivalence classes based on their condition attributes:

Table 1: A decision table for medicine.

	Age	Sex	Cholesterol	Blood pressure	Blood sugar	Result
x_1	3	1	2	1	1	+
x_2	3	1	2	1	1	+
x_3	2	1	3	2	2	−
x_4	3	0	2	3	2	?
x_5	3	0	2	3	2	−
x_6	2	1	3	2	2	−
x_7	3	0	2	2	2	−
x_8	3	0	1	2	3	+
x_9	3	0	2	3	2	−
x_{10}	2	0	3	3	3	?
x_{11}	3	0	2	2	2	−
x_{12}	3	0	1	2	2	−
x_{13}	3	0	1	2	2	−
x_{14}	3	0	1	1	1	+
x_{15}	3	0	1	1	1	+
x_{16}	3	0	2	3	2	+
x_{17}	3	0	2	3	2	−
x_{18}	2	1	3	2	2	−
x_{19}	3	0	1	2	3	−
x_{20}	2	0	3	3	3	+

$$
\begin{aligned}
[x]_1 &= \{x_1, x_2\},\\
[x]_2 &= \{x_3, x_6, x_{18}\},\\
[x]_3 &= \{x_4, x_5, x_9, x_{16}, x_{17}\},\\
[x]_4 &= \{x_7, x_{11}\},\\
[x]_5 &= \{x_8, x_{19}\},\\
[x]_6 &= \{x_{10}, x_{20}\},\\
[x]_7 &= \{x_{12}, x_{13}\},\\
[x]_8 &= \{x_{14}, x_{15}\}.
\end{aligned} \tag{6}
$$

Doctors divide suspected patients into three regions P_1, P_2, and P_3 based on the diagnosis result:

$$
\begin{aligned}
P_1 &= \{x_3, x_5, x_6, x_7, x_9, x_{11}, x_{12}, x_{13}, x_{17}, x_{18}, x_{19}\},\\
P_2 &= \{x_1, x_2, x_8, x_{14}, x_{15}, x_{16}, x_{20}\},\\
P_3 &= \{x_4, x_{10}\}.
\end{aligned} \tag{7}
$$

Taking $[x]_3$ as an example, according to equation (4), we can construct the decision rules, that is,

$$
r_{[x]_3}\colon \text{age} = 3 \wedge \text{sex} = 0 \wedge \text{chol} = 2 \wedge \text{bp} = 3 \wedge \text{bs} = 3 \Rightarrow \text{result} = \begin{cases} +, & = 1,\\ -, & = 3,\\ ?, & = 1. \end{cases} \tag{8}
$$

There are five different objects in $[x]_3$, one of which is diseased, three of which is disease-free, and one is uncertain. Therefore, conflicting information is common in an information system. All the condition attributes in the equivalence class $[x]_3$ are the same but derive different decision results. The existence of conflicting information has an enormous influence when mining the action strategy in three regions.

Taking $[x]_8$ as an equivalence class that needs to be moved, the decision maker hopes that the object in the diseased region moves to the disease-free region. The object in the uncertain region will be moved to the diseased or disease-free region under further medical examination. According to equation (5), we can mine some action strategies, that is,

$$
\begin{aligned}
&r_{[x]_8} \rightsquigarrow r_{[x]_2},\\
&r_{[x]_8} \rightsquigarrow r_{[x]_3},\\
&r_{[x]_8} \rightsquigarrow r_{[x]_4},\\
&r_{[x]_8} \rightsquigarrow r_{[x]_5}.
\end{aligned} \tag{9}
$$

The strategy $r_{[x]_8} \rightsquigarrow r_{[x]_3}$ means moving objects from $[x]_8$ to $[x]_3$ according to equation (5). However, there are diseased, disease-free, and uncertain objects in $r_{[x]_3}$. For the

decision maker, the outcome of movement is difficult to determine. There are different probabilities of movement:

$$r_{[x]_8} \rightsquigarrow r_{[x]_3}\text{: chol: } 1 \rightsquigarrow 2 \wedge \text{bp: } 1 \rightsquigarrow 3 \wedge \text{bs: } 1 \rightsquigarrow 3 \Rightarrow \text{result} = \begin{cases} +, & = p_1, \\ -, & = p_2, \\ ?, & = p_3, \end{cases} \quad \text{subject to: age} = 3 \wedge \text{sex} = 0. \tag{10}$$

where p_1, p_2, and p_3 represent the proportion or probability of moving disease-free, diseased, and uncertain regions, respectively.

The existence of inconsistent information makes a lot of noisy strategies when mining action strategies, such as $r_{[x]_8} \rightsquigarrow r_{[x]_3}$ and $r_{[x]_8} \rightsquigarrow r_{[x]_5}$. Therefore, it is necessary to consider conflicting information and analyze strategy when mining actionable rules in three regions.

3.2. Construct Three-Way Decision Model. The actionable rules affected by inconsistent information can generate a lot of noisy strategies. These noisy strategies are not helpful to the decision maker and may cause them to make wrong judgments. Therefore, we introduce credibility and coverage concepts to construct a three-way decision model for the action strategy set.

Definition 4. (see [38]). Suppose that IS $= \{U, C \cup D, V, f\}$ is an information system, and S is an action strategy mined in IS according to the target equivalence class $[x]$. The action strategy has a certain credibility. The definition is as follows:

$$\text{Credibility}(S) = \frac{\left|[x] \cap P_j\right|}{|[x]|}, \tag{11}$$

where $[x]$ is the equivalence class divided by $U/\text{ind}(C)$, $i = 1, 2, \ldots, m$, and P_j, $j = 1, 2, 3$, is the three regions divided by evaluation function.

The strategy is certain when $\text{Credibility}(S) = 1$. The strategy is uncertain when $0 < \text{Credibility}(S) < 1$. The credibility denotes the conditional probability of target region P_j to the target equivalence class $[x]$. When the credit is less than 1, the same condition attributes are divided into different regions. So, credibility reflects the uncertainty of strategies.

The credibility of strategy S only considers the proportion of the equivalence class $[x]$ in the target region. However, it is not enough to consider credibility in an inconsistent information system. It is necessary to consider the coverage of the strategy in the target region: how many objects induce the strategy.

Definition 5. (see [38]). Suppose that IS $= \{U, C \cup D, V, f\}$ is an information system, and S is an action strategy mined in IS according to the target equivalence class $[x]$. The action strategy has a certain coverage. The definition is as follows:

$$\text{Coverage}(S) = \frac{\left|[x] \cap P_j\right|}{\left|P_j\right|}, \tag{12}$$

where $[x]$ is the equivalence class divided by $U/\text{ind}(C)$, $i = 1, 2, \ldots, m$, and P_j, $j = 1, 2, 3$, is the three regions divided by evaluation function.

The coverage describes the proportion of objects meeting the strategy constraints in the target region. If the strategy's coverage is small, the objects that derive the strategy occupy a small part of the region P_j. Therefore, the causality of this strategy lacks sufficient data to support it.

Therefore, it is necessary to consider both the strategy's credibility and coverage when selecting a strategy. Based on the above description, combined with the trilevel thinking proposed by Yao [52], we constructed a novel three-way decision model for the strategy set. The model is given in Figure 2.

Given a strategy set $\text{AS} = \{S_1, S_2, \ldots, S_n\}$. The strategy set is divided into a top-down trilevel granularity structure according to the credibility threshold cre and the coverage threshold cov. The strategy set is gradual granulation from top to down.

The first level:

$$\text{AS} = \{S_1, S_2, \ldots, S_n\}. \tag{13}$$

The second level:

$$\text{AS/cre} = \{\{S_1, S_2, \ldots, S_m\}, \{S_{m+1}, S_{m+2}, \ldots, S_n\}\}. \tag{14}$$

The third level:

$$\text{AS/cre} \wedge \text{cov} = \left\{\left\{S_1, \ldots, S_{m_1}\right\}, \left\{S_{m_1+1}, \ldots, S_m\right\}\right\} \cup \left\{\left\{S_{m+1}, \ldots, S_{n_1}\right\}, \left\{S_{n_1+1}, \ldots, S_n\right\}\right\}. \tag{15}$$

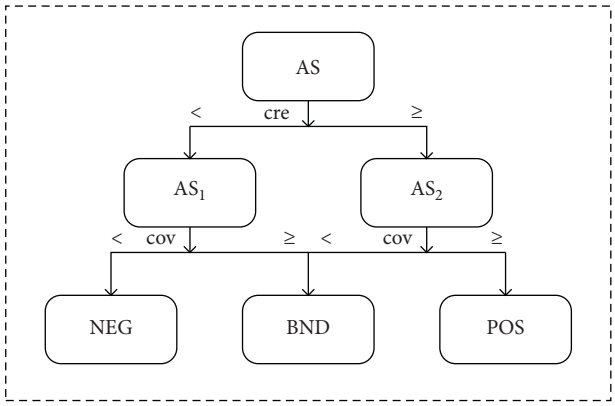

Figure 2: Three-way decision model for the strategy set.

The model of three-way decision for strategy set is as follows:

$$\begin{aligned}
\mathrm{POS}(S) &= \{S_i \in S | \mathrm{credibility}(S_i) \geq \mathrm{cre} \wedge \mathrm{coverage}(S_i) \geq \mathrm{cov}\},\\
\mathrm{NEG}(S) &= \{S_i \in S | \mathrm{credibility}(S_i) \leq \mathrm{cre} \wedge \mathrm{coverage}(S_i) \leq \mathrm{cov}\},\\
\mathrm{BND}(S) &= (\mathrm{POS}(S) \cup \mathrm{NEG}(S))^C\\
&= \{S_i \in S | \mathrm{credibility}(S_i) > \mathrm{acc} \wedge \mathrm{coverage}(S_i) < \mathrm{cov}\} \cup\\
&\quad | \{S_i \in S | \mathrm{credibility}(S_i) < \mathrm{cre} \wedge \mathrm{coverage}(S_i) > \mathrm{cov}\}.
\end{aligned} \tag{16}$$

The model introduces the concepts of credibility and coverage. In the first level, the strategy set does not introduce any concept. In the second level, the strategy set is divided into two subsets AS_1 and AS_2 through the credibility threshold cre. In the third level, the subsets AS_1 and AS_2 are classified again by the coverage threshold cov, which are above the threshold cov and below the threshold cov. Finally, the strategies whose credibility and coverage are higher than the threshold cre and cov are divided into POS region; the strategies whose accuracy and coverage are lower than the threshold cre and cov are divided into NEG region, and the remaining strategies are divided into BND region. The decision maker will give priority to the strategy in the POS region when selecting a strategy. The model enables the decision maker to choose a strategy with high credibility and coverage as much as possible, which can effectively avoid the influence of conflicting information.

At last, we summarize the key steps to construct the three-way decision for the strategy set. The approach is outlined in Algorithm 1.

4. Optimal Action Strategy Selection in M-3WD

This section analyzed the probabilistic preference in three regions and proposed an evidence theory-based approach to determine the probability of movement. The determination of the movement's probability is the basis for selecting the optimal action strategy. The optimal strategy is selected by comparing the difference between the ideal movement and the actual movement.

4.1. Probabilistic Preference in M-3WD. The model of the three-way decision for the strategy set can effectively avoid the influence of conflicting information by mining action strategy with high credibility and coverage. However, there may be many action strategies with high credibility and coverage. Therefore, we need to determine the probability of moving to three regions under different action strategies, which will help us select an optimal action strategy.

In a movement-based three-way decision, the decision maker has different preferences for different regions. For example, doctors want patients to move from a diseased region to a disease-free region in medical decision-making. According to the preference of decision makers, there are two types of movement. If the object's movement matches the preference of decision makers, we call it a favorable movement. If the object's movement does not match decision makers' preference, we call it an unfavorable movement. In a movement-based three-way decision, we first divide a set of objects into three different regions according to decision makers' needs. Then, we can mine action strategies between different regions.

Definition 6. Suppose that $\pi = \{P_1, P_2, P_3\}$ is a tripartition regions. We can mine action strategies and construct corresponding strategy sets:

$$\mathrm{AS} = (S_1, S_2, \ldots, S_n), \tag{17}$$

where AS denotes the set of all strategies for objects in P_i region to move to P_j region. Objects in three regions may have nine movements:

$$\begin{aligned}
&P_1 \rightsquigarrow P_1', P_1 \rightsquigarrow P_2', P_1 \rightsquigarrow P_3',\\
&P_2 \rightsquigarrow P_1', P_2 \rightsquigarrow P_2', P_2 \rightsquigarrow P_3',\\
&P_3 \rightsquigarrow P_1', P_3 \rightsquigarrow P_2', P_3 \rightsquigarrow P_3',
\end{aligned} \tag{18}$$

where $P_i \rightsquigarrow P_j'$, $i, j = 1, 2, 3$ denotes the object in P_i region move to P_j region and P_i and P_i' denote the region before and after the movement. In movement-based three-way decision, each kind of movement will generate the corresponding strategy set AS.

Due to the inconsistent information in the information system, the object moves from the unfavorable region to the favorable region with probability. According to the preference of decision maker, the probabilistic preference [53] movement matrix can be constructed as follows:

$$\begin{aligned}
&p_{11}, p_{12}, p_{13},\\
&p_{21}, p_{22}, p_{23},\\
&p_{31}, p_{32}, p_{33},
\end{aligned} \tag{19}$$

where p_{ij} denotes the probability of object's movement from P_i region to P_j region.

How to determine the probability of movement is an urgent problem to be solved. Considering the advantages of evidence theory in information fusion, we use the credibility of the equivalence class divided under a particular flexible attribute as the mass function of evidence theory. The

Input: IDIS = $(U, C \cup D, V, f)$, evaluation function $E(x)$, a pair of thresholds (α, β), cre, and cov.
Output: The three-way decision for strategy set.
(1) Divide equivalence classes according to condition attributes C.
(2) **for** $x \in U$ **do**
(3) Calculate the evaluation function $E(x)$.
(4) **if** $E(x) \geq \alpha$ **then**
(5) Divide x into P_1 region.
(6) **end**
(7) **else if** $E(x) \leq \beta$ **then**
(8) Divide x into P_3 region.
(9) **end**
(10) **else**
(11) Divide x into P_2 region.
(12) **end**
(13) Choose equivalence classes $[x]$ that need to be moved.
(14) Mining action strategies in P_1, P_2, and P_3 to generate corresponding strategy set AS.
(15) end
(16) **for** $S \in$ AS **do**
(17) **if** credibility$(S) \geq$ cre$\wedge$coverage$(S) \geq$ cov **then**
(18) Divide S into POS region.
(19) **end**
(20) **else if** credibility$(S) <$ cre$\wedge$coverage$(S) <$ cov **then**
(21) Divide S into NEG region.
(22) **end**
(23) **else**
(24) Divide S into BND region.
(25) **end**
(26) **end**

Algorithm 1: Three-way decision for the action strategy set.

probability of movement can be obtained by fusing multiple mass function under flexible attributes.

Evidence theory, also known as D-S evidence theory, is an uncertainty reasoning theory first proposed by Dempster. Shafer further researched and developed it. Evidence theory has been widely used in many fields such as information fusion [54], medical diagnosis [55], and uncertainty decision-making [56]. Suppose that m: $2^{\Theta} \longrightarrow [0, 1]$ is a function on the recognition framework Θ. The function satisfies the following two conditions:

$$\begin{aligned} &(1)\, m(\phi) = 0, \\ &(2) \sum_{A \subseteq \Theta} m(A) = 1, \end{aligned} \tag{20}$$

where the subset A denotes the focal elements, which meet the $m(A) > 0$. The value of $m(A)$ denotes the belief that supports the occurrence of A. The function is called a mass function or a basic credibility distribution function.

The synthesis rule [57] is the core of evidence theory. If there is multiple evidence under the recognition framework, different mass functions will be derived. The evidence synthesis formula synthesizes multiple mass functions to obtain a fused mass function. The fused mass function is used for decision-making, which can improve accuracy. Given the recognition framework Θ, for $\forall A \subseteq \Theta$, two mass functions under the same recognition frame Θ obtained from different evidences are m_1 and m_2. The synthesis formula of evidence m_1 and m_2 is as follows:

$$(m_1 \oplus m_2)(A) = \frac{1}{1 - K} \sum_{B \cap C = A} m_1(B) m_2(C), K = \sum_{B \cap C = \phi} m_1(B) m_2(C), \tag{21}$$

where K is the confidence assigned to the null value. In reality, the null value has no confidence, that is, $m(\phi) = 0$. When the two pieces of evidence are combined, the constraint condition $K < 1$ must be satisfied. If $K = 1$, the evidence is completely contradictory, and there is no $m_1 \oplus m_2$ at this time.

We use the credibility cre_{aj} of the equivalence class $[x]$ under a certain flexible attribute $a \in C$ as the mass function, that is, $m(P_j/[x]_a)$. The meaning of credibility is the proportion of equivalence classes divided by the condition attribute $a \in C$ in the target region P_j. The larger the ratio, the higher the

reliability. The mass function needs to satisfy two constraints in equation (20). The corresponding proof is as follows.

Proof. The mass function needs to satisfy two constraints, namely, $m(\phi) = 0$ and $\sum_{A\in\Theta} m(A) = 1$. According to the definition of credibility,

$$m\left(\phi/[x]_a\right) = \frac{\left|[x]_a \cap \phi\right|}{\left|[x]_a\right|} = 0,$$

$$\sum_{j=1}^{3} m\left(\frac{P_j}{[x]_a}\right) = \sum_{j=1}^{3} \frac{\left|[x]_a \cap P_j\right|}{\left|[x]_a\right|} = \frac{\left|[x]_a \cap (P_1 \cup P_2 \cup P_3)\right|}{\left|[x]_a\right|} = 1. \tag{22}$$

The credibility satisfies the above two constraints.

The credibility uses the value of each attribute and the decision result, that is, it makes full use of all the information in the information system. Therefore, the movement probability determined by evidence theory is more accurate.

The importance of different attributes to the decision maker is different. Considering the need for accuracy, the decision maker needs to consider the importance of different attributes when synthesizing the approximate movement probability. The attribute importance is taken as the weight factor, the greater the attribute's importance, the greater the weight of the mass function. The weight of the mass function under different attributes is represented by w_a.

Suppose that IS $= (U, C \cup D, V, f)$ is an information system, action strategies S derived in IS, the weight w_a of attribute a, and the mass function $m(P_j/[x]_a)$. The model of approximate movement probability assignment in three regions is as follows:

$$m\left(P_j\right) = \begin{cases} 0, & \dfrac{P_j}{[x]} = \phi, \\ \dfrac{\sum_{\cap P_j/[x]_a = P_j} \prod_{a\in C} w_a m\left(P_j/[x]_a\right)}{1 - \sum_{1\le i\le m} \prod_{a\in C} w_a m\left(P_j/[x]_a\right)}, & \dfrac{P_j}{[x]} \neq \phi. \\ \cap P_j/[x]_a = \phi & \end{cases} \tag{23}$$

The preferences of movement widely exist in the movement-based three-way decision. The preferences are often expressed in the form of probability. We analyze the probabilistic preference in the movement-based three-way decision. The evidence theory-based method is proposed to determine the probability of movement. The model uses all the information in the system and considers the importance of different attributes to improve the fusion results' reliability and objectivity. □

4.2. Optimal Action Strategy Selection. The movement-based three-way decision model aims to move objects from the unfavorable region to the favorable region. The movement of objects brings benefits and costs. We can select the optimal action strategy by analyzing the benefits and costs. However, the benefits and costs are difficult to determine. To select an optimal action strategy, we propose an action strategy selection method by analyzing the difference between the ideal movement and actual movement, the smaller the difference, the better the strategy. The ideal movement is determined by the decision maker, which can bring the highest utility.

Given the equivalence class $[x] = \{x_1, x_2, \ldots, x_n\}$ in the unfavorable region, the decision maker wants to move $[x]$ to a favorable region. We describe the equivalence class's probabilistic preference $[x]$ moving to three regions under the action strategy through a probability mass function. The probability mass function is the probability of a discrete random variable at each particular value. All values of the probability mass functions are nonnegative, and the sum of the probability is equal to 1.

For the equivalence class $[x]$, the probability mass function of moving to three regions under the action strategy is represented by

$$p_r = \{p(x_1), p(x_2), \ldots, p(x_n)\}. \tag{24}$$

For example, objects in the equivalence class $[x] = \{x_1, x_2, x_3, x_4, x_5\}$ are in P_3 region. After the action strategy, the distribution of objects in three regions is as follows:

$$\begin{aligned} P_1 &= \{x_1, x_3, x_4\}, \\ P_2 &= \{x_2\}, \\ P_3 &= \{x_5\}. \end{aligned} \tag{25}$$

The probability mass function of $[x]$ under the action strategy is $p_r = \{0.6, 0.2, 0.6, 0.6, 0.2\}$. It can be seen from the probability mass function that $p(P_1) + p(P_2) + p(P_3) = 0.6 + 0.2 + 0.2 = 1$. The probability mass function of ideal movement for decision maker is as follows:

$$p_e = \{p(x_1), p(x_2), \ldots, p(x_n)\}. \tag{26}$$

We use $u_{p_j}(x)$, $j = 1, 2, 3$, to represent the quality or utility of object x in different regions. So, the quality or utility of $[x]$ in three regions is represented as follows:

$$U([x]) = \left\{u_{P_j}(x_1), u_{P_j}(x_2), \ldots, u_{P_j}(x_n)\right\}. \quad (27)$$

Often objects have different utilities in different regions and have the same utility in the same region. For example, in an opinion poll, we usually divide voters into three types, those who support the candidate, those who oppose the candidate, and those who are neutral. The utility of the same type of voters is the same, and the utility of different types of voters is different. The utility of voters who support the candidate is more than the voters who neutral. The utility of voters who are neutral is more than voters who oppose the candidate.

The moment is the statistics commonly used. Moments of each order are often used to describe distribution characteristics. Moments have been fully applied in areas such as risk analysis and insurance dividends [58]. Suppose that X is a discrete random variable. We get the probability of all possible value of x, that is,

$$P(X = x_k) = p_k, \quad k = 1, 2, \ldots, n. \quad (28)$$

The mathematical expectation of X is expressed as $E(X)$ and the $k-$order moment of X is expressed as $E(X^k)$ $(k = 1, 2, \ldots, n)$. The first moment denotes the expectation and the second moment denotes the variance.

Given a discrete random variable X and its probability mass function $p(x)$, the moment generating function of [59] X is expressed as $M_X(t)$. The power series expansion of the function is as follows:

$$M_X(t) = \sum_{k=1}^{\infty} \frac{E\left(X^k\right)}{k!} t^k, \quad t \in R, \quad (29)$$

where $E(X)$ represents the expectation of the random variable X and $E(X^2)$ represents the variance of the random variable X. The moment generating function is a real-valued function of a random variable.

The optimal strategy not only has the highest expectations but also has the least uncertainty. Therefore, we use the first two order moments to construct the degree of difference between the ideal movement and the actual movement. The formula is as follows:

$$D\left(p_r \| p_e, S\right) = \left\{\sum_{k=1}^{2} \frac{\left[E\left(p_e^k\right) - E\left(p_r^k\right)\right]^2}{k!}\right\}^{1/2},$$
$$E\left(X^1\right) = \sum_{k=1}^{n} u_{P_j}(x_k) p(x_k), E\left(X^2\right) = \frac{\sum_{k=1}^{n}\left(u_{P_j}(x_k) - E\left(X^1\right)\right)^2}{n}, \quad (30)$$

where the first-order moment is the expectation and the second-order moment is the variance.

The proposed method selects an optimal action strategy by comparing the ideal movement and the actual movement, the smaller the difference, the better the strategy. The first moment compares the expectations between the ideal movement and the actual movement. The second-order moment compares the variance between the ideal movement and the actual movement. The framework can further consider the variance based on the expectations and help the decision maker select an optimal action strategy.

Finally, we summarize the key steps of approximate movement probability assignment and effectiveness measures framework for the trisecting-acting-outcome model. The specific procedure is given in Algorithm 2.

5. An Illustrative Example

In this section, we use an example of medical decision in Table 2 to illustrate the proposed method. There are 468 suspected patients and six symptoms or attributes. Chol, bp, and bs stand for cholesterol level, blood pressure, and blood sugar, respectively. The condition attributes are age, sex, chol, bp, and bs. The result is a decision attribute. Symbols "+," "−," and "?" stand for a suspected patient who has the disease, does not have the disease, and uncertain, respectively. For the convenience of representation, we divide objects into ten equivalence classes based on condition attributes. The right side of the decision attribute value indicates the number of objects in the equivalence class whose decision result is this type. For example, there are 50 objects in $[x]_1$, of which there are five objects with a decision result of "+," 30 objects with a decision result of "−," and 15 objects with a decision result of "?." We divide all objects into P_1, P_2, and P_3 according to the value "−," "+," and "?" of the decision attribute.

Taking $[x]_{10}$ as an example of the equivalence class that needs to be moved, from the information table, there are 105 objects in the equivalence class. Among them, 0 object does not have the disease, 100 objects have the disease, and 5 objects are uncertain. For diseased objects in $[x]_{10}$, action strategy are mined from the table according to equations (4)

Input: IDIS = $(U, C \cup D, V, f)$, P_1, P_2, P_3, and strategy set AS.
Output: effectiveness of strategy S.
(1) **for** $a \in A_f$ **do**
(2) Divide equivalence classes $[x]_a$.
(3) Calculate credibility cre_a under flexible attribute a.
(4) Assign weight for attribute a
(5) **end**
(6) Synthesize movement probability according to model of approximate movement probability assignment model $m(P_j)$.
(7) min difference = ∞.
(8) **for** $S \in$ AS **do**
(9) Formulate the probability quality function pe ideally expected by decision maker.
(10) Calculate the probability quality function pr according to model of approximate movement probability assignment.
(11) Calculate the degree of difference by $D(p_r \| p_e, S)$
(12) **if** $D(p_r \| p_e, S) \leq$ mindifference **then**
(13) min difference = $D(p_r \| p_e, S) \leq$
(14) **end**
(15) **end**

Algorithm 2: The algorithm for selecting an optimal action strategy.

Table 2: Table for medical decision-making.

	Age	Sex	chol	bp	bs	Result		
$[x]_1$	3	1	2	1	1	+= 5	−= 30	?= 15
$[x]_2$	3	0	2	2	2	+= 40	−= 5	?= 5
$[x]_3$	2	1	3	2	3	+= 30	−= 4	?= 6
$[x]_4$	3	0	2	3	2	+= 35	−= 10	?= 5
$[x]_5$	3	0	1	2	1	+= 15	−= 15	?= 20
$[x]_6$	1	1	3	2	2	+= 30	−= 6	?= 4
$[x]_7$	3	0	1	1	2	+= 2	−= 0	?= 0
$[x]_8$	3	0	1	2	3	+= 20	−= 10	?= 10
$[x]_9$	2	0	1	2	2	+= 30	−= 5	?= 6
$[x]_{10}$	3	0	3	3	3	+= 0	−= 100	?= 5

and (5), where age and sex are stable attributes and chol, bp, and bs are flexible attributes. The action strategy of $[x]_{10}$ is as follows:

$$\begin{aligned} S_1 &= \text{chol: } 3 \rightsquigarrow 2 \wedge \text{bp: } 3 \rightsquigarrow 2 \wedge \text{bs: } 3 \rightsquigarrow 2, \\ S_2 &= \text{chol: } 3 \rightsquigarrow 2 \wedge \text{bp: } 3 \rightsquigarrow 3 \wedge \text{bs: } 3 \rightsquigarrow 2, \\ S_3 &= \text{chol: } 3 \rightsquigarrow 2 \wedge \text{bp: } 3 \rightsquigarrow 2 \wedge \text{bs: } 3 \rightsquigarrow 1, \\ S_4 &= \text{chol: } 3 \rightsquigarrow 1 \wedge \text{bp: } 3 \rightsquigarrow 1 \wedge \text{bs: } 3 \rightsquigarrow 2, \\ S_5 &= \text{chol: } 3 \rightsquigarrow 1 \wedge \text{bp: } 3 \rightsquigarrow 2 \wedge \text{bs: } 3 \rightsquigarrow 3. \end{aligned} \tag{31}$$

Mining actionable rules in three regions and generating the corresponding strategy set $S = \{S_1, S_2, S_3, S_4, S_5\}$, calculate the credibility and coverage of each strategy in the strategy set, and the result is shown in Table 3.

Setting the credibility threshold to 0.5 and the coverage threshold to 0.1 to construct a three-way decision model for the strategy set, the model divides the strategy set into three regions POS, BND, and NEG through thresholds of accuracy and coverage. Each subset contains the following strategies:

$$\begin{aligned} \text{POS} &= \{S_1, S_2\}, \\ \text{BND} &= \{S_4, S_5\}, \\ \text{NEG} &= \{S_3\}. \end{aligned} \tag{32}$$

Table 3: Credibility and coverage of each strategy.

	S_1	S_2	S_3	S_4	S_5
cre	40/50	35/50	15/50	2/2	20/40
cov	40/207	35/207	15/207	2/207	20/207

The three regions have a partial order relationship of POS > BND > NEG. When the decision maker chooses a strategy, the strategy in the POS region is preferred. The accuracy of strategy S_4 is 1, but the coverage is 2/207. Two hundred and seven objects have no disease in the information system, but only two objects derived strategy S_4. This strategy is most likely a noise strategy that is affected by inconsistent information. This strategy is not helpful for the decision maker. Therefore, the strategy S_4 is effectively divided into the BND region. The strategy S_1 has an credibility of 40/50 and coverage of 40/207. Both credibility and coverage exceed the thresholds. Therefore, strategy S_1 is more effective and more reliable.

Both credibility and coverage are positive evaluation criteria, that is, the higher the value of two criteria, the better the strategy. This model can effectively avoid the influence of conflicting information for the decision maker. There are two action strategies in the POS region: S_1 and S_2. They both have high credibility and coverage. We select an optimal action strategy by the approximate movement probability assignment model and the effectiveness measures the framework.

The credibility of all flexible attributes of the strategies S_1 and S_2 in the POS region is used as a mass function. The approximate movement probability assignment is synthesized by the mass function under each flexible attributes. A total of 150 decision objects derived from strategy S_1 under the attribute chol, 80 of them do not have the disease, 45 of them have the disease, and 25 of them are uncertain. Strategy S_1 has a total of 261 objects under the attribute bp, 165 of them have not the disease, 45 of them have the disease, and 51 of them are uncertain. The strategy S_1 has a total of 183

objects under the attribute bs, 137 of them do not have the disease, 26 of them have the disease, and 20 are uncertain. The basic credibility allocation of strategy under the three attributes is shown in Table 4.

Given the flexible attribute chol, bp, and bs. The attribute weights are as follows:

$$w_{\text{chol}} = \frac{1}{3},$$
$$w_{\text{bp}} = \frac{1}{3}, \tag{33}$$
$$w_{\text{bs}} = \frac{1}{3}.$$

The approximate movement probability distribution of strategy S_1 is calculated by equation (23):

$$m(P_1) = \frac{\sum_{\cap P_1/[x]_a = P_1} \prod_{a\in C} w_a m(P_1/[x]_a)}{1 - \sum_{1\le i\le m \quad \cap P_1/[x]_a = \phi} \prod_{a\in C} w_a m(P_1/[x]_a)} = 0.96,$$

$$m((P_2) = \frac{\sum_{\cap P_2/[x]_a = P_2} \prod_{a\in C} w_a m(P_2/[x]_a)}{1 - \sum_{1\le i\le m \quad \cap P_2/[x]_a = \phi} \prod_{a\in C} w_a m(P_2/[x]_a)} = 0.03,$$

$$m((P_3) = \frac{\sum_{\cap P_3/[x]_a = P_3} \prod_{a\in C} w_a m(P_3/[x]_a)}{1 - \sum_{1\le i\le m \quad \cap P_3/[x]_a = \phi} \prod_{a\in C} w_a m(P_3/[x]_a)} = 0.01. \tag{34}$$

The basic credibility allocation of strategy S_2 under the three attributes is shown in Table 5. The approximate movement probability allocation of strategy S_2 is calculated by equation (23):

$$m(P_1) = \frac{\sum_{\cap P_1/[x]_a = P_1} \prod_{a\in C} w_a m(P_1/[x]_a)}{1 - \sum_{1\le i\le m \quad \cap P_1/[x]_a = \phi} \prod_{a\in C} w_a m(P_1/[x]_a)} = 0.74,$$

$$m(P_2) = \frac{\sum_{\cap P_2/[x]_a = P_2} \prod_{a\in C} w_a m(P_2/[x]_a)}{1 - \sum_{1\le i\le m \quad \cap P_2/[x]_a = \phi} \prod_{a\in C} w_a m(P_2/[x]_a)} = 0.25,$$

$$m((P_3) = \frac{\sum_{\cap P_3/[x]_a = P_3} \prod_{a\in C} w_a m(P_3/[x]_a)}{1 - \sum_{1\le i\le m \quad \cap P_3/[x]_a = \phi} \prod_{a\in C} w_a m(P_3/[x]_a)} = 0.01. \tag{35}$$

Table 4: Basic credibility assignment of strategy S_1.

	P_1	P_2	P_3
m(chol)	80/150	45/150	25/150
m(bp)	165/261	45/261	51/261
m(bs)	137/183	26/183	20/183

The probability quality function that the decision-maker ideal movement is pe and the probability quality of strategies S_1 and S_2 is pr_{S_1} and pr_{S_2}, respectively. Their utility is expressed as follows:

$$U_{\text{pe}}([x]_{10}) = \{\{u_{P_1}(x)\} \times 100, \{u_{P_2}(x)\} \times 0, \{u_{P_3}(x) \times 0\}\},$$
$$U_{\text{pr}_{S_1}}([x]_{10}) = \{\{u_{P_1}(x)\} \times 96, \{u_{P_2}(x)\} \times 3, \{u_{P_3}(x) \times 1\}\},$$
$$U_{\text{pr}_{S_2}}([x]_{10}) = \{\{u_{P_1}(x)\} \times 74, \{u_{P_2}(x)\} 25, \{u_{P_3}(x) \times 1\}\}. \tag{36}$$

In medical decision-making, the decision maker wants all objects in the diseased region to move to the disease-free region with appropriate action strategies, which will bring the greatest benefits to the decision-maker. The decision maker wants that the object in the diseased region in $[x]_{10}$ to move completely to the disease-free region with appropriate strategies. Therefore, the ideal probability distribution of the decision maker is recorded as $p_e = [1, 0, 0]$. Due to the influence of random errors in the actual cases, the strategy's effect is often difficult to meet the expectations of the decision maker. The above approximate movement probability allocation is used as its real movement probability distribution.

The objects in the P_1, P_2, and P_3 regions are assigned utility of 3, 1, and 2, respectively. That is to say, the utility of the object in the not disease region is 3, the utility of the object in the diseased region is 1, and the utility of the object in the uncertainty area is 2. According to equation (30), we can calculate the difference between the ideal expectation of the decision maker and strategy S_1:

$$D(p_r \| p_e), S_1) = \left\{ \sum_{k=1}^{2} \frac{\left[E(p_e^k) - E(p_r^k)\right]^2}{k!} \right\}^{1/2} = 0.1128. \tag{37}$$

The difference between the ideal expectation of the decision maker and strategy S_2 is as follows:

$$D(p_r \| p_e), S_2) = \left\{ \sum_{k=1}^{2} \frac{\left[E(p_e^k) - E(p_r^k)\right]^2}{k!} \right\}^{1/2} = 0.7357. \tag{38}$$

The degree of difference of S_1 is smaller, that is to say, the action strategy S_1 is more effective, with less uncertainty and more in line with the needs of the decision maker.

Table 5: Basic credibility allocation of strategy S_2.

	P_1	P_2	P_3
m (chol)	80/150	45/150	25/150
m (bp)	35/155	110/155	10/551
m (bs)	137/183	26/183	20/183

6. Conclusion

In this paper, we analyze the existence of conflicting information in a movement-based three-way decision. We construct a three-way decision model for the action strategy set by introducing the credibility and coverage. The model can effectively avoid the influence of conflicting information. To select an optimal action strategy, we analyzed the probabilistic preference in a movement-based three-way decision. An evidence-theory based method for determining the probability of movement has been proposed. The optimal action strategy can be selected by analyzing the difference between the ideal movement and the actual movement, the smaller the difference, the better the strategy. We illustrate the practicability of the proposed method through an example of medical decision-making. This model improves and enriches the movement-based three-way decision and widens its application range.

In future work, we will systematically study conflicting information in movement-based three-way decisions and establish a more effective evaluation framework to evaluate and select the optimal action strategy. Thresholds for credibility and coverage are given by expert experience, which is too subjective. In the future, we will study how to determine optimal thresholds. This paper only considers the case where the same region's objects have the same quality or utility. Therefore, the application of utility theory is also a future research direction.

Data Availability

All data, models, and code generated or used during the study are included within the article.

Conflicts of Interest

The authors declare that they have no conflicts of interest.

Acknowledgments

This work was supported in part by the Natural Science Foundation of Heilongjiang Province (LH2020F031).

References

[1] Y. Yao, "An outline of a theory of three-way decisions," in *Proceedings of the International Conference on Rough Sets and Current Trends in Computing*, pp. 1–17, Springer, Berlin, Germany, 2012.

[2] Y. Yao, "Three-way decision and granular computing," *International Journal of Approximate Reasoning*, vol. 103, pp. 107–123, 2018.

[3] C. Gao and Y. Yao, "Actionable strategies in three-way decisions," *Knowledge-Based Systems*, vol. 133, pp. 141–155, 2017.

[4] D. Liu and D. Liang, "Generalized three-way decisions and special three-way decisions," *Journal of Frontiers of Computer Science and Technology*, vol. 11, pp. 502–510, 2017.

[5] X. Deng and Y. Yao, "An information-theoretic interpretation of thresholds in probabilistic rough sets," in *Proceedings of the International Conference on Rough Sets and Knowledge Technology*, pp. 369–378, Springer, New York, NY, USA, 2012.

[6] Y. Zhang and J. Yao, "Gini objective functions for three-way classifications," *International Journal of Approximate Reasoning*, vol. 81, pp. 103–114, 2017.

[7] M. K. Afridi, N. Azam, and J. Yao, "Variance based three-way clustering approaches for handling overlapping clustering," *International Journal of Approximate Reasoning*, vol. 118, pp. 47–63, 2020.

[8] P. Wang, H. Shi, X. Yang, and J. Mi, "Three-way k-means: integrating k-means and three-way decision," *International Journal of Machine Learning and Cybernetics*, vol. 10, no. 10, pp. 2767–2777, 2019.

[9] H. Yu, Y. Chen, P. Lingras, and G. Wang, "A three-way cluster ensemble approach for large-scale data," *International Journal of Approximate Reasoning*, vol. 115, pp. 32–49, 2019.

[10] H. Yu, P. Jiao, Y. Yao, and G. Wang, "Detecting and refining overlapping regions in complex networks with three-way decisions," *Information Sciences*, vol. 373, pp. 21–41, 2016.

[11] H. Yu, Z. Liu, and G. Wang, "An automatic method to determine the number of clusters using decision-theoretic rough set," *International Journal of Approximate Reasoning*, vol. 55, no. 1, pp. 101–115, 2014.

[12] H. Yu, X. Wang, G. Wang, and X. Zeng, "An active three-way clustering method via low-rank matrices for multi-view data," *Information Sciences*, vol. 507, pp. 823–839, 2020.

[13] J. Qi, T. Qian, and L. Wei, "The connections between three-way and classical concept lattices," *Knowledge-Based Systems*, vol. 91, pp. 143–151, 2016.

[14] H. Zhi, J. Qi, T. Qian, and L. Wei, "Three-way dual concept analysis," *International Journal of Approximate Reasoning*, vol. 114, pp. 151–165, 2019.

[15] G. Lang, J. Luo, and Y. Yao, "Three-way conflict analysis: a unification of models based on rough sets and formal concept analysis," *Knowledge-Based Systems*, vol. 194, 2020.

[16] Y. Yao, "Three-way conflict analysis: reformulations and extensions of the pawlak model," *Knowledge-Based Systems*, vol. 180, pp. 26–37, 2019.

[17] M. K. Afridi, N. Azam, J. Yao, and E. Alanazi, "A three-way clustering approach for handling missing data using gtrs," *International Journal of Approximate Reasoning*, vol. 98, pp. 11–24, 2018.

[18] Y. Zhang and J. Yao, "Game theoretic approach to shadowed sets: a three-way tradeoff perspective," *Information Sciences*, vol. 507, pp. 540–552, 2020.

[19] J. Yao and N. Azam, "Web-based medical decision support systems for three-way medical decision making with game-theoretic rough sets," *IEEE Transactions on Fuzzy Systems*, vol. 23, pp. 3–15, 2014.

[20] X. Yang, T. Li, H. Fujita, D. Liu, and Y. Yao, "A unified model of sequential three-way decisions and multilevel incremental processing," *Knowledge-Based Systems*, vol. 134, pp. 172–188, 2017.

[21] X. Yang, T. Li, D. Liu, and H. Fujita, "A temporal-spatial composite sequential approach of three-way granular computing," *Information Sciences*, vol. 486, pp. 171–189, 2019.

[22] D. Liang, M. Wang, Z. Xu, and D. Liu, "Risk appetite dual hesitant fuzzy three-way decisions with todim," *Information Sciences*, vol. 507, pp. 585–605, 2020.

[23] M. Wang, D. Liang, and Z. Xu, "Sequential three-way multiple attribute group decisions with individual attributes and its consensus achievement based on social influence," *Information Sciences*, vol. 518, pp. 286–308, 2020.

[24] Y. Yao, "Three-way decisions with probabilistic rough sets," *Information Sciences*, vol. 180, no. 3, pp. 341–353, 2010.

[25] J. Qi, L. Wei, and Y. Yao, "Three-way formal concept analysis," in *Proceedings of the International Conference on Rough Sets and Knowledge Technology*, pp. 732–741, Springer, Berlin, Germany, 2014.

[26] H. Yu, C. Zhang, and G. Wang, "A tree-based incremental overlapping clustering method using the three-way decision theory," *Knowledge-Based Systems*, vol. 91, pp. 189–203, 2016.

[27] P. Wang and Y. Yao, "Ce3: a three-way clustering method based on mathematical morphology," *Knowledge-based Systems*, vol. 155, pp. 54–65, 2018.

[28] H. Li, L. Zhang, B. Huang, and X. Zhou, "Sequential three-way decision and granulation for cost-sensitive face recognition," *Knowledge-Based Systems*, vol. 91, pp. 241–251, 2016.

[29] L. Zhang, H. Li, X. Zhou, and B. Huang, "Sequential three-way decision based on multi-granular autoencoder features," *Information Sciences*, vol. 507, pp. 630–643, 2020.

[30] B. Zhou, Y. Yao, and J. Luo, "Cost-sensitive three-way email spam filtering," *Journal of Intelligent Information Systems*, vol. 42, no. 1, pp. 19–45, 2014.

[31] J. Xu, D. Miao, Y. Zhang, and Z. Zhang, "A three-way decisions model with probabilistic rough sets for stream computing," *International Journal of Approximate Reasoning*, vol. 88, pp. 1–22, 2017.

[32] H.-R. Zhang, F. Min, and B. Shi, "Regression-based three-way recommendation," *Information Sciences*, vol. 378, pp. 444–461, 2017.

[33] C. Jiang, Y. Duan, and J. Yao, "Resource-utilization-aware task scheduling in cloud platform using three-way clustering," *Journal of Intelligent & Fuzzy Systems*, vol. 37, no. 4, pp. 5297–5305, 2019.

[34] X. Deng and Y. Yao, "Decision-theoretic three-way approximations of fuzzy sets," *Information Sciences*, vol. 279, pp. 702–715, 2014.

[35] C. Jiang, D. Guo, Y. Duan, and Y. Liu, "Strategy selection under entropy measures in movement-based three-way decision," *International Journal of Approximate Reasoning*, vol. 37, 2020.

[36] C. Jiang and Y. Yao, "Effectiveness measures in movement-based three-way decisions," *Knowledge-Based Systems*, vol. 160, pp. 136–143, 2018.

[37] D. Q. Miao, Y. Zhao, Y. Y. Yao, H. X. Li, and F. F. Xu, "Relative reducts in consistent and inconsistent decision tables of the pawlak rough set model," *Information Sciences*, vol. 179, no. 24, pp. 4140–4150, 2009.

[38] Z. Pawlak, "Rough sets: theoretical aspects of reasoning about data," *Springer Science & Business Media*, vol. 9, 2012.

[39] Y. Yao, "Three-way decisions and cognitive computing," *Cognitive Computation*, vol. 8, no. 4, pp. 543–554, 2016.

[40] Y. Yao, "Set-theoretic models of three-way decision," *Granular Computing*, vol. 1–16, 2014.

[41] M. Hu and Y. Yao, "Structured approximations as a basis for three-way decisions in rough set theory," *Knowledge-Based Systems*, vol. 165, pp. 92–109, 2019.

[42] D. Liu and D. Liang, "Three-way decisions in ordered decision system," *Knowledge-Based Systems*, vol. 137, pp. 182–195, 2017.

[43] J. Luo, M. Hu, and K. Qin, "Three-way decision with incomplete information based on similarity and satisfiability," *International Journal of Approximate Reasoning*, vol. 2, 2020.

[44] M. Gao, Q. Zhang, F. Zhao, and G. Wang, "Mean-entropy-based shadowed sets: a novel three-way approximation of fuzzy sets," *International Journal of Approximate Reasoning*, vol. 13, 2020.

[45] X. R. Zhao and Y. Yao, "Three-way fuzzy partitions defined by shadowed sets," *Information Sciences*, vol. 497, pp. 23–37, 2019.

[46] D. Liang and D. Liu, "Deriving three-way decisions from intuitionistic fuzzy decision-theoretic rough sets," *Information Sciences*, vol. 300, pp. 28–48, 2015.

[47] D. Liang, Z. Xu, and D. Liu, "Three-way decisions with intuitionistic fuzzy decision-theoretic rough sets based on point operators," *Information Sciences*, vol. 375, pp. 183–201, 2017.

[48] Q. Zhang, F. Zhao, J. Yang, and G. Wang, "Three-way decisions of rough vague sets from the perspective of fuzziness," *Information Sciences*, vol. 50, 2020.

[49] J. Yang and Y. Yao, "Semantics of soft sets and three-way decision with soft sets," *Knowledge-Based Systems*, vol. 194, 2020.

[50] J. Kacprzyk, S. Zadrożny, and Z. W. Raś, "How to support consensus reaching using action rules: a novel approach," *International Journal of Uncertainty, Fuzziness and Knowledge-Based Systems*, vol. 18, no. 04, pp. 451–470, 2010.

[51] Z. W. Raś and A. Dardzińska, "From data to classification rules and actions," *International Journal of Intelligent Systems*, vol. 26, pp. 572–590, 2011.

[52] Y. Yao, "Tri-level thinking: models of three-way decision," *International Journal of Machine Learning and Cybernetics*, vol. 11, pp. 1–13, 2019.

[53] Y. Zhang, Z. Xu, H. Wang, and H. Liao, "Consistency-based risk assessment with probabilistic linguistic preference relation," *Applied Soft Computing*, vol. 49, pp. 817–833, 2016.

[54] J. Liu, X. Liao, and J.-B. Yang, "A group decision-making approach based on evidential reasoning for multiple criteria sorting problem with uncertainty," *European Journal of Operational Research*, vol. 246, no. 3, pp. 858–873, 2015.

[55] Y. Wang, Y. Dai, Y.-W. Chen, and F. Meng, "The evidential reasoning approach to medical diagnosis using intuitionistic fuzzy dempster-shafer theory," *International Journal of Computational Intelligence Systems*, vol. 8, no. 1, pp. 75–94, 2015.

[56] J. B. Yang and D. L. Xu, "On the evidential reasoning algorithm for multiple attribute decision analysis under uncertainty," *IEEE Transactions on Systems, Man, and Cybernetics-Part A: Systems and Humans*, vol. 32, pp. 289–304, 2002.

[57] L. Han and L. P. Shi, "Approach to evidence combination based on rough set," in *Proceedings of the 2009 International Conference on Electronic Computer Technology*, pp. 693–697, IEEE, New York, NY, USA, 2009.

[58] Y. Huang and W. Yu, "Studies on a double Poisson-geometric insurance risk model with interference," *Discrete Dynamics in Nature and Society*, vol. 2013, 2013.

[59] G. Tao, L. Han, and J. Song, "Divergence measure between the probability distributions based on moments," *Journal of Systems Science and Mathematical Sciences*, vol. 33, pp. 1071–1082, 2013.

Hindawi
Mathematical Problems in Engineering
Volume 2020, Article ID 6537048, 19 pages
https://doi.org/10.1155/2020/6537048

Research Article

Multiple Criteria Group Decision-Making Method with Dempster–Shafer Theory and Probabilistic Linguistic Term Sets

Yuanwei Du [1,2] **and Susu Wang** [1]

[1] *Management College, Ocean University of China, Qingdao 266100, China*
[2] *Marine Development Studies Institute of OUC, Key Research Institute of Humanities and Social Sciences at Universities, Ministry of Education, Qingdao 266100, China*

Correspondence should be addressed to Susu Wang; wangsusu@stu.ouc.edu.cn

Received 23 July 2020; Accepted 17 November 2020; Published 8 December 2020

Academic Editor: Zeshui Xu

The motivation of this study is to propose a novel multiple criteria group decision-making (MCDGM) method based on Dempster–Shafer theory (DST) and probabilistic linguistic term sets (PLTSs) to handle the distinctions between compensatory information at the criterion level and noncompensatory information at the individual level in the process of information fusion. Initially, the information at the individual level is extracted by BPA functions. Then, they are fused with DST considering ignorance and DMs' reliabilities. Next, the obtained BPA functions are transformed into interval-valued PLTSs with the assistance of intermediate belief and plausibility. Subsequently, the interval-valued PLTSs are converted into standard PLTSs. After normalization, the holistic PLTS is obtained with weighted addition operation and the round function is applied to determine the ultimate evaluation result. Finally, a case simulation study of evaluating the marine ranching ecological security is presented to verify and improve the validity and feasibility of the proposed method and algorithm in practical application. The proposed method and its relevant algorithm are both innovative combination of DST and PLTSs from the perspective of compensatory and noncompensatory features of information, which provides a new angle of view for the development of probabilistic preference theory and is beneficial to apply probabilistic preference theory in practice.

1. Introduction

Multiple criteria decision-making (MCDM) theory is composed of a series of methods that deal with alternative ranking or selection problems that are characterized by multiple attributes and conflicting noncommensurable objectives. Introduced in the 1950s [1, 2], MCDM has since received extensive attention from two kinds of methods: the multiple attribute decision-making (MADM) method and the multiple objective decision-making (MODM) method. MCGDM is an indispensable branch of modern decision-making theory. The representative methods of MCDM, such as multiobjective programming, analytic hierarchy process (AHP), ELimination Et Choice Translating REality (ELECTRE), and technique for order preference by similarity to an ideal solution (TOPSIS), have been applied in solving diversified practical MCDM problems [3–8]. As decision-making problems are getting more complicated, researchers have studied MCDM from the perspectives of utility achievement, weight determination, consistency measurement, fuzziness information, and so on [9–13].

MCDM methods usually comprehensively analyze MCDM problems from all angles. Their applications are achieved by balancing multiple attributes or objectives to find the best one among several given alternatives. In the implementation process of classical MCDM, an individual decision maker (DM) is the single source providing the decision information that involves all the factors and forms the final decision results. However, limited by the incomplete knowledge reserve, restricted ability of judgment, inadequate experience, and other such issues, an individual DM cannot provide sufficient valid information for today's

complex and synthetic MCDM. Consequently, multiple criteria group decision-making (MCGDM) methods [14–16] have been proposed to solve MCDM problems that arise under the group decision-making setting. The major MCGDM methods provide a basic framework for implementation that comprises extracting individual information first and then fusing it into group information. Here, two kinds of problems are of vital importance. One is about information expression and extraction, and the other is about information disposal and fusion. With respect to the former, existing literature has a lot of focus on enhancing the accuracy of the information given by each individual DM. Linguistic term, interval value, fuzzy number, membership, and other forms of information [17–20] are incorporated to facilitate DMs determining or expressing their preference. The information characteristics of uncertainty, fuzziness, and incompleteness [21–24] are also key concerns of MCGDM. With respect to the problem of information disposal and fusion, researchers have proposed several fusion methods to fuse individual information, such as the consensus model, fuzzy operators, Dempster–Shafer theory (DST), evidence reasoning (ER) approach, and probabilistic linguistic term set (PLTS) operations [25–27]. Different disposal and fusion processes usually cause different degrees of information loss, which affects the feasibility and validity of the decision results. To address this issue, several solutions, such as information conflict, reliability and weight of single information, consistency measure, and correlation measure [28–31] have been proposed in the published literature.

The motivation of this study is to propose a novel MCGDM method based on DST and PLTSs to overcome the problem of distinctions between information at different dimensions potentially disturbing the process of information fusion and thus influencing the final result of the MCGDM. These distinctions are performed since the information at the individual level is noncompensatory and that at the criterion level is compensatory in the process of information fusion. Note that MCGDM is the combination of MCDM and group decision making (GDM). In MCDM, the information at the criterion level is fused into a holistic score or value pertaining to the whole alternative, and according to this, the alternatives are ranked or selected [32]. In GDM, the final group decisions are derived through fusing information at the individual level [33]. The information involved in MCGDM is related to both the criterion and individual level. Therefore, the above distinctions should be considered carefully in MCGDM and distinct fusion rules corresponding to different information dimensions should be utilized.

In the process of implementing MCGDM, a set of criteria are selected to characterize the alternative in different aspects that are essential for the MCGDM problem [34]. For a specific MCGDM problem, the alternative always has good or poor performance (information at the criterion level) on different criteria with different weights, and these performances can compensate for each other [34–38] in additive fusion. Additive fusion is a process of trade-off where poor (good) performance on one criterion can be offset by good (poor) performance on other criteria [34] and performance on a high (low) weighted criterion can be offset by performance on a low (high) weighted criterion [36]. Consequently, the advantages or weaknesses of the alternative may not be revealed in the final comprehensive results [35]. Based on the above features, we believe that the fusion of information at the criterion level should follow compensatory strategies, which means that the holistic performance of the alternative is derived by adding performances on the criteria with equal or unequal weights [38]. In the published literature, common compensatory models are weighted additive, including but not limited to simple additive weighting (SAW), TOPSIS, AHP, and fuzzy AHP [39]. Among the existing compensatory methods, PLTSs [27] are an effective technique owing to their advantages of linguistic preference expression, probability measure, and multiple operations [40, 41]. PLTSs and its variants have solved various practical problems. For example, the reliable participant selection problem in mobile crowdsensing has been solved by a probabilistic linguistic VIKOR method based on TODIM [42], the edge node selection problem in edge computing has been solved using the probabilistic linguistic ELECTRE II method [43], and the problem of evaluating the Internet of things platforms has been solved using an integrated probabilistic linguistic MCDM method [44].

In addition to the criteria, individual DMs constitute another dimension in the process of MCGDM. DMs in a group are invited to give judgment information based on their preference about the performance of the alternative on a single criterion, and information at the individual level is then fused into group judgment information on a single criterion or an alternative (after information fusion at the criterion level). However, limited by different degrees of bounded rationality [38, 45], the information given by different DMs is usually uncertain and has different degrees of reliability, which is a key factor in the fusion of information at the individual level. When a DM is definitely reliable, their judgment information is assigned total belief in the process of fusion. If a DM is not entirely reliable, their judgment information is assigned a certain degree of belief instead of total belief in the process of information fusion. In other words, the fusion result is relative to the most reliable judgment and cannot be reserved by others [34, 37, 38]. Influenced by lower reliable information, information at the individual level is incomplete, and therefore, the compensatory strategies cannot be applied in the process of fusion [38]. Hence, noncompensatory strategies are employed. Compared with the analytic cognition in compensatory strategies, noncompensatory strategies are akin to intuitive cognition [46]. Noncompensatory strategies are more suitable for explaining DMs' decision-making behavior because of their lower computational demand and dependence on the most reliable information [36, 38]. In the published literature, classical noncompensatory models include conjunctive, disjunctive, elimination by aspects, lexicographic, and "take the best" [37]. DST [26, 47] is a superior method for noncompensatory strategies [48] because of its ability of expressing and fusing uncertain information. DST and its subsequent versions have been

employed to solve multiple practical problems, such as mapping flood susceptibility [49], predicting rolling bearing faults [50], and determining artificial recharge location [51], among others.

To sum up, compensatory and noncompensatory strategies are two indispensable information fusion strategies that are suitable when information belongs to different dimensions. However, the published MCGDM methods have not considered the distinctions between compensatory information at the criterion level in MCDM and noncompensatory information at the individual level in GDM, which could result in compromised decision validity and quality. As MCGDM problems are getting more and more complex, it is advisable and effective to choose both type of strategies in the process of information fusion. We propose a new MCGDM method that considers both compensatory and noncompensatory strategies. The rest of this paper is organized as follows. In Section 2, we introduce the background knowledge about DST and PLTSs. In Section 3, a novel MCGDM method is proposed considering both compensatory and noncompensatory strategies based on DST and PLTSs, and the corresponding algorithm is constructed. A case simulation study of evaluating marine ranching ecological security (MRES) is presented to test the scientific validity and practical feasibility of the proposed method and algorithm in Section 4. Section 5 concludes the paper.

2. Preliminaries

2.1. Dempster–Shafer Theory. DST is an uncertainty reasoning technique proposed by Dempster [47] and Shafer [26]. It can handle uncertain information at the individual level on the basis of a frame of discernment, which is composed of a set of mutually exclusive and collectively exhaustive propositions. The basic probability assignment (BPA) function is applied to extract the uncertain information.

Definition 1 (see [47]). Suppose a possible proposition is $\theta_n (n = 1, 2, \ldots, N)$, and each of the proposition is exclusive. Then, a finite nonempty exhaustive set of all propositions $\Theta = \{\theta_1, \ldots, \theta_N\}$ is called a frame of discernment, and its power set that consists of 2^N subsets of Θ is usually expressed as

$$P(\Theta) = 2^{\Theta} = \{\varnothing, \theta_1, \ldots, \theta_N, \{\theta_1, \theta_2\}, \ldots, \{\theta_{N-1}, \theta_N\}, \ldots, \{\theta_1, \ldots, \theta_{N-1}\}, \Theta\}. \tag{1}$$

Definition 2 (see [47]). Suppose θ is a nonempty subset of Θ, and its belief is $p(\theta)$. If the mapping function p: $2^{\Theta} \longrightarrow [0, 1]$ fulfills

$$\begin{cases} p(\theta) = 0, & \theta = \varnothing, \\ p(\theta) \geqslant 0, \sum_{\theta \subseteq \Theta} p(\theta) = 1, & \theta \neq \varnothing, \end{cases} \tag{2}$$

where $\varnothing$ represents the empty set, then $p(\theta)$ is called the BPA function. If $p(\theta) > 0$, θ is named a focal element. $p(\theta)$ is a basic probability that is assigned exactly to θ and not to any smaller subset.

Considering the situation that counterintuitive problems [52, 53] may impede the combination of evidences with the orthogonal sum operator in Dempster's rule, Shafer proposed a discounting method, named Shafer discounting, to solve these kinds of problems.

Definition 3 (see [26]). Suppose the belief distribution given by a piece of evidence e_i that points to a proposition θ is $p_{\theta,i}$, and w_i is the weight of evidence e_i that is used to discount $p_{\theta,i}$ with $0 \leq w_i \leq 1$, $\forall i$ and $\sum_{i=1}^{I} w_i = 1$. Then, the Shafer discounting can be defined to modify the BPA function for the evidence as follows.

$$m_i = \begin{cases} w_i p_{\theta,i}, & \theta \subset \Theta. \\ w_i p_{\theta,i} + (1 - w_i), & \theta = \Theta. \end{cases} \tag{3}$$

Definition 4 (see [26]). Suppose the discounted BPA functions of two pieces of evidence e_1 and e_2 are, respectively, m_1 and m_2 on Θ, and $\otimes$ is the orthogonal sum operator. For any $\theta \subseteq \Theta$, Dempster's rule is described as follows.

$$m_{\theta,e(2)} = [m_1 \otimes m_2](\theta) = \begin{cases} 0, & \theta = \varnothing, \\ \dfrac{\sum_{\theta' \cap \theta'' = \theta, \theta', \theta'' \subseteq \Theta} m_{\theta',1} m_{\theta'',2}}{1 - \sum_{\theta' \cap \theta'' = \varnothing, \theta', \theta'' \subseteq \Theta} m_{\theta',1} m_{\theta'',2}}, & \theta \subseteq \Theta. \end{cases} \tag{4}$$

A belief measure associated with the BPA function and composed of the belief function and the plausibility function is necessary. The belief function measures the total mass that must be allocated to the elements of a certain subset of Θ, and the plausibility function measures the maximal amount of mass that can be allocated to the elements of a certain subset of Θ.

Definition 5 (see [47]). Suppose $m(\theta)$ is a piece of BPA function on the frame of discernment Θ. Then, the belief

function and the plausibility function of a subset θ of Θ can be denoted by

$$\begin{cases} \mathrm{Bel}(\theta) = \sum_{\theta' \subseteq \theta} m(\theta'), \\ Pl(\theta) = \sum_{\theta' \cap \theta \neq \varnothing} m(\theta'), \end{cases} \tag{5}$$

where $Pl(\theta) \geq \mathrm{Bel}(\theta)$ and $Pl(\theta) = 1 - \mathrm{Bel}(\overline{\theta})$. $\overline{\theta}$ is the classical complement of θ. In equation (5), $\mathrm{Bel}(\theta)$ is known as the belief function that represents the lower limit of the belief level of θ, and $Pl(\theta)$ is known as the plausibility function that represents the upper limit of the belief level of θ. Therefore, the confidence interval $[\mathrm{Bel}(\theta), Pl(\theta)]$ can describe the uncertainty about θ, where $\mathrm{Bel}(\theta)$ and $Pl(\theta)$, respectively, describe the minimal and maximal uncertainty about θ.

2.2. Probabilistic Linguistic Term Sets. PLTSs [27] are an extension of hesitant fuzzy linguistic term sets (HFLTSs) [54] with the intention of providing a more convenient way for DMs to express their preference with probability. A series of operational laws and aggregation operations are also introduced to facilitate the fusion of information. We firstly introduce the definition of linguistic term sets (LTSs).

Definition 6 (see [55]). Let $S = \{s_\alpha | \alpha = 0, 1, \ldots, \tau\}$ be an LTS and s_α, $\alpha = 0, 1, \ldots, \tau$ be an optional value for a linguistic variable, where τ is a positive integer that represents the total number of the linguistic terms in the LTS. Then, we have

(1) The set ordering rule as $s_\alpha > s_\beta$, if $\alpha > \beta$.

(2) The negation operator defined as $\mathrm{neg}(s_\alpha) = s_\beta$, such that $\beta = \tau - \alpha$.

Actually, HFLTSs mainly consider the situation wherein DMs hesitate among several optional linguistic terms in the moment of making their decision. HFLTSs ignore the probabilistic messages associated with linguistic terms [27]. Therefore, PLTSs are proposed by introducing probabilistic messages in LTSs as follows.

Definition 7 (see [27]). Suppose $S = \{s_\alpha | \alpha = 0, 1, \ldots, \tau\}$ is an LTS. Then, its relative PLTS is denoted by

$$L(p) = \left\{ L^{(k)}\left(p^{(k)}\right) | L^{(k)} \in S, p^{(k)} \geq 0, \; k = 1, 2, \ldots, \#L(p), \; \sum_{k=1}^{\#L(p)} p^{(k)} \leq 1 \right\}, \tag{6}$$

where $L^{(k)}(p^{(k)})$ means that the associated probability of the kth linguistic term $L^{(k)}$ in $L(p)$ is $p^{(k)}$ and $\#L(p)$ is the total number of the linguistic terms in PLTS $L(p)$. It is worth noting that $\sum_{k=1}^{\#L(p)} p^{(k)}$ represents the degree of information completeness with respect to the probabilistic distribution on all possible linguistic terms. We have $\sum_{k=1}^{\#L(p)} p^{(k)} = 1$ under complete information, $\sum_{k=1}^{\#L(p)} p^{(k)} = 0$ under complete ignorance, and $0 < \sum_{k=1}^{\#L(p)} p^{(k)} < 1$ under partial ignorance, where the ignorance represented by $1 - \sum_{k=1}^{\#L(p)} p^{(k)}$ should be averagely assigned to all of the linguistic terms in $L(p)$.

The PLTSs in equation (6) are called standard PLTSs [56] with a certain point value of probability. The interval value of probability is more suitable for solving practical decision-making problems because of its consideration of DMs' vagueness. However, it is also less computable. Therefore, Gu et al. [56] provided a method for converting interval-valued PLTSs into standard PLTSs as follows.

Definition 8 (see [56]). Suppose an interval-valued PLTS is given as $L(p) = \{L^{(k)}[l^{(k)}, u^{(k)}] | L^{(k)} \in S, 0 \leq l^{(k)} \leq u^{(k)} \leq 1, k = 1, 2, \ldots, \#L(p)\}$. Then, the method for converting interval-valued PLTSs into standard PLTSs is denoted by

$$\overline{p}^{(k)} = \frac{\sum_{k=1}^{\#L(p)} u^{(k)} - 1}{\sum_{k=1}^{\#L(p)} u^{(k)} - \sum_{k=1}^{\#L(p)} l^{(k)}} \times l^{(k)} + \frac{1 - \sum_{k=1}^{\#L(p)} l^{(k)}}{\sum_{k=1}^{\#L(p)} u^{(k)} - \sum_{k=1}^{\#L(p)} l^{(k)}} \times u^{(k)}, \tag{7}$$

where $l^{(k)}$ and $u^{(k)}$ are, respectively, the lower limit and upper limit of the given interval value of probability. Obviously, standard PLTSs are special interval-valued PLTSs when $l^{(k)} = u^{(k)}$.

Certain problems are caused by the different numbers of linguistic terms in PLTSs. Therefore, an extension rule for PLTSs is introduced. The normalization of PLTSs to avoid information distortion [57] follows the rules of association and extension, as below.

Definition 9 (see [27]). If $0 < \sum_{k=1}^{\#L(p)} p^{(k)} < 1$, the associated PLTS $\dot{L}(p)$ of a given PLTS $L(p)$ is denoted by

$$\dot{L}(p) = \left\{ L^{(k)}\left(\dot{p}^{(k)}\right) | k = 1, 2, \ldots, \#L(p) \right\}, \tag{8}$$

where $\dot{p}^{(k)} = p^{(k)} / \sum_{k=1}^{\#L(p)} p^{(k)}$, $k = 1, 2, \ldots, \#L(p)$.

Definition 10 (see [27]). If $\#L_1(p) \neq \#L_2(p)$, where $\#L_1(p)$ and $\#L_2(p)$ are the numbers of linguistic terms in $L_1(p)$ and

$L_2(p)$ respectively, suppose $L_1(p)$ and $L_2(p)$ are two PLTSs given as $L_1(p) = \left\{L_1^{(k)}(p_1^{(k)}) \mid k = 1, 2, \ldots, \#L_1(p)\right\}$ and $L_2(p) = \left\{L_2^{(k)}(p_2^{(k)}) \mid k = 1, 2, \ldots, \#L_2(p)\right\}$. Then, we should choose a PLTS with the smaller number of linguistic terms between $L_1(p)$ and $L_2(p)$ and add $|\#L_1(p) - \#L_2(p)|$ linguistic terms to it. The added linguistic terms are the smallest one(s) in the chosen PLTS, and the corresponding probability is equal to zero.

The elements in a PLTS are often disordered, which may cause operational problems. Therefore, the following ordering rule is introduced.

Definition 11 (see [27]). Given a PLTS $L(p) = \{L^{(k)}(p^{(k)}) \mid k = 1, 2, \ldots, \#L(p)\}$, let $r^{(k)}$ be the subscript of the linguistic term $L^{(k)}$. Then, the ordered PLTS is obtained by arranging the elements in the normalized PLTS in accordance to the values of $r^{(k)}p^{(k)}$ in descending order.

Remark 1. Considering the situation wherein two or more elements in a PLTS have equal values of $r^{(k)}p^{(k)}$, a complement for the ordering rule as in Definition 11 is introduced. Generally, when the values of $r^{(k)}$ in $r^{(k)}p^{(k)}$ are unequal, the chosen elements in $L(p)$ are arranged according to the values of $r^{(k)}$ in descending order. Otherwise, the chosen elements in $L(p)$ are arranged according to the values of $p^{(k)}$ in descending order [57].

Based on the above definitions, some operations are defined as follows.

Definition 12 (see [27]). Given two ordered PLTSs $L_1(p)$ and $L_2(p)$, where $L_1(p) = \left\{L_1^{(k)}(p_1^{(k)}) \mid k = 1, 2, \ldots, \#L_1(p)\right\}$ and $L_2(p) = \left\{L_2^{(k)}(p_2^{(k)}) \mid k = 1, 2, \ldots, \#L_2(p)\right\}$, then the addition operation is defined as

$$L_1(p) \oplus L_2(p) = \cup_{L_1^{(k)} \in L_1(p), L_2^{(k)} \in L_2(p)} \left\{p_1^{(k)} L_1^{(k)} \oplus p_2^{(k)} L_2^{(k)}\right\}, \tag{9}$$

where $L_1^{(k)}$ and $L_2^{(k)}$ are the kth linguistic terms in $L_1(p)$ and $L_2(p)$, respectively, and the condition $\lambda_1 S_\alpha \oplus \lambda_2 S_\beta = S_{\lambda_1\alpha+\lambda_2\beta}$ is satisfied [58]. Then, the uniqueness of PLTSs compared with the ordinary LTSs, that is, probability, is not revealed. Zhang et al. [59] defined a new operation for normalized and ordered PLTSs as

$$L_1^{N(k_1)}(p) \oplus L_2^{N(k_2)}(p) = \cup \left\{L_3^{N(k_3)}\left(p_3^{N(k_3)}\right) \middle| \quad k_1 = 1, 2, \ldots, \#L_1^N(p), k_2 = 1, 2, \ldots, \#L_2^N(p)\right\}, \tag{10}$$

where $L_3^{N(k_3)} = L_1^{N(k_1)} \oplus L_2^{N(k_2)}$, $p_3^{N(k_3)} = p_1^{N(k_1)} p_2^{N(k_2)}$, $L_1^{(k_1)}$ and $L_2^{(k_2)}$ are the k_1th and k_2th linguistic terms in $L_1^{N(k_1)}(p)$ and $L_2^{N(k_2)}(p)$, respectively, and N in $L_1^{N(k_1)}$ represents that $L_1^{N(k_1)}$ is a normalized PLTS.

Virtual linguistic terms may exist when PLTSs satisfy $\lambda_1 S_\alpha \oplus \lambda_2 S_\beta = S_{\lambda_1\alpha+\lambda_2\beta}$. Then, the round function is as follows.

Definition 13. (see [57]). Given a PLTS $L(p) = \{L^{(k)}(p^{(k)}) \mid k = 1, 2, \ldots, \#L(p)\}$, the integer score (linguistic term) of $L(p)$ is denoted by

$$E(L(p)) = \text{round}(s_\alpha), \tag{11}$$

where $\alpha = \sum_{k=1}^{\#L(p)} r^{(k)}p^{(k)} / \sum_{k=1}^{\#L(p)} p^{(k)}$, $r^{(k)}$ is the subscript of the kth linguistic term $L^{(k)}$, and $\text{round}(s_\alpha)$ is the classical round function that is used to determine the linguistic term that nearest to s_α with the rounding-off method.

3. The Proposed Method

3.1. Extraction of Information. MCGDM is usually conducted by a group of DMs who evaluate a set of given alternatives according to their own preference, with the aim to seek a satisfactory alternative or alternative rank based on a common criteria system. The only information sources in MCGDM are the DMs in the group, who may come from various fields with different degrees of knowledge reserves, experience, and cognitive styles, leading to diverse judgment information at the beginning of the MCGDM. The judgment information is subjectively given by DMs with different degrees of epistemic uncertainty, which could generate inaccurate decisions. Therefore, considering the uncertainty along with the preference expression of DMs is of vital importance in the extraction of information. In this regard, the BPA function in DST is an appropriate tool for extracting information, as it provides a unified way to represent preference and model uncertainty [60, 61].

For a specific MCGDM problem of evaluating alternatives, we give the following description. In order to solve the MCGDM problem, a group of DMs are invited to make judgment about the alternative on each given criterion. The DM set and criterion set are denoted by $E = \{e_i \mid i = 1, 2, \ldots, I\}$ and $C = \{c_n \mid n = 1, 2, \ldots, N\}$, where I and N represent the number of DMs and criteria, respectively. A set of linguistic terms denoted by $\Theta = \left\{\theta_j \mid j = 1, 2, \ldots, J\right\}$ is given for facilitating DMs to make their judgment based on their own preference with uncertainty. θ_j refers to the jth linguistic term in the given J ones. Linguistic terms in Θ are actually a series of variable values expressed in a way that conforms to human language, and each of them is mutually exclusive and exhaustive. Therefore, Θ is a finite nonempty set, called the frame of discernment, according to Definition 1. Then, the preference information given by DM e_i on criterion c_n can be extracted by a piece of the individual BPA function satisfying Definition 2 as

$$P_i^n = \left\{ (\theta, p_i^n(\theta)) | p_i^n(\theta) \geq 0, \sum_{\theta \subseteq \Theta} p_i^n(\theta) = 1, \theta \subseteq \Theta \right\}, \quad (12)$$

where θ is an element of the power set of the frame of discernment $P(\Theta)$ as in equation (1) and $p_i^n(\theta)$ is the probability related to θ. In terms of extracting and expressing information at the individual level, the BPA function is more suitable than PLTSs to reflect the actual cognitive competence of the DMs. Since PLTSs can just reflect judgment using single linguistic term with associated probability, the BPA function additionally has the ability of presenting judgment information with local ignorance. As shown in equation (12), the value of θ describes the completeness of the DMs' recognition. When $\theta = \theta_j$ and $P_i^n = \{(\theta_j, p_i^n(\theta_j)) | p_i^n(\theta_j) = 1\}$, we believe that DM e_i has complete recognition about the alternative's performance on criterion c_n, and he/she can give a certain judgment with no ignorance [63]. When $\theta = \Theta$ and $P_i^n = \{(\Theta, p_i^n(\Theta)) | p_i^n(\Theta) = 1\}$, it is believed that DM e_i can recognize nothing about the alternative's performance on criterion c_n, and he/she makes judgment with global ignorance [62]. $P_i^n = \{(\theta, p_i^n(\theta)) | p_i^n(\theta) = 1\}$ means that DM e_i has incomplete recognition about the alternative's performance on criterion c_n, and he/she can make judgment with local ignorance [62]; that is, DM e_i believes that the alternative's performance on criterion c_n can be depicted by linguistic terms in θ, but he/she cannot decide which one in θ is the best. Equation (12) represents a more general case wherein DM e_i believes that the alternative's performance on criterion c_n can be depicted by θ with several different values, and he/she can give relative probabilities to each of them.

3.2. Fusion of Information at the Individual Level. With the application of the BPA function, the DMs' judgment information about the alternative's performance on each criterion with corresponding probability is obtained. Then, the information at the individual level needs to be fused to get the group judgment about the alternative's performance on each criterion. It is worth noting that the BPA functions from different DMs are always associated with different degrees of uncertainty caused by objective environmental factors, subjective cognitive factors, and other factors. Even though the BPA function has abilities to express the judgments of "uncertain" or "unaware," the uncertainty caused by differences among DMs still needs to be attended. Generally, the differences among DMs are reflected in various aspects of the DMs, such as knowledge, experience, background, and authority, resulting in different degrees of reliabilities that play an important role in the process of information fusion for a particular MCGDM problem. Accordingly, the reliability of a DM is a key factor that needs to be considered in the fusion of information at the individual level.

From a group point of view, the reliability of DM e_i actually measures the degree of influence brought by his/her individual BPA function on the group result relative to the BPA functions given by other DMs. However, as mentioned in Section 1, this kind of influence is dominant in the process of information fusion, and influence with a low degree of reliability cannot offset that with a high degree of reliability. In other words, the information at the individual level, which is formalized as the individual BPA function, is noncompensatory, and the group result depends more on the individual BPA function given by a DM with greater reliability. For example, in the problem of evaluating the school performance of a student by three teachers, the final evaluation result is usually influenced more by (or even determined by) the teacher who knows the evaluated student more because their judgment is considered the most reliable. Suppose that the three invited teachers are e_1, e_2, and e_3. Teachers e_2 and e_3 just have information about the evaluated student in terms of learning and activities, and their judgments are given with local ignorance as (poor, average) and average, respectively. Teacher e_1, who has more information about the evaluated student in terms of various aspects, gives judgment as poor because he/she knows about a punishment the evaluated student has received. As a result, the final evaluation result should be poor because the judgment given by the most reliable teacher e_1 has vote power. In this example, the information given by teacher e_1 has dominant influence on the evaluation result and cannot be compensated by information given by teachers e_2 and e_3. Similarly, the judgments given by each DM in an MCGDM problem are also noncompensatory. In this scenario, DST is an effective tool for handling noncompensatory information in a more rational way [63]. In DST, an evidence with 100% reliability is totally supported; thus, it can have dominant influence on the fusion result. Otherwise, residual supports are assigned on the frame of discernment [63], which makes it possible that the residual supports are assigned on any element in the frame of discernment rather than to compensate other evidences.

Consequently, we applied DST to fuse information at the individual level. Suppose that the reliability set of DMs is $R = \{r_i | i = 1, 2, \ldots, I\}$. Subsequently, the extracted individual BPA functions as in equation (12) are first discounted with Shafer's discounting by taking P_i^n and R into equation (3). The discounted individual BPA functions can be represented as

$$M_i^n = \left\{ (\theta, m_i^n(\theta)) | m_i^n(\theta) \geq 0, \sum_{\theta \subseteq \Theta} m_i^n(\theta) = 1, \theta \subseteq \Theta \right\}, \quad (13)$$

where $m_i^n(\theta)$ is the discounted probability associated with the linguistic terms in θ, and we have $m_i^n(\theta) = r_i p_i^n(\theta) + (1 - r_i)$ when $\theta = \Theta$; otherwise, $m_i^n(\theta) = r_i p_i^n(\theta)$.

Next, the discounted individual BPA functions are fused with Dempster's rule by taking M_i^n into equation (4). For any two given individual BPA functions from DM e_i and $e_{i'}$, the fusion formula is described as

$$m_{e(2)}^{n}(\theta) = \left[m_i^n \otimes m_{i'}^n\right](\theta) = \begin{cases} 0, & \theta = \varnothing, \\ \dfrac{\sum_{\theta' \cap \theta'' = \theta, \theta', \theta'' \subseteq \Theta} m_i^n(\theta') m_{i'}^n(\theta'')}{1 - \sum_{\theta' \cap \theta'' = \varnothing, \theta', \theta'' \subseteq \Theta} m_i^n(\theta') m_{i'}^n(\theta'')}, & \theta \subseteq \Theta. \end{cases} \tag{14}$$

Accordingly, I pieces of individual BPA functions as demonstrated in equation (12) given by DM $e_1, e_2, \ldots, e_I$ can be recursively fused into a group BPA function relative to criterion c_n. In the above process of applying DST, the reliabilities of DMs are used to discount the extracted information, where the dominant influences of DMs with higher reliabilities on the group BPA function are enhanced. Furthermore, the group judgment depends more on BPA functions with higher degrees of reliabilities under the application of the orthogonal sum operator in Dempster' rule. As a result, the influence of each individual BPA function on the group BPA function cannot compensate one another in the process of fusion, and the influences of the total reliable individual BPA functions could be entirely brought to the group BPA function with no discount. Eventually, the group BPA function relative to criterion c_n is derived based on noncompensatory strategies as follows.

$$M^n = M_1^n \otimes M_2^n \otimes \cdots \otimes M_I^n = \left\{ \left(\theta, m^n(\theta)\right) | m^n(\theta) \geq 0, \sum_{\theta \subseteq \Theta} m^n(\theta) = 1, \theta \subseteq \Theta \right\}. \tag{15}$$

3.3. Transformation from BPA Functions into PLTSs. Based on the demonstration of DST, we have obtained N pieces of group BPA functions that describe the group judgments about the alternative's performance on each criterion. In fact, the expression of information by the BPA functions facilitates handling uncertainty in DMs' judgments through assigning probabilities on the power set of the frame of discernment. When probabilities are assigned to single elements of the frame of discernment like θ_j, we believe that the judgment is precise with no ignorance. When probabilities are assigned to a subset including more than one element like θ, we believe that the judgment is "uncertain" with local ignorance. When probabilities are assigned to the frame of discernment itself like Θ, we believe that the judgment is "unaware" with global ignorance. However, these kinds of data make it difficult and complicated to fuse the group judgments on each criterion. As mentioned above, the information at the criterion level, that is, the group BPA functions demonstrated by equation (15), is actually compensatory in the process of fusion. Thus, the influence given by the group BPA function on some criterion can offset that given by others in the process of fusion. Therefore, the fusion result of the information at the criterion level can reflect the comprehensive performance on all criteria and needs to be obtained with the weighted additive fusion rule. The information expression form of the BPA function is not suitable for the weighted additive fusion rule because of its assignment of probabilities. In order to establish links between information at the criterion level (group BPA functions) and the application of the weighted additive operations, the transformation method is proposed to convert the group BPA functions as in equation (15) into a simple expression appropriate for compensatory model, such as PLTSs.

In general, the probability in the BPA function usually describes the support degree of a proposition obtained from DMs. The higher the degree of support, the more certain is the proposition. In other words, the probabilities in the BPA functions are actually a kind of representation of uncertainty arising from DMs' judgments. In DST, this kind of uncertainty is measured by two functions with respect to each single linguistic term, namely, the belief function and plausibility function, which separately measure the lowest and highest probability of the proposition being true [64]. By taking the group BPA function as in equation (15) into equation (5), we can derive the belief and plausibility of the group BPA function M^n as $\mathrm{Bel}_n(\theta_j)$ and $Pl_n(\theta_j)$, which, respectively, depict the lower and upper limits of probabilities relative to single linguistic term θ_j on criterion c_n. From the perspective of PLTSs, $\mathrm{Bel}_n(\theta_j)$ and $Pl_n(\theta_j)$ actually constitute the probability associated with linguistic term θ_j in the form of an interval value. For convenience, illustration, and understanding, we redefine the frame of discernment $\Theta = \left\{\theta_j | \, j = 1, 2, \ldots, J\right\}$ as an LTS $S = \left\{s_\alpha | \, \alpha = 0, 1, \ldots, \tau\right\}$ that satisfies Definition 6, where $s_0 = \theta_1$, $s_1 = \theta_2$, $\ldots$, $s_\tau = \theta_J$. $\mathrm{Bel}_n(\theta_j)$ and $Pl_n(\theta_j)$ are redefined as $l_n^{(k)}$ and $u_n^{(k)}$, which separately represent the lower and upper limits of probability relative to the kth linguistic term in LTS S on criterion c_n. Accordingly, the group BPA function M^n as in equation (15) can be transformed into a PLTS $L_n(p)$ as follows according to Definition 8.

$$L_n(p) = \left\{ L_n^{(k)}\left[l_n^{(k)}, u_n^{(k)}\right] | L_n^{(k)} \in S, \quad 0 \leq l_n^{(k)} \leq u_n^{(k)} \leq 1, k = 1, 2, \ldots, \#L_n(p) \right\}, \tag{16}$$

where $L_n^{(k)}$ represents the kth linguistic term relative to criterion c_n and $\#L_n(p)$ represents the number of linguistic terms in $L_n(p)$. Note that standard PLTSs are a special case of interval-valued PLTSs as in equation (16) when $l_n^{(k)} = u_n^{(k)}$.

3.4. Fusion of Information at the Criterion Level. The obtained group judgments, which are demonstrated in the form of interval-valued PLTSs on each criterion, need to be further fused to derive the holistic judgment about the whole alternative. As mentioned in Section 1, the group judgments on each criterion are actually information at the criterion level and compensatory to each other. For the whole alternative or the MCGDM problem, each criterion is selected according to a set of principles, such as systematic, typical, scientific, and comprehensive, so that the constructed criterion system can consider aspects that are integrated and valid enough for describing the MCGDM problem. In other words, each criterion in an MCGDM problem describes an essential aspect of the alternative, and the final decision is made by comprehensively combining the alternative's performance on all aspects, which is a process of trade-off. For example, in the problem of evaluating a student from the aspects of academic record (c_1), student leader work (c_2), and activity achievements (c_3), bad performance on one aspect can usually be compensated by good work on other aspects because the school always train students following the principle of integrated development and any single aspect cannot decide the evaluation results. After a trade-off, a student with good performance on criterion c_1, excellent performance on criterion c_2, and poor performance on criterion c_3 may be evaluated as a good student because of the mutual compensation of performance on each aspect. Similarly, the information at the criterion level in an MCGDM problem is also compensatory. Therefore, the obtained PLTSs on each criterion as in equation (16) need to be fused into a holistic result in accordance with compensatory strategies.

As demonstrated in equation (16), the obtained PLTSs contain the information of criterion c_n, associated linguistic term $L_n^{(k)}$, and its corresponding interval value of probability $[l_n^{(k)}, u_n^{(k)}]$. As mentioned above, the interval value of probability is more suitable to demonstrate the vagueness of the linguistic term. However, it is not applicable for fusion operations on PLTSs. In order to solve this problem, several researchers have made strong attempts [65–67] by introducing new aggregation operators and comparison laws for interval values, which provide new calculation methods to accommodate the vagueness of linguistic terms and complicated calculations. We believe that the method as in equation (7) proposed by Gu et al. [56] is simple and applicable to deal with interval-valued probability. Additionally, it should be noticed that the situation of $\mathrm{Bel}_n(\theta_j) = Pl_n(\theta_j)$ actually exists in practice when DMs only definitely assign the probabilities with no ignorance on single elements of the frame of discernment rather than any subset including more than one element. Thus, it is possible to have $l_n^{(k)} = u_n^{(k)}$ when the interval value of probability in the PLTSs can be regarded as a certain point value, that is, $\overline{p}_n^{(k)} = (l_n^{(k)} + u_n^{(k)})/2$. Equation (7) does not work under this circumstance. Accordingly, the obtained interval values of probabilities in the PLTSs are first converted into equivalent certain point values of probabilities as follows.

$$\overline{p}_n^{(k)} = \begin{cases} \dfrac{l_n^{(k)} + u_n^{(k)}}{2}, & l_n^{(k)} = u_n^{(k)}, \\ \dfrac{\sum_{k=1}^{\#L_n(p)} u_n^{(k)} - 1}{\sum_{k=1}^{\#L_n(p)} u_n^{(k)} - \sum_{k=1}^{\#L_n(p)} l_n^{(k)}} \times l_n^{(k)} + \dfrac{1 - \sum_{k=1}^{\#L_n(p)} l_n^{(k)}}{\sum_{k=1}^{\#L_n(p)} u_n^{(k)} - \sum_{k=1}^{\#L_n(p)} l_n^{(k)}} \times u_n^{(k)}, & l_n^{(k)} \neq u_n^{(k)}. \end{cases} \tag{17}$$

Hence, the interval-valued PLTSs as in equation (16) can be converted into standard PLTSs as $L_n(\overline{p}) = \{L_n^{(k)}(\overline{p}_n^{(k)}) | L_n^{(k)} \in S, \quad \overline{p}_n^{(k)} \geq 0, \quad k = 1, 2, \ldots, \#L_n(\overline{p}), \sum_{k=1}^{\#L_n(\overline{p})} \overline{p}_n^{(k)} = 1\}$. Afterwards, the procedure of fusing information at the criterion level can be implemented through normalization of the standard PLTSs $L_n(\overline{p})$. In conformity to the procedure of normalization of PLTSs, association and extension need to be carried out. However, the situation explained in Definition 9 is out of consideration here because $\#L_n(p) = \#L_n(\overline{p})$ and $\sum_{k=1}^{\#L_n(\overline{p})} \overline{p}_n^{(k)} = 1$, which can be easily proven. Therefore, there is no need for association. Then, the PLTSs $L_n(\overline{p})$ need to be extended according to Definition 10. The probabilities assigned on the added linguistic terms are zero. Then, the extended PLTSs are arranged according to the value of $r_n^{(k)} \overline{p}_n^{(k)}$ in descending order, where $r_n^{(k)}$ is the subscript of linguistic term $L_n^{(k)}$ (see Definition 11). As a result, the normalized and ordered PLTSs are obtained as

$$\overline{L}_n(\overline{p}) = \left\{ \overline{L}_n^{(k)}\left(\overline{p}_n^{(k)}\right) | \overline{L}_n^{(k)} \in S, \overline{p}_n^{(k)} \geq 0, \quad k = 1, 2, \ldots, \#\overline{L}_n(\overline{p}), \sum_{k=1}^{\#\overline{L}_n(\overline{p})} \overline{p}_n^{(k)} = 1 \right\}. \tag{18}$$

Subsequently, we need to choose an operation to derive the fusion result of information at the criterion level, where the weight of the criterion is also a necessary factor that has substantial effect on the fusion result. Therefore, we apply the redefined addition operation [19] to fuse the normalized and ordered PLTSs. Let $W = \{w_n | 0t \le nw_n q \le h1, x \sum_{n=1}^{N} w_n = C1;, n = 1, 2, \ldots, N\}$ be the weight set corresponding to criterion set $C = \{c_n | n = 1, 2, \ldots, N\}$. Then, any two given PLTSs $\overline{L}_n(\overline{p})$ and $\overline{L}_{n'}(\overline{p})$ satisfy $w_n S_\alpha \oplus w_{n'} S_\beta = S_{w_n \alpha + w_{n'} \beta}$, $\alpha, \beta = 0, 1, \ldots, \tau$. Based on Definition 12, the weighted addition operation of any two given PLTSs $\overline{L}_n(\overline{p})$ and $\overline{L}_{n'}(\overline{p})$ is as follows.

$$w_n \overline{L}_n^{(k_n)}(\overline{p}) \oplus w_{n'} \overline{L}_{n'}^{\left(k_{n'}\right)}(\overline{p}) = \cup \left\{ \overline{L}_\delta^{(k_\delta)} \left(\overline{p}_\delta^{(k_\delta)} \right) \middle| \quad k_n = 1, 2, \ldots, \#\overline{L}_n(\overline{p}), k_{n'} = 1, 2, \ldots, \#\overline{L}_{n'}(\overline{p}) \right\}, \tag{19}$$

where

$$\begin{cases} \overline{L}_\delta^{(k_\delta)} = w_n L_n^{(k_n)} \oplus w_{n'} L_{n'}^{\left(k_{n'}\right)}, \\ \overline{p}_\delta^{(k_\delta)} = \overline{p}_n^{(k_n)} \overline{p}_{n'}^{\left(k_{n'}\right)}, \end{cases} \tag{20}$$

in which $\overline{L}_\delta^{(k_\delta)}$, $k_\delta = 1, 2, \ldots, \#\overline{L}_\delta(\overline{p})$ represents the k_δth linguistic term in the fusion result of PLTSs $\overline{L}_1(\overline{p})$ and $\overline{L}_2(\overline{p})$. The value of $\overline{L}_\delta^{(k_\delta)}$ is calculated by $w_n L_n^{(k_n)} \oplus w_{n'} L_{n'}^{\left(k_{n'}\right)}$, which obeys the rule $w_n S_\alpha \oplus w_{n'} S_\beta = S_{w_n \alpha + w_{n'} \beta}$, $\alpha, \beta = 0, 1, \ldots, \tau$. $\overline{p}_\delta^{(k_\delta)}$ is the probability relative to the linguistic term $\overline{L}_\delta^{(k_\delta)}$ in the fusion result, which is determined based on the redefined addition operation as in equation (10). For convenience of understanding, here we introduce a simple example to illustrate.

Example 1. Given two PLTSs demonstrated by equation (18) as $\overline{L}_1(\overline{p}) = \{(s_0, 0.1), (s_1, 0.3), (s_2, 0.6)\}$ and $\overline{L}_2(\overline{p}) = \{(s_0, 0.4), (s_1, 0.3), (s_2, 0.3)\}$ and their respective weights as $w_1 = 0.3$ and $w_2 = 0.7$, the calculation of fusing these two PLTSs by equations (19) and (20) is as follows.

$$\begin{aligned} w_1 \bar{L}_1(\bar{p}) \oplus w_2 \bar{L}_2(\bar{p}) = & \{(s_{0.3\times0+0.7\times0}, 0.1 \times 0.4), (s_{0.3\times0+0.7\times1}, 0.1 \times 0.3), (s_{0.3\times0+0.7\times2}, 0.1 \times 0.3), (s_{0.3\times1+0.7\times0}, 0.3 \times 0.4), \\ & (s_{0.3\times1+0.7\times1}, 0.3 \times 0.3), (s_{0.3\times1+0.7\times2}, 0.3 \times 0.3), (s_{0.3\times2+0.7\times0}, 0.6 \times 0.4), (s_{0.3\times2+0.7\times1}, 0.6 \times 0.3), \\ & (s_{0.3\times2+0.7\times2}, 0.6 \times 0.3)\} \\ = & \{(s_2, 0.18), (s_{1.3}, 0.18), (s_{1.7}, 0.09), (s_{0.6}, 0.24), (s_1, 0.09), (s_{1.4}, 0.03), (s_{0.3}, 0.12), (s_{0.7}, 0.03), (s_0, 0.04)\}. \end{aligned} \tag{21}$$

Subsequently, the information at the criterion level is fused into a piece of holistic PLTS relative to the whole alternative by recursively repeating the fusion as in equations (19) and (20) for $N - 1$ times, where the weight of each intermediate PLTS should be determined carefully. Suppose w_Δ is the weight of the intermediate PLTS that is the fusion result of the first few PLTSs. Initially, for $n = 1$, we have $w_\Delta = 0$ and then $\widehat{L}^{(k)} = \overline{L}_1^{(k_1)}$, $\widehat{p}^{(k)} = \overline{p}_1^{(k_1)}$. Then, for $n = 2$, we conduct the first fusion and have $w_\Delta = w_1$, and $\widehat{L}^{(k)} = w_\Delta \widehat{L}^{(k)} \oplus w_2 \overline{L}_2^{(k_2)}$, $\widehat{p}^{(k)} = \widehat{p}^{(k)} \overline{p}_2^{(k_2)}$. For $n = 3$, we conduct the second fusion and have $w_\Delta = w_\Delta + w_2$, and $\widehat{L}^{(k)} = w_\Delta \widehat{L}^{(k)} \oplus w_3 \overline{L}_3^{(k_3)}$, $\widehat{p}^{(k)} = \widehat{p}^{(k)} \overline{p}_3^{(k_3)}$. In general, for $\forall n = 2, \ldots, N$, we have $w_\Delta = w_\Delta + w_{n-1}$, and $\widehat{L}^{(k)} = w_\Delta \widehat{L}^{(k)} \oplus w_n \overline{L}_n^{(k_n)}$, $\widehat{p}^{(k)} = \widehat{p}^{(k)} \overline{p}_n^{(k_n)}$. Finally, the obtained holistic PLTS that describes the group judgment on all criteria is denoted by

$$\widehat{L}(\widehat{p}) = w_1 \overline{L}_1(\overline{p}) \oplus w_2 \overline{L}_2(\overline{p}) \oplus \cdots \oplus w_N \overline{L}_N(\overline{p}) = \left\{ \widehat{L}^{(k)} \left(\widehat{p}^{(k)} \right) \middle| \quad \widehat{L}^{(k)} \in S, \widehat{p}^{(k)} \ge 0, k = 1, 2, \ldots, \#\widehat{L}(\widehat{p}) \right\}. \tag{22}$$

Obviously, virtual linguistic terms may exist in $\widehat{L}(\widehat{p})$ (see Example 1). The ultimate result of MCGDM is calculated by taking $\widehat{L}(\widehat{p})$ into equation (11), and we have $\alpha = \sum_{k=1}^{\#\widehat{L}(p)} \widehat{r}^{(k)} \widehat{p}^{(k)} / \sum_{k=1}^{\#\widehat{L}(p)} \widehat{p}^{(k)}$, where $\widehat{r}^{(k)}$ is the subscript of the kth linguistic term $\widehat{L}^{(k)}$ in holistic PLTS $\widehat{L}(\widehat{p})$, and $\widehat{p}^{(k)}$ is its associated probability. Let the ultimate result of the MCGDM be s^*. Then, $s^* = \text{round}(s_\alpha)$ is the linguistic term that is nearest to s_α.

Example 2. Considering the situation that the criterion set is $C = \{c_1, c_2\}$ and the holistic PLTS is obtained as in Example

1, then the integer score of $\widehat{L}(\widehat{p})$ is calculated by $E(\widehat{L}(\widehat{p})) = \text{round}(s_\alpha)$, where

$$\alpha = \frac{0 \times 0.04 + 0.7 \times 0.03 + 1.4 \times 0.03 + 0.4 \times 0.12 + 1 \times 0.09 + 1.7 \times 0.09 + 0.6 \times 0.24 + 1.3 \times 0.18 + 2 \times 0.18}{0.04 + 0.03 + 0.03 + 0.12 + 0.09 + 0.09 + 0.24 + 0.18 + 0.18} = 1.092. \quad (23)$$

Thus, we have $s^* = \text{round}(s_{1.092}) = s_1$.

3.5. MCGDM Process and Algorithm. For convenience of illustration, the operational process of the proposed method is summarized in Figure 1. In summary, we present a novel MCGDM method using DST and PLTSs for distinguishing the noncompensatory information at the individual level and compensatory information at the criterion level in the process of information fusion. Firstly, the extraction of information based on the BPA function in DST is introduced considering ignorance that exists in DMs' judgments. Then, DST is applied to discount and obtain the group judgment on each criterion, where the reliabilities of DMs are considered. The information at the individual level is fused based on the noncompensatory strategy. In order to establish links between the group judgment formed in the group BPA function and the compensatory fusion strategy for information at the criterion level, we propose a transformation from BPA functions into PLTSs based on the belief and plausibility function in DST. Consequently, we obtain the information at the criterion level, which is in the form of interval-valued PLTSs. Thus, a method for converting interval-valued PLTSs into standard PLTSs is constructed. Finally, the standard PLTSs on each criterion are fused into a holistic PLTS with weighted addition operations, and the final MCGDM result is determined based on the round function. To facilitate practical demonstration, the above process is simplified as in the following Algorithm 1.

4. Case Simulation Study

In order to verify and improve the scientific validity and practical feasibility of the proposed method and algorithm, we give a case simulation study of evaluating marine ranching ecological security in this section to offer a simulative demonstration of the proposed MCGDM method. According to the definition given by the Chinese Academy of Aquatic Sciences, marine ranching is a fishery mode based on the principle of marine organisms to breed, grow bait, or avoid enemies, through releasing artificial reefs and stock enhancement. It is conductive to increase and protect fishery resources, improve the marine ecological environment, and realize sustainable utilization of fishery resources [57] (Aquatic Industry SC/T9111-2017). As a fishery mode that safeguards economic, social, and environmental revenue, marine ranching has received substantial attention in terms of various aspects, especially MRES. The objective of the case simulation study is to evaluate the MRES of a marine ranch by applying the proposed method and algorithm.

MRES is a kind of integral balance of the marine resources, marine environment, fishery activities, and other human activities. In order to keep this kind of balance, humans perform actions of releasing artificial reef and cultivating seaweed and other measures to develop a habitat for the target species. Other environmental actions are also taken to protect and improve the marine ranching ecosystem. Enhancement of fishery resources and sustainable increase of the fishery output are two main components of MRES. Consequently, we believe that the problem of evaluating MRES of a specific marine ranch includes five indispensable criteria: special funds acquisition and management (c_1), cost and profit of the marine ranch (c_2), monitoring system and regular inspections (c_3), main biomass index (c_4), and seawater and seaweed bed quality (c_5). Suppose five DMs, namely, marine environmental monitoring technician (e_1), aquaculture expert (e_2), manager of the evaluated marine ranching (e_3), marine environment and resource specialist (e_4), and local governmental personnel (e_5), are invited to participate in the evaluation of MRES. We denote the criterion set and DM set by $C = \{c_n | n = 1, 2, \ldots, 5\}$ and $E = \{e_i | i = 1, 2, \ldots, 5\}$. Correspondingly, the weight set of the criteria and reliability set of the DMs are obtained as $W = (0.150, 0.050, 0.100, 0.400, 0.300)$ and $R = (0.680, 0.920, 0.600, 1.000, 0.800)$, respectively. The DMs need to make judgment about the performance of the specific marine ranch on each criterion based on the given frame of discernment that includes three linguistic terms: $\Theta = (\theta_1 = \text{bad}, \theta_2 = \text{average}, \theta_3 = \text{good})$.

4.1. Extracting Information from the Five DMs. Based on the above description, the individual information on each criterion given by each DM is extracted with the BPA function as in equation (12), as shown in Table 1.

It is clearly shown in Table 1 that DMs $e_1, e_2, \ldots, e_5$ give their judgments about the MRES performance of the evaluated marine ranch on five criteria relative to the power set of frame of discernment with probabilities. For example, the extracted information given by DM e_1 on criterion c_1 can be expressed as $P_1^1 = \{(\theta_2, 0.300), (\theta_3, 0.600), (\Theta, 0.100)\}$, which means that DM e_1 believes that the MRES performance of the evaluated marine ranch on criterion c_1 has 30% probability to be average (θ_2), 60% probability to be good (θ_3), and 10% probability that the DM cannot make judgment with global ignorance. As another example, DM e_5 believes that the MRES performance of the evaluated marine ranch on criterion c_2 can be evaluated as average (θ_2) or good (θ_3); he/she only has 10% probability to hold average (θ_2). For the remaining 90% probability, he/she cannot

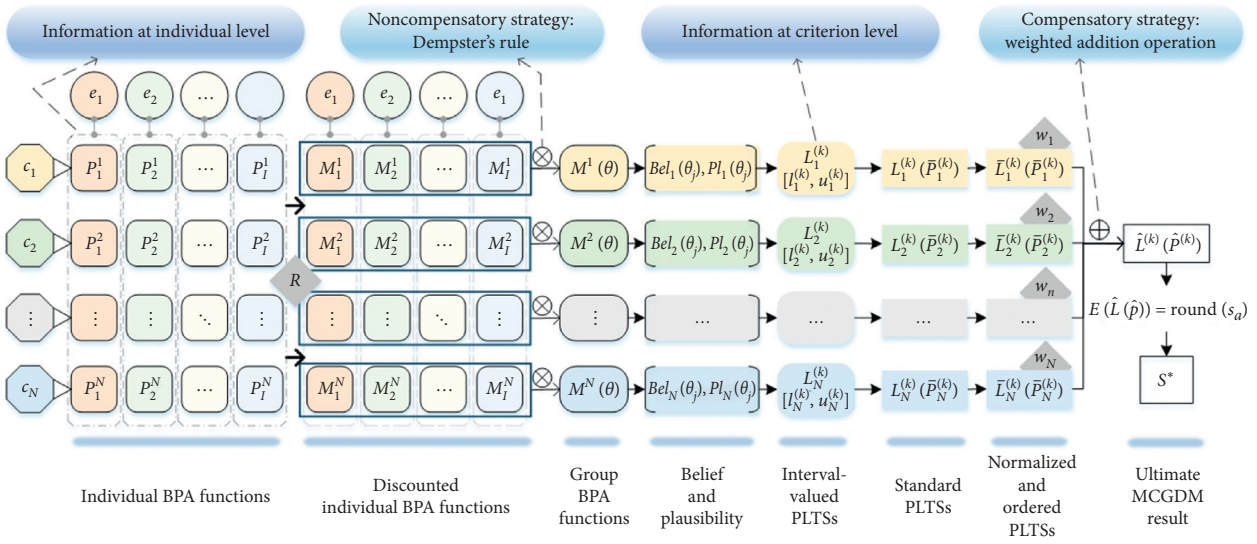

Figure 1: Operational process of the proposed method.

Input: extracted information from DM e_i on criterion c_n named P_i^n, $\forall i, n$, the DMs' reliability set R, and the criteria weight set W.
Output: the ultimate linguistic term s^*
Begin
% Fusion of information at the individual level based on noncompensatory strategies
  % Discount the individual BPA functions with Shafer discounting
  For $i = 1$ to I
    If $\theta = \Theta$
      Then $m_i^n(\theta) = r_i p_i^n(\theta) + (1 - r_i)$
      Else $m_i^n(\theta) = r_i p_i^n(\theta)$
    EndIf
  EndFor
  % Fuse the discounted individual BPA functions with Dempster's rule
  For $n = 1$ to N
    If $\theta = \varnothing$
      Then $m^n(\theta) = 0$
      Else $m^n(\theta) = m_1^n(\theta)$
      For $i = 2$ to I
        $m^n(\theta) = \sum_{\theta' \cap \theta'' = \theta, \theta', \theta'' \subseteq \Theta} m_i^n(\theta') m_{i'}^n(\theta'') / [1 - \sum_{\theta' \cap \theta'' = \varnothing, \theta', \theta'' \subseteq \Theta} m_i^n(\theta') m_{i'}^n(\theta'')]$
      EndFor
    EndIf
  EndFor
% Transformation from BPA function into PLTSs
  % Calculate the belief and plausibility of the group BPA functions
  For $n = 1$ to N
    For $j = 1$ to J
      $\mathrm{Bel}_n(\theta_j) = \sum_{\theta' \subseteq \theta_j} m^n(\theta')$
      $Pl_n(\theta_j) = \sum_{\theta' \cap \theta_j \neq \varnothing} m^n(\theta')$
    EndFor
  EndFor
  % Define the LTS and interval-valued probabilities
  For $\alpha = 0$ to τ
    $s_\alpha = \theta_{j-1}$
    $S = \{s_\alpha | \alpha = 0, 1, \ldots, \tau\} \Longleftrightarrow \Theta = \{\theta_j | j = 1, 2, \ldots, J\}$
    For $n = 1$ to N
      $[l_n^{(k)}, u_n^{(k)}] \Longleftrightarrow [Bel_n(\theta_j), Pl_n(\theta_j)]$
      % Form the interval-valued PLTSs
      $L_n(p) = \{L_n^{(k)}([l_n^{(k)}, u_n^{(k)}]) | L_n^{(k)} \in S, 0 \leq l_n^{(k)} \leq u_n^{(k)} \leq 1, k = 1, 2, \ldots, \#L_n(p)\}$
    EndFor

Algorithm 1: Continued.

EndFor
% Fuse information at the criterion level based on compensatory strategies
% Convert interval-valued PLTSs into standard PLTSs
For $n = 1$ to N
For $k = 1$ to $\#L_n(p)$
If $l_n^{(k)} = u_n^{(k)}$
Then $\overline{p}_n^{(k)} = (l_n^{(k)} + u_n^{(k)})/2$
Else $\overline{p}_n^{(k)} = l_n^{(k)} \times [\sum_{k=1}^{\#L_n(p)} u_n^{(k)} - 1]/[\sum_{k=1}^{\#L_n(p)} u_n^{(k)} - \sum_{k=1}^{\#L_n(p)} l_n^{(k)}] + u_n^{(k)} \times [1 - \sum_{k=1}^{\#L_n(p)} l_n^{(k)}]/[\sum_{k=1}^{\#L_n(p)} u_n^{(k)} - \sum_{k=1}^{\#L_n(p)} l_n^{(k)}]$
EndIf
EndFor
% Extend and arrange the linguistic terms in standard PLTSs and form the normalized and ordered PLTSs
$\overline{L}_n(\overline{p}) = \left\{\overline{L}_n^{(k)}(\overline{p}_n^{(k)}) | \overline{L}_n^{(k)} t \in nSq, h\overline{p}_n^{(k)} \geq x07, Ck; = 1, 2, \ldots, \#\overline{L}_n(\overline{p}), \sum_{k=1}^{\#\overline{L}_n(\overline{p})} \overline{p}_n^{(k)} = 1\right\}$
EndFor
% Fuse the normalized and ordered PLTSs with the weighted addition operation
For $n = 1$
$w_\Delta = 0$
$\widehat{L}^{(k)} = \overline{L}_1^{(k_1)}$
$\widehat{p}^{(k)} = \overline{p}_1^{(k_1)}$
For $n = 2$ to N
$w_\Delta = w_\Delta + w_{n-1}$
$\widehat{L}^{(k)} = w_\Delta \widehat{L}^{(k)} \oplus w_n \overline{L}_n^{(k_n)}$
$\widehat{p}^{(k)} = \widehat{p}^{(k)} \overline{p}_n^{(k_n)}$
EndFor
EndFor
% Determine the ultimate MCGDM result
For $k = 1$ to $\#L_n(p)$
$\alpha = \sum_{k=1}^{\#L(p)} r^{(k)} p^{(k)} / \sum_{k=1}^{\#L(p)} p^{(k)}$
$s^* = \text{round}(s_\alpha)$
EndFor
End

Algorithm 1: MCGDM with DST and PLTSs.

decide which one of the two linguistic terms ($\{\theta_2, \theta_3\}$) is the best. Accordingly, the extracted information is $P_5^2 = \{(\theta_2, 0.100), (\{\theta_2, \theta_3\}, 0.900)\}$, which includes local ignorance. DM e_3 thinks that the MRES performance of the evaluated marine ranching on criterion c_1 can definitely be evaluated as average (θ_2); thus, his/her individual BPA function on criterion c_1 is $P_3^1 = \{(\theta_2, 1.000)\}$ with no ignorance.

4.2. Fusing Information at the Individual Level. As mentioned in Section 3.2, the information given by different DMs has different degrees of reliabilities in the problem of evaluating MRES. To be specific, MRES is a complicated MCGDM problem with various aspects that are represented as the five criteria in this case. However, not every DM has enough ability, knowledge, and experience to give reliable judgment, as MRES involves many professional fields, such as government policy standards, marine sediment quality, marine environment monitoring technology, and so on. For the problem of evaluating MRES in this case, the invited marine environment and resource specialist (e_4) is authoritative in the field of marine environmental protection and marine resource management, and his/her judgment is the most reliable in the judgments given by the five DMs. This DM's reliability is 1.000. The marine environmental monitoring technician (e_1), aquaculture expert (e_2), and local governmental personnel (e_5), respectively, have a certain degree of abilities to make judgment with reliabilities of 0.680, 0.920, and 0.800. Even though the manager of the evaluated marine ranch (e_3) knows a lot about the operation and management of the evaluated marine ranch, such as the cost and profit of the marine ranch (c_2), he/she has the lowest reliability of 0.600 in the synthetic evaluation of the MRES. By taking the DM reliability set R and the information at the individual level in Table 1 into equation (13), we obtain the discounted individual BPA functions as follows.

In the process of fusion, the information from the DM with lower reliability (e.g., DM e_3) cannot compensate for the information from a DM with a higher reliability (e.g., DM e_4). So, the fusion result is effective and reliable as much as possible. Therefore, the fusion rule based on non-compensatory strategies, such as Dempster's rule, is applied, and the group BPA functions representing the group judgment of the five DMs on each criterion are obtained by taking the discounted BPA functions in Table 2 into equation (14). The obtained group BPA functions are shown in Table 3.

4.3. Transforming Group BPA Functions into PLTSs. As mentioned in Section 3.3, the BPA function provides a unified way to model and dispose the uncertainty existing in

Table 1: Extracted information at the individual level.

DM	Criterion	Individual probability assignment ($p_i^n(\theta)$)						
		$\{\theta_1\}$	$\{\theta_2\}$	$\{\theta_3\}$	$\{\theta_1,\theta_2\}$	$\{\theta_2,\theta_3\}$	$\{\theta_1,\theta_3\}$	Θ
e_1	c_1	0.000	0.300	0.600	0.000	0.000	0.000	0.100
	c_2	0.000	0.200	0.500	0.000	0.200	0.000	0.100
	c_3	0.000	0.300	0.000	0.150	0.550	0.000	0.000
	c_4	0.600	0.000	0.200	0.000	0.200	0.000	0.000
	c_5	0.600	0.000	0.000	0.000	0.000	0.000	0.400
e_2	c_1	0.000	0.600	0.000	0.000	0.350	0.000	0.050
	c_2	0.000	0.000	0.300	0.000	0.000	0.000	0.700
	c_3	0.000	0.000	0.400	0.000	0.400	0.000	0.200
	c_4	0.650	0.150	0.200	0.000	0.000	0.000	0.000
	c_5	0.000	0.500	0.500	0.000	0.000	0.000	0.000
e_3	c_1	0.000	1.000	0.000	0.000	0.000	0.000	0.000
	c_2	0.000	0.400	0.600	0.000	0.000	0.000	0.000
	c_3	0.000	0.200	0.200	0.600	0.000	0.000	0.000
	c_4	0.000	0.300	0.400	0.300	0.000	0.000	0.000
	c_5	0.000	0.000	0.300	0.300	0.000	0.000	0.400
e_4	c_1	0.300	0.000	0.000	0.400	0.000	0.000	0.300
	c_2	0.000	0.000	0.000	0.000	0.000	0.000	1.000
	c_3	0.000	0.200	0.200	0.600	0.000	0.000	0.000
	c_4	0.000	0.000	0.300	0.000	0.000	0.000	0.700
	c_5	0.300	0.700	0.000	0.000	0.000	0.000	0.000
e_5	c_1	0.000	0.200	0.200	0.600	0.000	0.000	0.000
	c_2	0.000	0.100	0.000	0.000	0.900	0.000	0.000
	c_3	0.100	0.000	0.000	0.900	0.000	0.000	0.000
	c_4	0.000	0.200	0.800	0.000	0.000	0.000	0.000
	c_5	0.000	0.000	0.500	0.000	0.000	0.000	0.500

DMs' judgments. As is shown in Table 3, the group BPA function on criterion c_1 is $M^1 = \{(\theta_1, 0.011), (\theta_2, 0.924), (\theta_3, 0.031), (\{\theta_1, \theta_2\}, 0.022), (\{\theta_2, \theta_3\}, 0.008), (\Theta, 0.003)\}$, which contains both local ignorance and global ignorance of the DM group. The group BPA function on criterion c_5 is $M^5 = \{(\theta_1, 0.097), (\theta_2, 0.903)\}$, which assigns the probabilities to single elements with no ignorance. Irrespective of the kind of ignorance contained, all information in the group BPA functions is associated with a degree of uncertainty, which is measured by the belief and plausibility function in DST. Therefore, we calculate the belief and plausibility of the group BPA functions by taking the group BPA functions in Table 3 into equation (5). The calculation result is provided in Table 4.

As a result, we obtain the lower and upper limits of the probability assigned to each linguistic term. For convenience of illustration and understandability, we redefine the LTS and its associated value limit of probability. According to the explanation in Section 3.3, the frame of discernment $\Theta = (\theta_1 = \text{bad}, \theta_2 = \text{average}, \theta_3 = \text{good})$ is redefined as an LTS $S = (s_0 = \text{bad}, s_1 = \text{average}, s_2 = \text{good})$, and the associated value limit of the probability is redefined each to each. For example, the belief ($\text{Bel}_2(\theta_1)$) and plausibility ($Pl_2(\theta_1)$) of the group BPA function M^2 relative to linguistic term θ_1 are redefined as $l_2^{(1)}$ and $u_2^{(1)}$, respectively. Accordingly, the group BPA functions in Table 3 are transformed into interval-valued PLTSs as shown in Table 5.

4.4. Fusing Information at the Criterion Level. Based on the above procedure, we obtain the interval-valued PLTSs on each criterion, which describe the possible linguistic terms and associated probabilities. For example, the interval-valued PLTS on criterion c_1 is $L_1(p) = \{s_0[0.011, 0.037], s_1[0.924, 0.958], s_2[0.031, 0.042]\}$, which represents that the MRES performance on special funds acquisition and management (c_1) situation of the evaluated marine ranch is possible to be evaluated as bad (s_0),average (s_1), and good (s_2). Correspondingly, the associated possibilities are, respectively, between intervals [1.1%, 3.7%], [92.4%, 95.8%], and [3.1%, 4.2%]. Subsequently, the five interval-valued PLTSs need to be fused to get the holistic PLTS. We should convert the interval-valued PLTSs into standard PLTSs with certain point-valued probabilities first so that the compensatory operations of PLTSs are applicable. By taking the interval-valued PLTSs in Table 5 into equation (17), we derive the standard PLTSs. After normalization and arrangement, the normalized and ordered PLTSs are obtained (Table 6), where $r_n^{(k)}$ is the subscript of the kth linguistic term in the normalized and ordered PLTSs and $r_n^{(k)}\overline{p}_n^{(k)}$ is the value that is used to arrange the linguistic terms in descending order.

Generally, each PLTS in Table 6 describes the information at the criterion level. As illustrated in Section 3.4, each criterion of MRES is an independent and indispensable aspect, and all criteria compose the MCGDM problem jointly. In this case, the evaluation of MRES includes five criteria, and the information at the criterion level is

Table 2: The discounted individual BPA functions.

DM	Criterion	Discounted individual probability assignment ($m_i^n(\theta)$)						
		$\{\theta_1\}$	$\{\theta_2\}$	$\{\theta_3\}$	$\{\theta_1,\theta_2\}$	$\{\theta_2,\theta_3\}$	$\{\theta_1,\theta_3\}$	Θ
e_1	c_1	0.000	0.204	0.408	0.000	0.000	0.000	0.388
	c_2	0.000	0.136	0.340	0.000	0.136	0.000	0.388
	c_3	0.000	0.204	0.000	0.102	0.374	0.000	0.320
	c_4	0.408	0.000	0.136	0.000	0.136	0.000	0.320
	c_5	0.408	0.000	0.000	0.000	0.000	0.000	0.592
e_2	c_1	0.000	0.552	0.000	0.000	0.322	0.000	0.126
	c_2	0.000	0.000	0.276	0.000	0.000	0.000	0.724
	c_3	0.000	0.000	0.368	0.000	0.368	0.000	0.264
	c_4	0.598	0.138	0.184	0.000	0.000	0.000	0.080
	c_5	0.000	0.460	0.460	0.000	0.000	0.000	0.080
e_3	c_1	0.000	0.600	0.000	0.000	0.000	0.000	0.400
	c_2	0.000	0.240	0.360	0.000	0.000	0.000	0.400
	c_3	0.000	0.120	0.120	0.360	0.000	0.000	0.400
	c_4	0.000	0.180	0.240	0.180	0.000	0.000	0.400
	c_5	0.000	0.000	0.180	0.180	0.000	0.000	0.640
e_4	c_1	0.300	0.000	0.000	0.400	0.000	0.000	0.300
	c_2	0.000	0.000	0.000	0.000	0.000	0.000	1.000
	c_3	0.000	0.200	0.200	0.600	0.000	0.000	0.000
	c_4	0.000	0.000	0.300	0.000	0.000	0.000	0.700
	c_5	0.300	0.700	0.000	0.000	0.000	0.000	0.000
e_5	c_1	0.000	0.160	0.160	0.480	0.000	0.000	0.200
	c_2	0.000	0.080	0.000	0.000	0.720	0.000	0.200
	c_3	0.080	0.000	0.000	0.720	0.000	0.000	0.200
	c_4	0.000	0.160	0.640	0.000	0.000	0.000	0.200
	c_5	0.000	0.000	0.400	0.000	0.000	0.000	0.600

Table 3: The group BPA functions.

Criterion	Group probability assignment ($m^n(\theta)$)						
	$\{\theta_1\}$	$\{\theta_2\}$	$\{\theta_3\}$	$\{\theta_1,\theta_2\}$	$\{\theta_2,\theta_3\}$	$\{\theta_1,\theta_3\}$	Θ
c_1	0.011	0.924	0.031	0.022	0.008	0.000	0.003
c_2	0.000	0.216	0.603	0.000	0.152	0.000	0.029
c_3	0.009	0.848	0.034	0.109	0.000	0.000	0.000
c_4	0.273	0.118	0.590	0.005	0.004	0.000	0.010
c_5	0.097	0.903	0.000	0.000	0.000	0.000	0.000

Table 4: The belief and plausibility of the group BPA functions.

Criterion	Belief and plausibility of the group BPA functions ($\mathrm{Bel}_n(\theta_j)$ & $Pl_n(\theta_j)$)					
	$\mathrm{Bel}_n(\theta_1)$	$Pl_n(\theta_1)$	$\mathrm{Bel}_n(\theta_2)$	$Pl_n(\theta_2)$	$\mathrm{Bel}_n(\theta_3)$	$Pl_n(\theta_3)$
c_1	0.011	0.037	0.924	0.958	0.031	0.042
c_2	0.000	0.029	0.216	0.397	0.603	0.784
c_3	0.009	0.119	0.848	0.957	0.034	0.034
c_4	0.273	0.288	0.118	0.137	0.590	0.604
c_5	0.097	0.097	0.903	0.903	0.000	0.000

Table 5: The interval-valued PLTSs.

Criterion	Interval value of probability ($[l_n^{(k)}, u_n^{(k)}]$)		
	$L_n^{(1)}[l_n^{(1)}, u_n^{(1)}]$	$L_n^{(2)}[l_n^{(2)}, u_n^{(2)}]$	$L_n^{(3)}[l_n^{(3)}, u_n^{(3)}]$
c_1	$s_0[0.011, 0.037]$	$s_1[0.924, 0.958]$	$s_2[0.031, 0.042]$
c_2	$s_0[0.000, 0.029]$	$s_1[0.216, 0.397]$	$s_2[0.603, 0.784]$
c_3	$s_0[0.009, 0.119]$	$s_1[0.848, 0.957]$	$s_2[0.034, 0.034]$
c_4	$s_0[0.273, 0.288]$	$s_1[0.118, 0.137]$	$s_2[0.590, 0.604]$
c_5	$s_0[0.097, 0.097]$	$s_1[0.903, 0.903]$	–

Table 6: The normalized and ordered PLTSs.

Criterion	Probability and associated value $(r_n^{(k)}\overline{p}_n^{(k)})$								
	$\overline{L}_n^{(1)}$	$\overline{p}_n^{(1)}$	$r_n^{(1)}\overline{p}_n^{(1)}$	$\overline{L}_n^{(2)}$	$\overline{p}_n^{(2)}$	$r_n^{(2)}\overline{p}_n^{(2)}$	$\overline{L}_n^{(3)}$	$\overline{p}_n^{(3)}$	$r_n^{(3)}\overline{p}_n^{(3)}$
c_1	s_1	0.940	0.940	s_2	0.036	0.072	s_0	0.023	0.000
c_2	s_2	0.687	1.374	s_1	0.300	0.300	s_0	0.014	0.000
c_3	s_1	0.902	0.902	s_2	0.034	0.068	s_0	0.064	0.000
c_4	s_2	0.595	1.190	s_1	0.125	0.125	s_0	0.279	0.000
c_5	s_1	0.903	0.903	s_0	0.097	0.000	s_0	0.000	0.000

Table 7: The holistic PLTS.

Linguistic term	Probability assignment	
	$\widehat{r}^{(k)}$	$\widehat{p}^{(k)}$
$\widehat{L}^{(1)}$	0.0000	0.0000005
$\widehat{L}^{(2)}$	0.0021	0.0000121
$\widehat{L}^{(3)}$	0.0042	0.0000276
$\widehat{L}^{(4)}$	0.0063	0.0000220
$\widehat{L}^{(5)}$	0.0084	0.0004887
$\widehat{L}^{(6)}$	0.0105	0.0011203
$\widehat{L}^{(7)}$	0.0126	0.0000009
$\widehat{L}^{(8)}$	0.0147	0.0000189
$\widehat{L}^{(9)}$	0.0168	0.0000434
$\widehat{L}^{(10)}$	0.0210	0.0000076
$\widehat{L}^{(11)}$	0.0231	0.0001697
$\widehat{L}^{(12)}$	0.0252	0.0003890
$\widehat{L}^{(13)}$	0.0273	0.0003098
$\widehat{L}^{(14)}$	0.0294	0.0068758
$\widehat{L}^{(15)}$	0.0315	0.0157618
$\widehat{L}^{(16)}$	0.0336	0.0000120
$\widehat{L}^{(17)}$	0.0357	0.0002661
$\widehat{L}^{(18)}$	0.0378	0.0006101
$\widehat{L}^{(19)}$	0.0420	0.0000003
$\widehat{L}^{(20)}$	0.0441	0.0000063
$\widehat{L}^{(21)}$	0.0462	0.0000145
$\widehat{L}^{(22)}$	0.0483	0.0000116
$\widehat{L}^{(23)}$	0.0504	0.0002572
$\widehat{L}^{(24)}$	0.0525	0.0005895
$\widehat{L}^{(25)}$	0.0546	0.0000004
$\widehat{L}^{(26)}$	0.0567	0.0000100
$\widehat{L}^{(27)}$	0.0588	0.0000228
$\widehat{L}^{(28)}$	0.2800	0.0000002
$\widehat{L}^{(29)}$	0.2821	0.0000054
$\widehat{L}^{(30)}$	0.2842	0.0000124
$\widehat{L}^{(31)}$	0.2863	0.0000099
$\widehat{L}^{(32)}$	0.2884	0.0002192
$\widehat{L}^{(33)}$	0.2905	0.0005025
$\widehat{L}^{(34)}$	0.2926	0.0000004
$\widehat{L}^{(35)}$	0.2947	0.0000085
$\widehat{L}^{(36)}$	0.2968	0.0000194
$\widehat{L}^{(37)}$	0.3000	0.0000051
$\widehat{L}^{(38)}$	0.3010	0.0000034
$\widehat{L}^{(39)}$	0.3021	0.0001125
$\widehat{L}^{(40)}$	0.3031	0.0000761
$\widehat{L}^{(41)}$	0.3042	0.0002578
$\widehat{L}^{(42)}$	0.3052	0.0001745
$\widehat{L}^{(43)}$	0.3063	0.0002053
$\widehat{L}^{(44)}$	0.3073	0.0001389
$\widehat{L}^{(45)}$	0.3084	0.0045567
$\widehat{L}^{(46)}$	0.3094	0.0030839
$\widehat{L}^{(47)}$	0.3105	0.0104456
$\widehat{L}^{(48)}$	0.3115	0.0070694
$\widehat{L}^{(49)}$	0.3126	0.0000079
$\widehat{L}^{(50)}$	0.3136	0.0000054
$\widehat{L}^{(51)}$	0.3147	0.0001764
$\widehat{L}^{(52)}$	0.3157	0.0001194
$\widehat{L}^{(53)}$	0.3168	0.0004043
$\widehat{L}^{(54)}$	0.3178	0.0002736
$\widehat{L}^{(55)}$	0.3210	0.0000713
$\widehat{L}^{(56)}$	0.3220	0.0000001
$\widehat{L}^{(57)}$	0.3231	0.0015821
$\widehat{L}^{(58)}$	0.3241	0.0000028
$\widehat{L}^{(59)}$	0.3252	0.0036268
$\widehat{L}^{(60)}$	0.3262	0.0000065
$\widehat{L}^{(61)}$	0.3273	0.0028885
$\widehat{L}^{(62)}$	0.3283	0.0000052
$\widehat{L}^{(63)}$	0.3294	0.0641101
$\widehat{L}^{(64)}$	0.3304	0.0001153
$\widehat{L}^{(65)}$	0.3315	0.1469629
$\widehat{L}^{(66)}$	0.3325	0.0002644
$\widehat{L}^{(67)}$	0.3336	0.0001118
$\widehat{L}^{(68)}$	0.3346	0.0000002
$\widehat{L}^{(69)}$	0.3357	0.0024815
$\widehat{L}^{(70)}$	0.3367	0.0000045
$\widehat{L}^{(71)}$	0.3378	0.0056885
$\widehat{L}^{(72)}$	0.3388	0.0000102
$\widehat{L}^{(73)}$	0.3420	0.0000027
$\widehat{L}^{(74)}$	0.3441	0.0000592
$\widehat{L}^{(75)}$	0.3462	0.0001356
$\widehat{L}^{(76)}$	0.3483	0.0001080
$\widehat{L}^{(77)}$	0.3504	0.0023977
$\widehat{L}^{(78)}$	0.3525	0.0054965
$\widehat{L}^{(79)}$	0.3546	0.0000042
$\widehat{L}^{(80)}$	0.3567	0.0000928
$\widehat{L}^{(81)}$	0.3588	0.0002128
$\widehat{L}^{(82)}$	0.5600	0.0000012
$\widehat{L}^{(83)}$	0.5621	0.0000257
$\widehat{L}^{(84)}$	0.5642	0.0000590
$\widehat{L}^{(85)}$	0.5663	0.0000470
$\widehat{L}^{(86)}$	0.5684	0.0010422
$\widehat{L}^{(87)}$	0.5705	0.0023890
$\widehat{L}^{(88)}$	0.5726	0.0000018
$\widehat{L}^{(89)}$	0.5747	0.0000403
$\widehat{L}^{(90)}$	0.5768	0.0000925
$\widehat{L}^{(91)}$	0.5800	0.0000023
$\widehat{L}^{(92)}$	0.5810	0.0000163
$\widehat{L}^{(93)}$	0.5821	0.0000504
$\widehat{L}^{(94)}$	0.5831	0.0003618
$\widehat{L}^{(95)}$	0.5842	0.0001156
$\widehat{L}^{(96)}$	0.5852	0.0008295
$\widehat{L}^{(97)}$	0.5863	0.0000921
$\widehat{L}^{(98)}$	0.5873	0.0006606
$\widehat{L}^{(99)}$	0.5884	0.0020438
$\widehat{L}^{(100)}$	0.5894	0.0146624

Table 7: Continued.

$\widehat{L}^{(101)}$	0.5905	0.0046850
$\widehat{L}^{(102)}$	0.5915	0.0336114
$\widehat{L}^{(103)}$	0.5926	0.0000036
$\widehat{L}^{(104)}$	0.5936	0.0000256
$\widehat{L}^{(105)}$	0.5947	0.0000791
$\widehat{L}^{(106)}$	0.5957	0.0005675
$\widehat{L}^{(107)}$	0.5968	0.0001813
$\widehat{L}^{(108)}$	0.5978	0.0013010
$\widehat{L}^{(109)}$	0.6010	0.0000320
$\widehat{L}^{(110)}$	0.6020	0.0000006
$\widehat{L}^{(111)}$	0.6031	0.0007096
$\widehat{L}^{(112)}$	0.6041	0.0000135
$\widehat{L}^{(113)}$	0.6052	0.0016267
$\widehat{L}^{(114)}$	0.6062	0.0000310
$\widehat{L}^{(115)}$	0.6073	0.0012955
$\widehat{L}^{(116)}$	0.6083	0.0000247
$\widehat{L}^{(117)}$	0.6094	0.0287542
$\widehat{L}^{(118)}$	0.6104	0.0005484
$\widehat{L}^{(119)}$	0.6115	0.0659149
$\widehat{L}^{(120)}$	0.6125	0.0012571
$\widehat{L}^{(121)}$	0.6136	0.0000501
$\widehat{L}^{(122)}$	0.6146	0.0000010
$\widehat{L}^{(123)}$	0.6157	0.0011130
$\widehat{L}^{(124)}$	0.6167	0.0000212
$\widehat{L}^{(125)}$	0.6178	0.0025514
$\widehat{L}^{(126)}$	0.6188	0.0000487
$\widehat{L}^{(127)}$	0.6220	0.0000012
$\widehat{L}^{(128)}$	0.6241	0.0000265
$\widehat{L}^{(129)}$	0.6262	0.0000608
$\widehat{L}^{(130)}$	0.6283	0.0000485
$\widehat{L}^{(131)}$	0.6304	0.0010754
$\widehat{L}^{(132)}$	0.6325	0.0024652
$\widehat{L}^{(133)}$	0.6346	0.0000019
$\widehat{L}^{(134)}$	0.6367	0.0000416
$\widehat{L}^{(135)}$	0.6388	0.0000954
$\widehat{L}^{(136)}$	0.8600	0.0000108
$\widehat{L}^{(137)}$	0.8621	0.0002398
$\widehat{L}^{(138)}$	0.8642	0.0005497
$\widehat{L}^{(139)}$	0.8663	0.0004378
$\widehat{L}^{(140)}$	0.8684	0.0097171
$\widehat{L}^{(141)}$	0.8705	0.0222749
$\widehat{L}^{(142)}$	0.8726	0.0000169
$\widehat{L}^{(143)}$	0.8747	0.0003761
$\widehat{L}^{(144)}$	0.8768	0.0008622
$\widehat{L}^{(145)}$	0.8810	0.0001520
$\widehat{L}^{(146)}$	0.8831	0.0033738
$\widehat{L}^{(147)}$	0.8852	0.0077340
$\widehat{L}^{(148)}$	0.8873	0.0061597
$\widehat{L}^{(149)}$	0.8894	0.1367123
$\widehat{L}^{(150)}$	0.8915	0.3133927
$\widehat{L}^{(151)}$	0.8936	0.0002384
$\widehat{L}^{(152)}$	0.8957	0.0052917
$\widehat{L}^{(153)}$	0.8978	0.0121304
$\widehat{L}^{(154)}$	0.9020	0.0000057
$\widehat{L}^{(155)}$	0.9041	0.0001262
$\widehat{L}^{(156)}$	0.9062	0.0002893
$\widehat{L}^{(157)}$	0.9083	0.0002304
$\widehat{L}^{(158)}$	0.9104	0.0051131
$\widehat{L}^{(159)}$	0.9125	0.0117210
$\widehat{L}^{(160)}$	0.9146	0.0000089
$\widehat{L}^{(161)}$	0.9167	0.0001979
$\widehat{L}^{(162)}$	0.9188	0.0004537

synthetically fused to derive the final evaluation result, which cannot be decided by a single criterion. In this process, any criterion cannot decide the evaluation result of MRES. Even though the information values on monitoring system and regular inspections (c_3) and main biomass index (c_4) are both definitely good, the final evaluation result is still influenced by three other criteria. Thus, the fusion of information at the criterion level is actually a process of trade-off, which should follow compensatory strategies. Accordingly, we derive the holistic PLTSs (Table 7) by taking the criterion weight set $W = (0.150, 0.050, 0.100, 0.400, 0.300)$ and the normalized and ordered PLTSs as shown in Table 6 into equation (22).

As demonstrated in Table 7, values in the column of $\widehat{r}^{(k)}$ represent the subscripts of 162 virtual linguistic terms in the holistic PLTS, and values in the column of $\widehat{p}^{(k)}$ are their associated probabilities. Then, we apply the round function as in equation (11) to compute the integer score of the holistic PLTS and obtain $\alpha = 0.670$. Then, we have $s^* = \text{round}(s_\alpha) = s_1$. Thus, the ultimate evaluation result is that the MRES is evaluated as average.

5. Conclusion

MCGDM is a decision-making theory that has gained wide attention and applications. As a combination of MCDM and GDM, MCGDM contains two dimensions of information: individual and criterion. Distinction between these two kinds of information is important. Specifically, information at the individual level is noncompensatory in the process of fusion and influence brought by information with a lower degree of reliability cannot offset that brought by information with a higher degree of reliability. Information at the criterion level is compensatory in the process of fusion; the information offsets one another and jointly forms the fusion result. Unfortunately, existing MCGDM methods do not pay attention to this kind of distinction. Therefore, this paper proposes a novel MCGDM method with DST and PLTSs under the consideration of both compensatory and noncompensatory strategies. To conclude, this paper provides contributions in terms of the following aspects.

Firstly, this paper proposes that the information in the two dimensions in MCGDM is distinct, that is, information at the individual level is noncompensatory in the process of fusion, and information at the criterion level is compensatory. Accordingly, the proposed MCGDM method provides a comprehensive information fusion procedure that can fuse information at different levels.

Secondly, the proposed method provides a new orientation for the development of probabilistic preference theory in MCGDM by distinguishing noncompensatory information at the individual level and compensatory information at the criterion level. With the assistance of DST, PLTSs were developed to support information fusion and improve the scientific validity of the MCGDM.

Thirdly, this paper provides a method of building links between group BPA functions and PLTSs. Consequently, a framework based on belief and plausibility for transforming the certain point-valued probabilities assigned on power set

of the frame of discernment into interval-valued probabilities associated with single linguistic terms is proposed, which also provides way of correlating BPA functions with PLTSs.

Finally, this paper contributes to improving the application of probabilistic preference theory for evaluating MRES. This paper provides a relative algorithm for the proposed method, which can be easily converted into a core algorithm of a decision system to promote its application. A case simulation study is also presented by applying the proposed method to evaluate the MRES.

It is worth noting that this paper just uses DST and PLTSs for reference to support noncompensatory and compensatory fusion, respectively. Other effective noncompensatory and compensatory modes could also be applied following the framework in this paper according to different problem characteristics. In the process of fusing compensatory information at the criterion level, the weights of the criteria are assumed to be known in advance. This paper does not address the way of determining the criteria weights. However, as the weights of the criteria influence the value of the virtual linguistic terms in the holistic PLTS a lot during the application of the weighted addition operation, they may lead to distortion of the fusion result. Therefore, the criteria weights should be determined carefully and an appropriate determination principle of criteria weights that suits the weighted addition operation of PLTSs in MCGDM is a worthy future research direction.

Data Availability

The data used to support the findings of this study are available from the corresponding author upon request.

Conflicts of Interest

The authors declare that there are no conflicts of interest regarding the publication of this paper.

Acknowledgments

This research was supported by the Major Program of National Social Science Foundation of China under grant no. 18ZDA055, the National Natural Science Foundation of China (NSFC) under grant nos. 71874167, 71804170, 71901199, and 71462022, the Fundamental Research Funds for the Central Universities under grant no. 202041005, and the Special Funds of Taishan Scholars Project of Shandong Province under grant no. tsqn20171205.

References

[1] C. W. Churchman Jr. and R. L. Ackoff, "An approximate measure of value," *Journal of the Operations Research Society of America*, vol. 2, no. 2, pp. 172–187, 1954.

[2] T. Koopmans, *Activity Analysis of Production and Allocation*, Wiley, Hoboken, NJ, USA, 1951.

[3] S. Fan, J. Zhang, E. Blanco-Davis, Z. Yang, and X. Yan, "Maritime accident prevention strategy formulation from a human factor perspective using Bayesian networks and topsis," *Ocean Engineering*, vol. 210, p. 107544, 2020.

[4] S. Komsiyah, R. Wongso, and S. W. Pratiwi, "Applications of the fuzzy ELECTRE method for decision support systems of cement vendor selection," *Procedia Computer Science*, vol. 157, pp. 479–488, 2019.

[5] H. Liao, L. Jiang, B. Lev, and H. Fujita, "Novel operations of pltss based on the disparity degrees of linguistic terms and their use in designing the probabilistic linguistic ELECTRE III method," *Applied Soft Computing*, vol. 80, pp. 450–464, 2019.

[6] H.-M. Lyu, W.-H. Zhou, S.-L. Shen, and A.-N. Zhou, "Inundation risk assessment of metro system using Ahp and Tfn-Ahp in Shenzhen," *Sustainable Cities and Society*, vol. 56, Article ID 102103, 2020.

[7] R. Micale, C. M. La Fata, and G. La Scalia, "A combined interval-valued ELECTRE tri and topsis approach for solving the storage location assignment problem," *Computers & Industrial Engineering*, vol. 135, pp. 199–210, 2019.

[8] Y. Zhang, Z. Xu, and H. Liao, "Water security evaluation based on the todim method with probabilistic linguistic term sets," *Soft Computing*, vol. 23, no. 15, pp. 6215–6230, 2019.

[9] H. Li, W. Wang, L. Fan, Q. Li, and X. Chen, "A novel hybrid MCDM model for machine tool selection using fuzzy dematel, entropy weighting and later defuzzification vikor," *Applied Soft Computing*, vol. 91, p. 106207, 2020.

[10] S.-f. Zhang, S.-y. Liu, and R.-h. Zhai, "An extended gra method for MCDM with interval-valued triangular fuzzy assessments and unknown weights," *Computers & Industrial Engineering*, vol. 61, no. 4, pp. 1336–1341, 2011.

[11] G. Pineda, P. Jose, J. James, H. Liou, C.-C. Hsu, and Y.-C. Chuang, "An integrated MCDM model for improving airline operational and financial performance," *Journal of Air Transport Management*, vol. 68, pp. 103–117, 2018.

[12] A. Abdelli, L. Mokdad, and Y. Hammal, "Dealing with value constraints in decision making using MCDM methods," *Journal of Computational Science*, vol. 44, p. 101154, 2020.

[13] Ž. Stević, D. Pamučar, A. Puška, and P. Chatterjee, "Sustainable supplier selection in healthcare industries using a new MCDM method: measurement of alternatives and ranking according to compromise solution (marcos)," *Computers & Industrial Engineering*, vol. 140, p. 106231, 2020.

[14] S. Barak and T. Mokfi, "Evaluation and selection of clustering methods using a hybrid group MCDM," *Expert Systems with Applications*, vol. 138, p. 112817, 2019.

[15] R. A. Krohling and V. C. Campanharo, "Fuzzy topsis for group decision making: a case study for accidents with oil spill in the sea," *Expert Systems with Applications*, vol. 38, no. 4, pp. 4190–4197, 2011.

[16] J. Pang, X. Guan, J. Liang, B. Wang, and P. Song, "Multi-Attribute group decision-making method based on multi-granulation weights and three-way decisions," *International Journal of Approximate Reasoning*, vol. 117, pp. 122–147, 2020.

[17] H. Karimi, M. Sadeghi-Dastaki, and M. Javan, "A fully fuzzy best-worst multi attribute decision making method with triangular fuzzy number: a case study of maintenance assessment in the hospitals," *Applied Soft Computing*, vol. 86, p. 105882, 2020.

[18] Y.-J. Wang, "Interval-valued fuzzy multi-criteria decision-making based on simple additive weighting and relative preference relation," *Information Sciences*, vol. 503, pp. 319–335, 2019.

[19] F. Meng, S.-M. Chen, and S. Zhang, "Group decision making based on acceptable consistency analysis of interval linguistic

hesitant fuzzy preference relations," *Information Sciences*, vol. 530, pp. 66–84, 2020.

[20] X. Tan, J. Zhu, and Y. Zhang, "A consensus reaching process with quantum subjective adjustment in linguistic group decision making," *Information Sciences*, vol. 533, pp. 150–168, 2020.

[21] J. Qu, X. Meng, X. Jiang et al., "Effective aggregation of expert opinions to inform environmental management: an integrated fuzzy group decision-making framework with application to cadmium-contaminated water treatment alternatives evaluation," *Journal of Cleaner Production*, vol. 209, pp. 834–845, 2019.

[22] J. Tang, S.-M. Chen, and F. Meng, "Heterogeneous group decision making in the setting of incomplete preference relations," *Information Sciences*, 2019.

[23] F. Zhu, P.-a. Zhong, and Y. Sun, "Multi-criteria group decision making under uncertainty: application in reservoir flood control operation," *Environmental Modelling & Software*, vol. 100, pp. 236–251, 2018.

[24] X. Zhang, H. Liao, B. Xu, and M. Xiong, "A probabilistic linguistic-based deviation method for multi-expert qualitative decision making with aspirations," *Applied Soft Computing*, vol. 93, Article ID 106362, 2020.

[25] J.-B. Yang and D.-L. Xu, "Evidential reasoning rule for evidence combination," *Artificial Intelligence*, vol. 205, pp. 1–29, 2013.

[26] G. A. Shafer, *A Mathematical Theory of Evidence*, Princeton University Press, Princeton, NJ, USA, 1976.

[27] Q. Pang, H. Wang, and Z. Xu, "Probabilistic linguistic term sets in multi-attribute group decision making," *Information Sciences*, vol. 369, pp. 128–143, 2016.

[28] M. Zhou, X.-B. Liu, Y.-W. Chen, and J.-B. Yang, "Evidential reasoning rule for Madm with both weights and reliabilities in group decision making," *Knowledge-Based Systems*, vol. 143, pp. 142–161, 2018.

[29] B. Liu, Q. Zhou, R.-X. Ding, I. Palomares, and F. Herrera, "Large-scale group decision making model based on social network analysis: trust relationship-based conflict detection and elimination," *European Journal of Operational Research*, vol. 275, no. 2, pp. 737–754, 2019.

[30] H. Liao, X. Gou, Z. Xu, X. J. Zeng, and F. Herrera, "Hesitancy degree-based correlation measures for hesitant fuzzy linguistic term sets and their applications in multiple criteria decision making," *Information Ences*, vol. 508, pp. 275–292, 2020.

[31] M. Xue, C. Fu, and S.-L. Yang, "Group consensus reaching based on a combination of expert weight and expert reliability," *Applied Mathematics and Computation*, vol. 369, p. 124902, 2020.

[32] R. K. Bhattacharya, N. D. Chatterjee, and K. Das, "Sub-basin prioritization for assessment of soil erosion susceptibility in Kangsabati, a plateau basin: a comparison between MCDM and swat models," *Science of the Total Environment*, vol. 734, p. 139474, 2020.

[33] J. Xiao, X. Wang, and H. Zhang, "Managing classification-based consensus in social network group decision making: an optimization-based approach with minimum information loss," *Information Fusion*, vol. 63, pp. 74–87, 2020.

[34] T. Elrod, R. D. Johnson, and J. White, "A new integrated model of noncompensatory and compensatory decision strategies," *Organizational Behavior and Human Decision Processes*, vol. 95, no. 1, pp. 1–19, 2004.

[35] M. E. Banihabib, F.-S. Hashemi-Madani, and A. Forghani, "Comparison of compensatory and non-compensatory multi criteria decision making models in water resources strategic management," *Water Resources Management*, vol. 31, no. 12, pp. 3745–3759, 2017.

[36] S. Luan and J. Reb, "Fast-and-Frugal trees as non-compensatory models of performance-based personnel decisions," *Organizational Behavior and Human Decision Processes*, vol. 141, pp. 29–42, 2017.

[37] L. Rothrock and J. Yin, *Integrating Compensatory and Non-compensatory Decision-Making Strategies in Dynamic Task Environments*, pp. 125–141, Springer, New York, NY, USA, 2008.

[38] C. D. Von Gunten, L. D. Scherer, and L. D. Scherer, "Self-other differences in multiattribute decision making: compensatory versus noncompensatory decision strategies," *Journal of Behavioral Decision Making*, vol. 32, no. 2, pp. 109–123, 2019.

[39] H. Liao, Z. Xu, and F. Herrera, "Applications of contemporary decision-making methods to the development of economy and technology," *Technological and Economic Development of Economy*, vol. 26, no. 3, pp. 546–548, 2020.

[40] P. Li and C. Wei, "An emergency decision-making method based on D-S evidence theory for probabilistic linguistic term sets," *International Journal of Disaster Risk Reduction*, vol. 37, Article ID 101178, 2019.

[41] X. Wu and H. Liao, "An approach to quality function deployment based on probabilistic linguistic term sets and oreste method for multi-expert multi-criteria decision making," *Information Fusion*, vol. 43, pp. 13–26, 2018.

[42] C. Huang, M. Lin, and R. Chen, "Probabilistic linguistic VIKOR method based on TODIM for reliable participant selection problem in mobile crowdsensing," in *IEEE International Conference on Big Data and Cloud Computing (BdCloud)*, Xiamen, China, December 2019.

[43] M. Lin, Z. Chen, H. Liao, and Z. Xu, "ELECTRE II method to deal with probabilistic linguistic term sets and its application to edge computing," *Nonlinear Dynamics*, vol. 96, no. 3, pp. 2125–2143, 2019.

[44] M. Lin, C. Huang, Z. Xu, and R. Chen, "Evaluating IoT platforms using integrated probabilistic linguistic MCDM method," *IEEE Internet of Things Journal*, vol. 7, no. 11, pp. 11195–11208, 2020.

[45] H. A. Simon, *Administrative Behavior: A Study of Decision-Making Process in Administrative Organization*, Macmillan, New York, NY, USA, 1947.

[46] J. K. Nuamah and Y. Seong, "A machine learning approach to predict human judgments in compensatory and non-compensatory judgment tasks," *IEEE Transactions on Human-Machine Systems*, vol. 49, no. 4, pp. 326–336, 2019.

[47] A. P. Dempster, "Upper and lower probabilities induced by a multivalued mapping," *The Annals of Mathematical Statistics*, vol. 38, no. 2, pp. 325–339, 1967.

[48] Y.-W. Du, S.-S. Wang, N. Yang, and W. Zhou, "Multiple attribute large-group decision-making method with incomplete information by considering expert's knowledge structure," *Chinese Journal of Management Science*, vol. 25, no. 12, pp. 167–178, 2017.

[49] T. Gudiyangada, Sepideh Tavakkoli Piralilou, K. Gholamnia, O. Ghorbanzadeh, and T. Blaschke, "Flood susceptibility mapping with machine learning, multi-criteria decision analysis and ensemble using Dempster Shafer theory," *Journal of Hydrology*, vol. 590, Article ID 125275, 2020.

[50] L. Wan, H. Li, Y. Chen, and C. Li, "Rolling bearing fault prediction method based on QPSO-BP neural network and Dempster-Shafer evidence theory," *Energies*, vol. 13, no. 5, p. 1094, 2020.

[51] M. Mokarram, S. Ali, P. Mohammadizadeh, and A. Ali, "Determination of artificial recharge location using analytic hierarchy process and Dempster–Shafer theory," *Environmental Earth Ences*, vol. 79, p. 10, 2020.
[52] Y.-M. Wang, J.-B. Yang, D.-L. Xu, and K.-S. Chin, "The evidential reasoning approach for multiple attribute decision analysis using interval belief degrees," *European Journal of Operational Research*, vol. 175, no. 1, pp. 35–66, 2006.
[53] R. Haenni, "Shedding new light on Zadeh's criticism of Dempster's rule of combination," in *Proceedings of the Paper Presented at the 2005 7th International Conference on Information Fusion*, Philadelphia, PA, USA, July 2005.
[54] R. M. Rodriguez, L. Martinez, and F. Herrera, "Hesitant fuzzy linguistic term sets for decision making," *IEEE Transactions on Fuzzy Systems*, vol. 20, no. 1, pp. 109–119, 2012.
[55] F. Herrera, E. Herrera-Viedma, and J. L. Verdegay, "A sequential selection process in group decision making with a linguistic assessment approach," *Information Sciences*, vol. 85, no. 4, pp. 223–239, 1995.
[56] J. Gu, Y. Zheng, X. Tian, and Z. Xu, "A decision-making framework based on prospect theory with probabilistic linguistic term sets," *Journal of the Operational Research Society*, pp. 1–10, 2020.
[57] Y.-W. Du and X.-L. Sun, "Influence paths of marine ranching ecological security in China based on probabilistic linguistic term sets and qualitative comparative analysis," *International Journal of Fuzzy Systems*, 2020.
[58] Z. Xu and H. Wang, "On the syntax and semantics of virtual linguistic terms for information fusion in decision making," *Information Fusion*, vol. 34, pp. 43–48, 2017.
[59] Y. Zhang, Z. Xu, H. Wang, and H. Liao, "Consistency-based risk assessment with probabilistic linguistic preference relation," *Applied Soft Computing*, vol. 49, pp. 817–833, 2016.
[60] R. R. Yager, "Decision making under Dempster-Shafer uncertainties," *International Journal of General Systems*, vol. 20, no. 3, pp. 233–245, 1992.
[61] B. Suo, L. Zhao, and Y. Yan, "A novel Dempster-Shafer theory-based approach with weighted average for failure mode and effects analysis under uncertainty," *Journal of Loss Prevention in the Process Industries*, vol. 65, Article ID 104145, 2020.
[62] Y.-W. Du, S.-S. Wang, and Y.-M. Wang, "Group fuzzy comprehensive evaluation method under ignorance," *Expert Systems With Applications*, vol. 126, pp. 92–111, 2019.
[63] J. Yang and M. G. Singh, "An evidential reasoning approach for multiple-attribute decision making with uncertainty," *IEEE Transactions on Systems, Man, and Cybernetics*, vol. 24, no. 1, pp. 1–18, 1994.
[64] Z. Wang, J.-M. Gao, R.-X. Wang, K. Chen, Z.-Y. Gao, and Y. Jiang, "Failure mode and effects analysis using Dempster-Shafer theory and topsis method: application to the gas insulated metal enclosed transmission line (gil)," *Applied Soft Computing*, vol. 70, pp. 633–647, 2018.
[65] C. Bai, R. Zhang, S. Shen, C. Huang, and X. Fan, "Interval-valued probabilistic linguistic term sets in multi-criteria group decision making," *International Journal of Intelligent Systems*, vol. 33, no. 6, pp. 1301–1321, 2018.
[66] P. Liu and S. Cheng, "Interval-valued probabilistic dual hesitant fuzzy sets for multi-criteria group decision-making," *International Journal of Computational Intelligence Systems*, vol. 2, no. 12, pp. 1393–1411, 2019.
[67] R. Krishankumar, A. R. Mishra, K. S. Ravichandran et al., "A group decision framework for renewable energy source selection under interval-valued probabilistic linguistic term set," *Energies*, vol. 13, no. 4, p. 986, 2020.

Hindawi
Mathematical Problems in Engineering
Volume 2020, Article ID 4792679, 15 pages
https://doi.org/10.1155/2020/4792679

Research Article

Sustainable Supplier Evaluation and Selection of Fresh Agricultural Products Based on IFAHP-TODIM Model

Yupei Du,[1] Di Zhang,[2] and Yue Zou[3]

[1]*School of Aeronautics and Astronautics, Sichuan University, Chengdu 610065, China*
[2]*Cyberspace Administration of Sichuan, Chengdu 610065, China*
[3]*Business School, Sichuan University, Chengdu 610065, China*

Correspondence should be addressed to Yue Zou; 2019225025109@stu.scu.edu.cn

Received 26 June 2020; Accepted 21 November 2020; Published 4 December 2020

Academic Editor: Luigi Rodino

In recent years, increasing pollution of the ecological environment, excessive use of pesticides, and lack of effective management of agricultural product supply chains have made the problem of having a green and safe supply of fresh food increasingly prominent. The sustainability of the fresh agricultural products supply has become an inevitable focus in the development of agricultural enterprises. There are some problems in the supply chain of fresh agricultural products, such as scattered production sites and difficult logistics transportation, which makes it difficult for enterprises to choose reliable suppliers. Supplier selection is a key component of sustainable supply chain management, and the criteria for evaluating the quality of sustainable suppliers are often affected by economic, social, and environmental factors. Therefore, from the perspective of sustainability, based on triple bottom line theory and comprehensively considering the three aspects of society, environment, and economy, this paper proposes a novel evaluation index system for the selection of sustainable suppliers of fresh agricultural products. This paper innovatively integrates the intuition fuzzy analytic hierarchy process and TODIM (an acronym in Portuguese of interactive and multiple attribute decision-making), and these are applied to select sustainable suppliers. Finally, the integration method is applied to the example, and a sensitivity analysis is carried out to verify the validity of the evaluation model.

1. Introduction

Selection of fresh agricultural product suppliers is one of the most critical links in the agricultural product supply chain. Green and sustainable agricultural product supply is not only related to the development of food enterprises, but it also has a greater impact on people's livelihood. In recent years, with the problems of ecological environment pollution, excessive use of pesticides and fertilizers, and excessive use of additives in food processing in farmland, ensuring the sustainability of agricultural products has become increasingly problematic. For example, "Sudan red," "poisonous cowpea," and other vicious events have aroused widespread public concern about the safety of agricultural product supply. Taking China as an example, due to the lagging development of logistics transportation in the agricultural product supply chain, agricultural product production is relatively fragmented, and intersubject information cannot be circulated quickly and effectively. This makes it difficult to choose safe and sustainable suppliers in the agricultural product supply chain. Therefore, sustainable supplier selection of fresh agricultural products has become a key link in the management of green agricultural product supply chains. Selection of fresh agricultural product suppliers must not only consider the cost and technology but also environmental pollution, resource consumption, and social responsibility. In summary, how to effectively assess the sustainability of fresh agricultural product suppliers is an important issue for companies to implement sustainable supply chain management.

2. Literature Review

At present, domestic and foreign studies on the food supply chain and supplier selection methods are relatively numerous, while there are relatively few studies on the selection

of sustainable suppliers of fresh agricultural products. A characteristic of the food supply chain is that food is perishable [1], and the freshness of food will directly affect the quality and safety [2]. Fresh food is a critical part in the food supply chain, which greatly affects the safety of consumers' diets. However, in this supply chain, there are a large number of intermediaries between farmers and retailers [3]. Under the trend of continuous development of food safety and quality standards, supermarkets and other suppliers have to pay a huge cost to purchase from many small-scale agricultural producers [4]. Therefore, the selection of sustainable suppliers in the fresh food supply chain has become a key issue that needs to be studied.

Supplier selection is a key component of sustainable supply chain management [5]. The focus of sustainable supply chain development is the type of supply chain and the social and environmental responsibilities of products [6], while the sustainability of agricultural food supply chains obviously involves significant environmental and social impacts [7]. The sustainability of food includes environmental issues, social issues, and expected returns [8]. Therefore, previous research has attempted to establish a sustainable agricultural food supply chain evaluation index system from the three dimensions of social responsibility, economic benefits, and environmental protection. As the material basis for agricultural product production, the ecological environment has always been the main consideration in constructing a sustainable evaluation index system. Gerbens-Leenes et al. [9] applied environmental indicators to their evaluation of the environmental sustainability of food production. Solér et al. [10] explored the use of environmental information at different stages in the food supply chain. Cellura et al. [11] evaluated the sustainability of crop production and consumption from the perspectives of energy consumption and environmental burden.

Corporate social responsibility is considered to be one of the major factors impacting the food supply chain [12]. Spence et al. [13] discussed the evolution from corporate social responsibility to food supply chain responsibility. Chkanikova and Mont [14] systematically elaborated the reasons and obstacles for food retailers to fulfill their supply chain responsibilities. Krejci et al. [15] studied the influence of social factors on the long-term sustainability of food supply centers. Chen et al. [16] determined optimal suppliers in the sustainable food supply chain from the perspective of social responsibility. Stranieri et al. [17] discussed the effect of implementing corporate social responsibility activities on the vertical restructuring of the food supply chain.

Economic benefit is the basic indicator of sustainable supply assessment. It is generally combined with environmental performance or social performance to evaluate the sustainability of the supply chain [18–20]. In addition, some researchers have combed the existing literature on agricultural fresh food supply chain quality (AFSCQ). They found that sustainable management is one of the key issues in AFSCQ research, and performance evaluations of the agricultural fresh food supply chain are still in the development stage [21]. However, most of the previous research has focused on sustainability assessment of the food supply chain and agricultural product supply chain. Sustainability assessments of fresh agricultural product suppliers are basically nonexistent and lack a systematic measurement framework.

Selection of sustainable suppliers requires evaluation of supplier performance based on multiple criteria [22], which includes two stages: determination of indicator weights and supplier ranking. The two-stage evaluation part involves two types of uncertainty: individual uncertainty and group uncertainty [23]. Individual uncertainty refers to the ambiguity of an individual's thinking and expression [24], and group uncertainty refers to the ambiguity of different people's preferences for something [23]. Since the decision process involves uncertain information, various methods based on fuzzy set theory are often used in the field of supplier selection to capture fuzzy or ambiguous information [25]. Among the commonly used multiattribute decision-making methods for determining weights, there are, for example, AHP [26], ANP [27], and DEMATEL [28]. These traditional weighting methods cannot deal well with the uncertainty and inaccuracy of decision information. In the supplier ranking method, compared with DEA [29], PROMETHEE [30], and TOPSIS [31] methods, the TODIM multiattribute decision-making method considers the psychological behavior of decision-makers [32] and can deal with uncertainties The problem is in the environment [33], but the TODIM method directly measures the distance between the fuzzy numbers and decomposes the fuzzy information into clear values at the beginning, which may lead to the loss of important information in decision-making problems [34]. Considering the ambiguity of decision information, applying the IF intuitionistic fuzzy set theory to the AHP method (i.e., IFAHP) can better deal with the hesitation in decision-making [35]. Thus, this article chose the IFAHP-TODIM integration method and applied it to the selection of sustainable suppliers of fresh agricultural products. Existing research on the selection of sustainable suppliers of fresh agricultural products has not yet used this integrated method, so we also expand on new ideas for subsequent scholars to study.

3. The Evaluation Index System of Fresh Agricultural Product Sustainable Suppliers Based on Triple Bottom Line

Sustainable supply chain management has become the focus of supply chain field. One of the most basic means of sustainable supply chain management is supplier selection [36]. Sustainable supplier selection is a key factor in sustainable supply chain management [37], because the supplier is at the beginning of the supply chain, and its economic, environmental, and social performance will have a significant impact on the downstream enterprises of the supply chain [25]. Traditional supplier selection only focuses on economic factors, but in the changing market, sustainable supply chain management should be adopted, that is,

environmental and social standards [38, 39] should be considered. Choosing the right supplier based on sustainability criteria (economy, environment, and society) can help enterprises achieve sustainable development [40]. Sustainable supply chain management in the field of fresh agricultural products is facing economic, social, and ecological challenges. This sustainability is influenced by many factors, including economic, social, and environmental aspects, namely, the triple bottom line (TBL) principle (Figure 1). In the organization of production activities, enterprises not only focus on economic development but also consider their own social responsibilities and possible environmental pollution. If you simply pursue profitability and ignore social and environmental responsibilities, companies may move to oppose consumers and society and will face the dilemma of rootless trees. Unification of economic development, social responsibility, and environmental responsibility is the foundation for sustainable development of an enterprise and its longevity.

3.1. "Economic Bottom Line" Evaluation Index. Economic development is the lifeblood of an enterprise, and economic benefits (gross output value/production cost) are an important part of measuring enterprise performance. This article selects three indicators of energy consumption, logistics cost, and net product price from the cost dimension to construct an economic bottom line indicator system.

3.2. "Social Bottom Line" Evaluation Index. The social bottom line measures the ability of business organizations to fulfill their social responsibilities. Social responsibility includes protection of consumer rights, social welfare, green safety, and other components. This article selects six specific indicators from the dimensions of food safety and packaging materials—to reduce food additives, green R & D and innovation, reusability, biodegradable products, use of recycled materials, and use of hazardous substances—to build a social bottom line indicator system.

3.3. "Environmental Bottom Line" Evaluation Index. Sustainable development focuses on the coordinated development of social, economic, and environmental aspects. Changes in the vectors of indicators in these areas are expected to increase incrementally. Among them, ecological environmental protection is the prerequisite for sustainable economic development. Based on the theory of sustainable development, this article refers to the indicators recommended by the "Guide to Sustainability Reporting." The article selects seven indicators—ISO14000 certification, environmental policies and plans, environmental remediation, environmental governance, air pollutant production, wastewater production, and solid waste production—from three dimensions—environmental management system, environmental protection, and pollution generation—and builds an environmental baseline indicator system. The established evaluation index system for the suppliers of fresh agricultural products is shown in Table 1.

4. Methodology

The intuitionistic fuzzy analytic hierarchy process decomposes complex decision-making problems into an orderly hierarchical structure in the order of general goals, subgoals at various levels, and evaluation criteria, and then relevant experts score the indicators in the structural model. With the help of expert scores and an intuitionistic fuzzy number correspondence table (Table 2), an intuitionistic fuzzy judgment matrix is established. Then, after a consistency test, the index weights at all levels are finally obtained to assist decision-making. This method can accurately reflect the uncertainty of the decision-making subject to the evaluated object to a certain extent, and it can unify the quantitative and qualitative indicators. In addition, when the judgment matrix is not consistent, an intuitionistic fuzzy judgment matrix that meets the requirements can be obtained by adjusting the parameters, and distortion of the original data is avoided as much as possible. The TODIM multiattribute decision-making method has been widely used in multiattribute decision-making problems such as intuitionistic fuzzy numbers, hesitant fuzzy numbers, and hesitant fuzzy language because it can fully consider the psychological behavior of decision-makers and obtain decision results that meet the preferences of decision-makers. In this study, the intuitionistic fuzzy analytic hierarchy process combined with the TODIM multiattribute decision-making method was used to select suppliers of fresh agricultural products. This process is specified in Figure 2.

4.1. Construction of the Intuitionistic Fuzzy Judgment Matrix. The first step was to collect the opinions of relevant experts on the importance of each indicator. For the 6 first-level indicators and 16 second-level indicators in the indicator system, we established seven intuitive fuzzy judgment matrices according to the criteria corresponding to the scores in Table 2 and the fuzzy numbers. Then, we made a pairwise comparison of the indicators of each layer to construct a $R = (r_{ij})_{n\times n}$ square matrix, where i and j represent the rows and columns in the judgment matrix, respectively. $r_{ij} = (u_{ij}, v_{ij})\,(i, j = 1, 2, \ldots, n)$, where $r_{ij} = (u_{ij}, v_{ij})$, in which u_{ij} indicates the degree that the ith index is better than the jth index; v_{ij} indicates the ith index is inferior to the jth index; π_{ij} represents the degree of hesitation, $\pi_{ij} = 1 - u_{ij} - v_{ij}$.

The basis for constructing the intuitionistic fuzzy judgment matrix is to grade the opinions of experts in the field of fresh agricultural product suppliers. For the comparison between qualitative indicators, see Table 2. The scale corresponds to expert score and intuitionistic fuzzy number. The last digit of the intuitionistic fuzzy number represents uncertainty (i.e., ambiguity). An intuitionistic fuzzy judgment matrix was constructed according to the corresponding fuzzy numbers obtained in Table 2, so as to visually

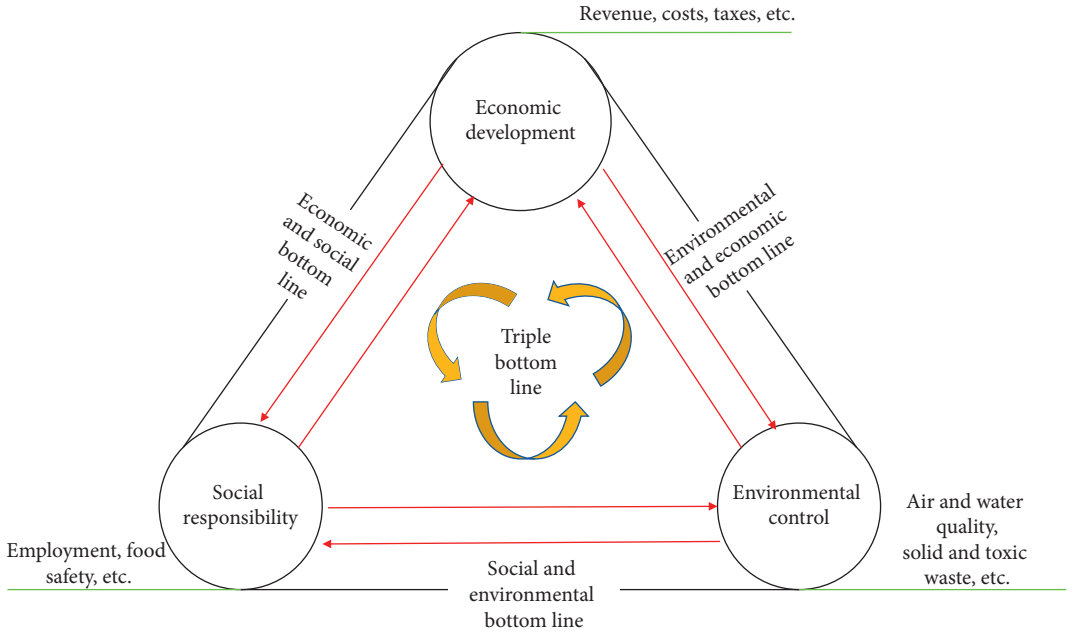

Figure 1: Triple bottom line.

Table 1: Evaluation index system of fresh agricultural product sustainable suppliers based on triple bottom line.

Target layer	Standard layer	Indicator layer	Explanation layer
Environmental control	Environmental management system A_1	ISO 14000 certification B_{11}	Environmental certification held by the supplier
		Environmental policy and plan B_{12}	Supplier environmental protection policy planning, implementation, and review
	Environmental protection A_2	Environmental restoration B_{21}	Supplier efforts to eliminate contamination in the media
		Environmental governance B_{22}	Suppliers efforts to harmlessly dispose of waste
Economic development	Cost A_3	Energy consumption B_{31}	Energy consumption per unit of agricultural product
		Logistics costs B_{32}	Total cost of agricultural products
		Product net price B_{33}	Average net price per unit of agricultural product
	Pollution A_4	Air pollutant production B_{41}	The average amount of air pollutants emitted per day
		Wastewater production B_{42}	Daily average volume of wastewater
		Solid waste generation B_{43}	Average daily solid waste volume
Social responsibility	Use of packaging materials A_5	Reusability B_{51}	Reusable product percentage
		Biodegradable products B_{52}	Percentage of biodegradable products
		Use recycled materials B_{53}	Percentage of products using recycled materials
		Use of hazardous substances B_{54}	Daily use of harmful substances
	Food safety A_6	Reduce food additives B_{61}	Ability to ensure green food safety
		Green R & D and innovation B_{62}	Ability to innovate new clean technologies, processes, and practices

check the relative importance of the indicators, and then a data consistency test was constructed.

4.2. Inspection Consistency Calculation. The second step was to conduct a consistency test on the collected expert evaluation opinions. If the requirements are not met, it means that the experts' evaluations of the relative importance of the indicators are not uniform. Unlike traditional analytic hierarchy processes, intuitionistic fuzzy analytic hierarchy processes can iterate through formulas and set parameters to avoid rescoring experts. The consistency test

Table 2: Scale table corresponding to fuzzy numbers and ratings.

Preference evaluation	Intuitionistic fuzzy number
Extremely important	(0.90, 0.10, 0.00)
Very important	(0.80, 0.15, 0.05)
Important	(0.70, 0.20, 0.10)
More important	(0.60, 0.25, 0.15)
Equally important	(0.50, 0.30, 0.20)
Less important	(0.40, 0.45, 0.15)
Unimportant	(0.30, 0.60, 0.10)
Very unimportant	(0.20, 0.75, 0.05)
Extremely unimportant	(0.10, 0.90, 0.00)

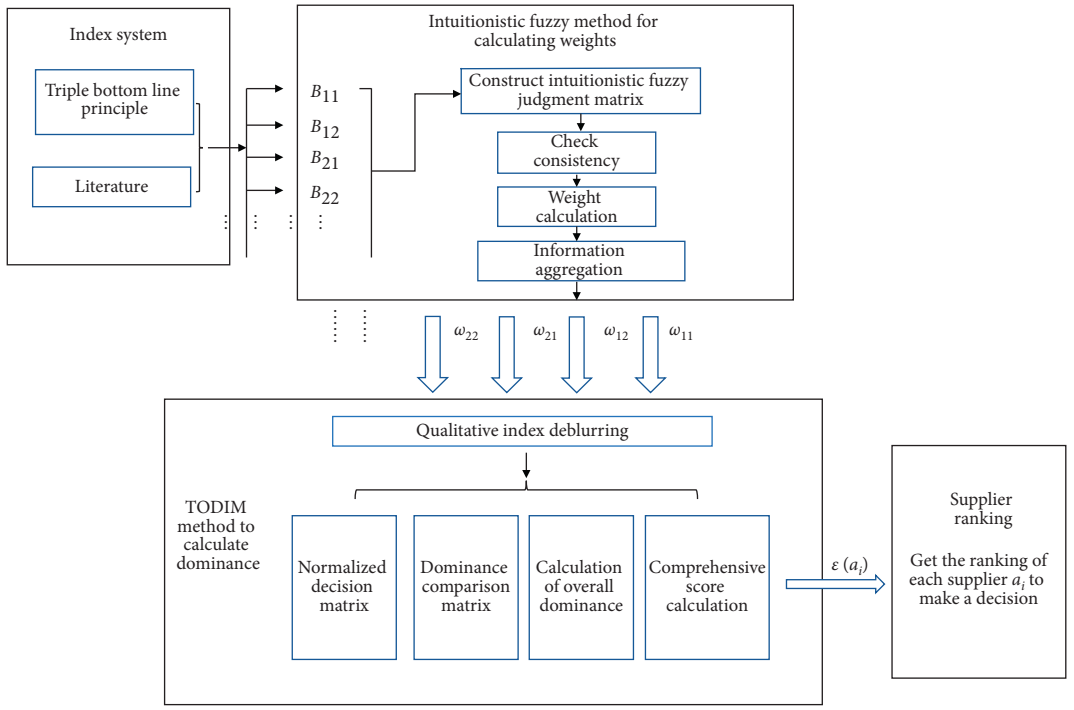

Figure 2: Supplier selection flowchart.

formula for distance measurements [41] based on intuitionistic fuzzy information is given as follows [42]:

$$d(\overline{R}, R) = \frac{1}{2(n-1)(n-2)} \sum_{i=1}^{n} \sum_{j=1}^{n} \left(\left| \overline{u_{ij}} - u_{ij} \right| + \left| \overline{v_{ij}} - v_{ij} \right| + \left| \overline{\pi_{ij}} - \pi_{ij} \right| \right), \tag{1}$$

where R is the intuitionistic fuzzy judgment matrix obtained by comparing pairs of indicators at all levels and $\overline{R}$ is the intuitionistic fuzzy consistency judgment matrix $\overline{R} = (\overline{r_{ij}})_{n\times n}$ obtained according to the following calculation formula [42]:

(1) When $j > i + 1$, let $\overline{R} = (\overline{u}_{ij}, \overline{v}_{ij})$, where

$$\overline{u}_{ij} = \sqrt[j-i-1]{\frac{\prod_{t=i+1}^{j-1} u_{it} u_{tj}}{\sqrt[j-i-1]{\prod_{t=i+1}^{j-1} u_{it} u_{tj}} + \sqrt[j-i-1]{\prod_{t=i+1}^{j-1} (1-u_{it})(1-u_{tj})}}}, \tag{2}$$

$$\overline{v}_{ij} = \sqrt[j-i-1]{\frac{\prod_{t=i+1}^{j-1} v_{it} v_{tj}}{\sqrt[j-i-1]{\prod_{t=i+1}^{j-1} v_{it} v_{tj}} + \sqrt[j-i-1]{\prod_{t=i+1}^{j-1} (1-v_{it})(1-v_{tj})}}}. \tag{3}$$

(2) When $j = i + 1$, $\overline{r_{ij}} = r_{ij}$.

(3) When $j < i + 1$, $\overline{r_{ij}} = (\overline{v}_{ij}, \overline{u}_{ij})$.

The intuitionistic fuzzy consistency judgment matrix $\overline{R} = (\overline{r_{ij}})_{n\times n}$ is calculated according to the above formula and substituted into equation (1) for a consistency check. If $d(\overline{R}, tR) < 0.1$, it passes the consistency test, and otherwise, it fails the consistency test. When the consistency test fails, the parameter σ is introduced into the iteration, that is, the intuitionistic fuzzy consistency judgment matrix is transformed by adjusting the parameter σ until the consistency test is passed. Let the parameter $\sigma \in [0, 1]$, then the consistency check formula is as follows [42]:

$$\widetilde{u_{ij}} = \frac{\left(u_{ij}\right)^{1-\sigma}\left(\overline{u_{ij}}\right)^{\sigma}}{\left(u_{ij}\right)^{1-\sigma}\left(\overline{u_{ij}}\right)^{\sigma} + \left(1 - u_{ij}\right)^{1-\sigma}\left(1 - \overline{u_{ij}}\right)^{\sigma}}, \quad i, j = 1, 2, \ldots, n,$$
$$\widetilde{v_{ij}} = \frac{\left(v_{ij}\right)^{1-\sigma}\left(\overline{v_{ij}}\right)^{\sigma}}{\left(v_{ij}\right)^{1-\sigma}\left(\overline{v_{ij}}\right)^{\sigma} + \left(1 - v_{ij}\right)^{1-\sigma}\left(1 - \overline{v_{ij}}\right)^{\sigma}}, \quad i, j = 1, 2, \ldots, n. \tag{4}$$

Through calculations of the above formula, the transformed consistency judgment matrix $\widetilde{R} = (\widetilde{r_{ij}})_{n\times n}$ is obtained, where $\widetilde{r_{ij}} = (\widetilde{u_{ij}}, t\widetilde{v_{ij}})$. Then, according to formula (5), the consistency test is performed on the new consistency judgment matrix, and the above process is continued until the consistency test is passed. This is calculated as follows:

$$d(\overline{R}, R) = \frac{1}{2(n-1)(n-2)} \sum_{i=1}^{n}\sum_{j=1}^{n}\left(\left|\widetilde{u_{ij}} - u_{ij}\right| + \left|\widetilde{v_{ij}} - v_{ij}\right| + \left|\widetilde{\pi_{ij}} - \pi_{ij}\right|\right). \tag{5}$$

4.3. Weight Calculation. Based on the intuitionistic fuzzy judgment matrix that passed the consistency test, the weight of each index is calculated, and the calculation formula is as follows [42]:

$$\omega_i = \left(\frac{\sum_{j=1}^{n} u_{ij}}{\sum_{i=1}^{n}\sum_{j=1}^{n}\left(1 - v_{ij}\right)}, 1 - \frac{\sum_{j=1}^{n}\left(1 - u_{ij}\right)}{\sum_{i=1}^{n}\sum_{j=1}^{n} v_{ij}}\right), \quad i = 1, 2, \ldots, n. \tag{6}$$

4.4. Information Gathering. It can be seen from Table 1 that this evaluation system has 6 first-level indicators and 16 second-level indicators. Let the weight of the first-level indicator be $\omega_k (k = 1, 2, \ldots, 6)$, and the weight of the second-level indicator relative to the first-level indicator be $\omega_{kl} (k = 1, 2, \ldots, 6; l = 1, 2, \ldots, 4)$. The comprehensive weight of the secondary indicators relative to the total score of the plan is W_{kl}, and the number of secondary indicators under the primary indicator A_i is between two and four. Since both ω_k and ω_{kl} are intuitionistic fuzzy numbers, their calculation should be performed using the algorithm of intuitionistic fuzzy numbers [43]:

$$\alpha_1 \oplus \alpha_2 = \left(u_{\alpha 1} + u_{\alpha 2} - u_{\alpha 1} * u_{\alpha 2}, v_{\alpha 1} * v_{\alpha 2}\right), \tag{7}$$

$$\alpha_1 \otimes \alpha_2 = \left(u_{\alpha 1} * u_{\alpha 2}, v_{\alpha 1} + v_{\alpha 2} - v_{\alpha 1} * v_{\alpha 2}\right). \tag{8}$$

Integration of qualitative index information uses the above formula, while the quantitative index uses the simulated value of the actual statistics.

The qualitative indicators should be deblurred so that they can form an initial decision matrix with the quantitative indicators. The deblurring algorithms of intuitionistic fuzzy sets mainly include the maximum truth value method, weighted average method, and centroid method [44]. This article uses the maximum truth method, and the formula is as follows:

$$T_v(u) = \mu_v(u) + \frac{1 + \mu_v(u) - \pi_v(u)}{2}\pi_v(u). \tag{9}$$

Here, $\mu_v(u)$ represents the degree of membership, $\pi_v(u)$ represents the degree of hesitation, and $T_v(u)$ is the true value of the intuitionistic fuzzy number.

4.5. Normalized Processing. The actual value of the quantitative index obtained from statistics and the real value of the qualitative index after deblurring constitute the initial decision-making matrix for the selection of fresh agricultural product suppliers, which are standardized to obtain a standardized decision matrix. The attributes of the indicator are divided into the benefit type and the cost type. The greater the value of the benefit-type index, the better, and the smaller the value of the cost-type index, the better. Therefore, the standardized formulas for different attribute indicators are as follows:

Benefit index:

$$c_{ij} = \frac{c_{ij}^{M} - \min c_{ij}^{M}}{\max c_{ij}^{M} - \min c_{ij}^{M}}. \tag{10}$$

Cost index:

$$c_{ij} = \frac{\max c_{ij}^{M} - c_{ij}^{M}}{\max c_{ij}^{M} - \min c_{ij}^{M}}. \tag{11}$$

4.6. TODIM Method to Calculate Dominance. This method is based on the description provided by expert experience, and it judges the merits of each evaluation object by calculating the overall superiority of the evaluation object relative to other evaluation objects. The main steps are as follows [45]:

(1) The predominance matrix $V = [\delta(a_i, a_k)_{n\times n}]$ of the evaluation objects is calculated, and $\delta(a_i, a_k)$ represents the predominance of the evaluation object a_i relative to the evaluation object a_k. The calculation formula is given by

$$\delta(a_i, a_k) = \sum_{j=1}^{n} \varphi_j(a_i, a_k). \tag{12}$$

Here, $\varphi_j(a_i, a_k)$ represents the dominance of the evaluation object a_i relative to the evaluation object a_k with respect to the index c_j. The calculation formula of $\varphi_j(a_i, a_k)$ is as follows:

$$\begin{aligned}
&\text{(a) } \varphi_j(a_i, a_k) = \sqrt{\frac{(x_{ij} - x_{kj}) w_{rj}}{\sum_{j=1}^{n} w_{rj}}}, \quad x_{ij} - x_{kj} > 0,\\
&\text{(b) } \varphi_j(a_i, a_k) = 0, \quad x_{ij} - x_{kj} = 0,\\
&\text{(c) } \varphi_j(a_i, a_k) = -\frac{1}{\theta}\sqrt{\frac{(x_{kj} - x_{ij}) \sum_{j=1}^{n} w_{rj}}{w_{rj}}}, \quad x_{ij} - x_{kj} < 0,
\end{aligned} \tag{13}$$

where x_{ij}, x_{kj} are real numbers; w_{rj} is the relative weight of the index relative to the reference index c_j, $w_{rj} = (w_{cj}/w^*)$, where $w^* = \max\{w_{cj}, j = 1, 2, \ldots, n\}$; θ is the attenuation coefficient in the face of loss, and its value range is $0 < \theta < ((\sum_{j=1}^{n} w_{rj})/(w_{rj}))$, which is generally 2.25, indicating the ability of the decision-maker to avoid mistakes.

(2) The formula for calculating the overall advantage T_d of the evaluation object a_i relative to all other evaluation objects is as follows:

$$T_d = \sum_{k=1}^{m} \delta(a_i, a_k). \tag{14}$$

(3) A comprehensive score of the evaluation object is calculated.

The comprehensive score $\varepsilon(a_i)$ of the evaluation object a_i is obtained by normalizing the overall advantage T_d of the evaluation object. Then, all evaluation objects are sorted according to the size of $\varepsilon(a_i)$. The larger the $\varepsilon(a_i)$, the better the evaluation object a_i. The calculation formula of $\varepsilon(a_i)$ is as follows:

$$\varepsilon(a_i) = \frac{T_d - \min\{T_d\}}{\max\{T_d\} - \min\{T_d\}}. \tag{15}$$

5. Case Study

5.1. Consistency Check. The intuitionistic fuzzy data in the intuitionistic fuzzy judgment matrix in this paper were obtained by experts. Based on the established index system for supplier selection criteria (Table 1), this paper established seven intuitionistic fuzzy judgment matrices as shown in Table 3.

According to equations (2) and (3), the intuitionistic fuzzy consistency test matrix $\overline{R}$ was calculated and transformed as shown in Table 4.

The next step was to calculate the consistency according to equation (1) and get $\mathrm{d}(\overline{R}, R) = 0.0940 < 0.1$. This shows that the consistency test passed.

Table 5 shows the original matrix. According to equations (2) and (3), the intuitionistic fuzzy consistency test matrix $\overline{R}$ was calculated and transformed as shown in Table 6.

It can be seen that $\overline{R} = R$, that is, the consistency check matrix was the same as the original matrix (Table 5). In the next step, the consistency was calculated according to equation (1) as $\mathrm{d}(\overline{R}, R) = 0 < 0.1$, which shows that the consistency test passed. All the following 2×2 matrices (Tables 7 and 8) have the same reasoning.

Table 9 shows the original matrix. According to equations (2) and (3), the intuitionistic fuzzy consistency test matrix $\overline{R}$ was calculated and transformed as shown in Table 10.

In the same way, according to formula (1), the consistency was calculated as $\mathrm{d}(\overline{R}, R) = 0.0702 < 0.1$, which shows the consistency test passed.

Table 11 shows the original matrix. According to equations (2) and (3), the intuitionistic fuzzy consistency test matrix $\overline{R}$ was calculated and transformed as shown in Table 12.

According to formula (1), the consistency was calculated as $\mathrm{d}(\overline{R}, R) = 0.0976 < 0.1$, which shows the consistency test passed.

Table 13 shows the original matrix. According to equations (2) and (3), the intuitionistic fuzzy consistency test matrix $\overline{R}$ was calculated and transformed as shown in Table 14.

According to formula (1), the consistency was calculated as $\mathrm{d}(\overline{R}, R) = 0.0791 < 0.1$, which shows the consistency test passed.

5.2. Weight Calculation. After calculations in the previous step, all intuitionistic fuzzy judgment matrices passed the consistency test. Substituting all the matrices $\overline{R}$ that passed the test into equation (6), the weights in the first-level index are as follows:

$$\begin{aligned}
\omega_1 &= (0.1428, 0.7735),\\
\omega_2 &= (0.1863, 0.7366),\\
\omega_3 &= (0.1527, 0.7672),\\
\omega_4 &= (0.1241, 0.7804),\\
\omega_5 &= (0.0741, 0.8516),\\
\omega_6 &= (0.1056, 0.8178).
\end{aligned} \tag{16}$$

Table 3: Intuitionistic fuzzy judgment matrix of first-level indicators.

First-level indicators	Environmental management system $\mathbf{A}_1$	Environmental protection $\mathbf{A}_2$	Cost $\mathbf{A}_3$	Pollution $\mathbf{A}_4$	Use of packaging materials $\mathbf{A}_5$	Food safety $\mathbf{A}_6$
Environmental management system $\mathbf{A}_1$	(0.5, 0.5)	(0.35, 0.6)	(0.4, 0.5)	(0.45, 0.35)	(0.65, 0.25)	(0.5, 0.3)
Environmental protection $\mathbf{A}_2$	(0.6, 0.35)	(0.5, 0.5)	(0.6, 0.4)	(0.65, 0.25)	(0.75, 0.2)	(0.7, 0.2)
Cost $\mathbf{A}_3$	(0.5, 0.4)	(0.4, 0.6)	(0.5, 0.5)	(0.5, 0.35)	(0.7, 0.25)	(0.65, 0.2)
Pollution $\mathbf{A}_4$	(0.35, 0.45)	(0.25 , 0.65)	(0.35, 0.5)	(0.5, 0.5)	(0.6, 0.2)	(0.6, 0.4)
Use of packaging materials $\mathbf{A}_5$	(0.25, 0.65)	(0.2, 0.75)	(0.25, 0.7)	(0.2, 0.6)	(0.5, 0.5)	(0.35, 0.6)
Food safety $\mathbf{A}_6$	(0.3, 0.5)	(0.2, 0.7)	(0.2, 0.65)	(0.4, 0.6)	(0.6, 0.35)	(0.5, 0.5)

Table 4: Intuitionistic fuzzy consistency test matrix of first-level indicators.

First-level indicators	Environmental management system $\mathbf{A}_1$	Environmental protection $\mathbf{A}_2$	Cost $\mathbf{A}_3$	Pollution $\mathbf{A}_4$	Use of packaging materials $\mathbf{A}_5$	Food safety $\mathbf{A}_6$
Environmental management system $\mathbf{A}_1$	(0.5, 0.5)	(0.35, 0.6)	(0.4468, 0.5)	(0.4495, 0.3416)	(0.5927, 0.2061)	(0.5403, 0.2648)
Environmental protection $\mathbf{A}_2$	(0.6, 0.35)	(0.5, 0.5)	(0.6, 0.4)	(0.6, 0.2642)	(0.7574, 0.1198)	(0.6991, 0.1937)
Cost $\mathbf{A}_3$	(0.5, 0.4468)	(0.4, 0.6)	(0.5, 0.5)	(0.5, 0.35)	(0.6, 0.1186)	(0.5785, 0.2975)
Pollution $\mathbf{A}_4$	(0.3416, 0.4495)	(0.2642, 0.6)	(0.35, 0.5)	(0.5, 0.5)	(0.6, 0.2)	(0.4468, 0.2727)
Use of packaging materials $\mathbf{A}_5$	(0.2061, 0.5927)	(0.1198, 0.7574)	(0.1186, 0.6)	(0.2, 0.6)	(0.5, 0.5)	(0.35, 0.6)
Food safety $\mathbf{A}_6$	(0.2648, 0.5403)	(0.1937, 0.6991)	(0.2975, 0.5785)	(0.2727, 0.4468)	(0.6, 0.35)	(0.5, 0.5)

Table 5: Intuitionistic fuzzy judgment matrix of secondary indicators of the environmental management system.

A1 second-level indicator	ISO 14000 certification $\mathbf{B}_{11}$	Environmental policy and plan $\mathbf{B}_{12}$
ISO 14000 certification $\mathbf{B}_{11}$	(0.5, 0.5)	(0.5, 0.45)
Environmental policy and plan $\mathbf{B}_{12}$	(0.45, 0.5)	(0.5, 0.5)

Table 6: Intuitionistic fuzzy consistency test matrix of secondary indicators of environmental management system.

A1 second-level indicator	ISO 14000 certification $\mathbf{B}_{11}$	Environmental policy and plan $\mathbf{B}_{12}$
ISO 14000 certification $\mathbf{B}_{11}$	(0.5, 0.5)	(0.5, 0.45)
Environmental policy and plan $\mathbf{B}_{12}$	(0.45, 0.5)	(0.5, 0.5)

Table 7: Intuitionistic fuzzy judgment matrix of secondary indicators of environmental protection.

A2 second-level indicator	Environmental restoration $\mathbf{B}_{21}$	Environmental governance $\mathbf{B}_{22}$
Environmental restoration $\mathbf{B}_{21}$	(0.5, 0.5)	(0.5, 0.5)
Environmental governance $\mathbf{B}_{22}$	(0.5, 0.5)	(0.5, 0.5)

Table 8: Intuitionistic fuzzy judgment matrix of the second-level food safety index.

A6 second-level indicator	Reduce food additives $\mathbf{B}_{61}$	Green R & D and innovation $\mathbf{B}_{62}$
Reduce food additives $\mathbf{B}_{61}$	(0.5, 0.5)	(0.45, 0.5)
Green R & D and innovation $\mathbf{B}_{62}$	(0.5, 0.45)	(0.5, 0.5)

Table 9: Intuitionistic fuzzy judgment matrix of secondary cost indicators.

A3 second-level indicator	Energy consumption $\mathbf{B}_{31}$	Logistics costs $\mathbf{B}_{32}$	Product net price $\mathbf{B}_{33}$
Energy consumption $\mathbf{B}_{31}$	(0.5, 0.5)	(0.65, 0.15)	(0.45, 0.35)
Logistics costs $\mathbf{B}_{32}$	(0.15, 0.65)	(0.5, 0.5)	(0.3, 0.7)
Product net price $\mathbf{B}_{33}$	(0.35, 0.45)	(0.7, 0.3)	(0.5, 0.5)

Table 10: Intuitionistic fuzzy consistency test matrix of the second-level cost index.

A3 second-level indicator	Energy consumption $\mathbf{B}_{31}$	Logistics costs $\mathbf{B}_{32}$	Product net price $\mathbf{B}_{33}$
Energy consumption $\mathbf{B}_{31}$	(0.5, 0.5)	(0.65, 0.15)	(0.4432, 0.2916)
Logistics costs $\mathbf{B}_{32}$	(0.15, 0.65)	(0.5, 0.5)	(0.3, 0.7)
Product net price $\mathbf{B}_{33}$	(0.2916, 0.4432)	(0.7, 0.3)	(0.5, 0.5)

The weights of the secondary indicators are as follows:

Table 11: Intuitionistic fuzzy judgment matrix for secondary indicators of pollution.

A4 second-level indicator	Air pollutant production $\mathbf{B}_{41}$	Wastewater production $\mathbf{B}_{42}$	Solid waste generation $\mathbf{B}_{43}$
Air pollutant production $\mathbf{B}_{41}$	(0.5, 0.5)	(0.45, 0.6)	(0.6, 0.35)
Wastewater production $\mathbf{B}_{42}$	(0.6, 0.45)	(0.5, 0.5)	(0.5, 0.45)
Solid waste generation $\mathbf{B}_{43}$	(0.35, 0.6)	(0.45, 0.5)	(0.5, 0.5)

Table 12: Intuitionistic fuzzy consistency test matrix for secondary indicators of pollution.

A4 second-level indicator	Air pollutant production $\mathbf{B}_{41}$	Wastewater production $\mathbf{B}_{42}$	Solid waste generation $\mathbf{B}_{43}$
Air pollutant production $\mathbf{B}_{41}$	(0.5, 0.5)	(0.45, 0.6)	(0.45, 0.3058)
Wastewater production $\mathbf{B}_{42}$	(0.6, 0.45)	(0.5, 0.5)	(0.5, 0.45)
Solid waste generation $\mathbf{B}_{43}$	(0.3058, 0.45)	(0.45, 0.5)	(0.5, 0.5)

Table 13: Intuitionistic fuzzy judgment matrix for the use of secondary indicators for packaging materials.

A5 second-level indicator	Reusability $\mathbf{B}_{51}$	Biodegradable products $\mathbf{B}_{52}$	Use recycled materials $\mathbf{B}_{53}$	Use of hazardous substances $\mathbf{B}_{54}$
Reusability $\mathbf{B}_{51}$	(0.5, 0.5)	(0.55, 0.4)	(0.45, 0.55)	(0.4, 0.5)
Biodegradable products $\mathbf{B}_{52}$	(0.4, 0.55)	(0.5, 0.5)	(0.5, 0.45)	(0.5, 0.3)
Use recycled materials $\mathbf{B}_{53}$	(0.55, 0.45)	(0.45, 0.5)	(0.5, 0.5)	(0.55, 0.45)
Use of hazardous substances $\mathbf{B}_{54}$	(0.5, 0.4)	(0.3, 0.5)	(0.45, 0.55)	(0.5, 0.5)

Table 14: Intuitionistic fuzzy consistency test matrix for the use of secondary indicators for packaging materials.

A5 second-level indicator	Reusability $\mathbf{B}_{51}$	Biodegradable products $\mathbf{B}_{52}$	Use recycled materials $\mathbf{B}_{53}$	Use of hazardous substances $\mathbf{B}_{54}$
Reusability $\mathbf{B}_{51}$	(0.5, 0.5)	(0.55, 0.4)	(0.55, 0.3529)	(0.525, 0.3483)
Biodegradable products $\mathbf{B}_{52}$	(0.4, 0.55)	(0.5, 0.5)	(0.5, 0.45)	(0.55, 0.401)
Use recycled materials $\mathbf{B}_{53}$	(0.3529, 0.55)	(0.45, 0.5)	(0.5, 0.5)	(0.55, 0.45)
Use of hazardous substances $\mathbf{B}_{54}$	(0.3483, 0.525)	(0.401, 0.55)	(0.45, 0.55)	(0.5, 0.5)

$$\begin{aligned}
\omega_{11} &= (0.4878, 0.4615),\\
\omega_{12} &= (0.4634, 0.4872),\\
\omega_{21} &= (0.5, 0.5),\\
\omega_{22} &= (0.5, 0.5),\\
\omega_{31} &= (0.3209, 0.4898),\\
\omega_{32} &= (0.1913, 0.7150),\\
\omega_{33} &= (0.3004, 0.5646),\\
\omega_{41} &= (0.2951, 0.6254),\\
\omega_{42} &= (0.3373, 0.6240),\\
\omega_{43} &= (0.2647, 0.6358),\\
\omega_{51} &= (0.2538, 0.6855),\\
\omega_{52} &= (0.2329, 0.7248),\\
\omega_{53} &= (0.2213, 0.7378),\\
\omega_{54} &= (0.2030, 0.7542),\\
\omega_{61} &= (0.4634, 0.4872),\\
\omega_{62} &= (0.4878, 0.4615).
\end{aligned} \tag{17}$$

5.3. Information Aggregation

5.3.1. Calculating the Total Weight. After calculating the weights of the first-level indicators and the second-level indicators, they are used in equation (8) for information integration to obtain the total weight. The results are shown in Table 15.

5.3.2. Deblurring. The total weight of the information aggregation in the previous step is a fuzzy number, which is then used in equation (9) to calculate the true value of the total weight as follows: [0.0963, 0.0916, 0.1135, 0.1135, 0.0832, 0.0476, 0.0734, 0.0592, 0.0623, 0.0561, 0.0326, 0.0290, 0.0276, 0.0257, 0.0712, 0.0749]. Then, it is normalized to get [0.0911, 0.0866, 0.1073, 0.1073, 0.0786, 0.0450, 0.0694, 0.0560, 0.0589, 0.0530, 0.0308, 0.0274, 0.0261, 0.0243, 0.0674, 0.0708].

5.3.3. Weight Ratio Analysis. It can be seen from Figure 3 that the highest proportions of index weights were B_{11}, B_{12}, B_{21}, B_{22}, B_{31}, and B_{62}, followed by B_{33} and B_{61}. The sum of the two accounted for 67.6%, which can be regarded as the most influential indicator. From the perspective of the meaning of the indicators, environmental policies and certification, environmental restoration, and governance reflect the suppliers' ability to harmlessly deal with pollution and their efforts to protect the ecological environment. The second is the cost of energy consumed by agricultural products and the ability to develop new clean technologies, which shows the economic profitability of the organization and the level of waste disposal. From the perspective of sustainability combined with the weight of indicators, the two were in line with objective cognition and scientific laws. The results show that suppliers should first consider possible ecological damage and pollution control, and then they should pay attention to controlling product cost and technological innovation for disposal.

5.4. Decision Matrix Normalization. Experts scored the qualitative indicators of the four suppliers, and then the maximum value method was used to decompose the fuzzy numbers to obtain the true values of the qualitative indicators of each supplier. The quantitative values obtained approximately accurate values through statistical data and simulation. Finally, the initial decision matrix composed of qualitative indicators and quantitative indicators is shown in Table 16.

Among them, the yellow part indicates that the indicator is a cost-based indicator, and the rest are benefit-based indicators. Then, the above indicators were divided into cost-type indicators and benefit-type indicators, and they were substituted into formulas (10) and (11), respectively. The standardized decision matrix is shown in Table 17.

5.5. Computing Dominance. After obtaining the normalized decision matrix and the weight of each indicator, the predominance $\delta(a_i, a_k)$ of supplier a_i relative to supplier a_k with respect to indicator c_j was calculated according to equation (13), where θ takes 2.25 [34]. Then, according to equation (12), the matrix of comparative advantages between suppliers was obtained as shown in Table 18.

The advantage comparison matrix was standardized according to equations (14) and (15) to obtain the comprehensive score $\varepsilon(a_i)$ of each supplier: $\varepsilon(a_1) = 0.7476$, $\varepsilon(a_2) = 0.6643$, $\varepsilon(a_3) = 0$, and $\varepsilon(a_4) = 1$. Sorting by size shows that a_4 was the best supplier, and the enterprise should choose supplier a_4 to supply fresh agricultural products.

As shown in Figure 4, the overall advantage of each supplier and the trend of the final comprehensive score were the same. Compared with other suppliers, supplier C4 had a maximum advantage of 3.9266 and the highest overall score of 1, followed by suppliers C1, C2, and C3. The figure shows that the overall advantage of supplier C3 was far lower than that of other manufacturers. From the above calculations, it can be seen that the largest of the cost-based indicators came from C3. This means that, in terms of environmental pollution and product costs, supplier C3 had the highest proportion compared with other manufacturers, so it had the lowest sustainability and the lowest ranking. Supplier C4 was mostly in the bottom position regarding cost-based indicators, and mostly in the first place in

Table 15: Total weight table.

First-level indicators	Secondary indicators	Total weight
(0.1428, 0.7735)	(0.4878, 0.4615)	(0.0697, 0.8780)
	(0.4634, 0.4872)	(0.0662, 0.8839)
(0.1863, 0.7366)	(0.5, 0.5)	(0.0932, 0.8683)
	(0.5, 0.5)	(0.0932, 0.8683)
(0.1527, 0.7672)	(0.3209, 0.4898)	(0.0490, 0.8812)
	(0.1913, 0.7150)	(0.0292, 0.9337)
	(0.3004, 0.5646)	(0.0459, 0.8986)
(0.1241, 0.7804)	(0.2951, 0.6254)	(0.0366, 0.9177)
	(0.3373, 0.6240)	(0.0419, 0.9174)
	(0.2647, 0.6358)	(0.0328, 0.9200)
(0.0741, 0.8516)	(0.2538, 0.6855)	(0.0188, 0.9533)
	(0.2329, 0.7248)	(0.0173, 0.9592)
	(0.2213, 0.7378)	(0.0164, 0.9611)
	(0.2030, 0.7542)	(0.0150, 0.9635)
(0.1056, 0.8178)	(0.4634, 0.4872)	(0.0489, 0.9066)
	(0.4878, 0.4615)	(0.0515, 0.9019)

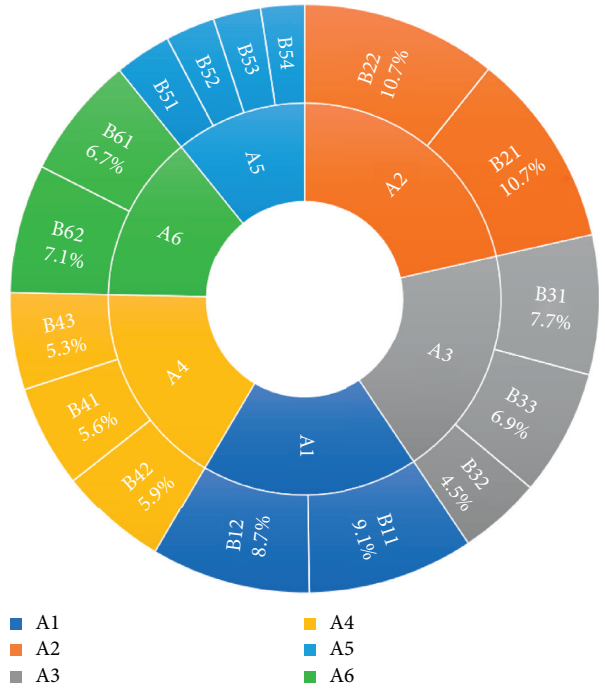

Figure 3: Proportion of total weight.

efficiency-based indicators. This shows that supplier C4 achieved a better balance between economic development, social responsibility, and environmental protection than other manufacturers, which ultimately makes it the most sustainable and gives it the highest comprehensive score.

5.6. Sensitivity Analysis. The purpose of the sensitivity analysis is to verify whether there are differences in the results of the selection of sustainable suppliers of fresh agricultural products under different θ values (representing the different ability of decision-makers to avoid risks). In this

Table 16: Initial decision matrix.

Index/supplier	C1	C2	C3	C4	maxcj	mincj
b1 ISO 14000 certification	0.7716	0.78	0.6675	0.7513	0.78	0.6675
b2 environmental policy and plan	0.4338	0.6456	0.36	0.675	0.675	0.36
b3 environmental restoration	0.6464	0.7195	0.3648	0.8613	0.8613	0.3648
b4 environmental governance	0.6563	0.6	0.408	0.6225	0.6563	0.408
b5 energy consumption	518	532	568	504	568	504
b6 logistics costs	1320	1632	1893	1100	1893	1100
b7 product net price	2530	2715	2900	2300	2900	2300
b8 air pollutant production	54	55	58	52	58	52
b9 wastewater production	1300	1520	1890	1100	1890	1100
b10 solid waste generation	4330	4650	4882	4210	4882	4210
b11 reusability	50	55	32	60	60	32
b12 biodegradable products	62	50	43	75	75	43
b13 use recycled materials	30	32	28	38	38	28
b14 use of hazardous substances	120	130	150	105	150	105
b15 reduce food additives	0.3863	0.4077	0.2409	0.4125	0.4125	0.2409
b16 green R & D and innovation	0.2288	0.2334	0.1713	0.2176	0.2334	0.1713

Table 17: Normalized decision matrix.

Index/supplier	C1	C2	C3	C4
b1 ISO 14000 certification	0.9259	1	0	0.7456
b2 environmental policy and plan	0.2343	0.9067	0	1
b3 environmental restoration	0.5672	0.7144	0	1
b4 environmental governance	1	0.7733	0	0.8639
b5 energy consumption	0.7813	0.5625	0	1
b6 logistics costs	0.7226	0.3291	0	1
b7 product net price	0.6167	0.3083	0	1
b8 air pollutant production	0.6667	0.5	0	1
b9 wastewater production	0.7468	0.4684	0	1
b10 solid waste generation	0.8214	0.3452	0	1
b11 reusability	0.6429	0.8214	0	1
b12 biodegradable products	0.5938	0.2188	0	1
b13 use recycled materials	0.2	0.4	0	1
b14 use of hazardous substances	0.6667	0.4444	0	1
b15 reduce food additives	0.8473	0.9720	0	1
b16 green R & D and innovation	0.9259	1	0	0.7456

Table 18: Dominant comparison matrix.

	C1	C2	C3	C4	$\mathbf{T_d}$	$\varepsilon(\mathbf{a_i})$
C1	0	−4.3945	3.2165	−15.5640	−16.7420	0.7476
C2	−8.9332	0	3.0584	−17.6883	−23.5631	0.6643
C3	−24.7402	−22.8435	0	−30.3814	−77.9651	0
C4	−0.0538	0.3925	3.5879	0	3.9266	1

paper, two values of $\theta = 3$, 4 [34] were used for sensitivity analysis. Table 19 shows the comprehensive scores of various suppliers under different attenuation coefficients. According to Table 19, as the attenuation coefficient increased, the scores of suppliers C1 and C2 declined. This is because the ability of decision-makers to avoid risks became weaker and weaker, resulting in more errors in the judgment of suppliers. Figure 5 reflects the comprehensive score trend of various suppliers under different attenuation coefficient θ values. It can be seen that under the four different θ values, no matter how the decision-makers' circumvention ability changed, the final supplier selection results tended to be consistent.

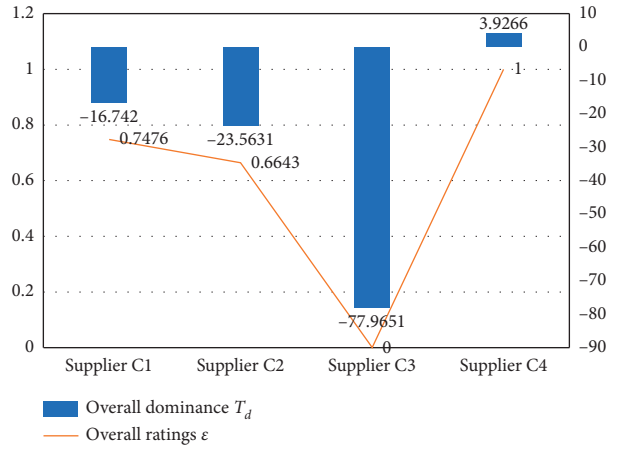

Figure 4: Dominance and comprehensive score table.

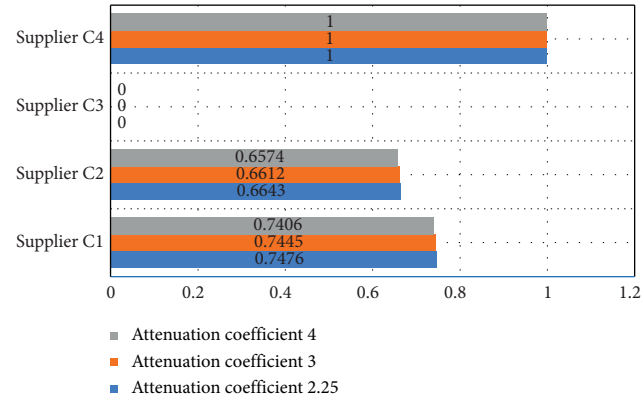

Figure 5: Comprehensive scores under different attenuation coefficients.

Table 19: Comprehensive supplier scores under different attenuation coefficients.

Attenuation coefficient/supplier	C1	C2	C3	C4
2.25	0.7476	0.6643	0	1
3	0.7445	0.6612	0	1
4	0.7406	0.6574	0	1

6. Conclusion

At present, there are very few studies that evaluate the sustainability of fresh agricultural product suppliers, and most indicators are selected based on economic indicators or financial indicators. However, noneconomic indicators such as social responsibility and environmental protection should be considered under the requirements of sustainable development. Therefore, this paper comprehensively considered the impact of economic development, social responsibility, and environmental protection (that is, the triple bottom line) on the sustainability of the supply of fresh agricultural products, and it built a more reasonable index system based on reference to the selection criteria of conventional suppliers. The evaluation system can help future decision-makers in selecting sustainable fresh agricultural product suppliers. This paper also combined intuitionistic fuzzy AHP and TODIM multiattribute decision-making methods to select sustainable suppliers.

When determining the index weight, the traditional supplier selection methods such as AHP, ANP, and DEMATEL cannot accurately deal with the uncertainty of expert evaluation information, and the decision information lacks scientific quantitative means. The fuzzy AHP method can better deal with the fuzziness of natural language and transform fuzzy information into accurate numbers. This fully considers the uncertainty in expert evaluation and better guarantees that the original information is not distorted.

When ranking suppliers, the supplier ranking methods such as DEA, PROMETHEE, and TOPSIS do not consider the decision-maker's subjective preference behavior, which often loses a lot of qualitative information. TODIM multiattribute decision-making method takes into account the psychological behavior of decision-makers, which can deal with environmental uncertainty and ensure the original information is not distorted.

In the field of sustainable supplier selection of fresh agricultural products, from the perspective of sustainability, most of the previous literature did not consider the combination of fuzzy weight determination method and traditional supplier ranking method to select fresh agricultural products suppliers. Therefore, based on the concept of sustainability, this paper uses FAHP and TODIM to select the best supplier. In order to verify the feasibility of the proposed integration method, an example sensitivity analysis was carried out in this paper. According to the final calculation results, it was found that intuitionistic fuzzy AHP and TODIM were feasible and effective for supplier selection.

In summary, this article is based on the "triple bottom line" theory to assess and enrich the sustainability model of fresh agricultural products suppliers. This research fills the gap of applying the "triple bottom line" theory and the IFAHP-TODIM method to the selection of sustainable suppliers of fresh agricultural products. Finally, the limitations and future research directions of this article are as follows:

(1) The model adopted in this paper still cannot avoid subjectivity in determining the weight of each indicator, so further research is needed.

(2) Due to the lack of research in this field, the evaluation index system in this article may not be universally applied. In the future, it is necessary to adjust the selection of indicators according to the actual economic and policy situation of various regions, so as to make the decision more effective.

(3) The future research can also start from the weight section. Further, the combination of subjective and objective weights makes the decision more reliable.

(4) The supplier selection of fresh agricultural products can make decisions more accurately with the help of big data and other data mining algorithms.

Data Availability

The data used to support the findings of this study were supplied by experts. Data are available from the corresponding author (2019225025109@stu.scu.edu.cn) for researchers who meet the criteria for access to confidential data.

Conflicts of Interest

The authors declare that they have no conflicts of interest.

References

[1] M. M. Aung and Y. S. Chang, "Temperature management for the quality assurance of a perishable food supply chain," *Food Control*, vol. 40, pp. 198–207, 2014.

[2] X. Ma, S. Wang, S. M. N. Islam, and X. Liu, "Coordinating a three-echelon fresh agricultural products supply chain considering freshness-keeping effort with asymmetric information," *Applied Mathematical Modelling*, vol. 67, pp. 337–356, 2019.

[3] C. Aysoy, D. H. Kirli, and S. Tumen, "How does a shorter supply chain affect pricing of fresh food? evidence from a natural experiment," *Food Policy*, vol. 57, pp. 104–113, 2015.

[4] S. Henson, O. Masakure, and D. Boselie, "Private food safety and quality standards for fresh produce exporters: the case of Hortico Agrisystems, Zimbabwe," *Food Policy*, vol. 30, no. 4, pp. 371–384, 2005.

[5] A. Amindoust, S. Ahmed, A. Saghafinia, and A. Bahreininejad, "Sustainable supplier selection: a ranking model based on fuzzy inference system," *Applied Soft Computing*, vol. 12, no. 6, pp. 1668–1677, 2012.

[6] B. G. Smith, "Developing sustainable food supply chains," *Philosophical Transactions of the Royal Society B: Biological Sciences*, vol. 363, no. 1492, pp. 849–861, 2007.

[7] H. Allaoui, Y. Guo, A. Choudhary, and J. Bloemhof, "Sustainable agro-food supply chain design using two-stage hybrid multi-objective decision-making approach," *Computers & Operations Research*, vol. 89, pp. 369–384, 2018.

[8] P. M. Wognum, H. Bremmers, J. H. Trienekens, J. G. A. J. van der Vorst, and J. M. Bloemhof, "Systems for sustainability and transparency of food supply chains—current status and challenges," *Advanced Engineering Informatics*, vol. 25, no. 1, pp. 65–76, 2011.

[9] P. W. Gerbens-Leenes, H. C. Moll, and A. J. M. Schoot Uiterkamp, "Design and development of a measuring method for environmental sustainability in food production systems," *Ecological Economics*, vol. 46, no. 2, pp. 231–248, 2003.

[10] C. Solér, K. Bergström, and H. Shanahan, "Green supply chains and the missing link between environmental information and practice," *Business Strategy and the Environment*, vol. 19, no. 1, pp. 14-15, 2009.

[11] M. Cellura, F. Ardente, and S. Longo, "From the LCA of food products to the environmental assessment of protected crops districts: a case-study in the south of Italy," *Journal of Environmental Management*, vol. 93, no. 1, pp. 194–208, 2012.

[12] M. J. Maloni and M. E. Brown, "Corporate social responsibility in the supply chain: an application in the food industry," *Journal of Business Ethics*, vol. 68, no. 1, pp. 35–52, 2006.

[13] L. Spence and M. Bourlakis, "The evolution from corporate social responsibility to supply chain responsibility: the case of Waitrose," *Supply Chain Management: An International Journal*, vol. 14, no. 4, pp. 291–302, 2009.

[14] O. Chkanikova and O. Mont, "Corporate supply chain responsibility: drivers and barriers for sustainable food retailing," *Corporate Social Responsibility and Environmental Management*, vol. 22, no. 2, pp. 65–82, 2012.

[15] C. C. Krejci, R. T. Stone, M. C. Dorneich, and S. B. Gilbert, "Analysis of food hub commerce and participation using agent-based modeling: integrating financial and social drivers," *Human Factors*, vol. 58, no. 1, pp. 58–79, 2016.

[16] Y. Chen, S. Wang, J. Yao, Y. Li, and S. Yang, "Socially responsible supplier selection and sustainable supply chain development: a combined approach of total interpretive structural modeling and fuzzy analytic network process," *Business Strategy and the Environment*, vol. 27, no. 8, pp. 1708–1719, 2018.

[17] S. Stranieri, L. Orsi, A. Banterle, and E. C. Ricci, "Sustainable development and supply chain coordination: the impact of corporate social responsibility rules in the European Union food industry," *Corporate Social Responsibility and Environmental Management*, vol. 26, no. 2, pp. 481–491, 2019.

[18] N. Yakovleva, J. Sarkis, and T. Sloan, "Sustainable benchmarking of supply chains: the case of the food industry," *International Journal of Production Research*, vol. 50, no. 5, pp. 1297–1317, 2012.

[19] R. Accorsi, S. Cholette, R. Manzini, C. Pini, and S. Penazzi, "The land-network problem: ecosystem carbon balance in planning sustainable agro-food supply chains," *Journal of Cleaner Production*, vol. 112, pp. 158–171, 2015.

[20] H. Allaoui, Y. Guo, and J. Sarkis, "Decision support for collaboration planning in sustainable supply chains," *Journal of Cleaner Production*, vol. 229, pp. 761–774, 2019.

[21] M. M. Siddh, G. Soni, R. Jain, M. K. Sharma, and V. Yadav, "Agri-fresh food supply chain quality (AFSCQ): a literature review," *Industrial Management & Data Systems*, vol. 117, no. 9, pp. 2015–2044, 2017.

[22] G. Büyüközkan and G. Çifçi, "A novel fuzzy multi-criteria decision framework for sustainable supplier selection with incomplete information," *Computers in Industry*, vol. 62, no. 2, pp. 164–174, 2011.

[23] D. Wu and J. M. Mendel, "Computing with words for hierarchical decision making applied to evaluating a weapon system," *IEEE Transactions on Fuzzy Systems*, vol. 18, no. 3, pp. 441–460, 2010.

[24] Z. Chen, X. Ming, X. Zhang, D. Yin, and Z. Sun, "A rough-fuzzy DEMATEL-ANP method for evaluating sustainable value requirement of product service system," *Journal of Cleaner Production*, vol. 228, pp. 485–508, 2019.

[25] J. Li, H. Fang, and W. Song, "Sustainable supplier selection based on SSCM practices: a rough cloud TOPSIS approach," *Journal of Cleaner Production*, vol. 222, pp. 606–621, 2019.

[26] S. Hosseini and A. A. Khaled, "A hybrid ensemble and AHP approach for resilient supplier selection," *Journal of Intelligent Manufacturing*, vol. 30, no. 1, pp. 207–228, 2016.

[27] M. Giannakis, R. Dubey, I. Vlachos, and Y. Ju, "Supplier sustainability performance evaluation using the analytic network process," *Journal of Cleaner Production*, vol. 247, Article ID 119439, 2020.

[28] W. Song, Z. Xu, and H.-C. Liu, "Developing sustainable supplier selection criteria for solar air-conditioner manufacturer: an integrated approach," *Renewable and Sustainable Energy Reviews*, vol. 79, pp. 1461–1471, 2017.

[29] A. Torres-Ruiz and A. R. Ravindran, "Use of interval data envelopment analysis, goal programming and dynamic eco-efficiency assessment for sustainable supplier management,"

Computers & Industrial Engineering, vol. 131, pp. 211–226, 2019.

[30] M. Segura, C. Maroto, and B. Segura, "Quantifying the sustainability of products and suppliers in food distribution companies," *Sustainability*, vol. 11, no. 21, pp. 58–75, 2019.

[31] C. Yu, Y. Shao, K. Wang, and L. Zhang, "A group decision making sustainable supplier selection approach using extended TOPSIS under interval-valued Pythagorean fuzzy environment," *Expert Systems with Applications*, vol. 121, pp. 1–17, 2019.

[32] Y. Liang, J. Liu, J. Qin, and Y. Tu, "An improved multigranularity interval 2-tuple TODIM approach and its application to green supplier selection," *International Journal of Fuzzy Systems*, vol. 21, no. 1, pp. 129–144, 2018.

[33] S. Nie, H. Liao, X. Wu, and Z. Xu, "Green supplier selection with a continuous interval-valued linguistic TODIM method," *IEEE Access*, vol. 7, pp. 124315–124328, 2019.

[34] L. Wang, Y.-M. Wang, and L. Martínez, "Fuzzy TODIM method based on alpha-level sets," *Expert Systems With Applications*, vol. 140, Article ID 112899, 2020.

[35] G. Büyüközkan and F. Göçer, "Application of a new combined intuitionistic fuzzy MCDM approach based on axiomatic design methodology for the supplier selection problem," *Applied Soft Computing*, vol. 52, pp. 1222–1238, 2017.

[36] A. Cheraghalipour and S. Farsad, "A bi-objective sustainable supplier selection and order allocation considering quantity discounts under disruption risks: a case study in plastic industry," *Computers & Industrial Engineering*, vol. 118, pp. 237–250, 2018.

[37] M. Abdel-Basset, M. Mohamed, and F. Smarandache, "A hybrid neutrosophic group ANP-TOPSIS framework for supplier selection problems," *Symmetry*, vol. 10, no. 6, p. 21, 2018.

[38] F. Ecer and D. Pamucar, "Sustainable supplier selection: a novel integrated fuzzy best worst method (F-BWM) and fuzzy CoCoSo with Bonferroni (CoCoSo'B) multi-criteria model," *Journal of Cleaner Production*, vol. 266, Article ID 121981, 2020.

[39] G. Bektur, "An integrated methodology for the selection of sustainable suppliers and order allocation problem with quantity discounts, lost sales and varying supplier availabilities," *Sustainable Production and Consumption*, vol. 23, pp. 111–127, 2020.

[40] A. H. Azadnia, M. Z. M. Saman, and K. Y. Wong, "Sustainable supplier selection and order lot-sizing: an integrated multiobjective decision-making process," *International Journal of Production Research*, vol. 53, no. 2, pp. 383–408, 2014.

[41] E. Szmidt and J. Kacprzyk, "Amount of information and its reliability in the ranking of Atanassov's intuitionistic fuzzy alternatives," *Studies in Computational Intelligence*, Springer, Berlin, Germany, pp. 7–19, 2009.

[42] Z. Xu and H. Liao, "Intuitionistic fuzzy analytic hierarchy process," *IEEE Transactions on Fuzzy Systems*, vol. 22, no. 4, pp. 749–761, 2014.

[43] X. Zeshui, "Intuitionistic fuzzy aggregation operators," *IEEE Transactions on Fuzzy Systems*, vol. 15, no. 6, pp. 1179–1187, 2007.

[44] A. Chandramohan, M. V. C. Rao, and M. S. Arumugam, "Two new and useful defuzzification methods based on root mean square value," *Soft Computing*, vol. 10, no. 11, pp. 1047–1059, 2006.

[45] Z.-P. Fan, X. Zhang, F.-D. Chen, and Y. Liu, "Extended TODIM method for hybrid multiple attribute decision making problems," *Knowledge-Based Systems*, vol. 42, pp. 40–48, 2013.

Hindawi
Mathematical Problems in Engineering
Volume 2020, Article ID 7839432, 11 pages
https://doi.org/10.1155/2020/7839432

Research Article

Reliability Estimation for Zero-Failure Data Based on Confidence Limit Analysis Method

Haiyang Li[1,2] **and Zeyu Zheng**[1,2]

[1]*Shenyang Institute of Automation, Chinese Academy of Sciences, Shenyang 110016, China*
[2]*Institutes for Robotics and Intelligent Manufacturing, Chinese Academy of Sciences, Shenyang 110169, China*

Correspondence should be addressed to Haiyang Li; lihaiyang@sia.cn

Received 28 May 2020; Revised 27 August 2020; Accepted 20 October 2020; Published 4 November 2020

Academic Editor: Huchang C. Liao

Due to the improvement of the quality of industrial products, zero-failure data often occurs during the reliability life test or in the service environment, and such problems cannot be handled using traditional reliability estimation methods. Regarding the processing and analysis of zero-failure data, the confidence limit assessment methods were proposed by some researchers. Based on the existing research, a confidence limit method set (CLMS) is established in the Weibull distribution for reliability estimation of zero-failure data. The method set includes the unilateral confidence limit method and optimal confidence limit method, so that almost all existing grouping types of zero-failure data can be quickly evaluated, and multiple methods can be used in parallel to deal with the same problem. The effectiveness and high efficiency of the CLMS combined with numerical simulation examples have been verified, and the possibility of analyzing multiple groups of zero-failure data with a confidence limit method suitable for processing single group of zero-failure data is expanded. Finally, the actual effect of the method set is verified by the single group of zero-failure data of rolling bearings and the multiple groups of zero-failure data of torque motors. The results of the example evaluation show that the CLMS has obvious advantages in practical engineering applications.

1. Introduction

For high-reliability industrial products, it takes quite a long time to test their samples failure data. Some of the industrial products with complicated structure and expensive cost are difficult to carry out damage tests because of economic reasons [1]. Research on reliability evaluation and life prediction methods of such products can often only rely on zero-failure data with limited capacity. The traditional reliability assessment method involves less processing of zero-failure data. Therefore, the theory of reliability evaluation under the condition of zero-failure data has been developed [2].

Estimating accurate sample reliability based on zero-failure data is challenging [3]. The reliability analysis of zero-failure data is a new question encountered in recent years with the improvement of product quality. The research work is not only of theoretical significance, but also of practical application value. Since the publication of research results by Martz and Waller [4], the research on zero-failure data has been studied for more than 40 years, which has gradually attracted the attention of related researchers [5]. Chen proposed the reliability assessment confidence limit method under the condition of zero-failure data in the 1990s and then proposed that the lower confidence limits of the reliability and reliable life are under the exponential distribution, Weibull distribution, and normal distribution [6]. Two years later, Chen et al. [7] proposed the optimal lower confidence limit method for average life, reliability, and reliable life using the product under several different life distribution conditions. Based on the previously mentioned results, Sun and Chen [8] used the confidence limit method for reliability assessment studies under the condition that the product lifetime obeys the Weibull distribution and the lognormal distribution.

The confidence limit evaluation method is an efficient way to deal with the reliability evaluation of zero-failure data. It is often used for reliability estimation in the case of

zero-failure data. Although the related research on reliability evaluation methods based on zero-failure data started late, the development in the past decade has also made some progress. Fu and Zhang [9] proposed a zero-failure data reliability analysis method with a known lower bound of shape parameters under the condition that the product life is subject to the Weibull distribution and gave a concrete expression of the one-side confidence lower limit of service life and reliability. After Monte Carlo simulation and simulation analysis, it is verified that the proposed method can make full use of zero-failure data and can accumulate the nonfailure data whose product life is subject to the distribution and increase the credibility of the information volume to improve the results. Jiang et al. [3, 10] extended the research on the product failure rate estimation method and proposed the least squares estimation and Bayesian estimation of the failure rate under the different life distributions. The estimation method combined with an example verifies the effectiveness and robustness of the method. Chambal and Bertkeats [11] proposed to use triangle distribution instead of Weibull distribution to describe the failure rate of components. The zero-failure data confidence limit evaluation method is widely used due to its strong generalization ability. Kayis [12] took the parameters related to product reliability as random variables and estimated the reliability under the unilateral confidence limit by using the parameters of different confidence intervals. Based on a class of nonlinear tunnel diode circuits with parameter perturbation, Chang et al. established the Takagi-Sugeno fuzzy model for the uncertainty of parameters, which effectively achieved the purpose of failure filtering errors [13]. In the process of expression of reliability uncertainty, the nonlinear functions are identified via neural networks can be effectively described, and the neural networks-based switched observer is constructed to approximate all unmeasurable states [14]. The uncertainty research in the reliability research process often used the neural network method to estimate the function, which would effectively solve the problem of considering the saturation nonlinearity [15]. Han [16] and Jiang and Jiang [17] put forward the optimal confidence limit method and applied it in different life distribution types and the single confidence limit of reliability was obtained according to the definite reliability analysis requirements.

Based on the existing research, a confidence limit method set (CLMS) is established in the Weibull distribution for reliability estimation of zero-failure data. The method set includes the unilateral confidence limit method and optimal confidence limit method, so that almost all existing grouping types of zero-failure data can be quickly evaluated, and multiple methods can be used in parallel to deal with the same problem. In this study, the grouping types of zero-failure data involved in the research object are combed in detail. Based on different zero-failure data grouping forms and related usage conditions, the confidence limit analysis methods used are different. The method set can be used to quickly and accurately select the appropriate confidence limit evaluation method for reliability estimation. The effectiveness and high efficiency of the CLMS combined with numerical simulation examples have been verified, and the possibility of analyzing multiple groups of zero-failure data with a confidence limit method suitable for processing single group of zero-failure data is expanded. Finally, in order to verify the effect of this method set in practical engineering, the actual case analysis of the single group of zero-failure data of rolling bearings and the multiple groups of zero-failure data of torque motors was conducted. This method set will facilitate future research, so that we can quickly find a way to solve the problem when encountering similar problems.

In this paper, the reliability estimation for zero-failure data based on confidence limit analysis method for industrial products is discussed. First of all, we introduce the characteristics of the Weibull distribution model and the physical properties of the product life distribution that each parameter can reflect. Then, we elaborate on the reasons and classification of zero-failure data. Third, in the section about the application and conditions of use of the confidence limit assessment method, the specific technical route and application scenarios of the method are described in detail. Finally, we use the representative rolling bearing and torque motor examples of industrial products to carry out verification research with the method proposed in this paper to further verify the effectiveness of the CLMS proposed in this paper.

2. Weibull Distribution

The Weibull distribution is widely used in the research of reliability assessment and product life prediction due to its own properties and good applicability in industrial product life statistics [18]. Most electronic, mechanical, and electrical products (such as bearings, generators, hydraulic pumps, and materials) are subjected to this distribution [19]. The probability density function (PDF) of the three-parameter Weibull distribution is defined as

$$f(t) = \frac{\beta}{\vartheta}\left(\frac{t-\gamma}{\vartheta}\right)^{\beta-1} \exp\left[-\left(\frac{t-\gamma}{\vartheta}\right)^{\beta}\right], \quad t \geq \gamma, \tag{1}$$

where β indicates shape parameters, ϑ indicates scale parameters, and γindicates position parameters.

When the value of position parameter γ is 0, the three-parameter Weibull distribution degenerates into two-parameter Weibull distribution. After nearly 80 years of research and application, the statistical analysis of a large number of engineering test data samples proves that Weibull distribution model plays an important role in the research of product life distribution type and reliability assessment [20]. The cumulative distribution function (CDF) is defined as

$$F(t) = P(T \leq t) = 1 - \exp\left[-\left(\frac{t-\gamma}{\vartheta}\right)^{\beta}\right], \quad t \geq \gamma, \tag{2}$$

where $T \sim W(\beta, \eta, \gamma)$, for$R(t) = 1 - F(t)$, and the reliability function is

$$R(t) = \exp\left[-\left(\frac{t-\gamma}{\vartheta}\right)^{\beta}\right], \quad t \geq \gamma. \tag{3}$$

The failure rate of industrial products such as bearings and motors usually has the characteristics of gradually

increasing and decreasing with time. With regard to the geometric meaning of the position parameter, the position parameter γ can determine the starting position of the distribution curve in the coordinate system, and its value change causes the curve to move in parallel on the coordinates. With regard to the physical meaning of the position parameter, when the position parameter $\gamma < 0$, this indicates that the product fails before use; when the position parameter $\gamma > 0$, this indicates that the product starts to fail, and when the mission time is greater than γ, the probability of failure before this time is 0. Therefore, the value of the position parameter in the process of actual engineering application is also called the minimum life or the safe life. The change of the position parameter causes the probability density function of the distribution to change as shown in Figure 1.

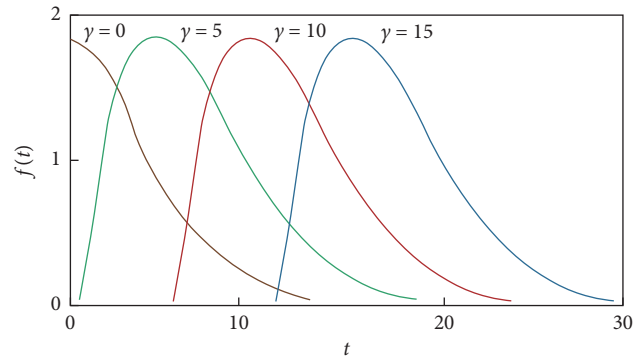

Figure 1: Probability density function curves with different position parameters.

3. The Grouping Type of Zero-Failure Data

Currently, there are mainly two kinds of zero-failure data grouping type, one is test data of a single group, and the other is test data of multiple groups [21]. Among them, the multipacket-type zero-failure data can be further subdivided into pretest grouping and posttest grouping. The censoring time is generally set in advance in the reliability life test, which has great subjectivity and dependence on expert experience. The preset value of the censoring time is further divided into regular and random settings. The grouping type of zero-failure data is shown in Figure 2.

3.1. Single Group of Zero-Failure Data. When n samples participate in the censoring test, it ends at time t, and all samples do not fail. At this time, a set of zero-failure data is obtained, which can be expressed as $Z = (n, t)$. The value of time t can be set before or after the censored test.

3.2. Multiple Groups of Zero-Failure Data. A batch of samples is randomly selected from the products of the study subjects for life test, and the sample capacity is represented by N. The batch of samples is divided into m groups, and the number of samples included in each group is represented by n_i, and the corresponding end time is t_1, t_2,..., t_m $(t_1 < t_2 < \cdots < t_m)$. At this time, the corresponding zero-failure data obtained according to the timing censored test can be expressed as $Z = (n_i, t_i)$. The value of m can be set before or after the start of the test, and the setting of the parameter n_i can be random or a regular value.

After the previously mentioned analysis, it is found that the single-group type of zero-failure data belongs to the special case of the multiple groups' type.

4. The Confidence Limit Assessment Method

4.1. Unilateral Confidence Limit Assessment Method

4.1.1. The Assessment for Single Group of Zero-Failure Data. If the premise of the life of the product obeying the two-parameter Weibull distribution after the statistical analysis of the previous empirical data is established, it is often difficult to directly estimate the shape parameters in the life distribution by using the zero-failure data. However, when the range of the shape parameters can be determined, the theoretical logic deduction can be used to derive the unilateral confidence limit of the reliability parameter of the samples.

There is such a set of zero-failure data, the sample size is n, and the censoring time is t_0. The value of time t_0 can be set before or after the censored test. According to the exponential distribution characteristics [9], the reliability R_l of the sample under the condition that the confidence level is $1 - \alpha$ can be expressed as

$$R_l(t) = \exp\left(\frac{t \ln(\alpha)}{N}\right), \tag{4}$$

where t indicates mission time, and $N = (n + 1)\,t_0$. Using formula (4), the lower confidence interval of the mean time between failures (MTBF) in the case of a single group zero-failure data can be obtained as

$$\theta_l = -\frac{(n+1)t_0}{\ln \alpha}. \tag{5}$$

If the shape parameter of Weibull distribution is known, let $X = t^\beta$, $\theta = \eta^\beta$, and then it can be considered that X obeys the exponential distribution. After transformation, the Weibull distribution is transformed into an exponential distribution, and the following can be obtained as

$$\theta_{u1} = \eta_{u1}^\beta = -\frac{(n+1)t_0^\beta}{\ln \alpha}. \tag{6}$$

The reliability unilateral confidence limit under the Weibull distribution is obtained by (6), and the R_{u1} of under the condition that the confidence level is $1 - \alpha$ can be expressed as

$$R_{u1}(t) = \exp\left[\frac{\ln \alpha}{n+1}\left(\frac{t}{t_0}\right)^\beta\right], \tag{7}$$

where t indicates mission time, β indicates shape parameters, and ϑ indicates scale parameters.

At the same time, under the condition that the confidence level is $1 - \alpha$, it is also possible to obtain the unilateral confidence limit of the reliability when the lower limit of the

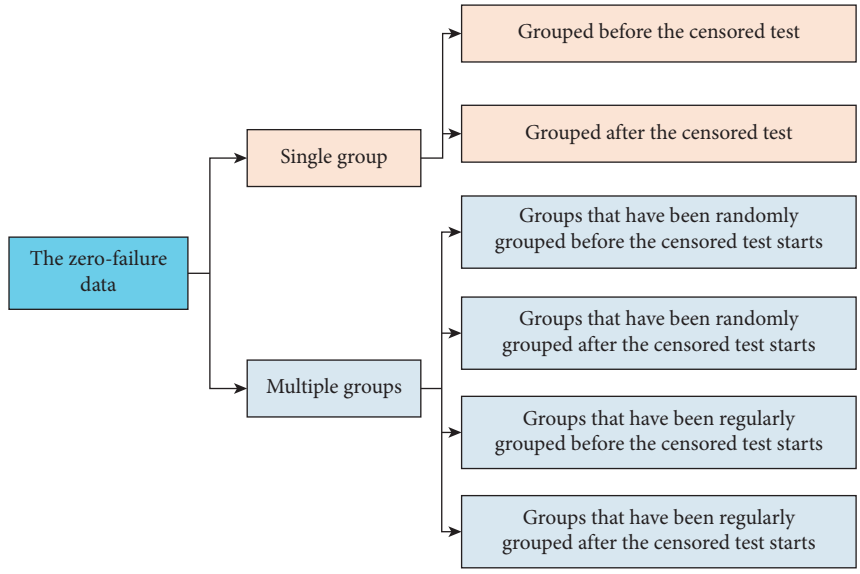

Figure 2: The grouping type chart of zero-failure data.

value range of the shape parameter in the Weibull distribution is known. The unilateral confidence limit of the reliability R'_{u1} can be expressed as

$$R'_{u1}(t) = \exp\left[\frac{\ln \alpha}{n+1}\left(\frac{t}{t_0}\right)^{\beta_0}\right], \quad (t > 0), \tag{8}$$

where t indicates the mission time and β_0 indicates the lower limit of the shape parameter.

4.1.2. The Assessment for Multiple Groups of Zero-Failure Data. There is such a batch of multiple groups of zero-failure data, and the sample size is n. The number of groups is m, each group contains the sample number n_i, $(i = 1, 2, \ldots, m)$, and the corresponding censoring time is t_1, t_2, …, $t_m$and the condition is $t_1 < t_2 < \cdots < t_m$. In this case, zero-failure data can be represented as $Z = (t_i, n_i)$, and the reliability R_{u2} of products under the condition that the confidence level is $1 - \alpha$ can be expressed as [10]

$$R_{u2}(t) = \exp\left[\frac{\left(t^{\beta} \ln \alpha\right)}{\sum_{i=1}^{m} n_i t_i^{\beta}}\right], \quad t > 0. \tag{9}$$

The derivation process of this reliability evaluation expression is also combined with the idea of exponential distribution parameter estimation, and the specific process is omitted here.

4.2. Optimal Confidence Limit Assessment Method

4.2.1. The Assessment for Single Group of Zero-Failure Data. According to the characteristics of zero-failure data of the single group, there is such a set of zero-failure data, the sample size is n, and the censoring time is t_0. The optimal confidence limit analysis method for single group of zero-failure data is a simplified result of multiple groups of forms.

Under the condition that the shape parameterβ in the two-parameter Weibull distribution is unknown [7], the reliability R_{o1} under the condition that the confidence level is $1 - \alpha$ can be expressed as

$$R_{o1}(t) = \begin{cases} 0, & t > t_0, \\ \alpha^{1/n}, & 0 < t \le t_0, \end{cases} \tag{10}$$

where t indicates the mission time.

If the shape parameter β has a value range of $[\beta_1, \beta_2]$, the reliability R'_{o1} under the condition that the confidence level is $1 - \alpha$ can be expressed as

$$R'_{o1}(t) = \begin{cases} \alpha^{1/\left[n\left(t_0/t\right)^{\beta_1}\right]}, & 0 < t < t_0, \\ \alpha^{1/\left[n\left(t_0/t\right)^{\beta_2}\right]}, & t \ge t_0, \end{cases} \tag{11}$$

where t indicates the mission time.

The range of shape parameters in the two-parameter Weibull distribution often comes from the statistical results of product life data in engineering practice. The optimal confidence limit analysis method under zero-failure data is more reliable because of the introduction of product life distribution parameter information.

4.2.2. The Assessment for Multiple Groups of Zero-Failure Data. According to the characteristics of zero-failure data of the multiple groups, the number of groups is m, each group contains the sample number n_i, $(i = 1, 2, \ldots, m)$, and the corresponding censored time is t_1, t_2, …, $t_m$and the condition is$t_1 < t_2 < \cdots < t_m$. In this case, zero-failure data can be represented as $Z = (t_i, n_i)$.

According to [7], when the confidence level is $1 - \alpha$, the lower confidence limit R_{o2} can be expressed as

$$R_{o2}(t) = \inf\left\{\exp\left[-\left(\frac{t}{\vartheta}\right)^{\beta}\right]\right\}: \prod_{i=1}^{m}\exp\left[-\left(\frac{t_i}{\vartheta}\right)^{\beta} > \alpha, \eta > 0, \beta > 0\right] = e^{-a}, \tag{12}$$

where $a = \sup[(t/\vartheta)^{\beta}: \sum_{i=1}^{m} t_i^{\beta}/-\ln\alpha < \vartheta^{\beta}, \vartheta > 0, \beta > 0] = -\ln\alpha/\inf\{f(\beta): \beta > 0\}$; at this time there is the equation-$f(\beta) = \sum_{i=1}^{m}(t_i/t)^{\beta}$.We can get the inequality $f'(\beta) \geq 0$when the condition is $t \leq (\prod_{i=1}^{m} t_i)^{1/m}$. So, $\inf\{f(\beta): \beta > 0\} = \lim_{\beta \longrightarrow 0} f(\beta) = m$. The lower confidence limit for reliability at this mission time is

$$R_{o2}(t) = \alpha^{1/m}. \tag{13}$$

The inequality is $f'(\beta) \leq 0$ when the condition is $t \geq t_{(m)}$, where, $t_{(m)} = \max(t_1, t_2, \ldots, t_m)$; therefore,

$$\inf\{f(\beta): \beta > 0\} = \lim_{\beta \longrightarrow \infty} f(\beta) = \begin{cases} 0, & \text{when } t > t_{(m)}, \\ P, & \text{when } t = t_{(m)}, \end{cases} \tag{14}$$

where the parameter P is an element in the set $\{i: 1 \leq i \leq m, t_i = t_{(m)}\}$, and the lower confidence limit for reliability at this time is

$$R_{o2}(t) = \begin{cases} 0, & \text{when } t > t_{(m)}, \\ \alpha^{1/P}, & \text{when } t = t_{(m)}. \end{cases} \tag{15}$$

The parameter β^* is the only solution of the equation $\sum_{i=1}^{m}(t_i/t)^{\beta}\ln(t_i/t) = 0$, when $(\prod_{i=1}^{m} t_i)^{1/m} < t < t_{(m)}$, and the$\inf\{f(\beta): \beta > 0\} = \lim f(\beta^*)$. The lower confidence limit for reliability at this time is $R_{o2} = \alpha^{1/f(\beta^*)}$. Under the condition that the shape parameter β in the two-parameter Weibull distribution is unknown, the reliability R_{o2} under the condition that the confidence level is $1-\alpha$ can be expressed as

$$R_{o2}(t) = \begin{cases} 0, & t > t_{(m)}, \\ \alpha^{1/P}, & t = t_{(m)}, \\ \alpha^{1/f(\beta^*)}, & c < t < t_{(m)}, \\ \alpha^{1/m}, & 0 < t \leq c, \end{cases} \tag{16}$$

where t indicates the mission time; $c = (\prod_{i=1}^{m} t_i)^{1/m}$.

If the shape parameter β has a value range of $[\beta_1, \beta_2]$, the reliability R_{o2}' under the condition that the confidence level is $1-\alpha$ can be expressed as follows:

$$R_{o2}'(t) = \begin{cases} \alpha^{1/f(\beta_1)}, & 0 < t \leq c, \\ \alpha^{1/f(\beta_2)}, & t \geq t_{(m)}, \\ \alpha^{1/f(\beta_1)}, & c < t < t_{(m)},\ \beta^* \leq \beta_1, \\ \alpha^{1/f(\beta_2)}, & c < t < t_{(m)},\ \beta^* \geq \beta_2, \\ \alpha^{1/f(\beta^*)}, & c < t < t_{(m)},\ \beta_1 \leq \beta^* \leq \beta_2, \end{cases} \tag{17}$$

where t indicates the mission time $t_{(m)} = \max(t_1, t_2, \ldots, t_m)$, the parameter β^* is the only solution of the equation $\sum_{i=1}^{m}(t_i/t)^{\beta}\ln(t_i/t) = 0$, and $f(\beta) = \sum_{i=1}^{m}(t_i/t)^{\beta}$, $c = (\prod_{i=1}^{m} t_i)^{1/m}$.

5. Establishing the Confidence Limit Method Set

In the Weibull distribution, all the current commonly used confidence limit analysis methods are collected into one framework to establish a method set, and we name it the confidence limit method set (CLMS). The purpose of the method set is to meet the random engineering characteristics of practical engineering cases in the application process of reliability evaluation based on zero-failure data. In order to use the single group optimal confidence limit method to process multiple groups of zero-failure data, a method to extend the application of optimal confidence limits is proposed in this method set. The basic structure of the CLMS is shown in Figure 3.

It can be seen from the schematic diagram that one side of the method set is the existing confidence limit analysis method, and the other side is the form of the zero-failure data case in actual engineering. The direction indicated by the arrow in the middle represents which cases the method can be used to evaluate. This makes it possible to apply multiple methods at the same time to solve a problem, and then select the optimal reliability evaluation result. The establishment of this method set belongs to a kind of ideological practice. With the deepening and development of research in this field, this method set can continue to expand to more methods and more types of life distribution. It can be seen from the source of zero-failure data that this type of life data does not contain the dispersive information of the actual life of the product, so it is difficult to estimate accurate shape parameters based on the zero-failure data. However, in the actual engineering application process, through past experience and actual product life statistics, we can often get the value range of the shape parameter in the Weibull distribution. It is feasible to conduct reliability assessment by introducing empirical life distribution parameter information into the confidence limit evaluation method of zero-failure data.

6. Simulation Verification and Discussion

According to previous research experience and results, it is assumed that the bearing life of the research object follows the three-parameters Weibull distribution. Yang [22] analyzed the fatigue life test data of 135 groups, 6 types, 52 models, and a total of 2031 sets of bearings from the National Bearing Quality Monitoring Center of Luoyang Bearing Research Institute and various bearing companies for a long time and obtained the shape parameter of ball bearings. Possible values are 1.5 and rolling bearings are 1.7. Therefore, under the condition that the bearing products are subject to Weibull distribution, assuming that the shape parameter value is 2.0, it can meet the analysis requirements of conventional reliability problems.

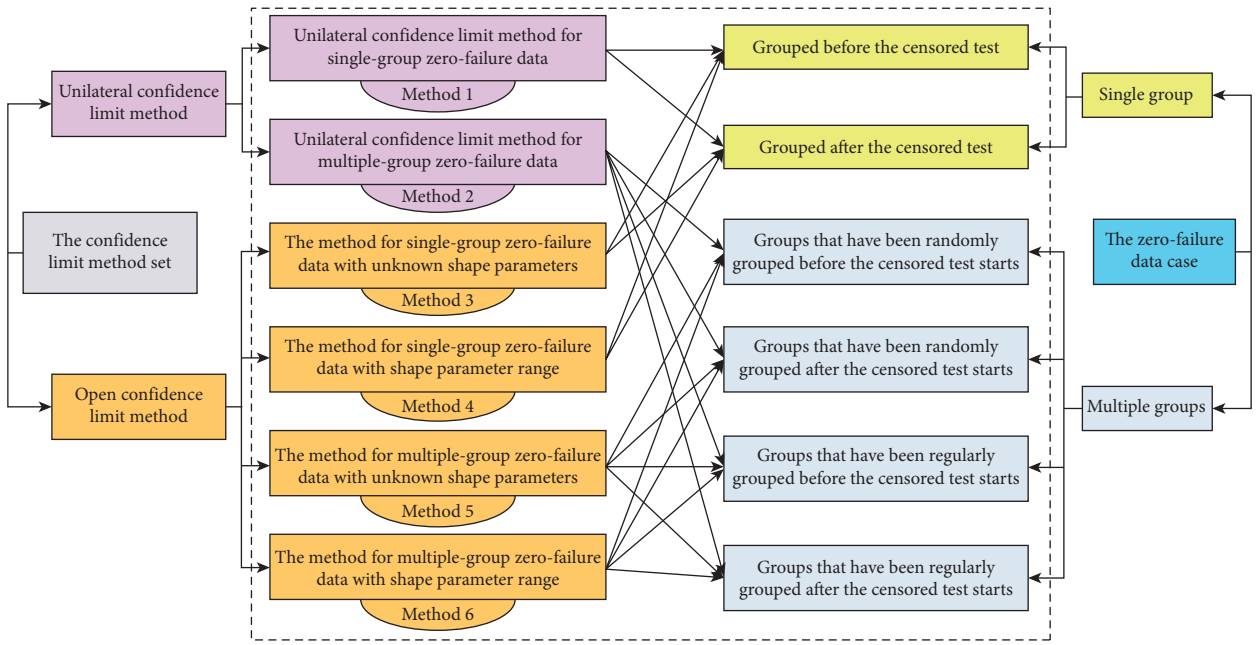

Figure 3: The CMLS for reliability evaluation based on zero-failure data.

The zero-failure data of the numerical simulation of bearings are listed in Table 1. The data are generated based on the method of generating zero-failure data samples [23] and the results of previous statistical studies on the life of rolling bearings of this type. Then, a set of pseudorandom numbers is generated under the conditions of specifying shape parameters and scale parameters based on the method of generating zero-failure data samples. Finally, a set of random numbers that follow the Weibull distribution (the number of random numbers should be much greater than the number in the bearing reliability test set) is generated by using the Monte Carlo method. The number of random numbers generated is 600. The values of relevant parameters in the zero-failure data of a group of bearings generated by simulation include the following: shape parameter is $\beta = 2.0$, scale parameter is $\vartheta = 2000$, and position parameter is $\gamma = 1000$. The mission time t in the two-parameter Weibull distribution is equivalent to the $t - \gamma$ in the three-parameter Weibull distribution.

There are 55 samples of zero-failure data for this group of bearings, as shown in Table 1. In order to use the single group optimal confidence limit method to process multiple groups of zero-failure data, a method to extend the application of optimal confidence limits is proposed in this part. The feasible solution is to average-equivalently process the total time $T = \sum_{i=1}^{m} n_i t_i$, and then the single censoring time $t_0 = \sum_{i=1}^{m} n_i t_i / n$, where n = 55. Using the optimal confidence limit method for single group of zero-failure data to calculate the reliability estimation results of this simulation example is shown in Figure 4; the confidence level is$1 - \alpha = 0.95$. It can be known that the life of the batch of bearings is subject to Weibull distribution, and the shape parameter values range from 1.8 to 2.3 [23]. Based on the current assumptions and the CMLS, we can use three methods to estimate the reliability of this group of bearings. The following analysis content is the lower confidence limit of product reliability in three cases, where the shape parameter is unknown (Method 3) and the shape parameter range is known (Method 1 and Method 4).

Although using the data set can quickly find the evaluation method, it can be seen from the evaluation results in Figure 4 that the evaluation effect after simplified processing is not ideal. The reason why the curve of the reliability estimate value in this figure is not smooth is that the value points of the reliability estimate are too scattered, but this does not affect the comparative analysis between different evaluation methods. Compared with the true value of the reliability change trend, the reliability estimates of the three methods are either too high or too low. The estimate of the lower limit of reliability in Method 3 is 0 under the condition that the task time is greater than the maximum censoring time t_0, and it has nothing to do with the confidence level. Therefore, Method 3 has certain limitations. According to the analysis of the results of this simulation example, the reliability estimation has always been on the high side by Methods 1 and 4. This will lead to underestimation of the probability of bearing risk in actual engineering applications.

Based on the data in Table 1, the lower confidence limit of product reliability is analyzed in the case where the shape parameter is unknown and the shape parameter range is known. In the following analysis, the confidence level parameter is $1 - \alpha = 0.95$, and the shape parameter assumption is still unknown or known to have a range of 1.8–2.3. After calculation, the parameter of critical time node is $c = 2375.8$ h. Based on the current assumptions and CMLS, three methods are used to estimate the reliability through this set of zero-failure data samples. The following analysis content is the lower confidence limit of product reliability in two cases, where the shape parameter is unknown (Method 5) and the shape parameter range is known (Method 2 and

Table 1: Zero-failure data sample of bearing based on three-parameter Weibull distribution.

Censoring time/h	The number of samples n_i	Censoring time (h)	The number of samples n_i
1030	10	2632	5
1617	9	2871	4
1915	8	3195	3
2180	7	3581	2
2379	6	4006	1
		Total number	55

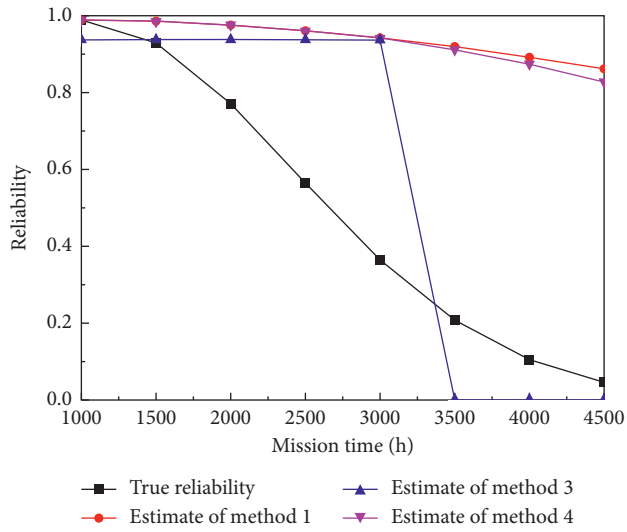

Figure 4: Reliability lower confidence limit estimate for single set of zero-failure data.

Method 6), and the results of the optimal confidence limit evaluation are shown in Figure 5.

From the results in Figure 5, the type of zero-failure data grouping has a direct impact on the reliability evaluation during the application of the optimal confidence limit analysis method. The reliability estimated by the unilateral confidence limit assessment method (Method 2) is significantly higher than the true value. The reliability estimates obtained by the two methods (Methods 5 and 6 are closest to the true value when the mission time is near critical time node c). The estimates of the lower confidence limits of reliability obtained by the two methods are conservative when the task time is less than 2000 hours. However, the estimates of the lower confidence limits of the reliability obtained by the two methods are biased when the task time is greater than 2000 hours. Although Method 6 considers more time stages to estimate the reliability, Method 5 is generally better. The optimal confidence limit evaluation method plays a role in dealing with rare events in failure analysis (reliability evaluation based on zero-failure data) and the estimates near critical time nodes are still very close to the true value of reliability, which can provide a reference for practical engineering applications.

7. Case Study

7.1. Single Group of Zero-Failure Data for Bearings. According to the rolling bearings used at the joints of a certain type of robot in the laboratory environment, we get such a set of zero-failure data. The sample size of this set of zero-failure data is 3, the censoring time is 1200 hours, and the zero-failure data of the bearing is expressed as $Z = (t_0, n) = (1200, 3)$. The photograph of the rolling bearing before it is not installed at the joint is shown in Figure 6. Therefore, for simplicity and without loss of generalization ability, it is assumed that the life of this group of bearings follows the two-parameter Weibull distribution, and the shape parameter ranges from 1.5 to 2.3. In the following analysis, the confidence level parameter is $1 - \alpha = 0.95$.

Based on the current assumptions and CMLS, we can use two methods (Methods 1 and 4) to estimate the reliability of this group of bearings. The reliability evaluation results of the bearings are shown in Figure 7.

Combined with the results of the numerical simulation study, it can be known that the reliability estimated by the optimal confidence limit method is closer to the true value, and it can be seen that Method 4 estimates the reliability of the bearing better. At the same time, it can also be found that the effects of the two methods when processing a single set of zero-failure data are very close. In order to analyze the influence of the sample size on the evaluation results; on the basis of this example, it is assumed that the sample size increases, and the results of the reliability evaluation according to the optimal confidence limit analysis method are shown in Figure 8.

From the results in Figure 8, it can be seen that the larger the sample size, the higher the final reliability estimate, and the change rate of the reliability estimate gradually decreases as the task time increases. Such conclusions are in accordance with the objective law of reliability evaluation through zero-failure data.

7.2. Multiple Groups of Zero-Failure Data for Torque Motor. The zero-failure data of this study came from the field operation data of the torque motors. Recording the time data of a product from start to failure (or failure-free) is an important data source for reliability evaluation. The reliability data of the actual work scene is extremely valuable. It reflects the operation of the product in the actual environment and maintenance conditions and is more representative of the product characteristics than the simulated data in the laboratory environment. The figure of the torque motor sample is obtained from [24] as shown in Figure 9.

In order to analyze the reliability of the torque motors, the operation records of 52 torque motors used in CNC machine tools are reviewed. After analysis and arrangement,

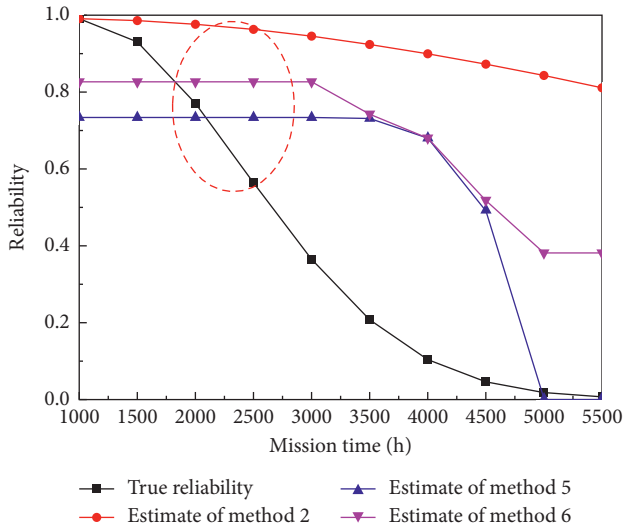

Figure 5: Reliability lower confidence limit estimate for multiple groups of zero-failure data.

Figure 6: The rolling bearing sample.

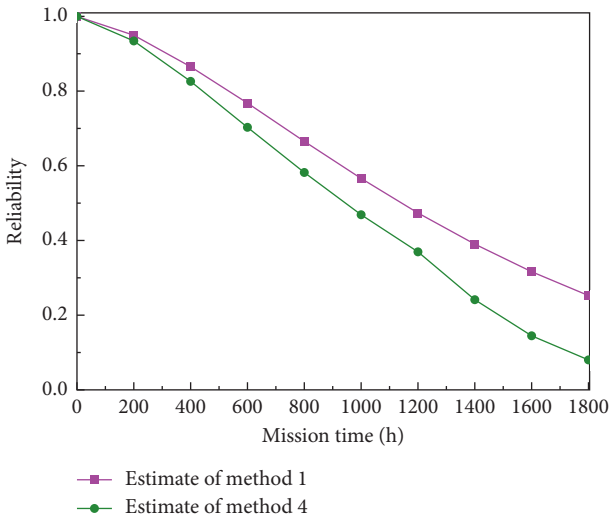

Figure 7: The comparison of reliability estimation results of two methods.

it is found that 52 torque motors have no fault in the mission time. As the starting time of the type-I censoring experiment, the time of the last recording of the motors in the CNC

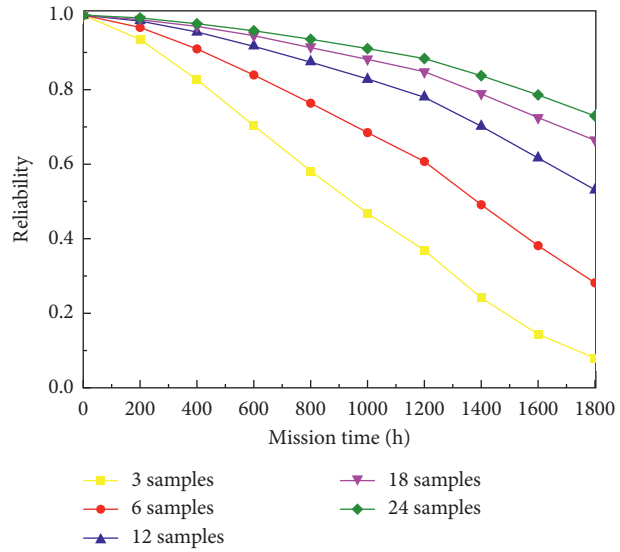

Figure 8: Changes in reliability estimates are based on different sample size.

Figure 9: A torque motor sample of this set [24].

machine tool is used as the censoring time of the experiment, and then the running time t_i corresponding to the torque motors is given. The sample data of the torque motor is obtained from [24] as shown in Table 2.

According to the previous research results [21], the batch of torque motors follows the two-parameter Weibull distribution, and the shape parameter range is between 1.5 and 1.8. Based on the previously mentioned analysis results and the confidence limit method set, for the reliability evaluation of the torque motor example, it is advisable to adopt multiple sets of zero-failure data evaluation methods in the unilateral confidence limit method and the optimal confidence limit method. Since the estimated value of the shape parameter is within a range, the interval estimation result of the reliability obtained by the unilateral confidence limit analysis method is evaluated. Although this example can refer to the range of the shape parameter interval, according to the results of numerical simulation analysis, Method 3 should be used when using the optimal confidence limit analysis. In the following analysis, the confidence level parameter is $1 - \alpha = 0.95$. Based on the current assumptions and the CMLS, we can use two methods

Table 2: The zero-failure data sample of torque motor [24].

Censoring time/h	The number of samples n_i	Censoring time/h	The number of samples n_i
256	2	2960	2
720	2	3600	2
960	2	4240	4
1200	2	4320	10
1360	2	4960	2
1440	6	5440	3
2400	2	5520	1
2560	2	5760	2
2640	2	7200	4
		Total number	52

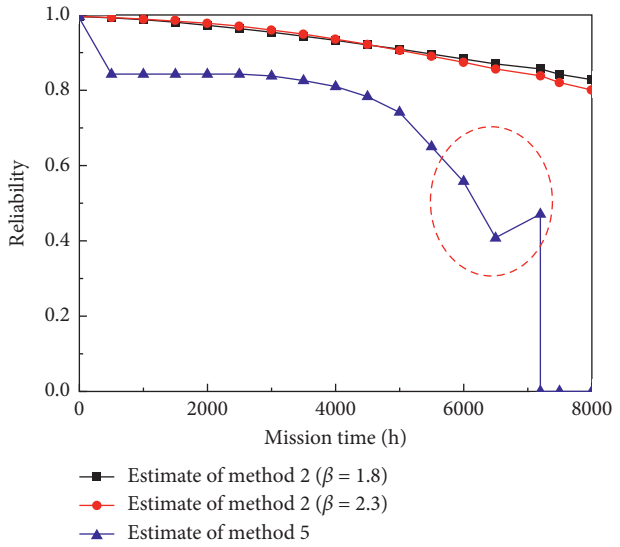

Figure 10: The comparison of reliability estimation results of two methods.

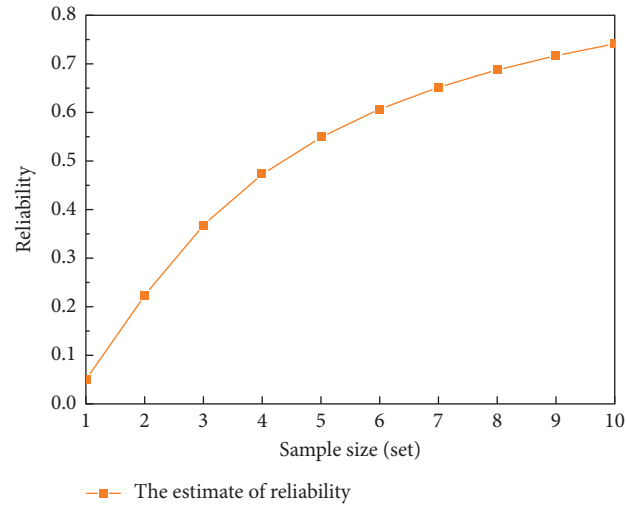

Figure 11: The increase in the number of samples leads to changes in reliability estimates value.

(Methods 2 and 5) to estimate the reliability of this group of torque motors.

As can be seen from Figure 10, the reliability evaluation results using Method 2 are not sensitive to the shape parameter values; that is to say, when the shape parameter values change a little, the reliability estimate value increases and the task time increase is almost negligible. According to the analysis of the evaluation results of Method 5, if the life distribution assumption of the torque motor is accurate, then the estimated value of the reliability of the accessory C at the critical time is about 0.85. It can be seen that the estimation results of Method 2 are biased. The result of the reliability estimation value using Method 5 has a fluctuation phenomenon when the task time is the maximum censoring time. This is because the expression of the reliability estimation value is $R_{o2}(t) = \alpha^{1/p}$. The relationship between the estimated reliability at this moment and the change in sample size is shown in Figure 11.

It can be seen that the number of samples corresponding to the maximum censoring time directly affects the size of the reliability estimate under the task time. In this case study, the occurrence of the final reliability estimate value fluctuating at the maximum truncation time point is the phenomenon caused by this reason.

8. Conclusion

This paper gives a unilateral confidence limit analysis method and an optimal confidence limit analysis method for product life that follow the Weibull distribution. According to past engineering experience, the shape parameter value information of the product life distribution is introduced to obtain a more accurate evaluation effect. By establishing a set of confidence limit methods for analyzing zero-failure data, a quick search method is realized, and the optimal reliability estimation result is selected using the comparative analysis results. The currently established method set is only applicable to the evaluation of various types of zero-failure data under the condition of Weibull distribution. Combining numerical simulation examples and case studies, the following conclusions are obtained.

(1) Through the method set established in this paper, the reliability evaluation of zero-failure data can be used to quickly select the methods that need to be adopted

in the case of the Weibull distribution, and the optimal evaluation results are selected through lateral comparison analysis.

(2) Through the analysis of examples and numerical simulation examples, it can be seen that the reliability estimate obtained by the confidence limit analysis method is closer to the real situation when the task time is shorter.

(3) The shape parameter of the life distribution of the research object is a crucial factor, which directly affects the accuracy of the reliability estimation under the condition of Weibull distribution.

In the future, the research object industrial products will adopt a variety of different distribution types of confidence limit analysis methods to establish a more comprehensive method set, which will be able to meet a wider range of practical engineering applications.

Data Availability

The data used to support the findings of this study are included within the article.

Conflicts of Interest

The authors declare that they have no conflicts of interest.

Acknowledgments

This work was supported by the National Key Research and Development Program of China (grant no. 2018YFF0214704).

References

[1] P. Rani and G. S. Mahapatra, "A neuro-particle swarm optimization logistic model fitting algorithm for software reliability analysis," *Proceedings of the Institution of Mechanical Engineers," Part O: Journal of Risk and Reliability*, vol. 233, no. 6, 14 pages, 2019.

[2] C.-Y. Wei, X.-Q. Cai, B. Liu, T.-Y. Wang, and F. Gao, "A generic construction of quantum-oblivious-key-transfer-based private query with ideal database security and zero failure," *IEEE Transactions on Computers*, vol. 67, no. 1, pp. 2–8, 2018.

[3] P. Jiang, Y. Y. Xing, X. Jia, and B. Guo, "Weibull failure probability estimation based on zero-failure data," *Mathematical Problems in Engineering*, vol. 2015, no. 3, 8 pages, Article ID 681232, 2015.

[4] H. F. Martz and R. A. Waller, "A bayesian zero-failure (BAZE) reliability demonstration testing procedure," *Journal of Quality Technology*, vol. 11, no. 3, pp. 128–138, 1979.

[5] C. L. Atwood and J. K. Vaurio, *Zero Failure Data, Encyclopedia of Quantitative Risk Analysis and Assessment*, John Wiley & Sons, Inc, Hoboken, NY, USA, 2008.

[6] J. D. Chen, W. L. Sun, and B. X. Li, "The confidence limits for reliability parameters in the case of no failure data," in *Proceedings of the Asian Conference on STA.Com*, pp. 17–20, Beijing, China, 1993.

[7] J. D. Chen, W. L. Sun, and B. X. Li, "On the confidence limits in the case of no failure data," *Acta Mathematicae Applicatae Sinica*, vol. 18, no. 1, pp. 90–100, 1995.

[8] W. L. Sun and J. D. Chen, "Some new results on the confidence limits for reliability parameters in the case of no failures," *Systems Science and Mathematical Sciences*, vol. 01, pp. 70–81, 1999.

[9] H. M. Fu and Y. B. Zhang, "Method of reliability analysis for time truncated zero-failure data based on normal distribution," *Journal of Aerospace Power*, vol. 25, no. 2, pp. 384–387, 2010.

[10] H. B. Zhao and Y. M. Cheng, "Statistical analysis about zero-failure data using memory less property of exponential distribution," *Chinese Journal of Applied Probability and Statistics*, vol. 20, no. 1, pp. 59–65, 2004.

[11] S. Chambal and J. Bertkeats, "Evaluating complex system reliability using reliability block diagram simulation when little or no failure data are available," *Quality Engineering*, vol. 13, no. 2, pp. 169–177, 2000.

[12] S. A. Kayis, "Evaluation of confidence limit estimates of cluster analysis on molecular marker data," *Journal of the Science of Food and Agriculture*, vol. 92, no. 4, pp. 776–780, 2012.

[13] X. H. Chang, X. Jun, and J. H Park, "Estimation for a class of parameter-controlled tunnel diode circuits," *IEEE Transactions on Systems, Man, and Cybernetics: Systems*, vol. 50, no. 11, pp. 4697–4707, 2018.

[14] L. Ma, X. Huo, X. Zhao, and G. D. Zong, "Observer-based adaptive neural tracking control for output-constrained switched MIMO nonstrict-feedback nonlinear systems with unknown dead zone," *Nonlinear Dynamics*, vol. 99, no. 2, pp. 1019–1036, 2020.

[15] L. Ma, G. Zong, X. Zhao et al., "Observed-based adaptive finite-time tracking control for a class of nonstrict-feedback nonlinear systems with input saturation," *Journal of the Franklin Institute*, vol. 357, no. 16, pp. 11518–11544, 2019.

[16] M. Han, "Confidence limit of reliability parameters in the case of zero-failure data," *Chinese Journal of Engineering Mathematics*, vol. 21, no. 2, pp. 245–244, 2004.

[17] R. B. Jiang and D. Y. Jiang, "Fiducial lower confidence limits of reliability for a standby system based on zero-failure data," *Zhejiang University.Science and Education*, vol. 6, p. 629, 2010.

[18] D. A. Burger, R. Schall, J. T. Ferreira, and D.-G. Chen, "A robust Bayesian mixed effects approach for zero inflated and highly skewed longitudinal count data emanating from the zero inflated discrete weibull distribution," *Statistics in Medicine*, vol. 39, no. 9, p. 2, 2020.

[19] H. Pham and C.-D. Lai, "On recent generalizations of the weibull distribution," *IEEE Transactions on Reliability*, vol. 56, no. 3, pp. 454–458, 2007.

[20] A. Z. Djeddi, A. Hafaifa, A. Kouzou et al., "Exploration of reliability algorithms using modified weibull distribution: application on gas turbine," *International Journal of System Assurance Engineering & Management*, vol. 8, no. 2, 10 pages, 2017.

[21] H. Li, L. Y. Xie, M. Li, J. Ren, B. Zhao, and S. Zhang, "Research on a new reliability assessment method for zero-failure data," *Journal of Military Engineering*, vol. 35, no. 01, pp. 1622–1631, 2019.

[22] X. W. Yang, *Study on Three Parameters of Weibull Distribution for Fatigue Life of Rolling Bearings*, Hefei University of Technology, Hefei, China, 2003.

[23] H. Y. Sun, *Research on Bearing Reliability Based on No Failure Data*, Northeastern University, Boston, MA, USA, 2014.

[24] H. Li, L. Xie, M. Li, J. Ren, B. Zhao, and S. Zhang, "Reliability assessment of high-quality and long-life products based on zero-failure data," *Quality and Reliability Engineering International*, vol. 35, no. 1, pp. 470–482, 2019.

Hindawi
Mathematical Problems in Engineering
Volume 2020, Article ID 2432806, 5 pages
https://doi.org/10.1155/2020/2432806

Research Article

Real-Time Prediction Model of Coal and Gas Outburst

Ru Yandong,[1] **Lv Xingfeng**,[2] **Guo Jikun**,[1] **Zhang Hongquan**,[1] **and Chen Lijuan**[1]

[1]*College of Electronics and Information Engineering, Heilongjiang University of Science and Technology, Haerbin, Heilongjiang 150027, China*
[2]*College of Computer Science and Technology, Heilongjiang University, Haerbin, Heilongjiang 150080, China*

Correspondence should be addressed to Ru Yandong; 10564006@qq.com

Received 14 July 2020; Revised 11 October 2020; Accepted 18 October 2020; Published 30 October 2020

Academic Editor: Zeshui Xu

Coal and gas outburst has been one of the main threats to coal mine safety. Accurate coal and gas outburst prediction is the key to avoid accidents. The data is actual and complete by default in the existing prediction model. However, in fact, data missing and abnormal data value often occur, which results in poor prediction performance. Therefore, this paper proposes to use the correlation coefficient to complete the missing data filling in real time for the first time. The abnormal data identification is completed based on the Pauta criterion. Random forest model is used to realize the prediction model. The prediction performance of sensitivity 100%, accuracy 97.5%, and specificity 84.6% were obtained. Experiments show that the model can complete the prediction of coal and gas outburst in real time under the condition of missing data and abnormal data value, which can be used as a new prediction model of coal and gas outburst.

1. Introduction

China is one of the countries with serious coal and gas outburst disasters which pose a great threat to the coal mine safety production [1]. The accidents caused by coal and gas outburst account for 38% of safety accidents in coal mine [2], which is the most dangerous and frequent accident type in coal mine accidents. Before coal and gas outburst, it is of great significance to complete the prediction of coal and gas outburst to ensure the safety of production and protect the life of miners.

The common prediction methods of coal and gas outburst include the index prediction method and mathematical model prediction method [3]. The index prediction method is to detect the values of various indexes and compare them with the standard values of indexes to determine whether they are dangerous for coal and gas outburst. Common indexes include gas content, gas pressure, coal strength coefficient, cuttings index, and comprehensive index [4–6]. There are many influencing factors and large measurement errors in these indexes, which often lead to low prediction accuracy. Therefore, in recent years, researchers pay more attention to mathematical model prediction methods. The method is to select several characteristics that affect coal and gas outburst and use the mathematical model to predict the outburst risk [7–9]. In fact, the existing prediction methods are based on the ideal data to complete the prediction of coal and gas outburst. However, there is still a long distance from the actual application, which is mainly reflected in three aspects. First, the data used by default is complete. In fact, in the process of data transmission and data fusion, data is often missing, resulting in partial or even all data missing. Second, the data used by default has the same value as the real value. In fact, due to the limitations of experimental conditions and experimental process, there may be some differences between the data and the real value. Third, the prediction model is based on the previous data. When the new abnormal data is coming, there is a lack of processing capacity resulting in the inability to complete the prediction in real time. For this reason, this paper proposes a coal and gas outburst prediction model. According to the characteristics of data from the coal mine, the data processing method is given, which can accurately predict coal and gas outburst in practical application. The prediction of coal and gas outburst ensures the safety of miner and property of miners.

2. Real-Time Prediction Model

There are many factors that affect coal and gas outburst. Commonly used factors include gas content, gas pressure, coal strength coefficient, drilling cuttings index, comprehensive index, initial gas release speed, porosity, and coal seam thickness [10]. In this paper, five index parameters are selected including gas content, gas pressure, coal strength coefficient, initial gas release speed, and porosity [11]. The mathematical prediction model is used to predict coal and gas outburst, which is shown in Figure 1. Three kinds of data including gas content, gas pressure, and initial velocity of gas emission collected from the underground are transmitted to the well through the transmission substation. These three kinds of data and coal strength coefficient and porosity of the coal body form the joint dataset. Data processing is used to deal with abnormal data and missing data. The prediction of coal and gas outburst is completed by using the random forest model. In case of coal and gas outburst, the manager shall be informed to take relevant measures at the same time. The audible and visual alarm shall be started to inform the miner to start the relevant risk avoidance equipment. The information shall be transmitted to the underground through the transmission substation. At the same time, the data storage and update are completed, and the new prediction model is trained by using the updated dataset regularly.

3. Experiments

3.1. Data Description. The data is divided into accident data and safe data, in which the safe data is easy to obtain and the data volume is large [12]. However, it is difficult to obtain accident data, even if there are some records of accident data, which are often incomplete, resulting in a small amount of accident data. Therefore, this paper adopts different methods for safe data and accident data. When the safe data is missing, delete the data directly. When the accident data is missing, fill the data according to the existing data. In this paper, five indexes including gas pressure, gas content, initial velocity of gas emission, porosity, and coal strength coefficient, which are closely related to coal and gas outburst, are selected as characteristics. Partial characteristic data is shown in Table 1.

3.2. Data Processing. According to the characteristics of coal mine data, this paper completes the data processing. The processing block diagram is shown in Figure 2. First, check whether there is data missing in the dataset. If there is data missing, use the corresponding processing method to complete the data filling. Secondly, check whether there are abnormal values in the dataset. If there are abnormal values, use the abnormal value processing method to process the data.

3.2.1. Missing Data Processing Method. There are many methods of data filling, but they are based on the existing dataset [13]. As the time goes, the amount of data will become very large, so it will take a lot of time to realize data filling so as to affect the prediction speed [7]. Therefore, this paper proposes a numerical filling data method based on the correlation of variables which can be considered as real time. For the first time, the correlation between existing data variables is considered, and Pearson correlation coefficient is used to complete the new missing data filling that ensures data integrity. Pearson correlation coefficient can be expressed by numerical value to measure the correlation between two variables, which can be described as follows:

$$\rho_{X,Y} = \frac{\operatorname{cov}(X,Y)}{\sigma_X \sigma_Y} = \frac{E\left((X-\mu_X)(Y-\mu_Y)\right)}{\sigma_X \sigma_Y}, \quad (1)$$

where $E(X)$ is the mathematical expectation of the variable, σ_X represents the standard deviation of variable X, and μ_X represents the mean value of variable X. In this paper, the correlation matrix of five characteristics is calculated, and the results are shown in Table 2.

When data from a certain feature in the dataset is missing, this article observes the correlation coefficient in the correlation matrix and finds out the maximum value of the correlation coefficient between the characteristics of the data and other characteristics. This article makes use of the correlation coefficient to filling the missing value. In this paper, the calculated values obtained by using the correlation when the five characteristics are missing are listed, respectively. The experimental results are shown in Table 3.

It can be seen from Table 3 that the correlation coefficient matrix method is used to fill the missing data, and the similarity between the filled data value and the actual value is from 83.3% to 98.6%. On the whole, the filled data is very similar to the actual data which ensures higher prediction performance.

3.2.2. Abnormal Data Value Processing Method. Due to the limitation of equipment precision and experimental conditions, noise will inevitably be mixed into the data, which will lead to abnormal data values. In this paper, after processing the missing value of the data, the abnormal value in the data is found according to the Pauta criterion. Pauta criterion is described as follows.

When the value meets the formula,

$$\left|X_i - \overline{X}\right| > 3^* S_x. \quad (2)$$

X_i is considered to be an abnormal, where X_i is the data point, $\overline{x} = (1/n)\sum_{i=1}^{n} x_i$ is the data mean value, and $S_x = [(1/n)\sum_{i=1}^{n}(x_i - \overline{x})^2]^{1/2}$ is the standard deviation of data.

In this paper, 5 characteristics of the dataset are detected for the abnormal data value. When detecting the abnormal data value, the missing value filling method mentioned above is used for data correction. In this paper, 530 pieces of accident data and safe data are selected, and the above methods are used to complete the abnormal data identification. The abnormal identification results are shown in Table 4.

It can be seen from Table 4 that there are some abnormal data in the dataset. The main reason is that the accuracy of data acquisition equipment and the limitations of

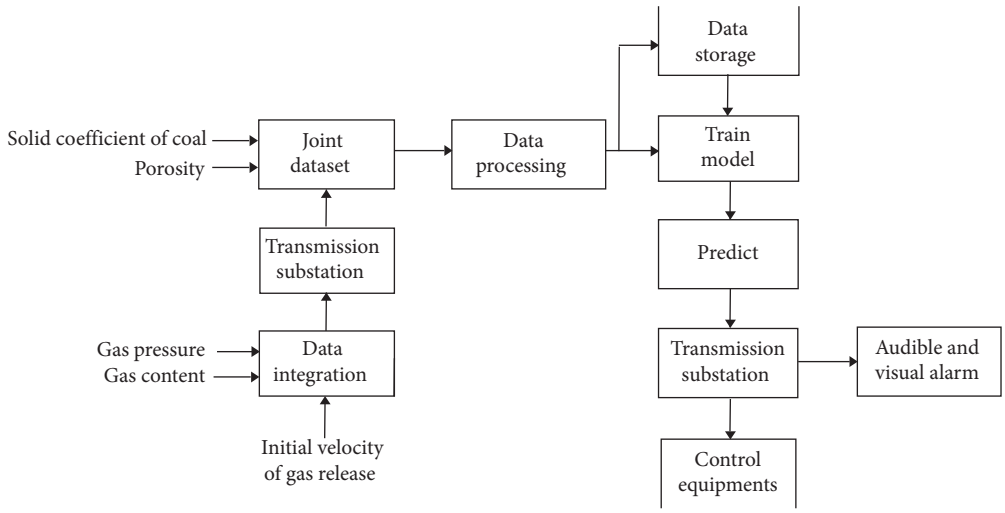

Figure 1: Block diagram of coal and gas prediction system.

Table 1: Characteristic data (partial).

Gas content	Gas pressure	Porosity	Coal strength coefficient	Initial velocity of gas release	Data class
17.40	1.40	6.20	0.52	10	Safe
16.42	1.60	3.60	0.36	15	Safe
13.62	1.80	4.36	0.39	8	Safe
12.34	0.70	7.36	0.35	13	Safe
11.26	0.39	9.60	0.59	14	Safe
9.54	2.95	3.50	0.24	11	Safe
9.32	4.40	6.30	0.57	10	Safe
8.36	3.10	8.30	0.45	12	Safe
7.55	0.97	4.36	0.52	7	Safe
7.36	2.95	3.60	1.30	7	Safe
8.87	1.20	5.49	1.11	8	Accidental
8.14	0.10	5.23	0.65	11	Accidental
7.80	0.89	5.80	1.30	5	Accidental
7.43	2.10	7.36	1.11	10	Accidental
6.67	0.80	3.56	0.65	6	Accidental
6.55	0.70	8.20	0.98	7	Accidental
5.30	0.65	7.36	0.98	2	Accidental
5.25	0.60	3.60	0.64	5	Accidental
4.38	0.89	8.20	0.64	5	Accidental
3.82	0.46	3.65	0.94	4	Accidental

experimental methods leading to part of the data value deviate from the actual value. Therefore, this part of abnormal signals must be identified and deleted, and the data filling method mentioned above should be used to complete the data filling, so as to ensure the high performance of prediction.

3.3. Realization of Coal and Gas Outburst Prediction. In this paper, accuracy, sensitivity, and specificity are used as performance evaluation indexes of the model, which are defined as follows:

$$\text{accuracy} = \frac{\text{TP} + \text{TN}}{\text{TP} + \text{FP} + \text{FN} + \text{TN}}, \tag{3}$$

$$\text{sensitivity} = \frac{\text{TP}}{\text{TP} + \text{FN}}, \tag{4}$$

$$\text{specificity} = \frac{\text{TN}}{\text{TP} + \text{FP}}. \tag{5}$$

TP is the number of correctly predicted safe data. FP is the number of wrongly divided safe data into accidental data. FN is the number of wrongly divided accidental data into safe data. TN is the number of correctly predicted accidental data.

In order to achieve high-performance detection and avoid overfitting, this paper uses the random forest model to achieve coal and gas outburst prediction. Random forest (RF) is an efficient integrated classification method composed of a large number of decision trees. According to the characteristics of decision trees, many improvements have been made so that the decision trees constructed are as uncorrelated as possible, thus significantly improving the classification performance of the system. In this paper, the

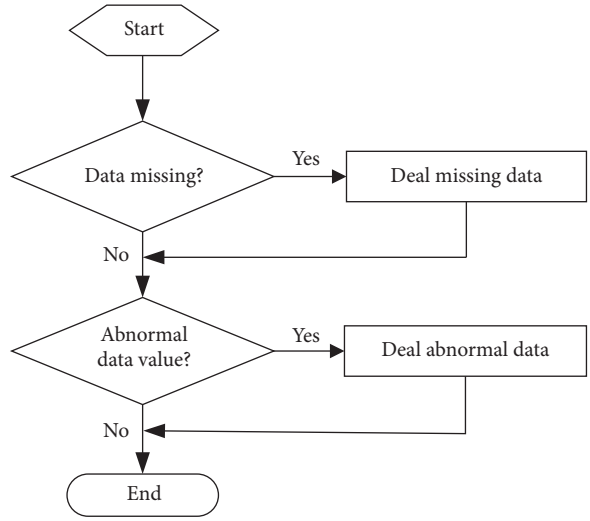

Figure 2: Overall block diagram of data processing.

Table 2: Correlation matrix of characteristics.

Correlation coefficient	Gas content	Gas pressure	Porosity	Coal strength coefficient	Initial velocity of gas release
Gas content	1	0.5518	0.0881	−0.3222	0.6531
Gas pressure	0.5518	1	−0.0005	−0.0787	0.4623
Porosity	0.0881	−0.0005	1	−0.1294	0.0901
Coal strength coefficient	−0.3222	−0.0787	−0.1294	1	−0.4413
Initial velocity of gas release	0.6531	0.4623	0.0901	−0.4413	1

Table 3: Calculation value of feature.

	Gas content	Gas pressure	Porosity	Coal strength coefficient	Initial velocity of gas release
(a) Calculation value of initial velocity of gas emission					
Experimental value	15.36	2	4.60	0.53	Null value
Calculated value	—	—	—	—	10.20
Actual value	15.36	2	4.60	0.53	10.06
Similarity degree	—	—	—	—	98.6%
(b) Calculation value of porosity					
Experimental value	19.72	1.90	Null value	0.15	13
Calculated value	—	—	5.70	—	—
Actual value	19.72	1.90	4.75	0.15	13
Similarity degree	—	—	83.3%	—	—
(c) Calculation value of coal seam firmness coefficient					
Experimental value	16.23	3	9.20	Null value	9
Calculated value	—	—	—	0.18	—
Actual value	16.23	3	9.20	0.16	9
Similarity degree	—	—	—	88.9%	
(d) Calculation value of gas content					
Experimental value	Null value	1.30	4.60	0.26	13
Calculated value	23.10	—	—	—	—
Actual value	21.68	1.30	4.60	0.26	13
Similarity degree	93.9%	—	—	—	—
(e) Calculation value of gas pressure					
Experimental value	9.32	Null value	4.60	0.26	13
Calculated value	—	2.30	—	—	—
Actual value	9.32	2.10	4.60	0.26	13
Similarity degree	—	91.3%	—	—	—

grid search method is used to optimize the model parameters, the number of optimal decision trees is 500, and the number of random variables is 3. The 10 fold crossvalidation method is used to complete the cross validation, and the R language is used to realize the model. The prediction results are shown in Table 5.

Table 4: Abnormal data identification results.

	Gas content	Gas pressure	Porosity	Coal strength coefficient	Initial velocity of gas release
Data volume	530	530	530	530	530
Amount of abnormal data	15	10	1	5	10
Ratio of abnormal data to dataset (%)	2.83	1.89	0.19	0.94	1.89

Table 5: Prediction results.

	Safe data (predicted)	Accidental data (predicted)
Safe data (actual)	340	10
Accidental data (actual)	0	55

Through the prediction results in Table 5, we calculated that the model has high performance of sensitivity 100%, accuracy 97.5%, and specificity 84.6%. From the experimental results, we can conclude that the model can completely detect coal and gas outburst with high performance.

4. Conclusion

In this paper, the prediction model of coal and gas outburst is realized. The correlation between the five important characteristics affecting coal and gas outburst is analyzed. This paper completes the filling of missing data according to the correlation between characteristics for the first time which can guarantee to consume very little time. Abnormal values are identified and processed in order to ensure the analyzed data getting closer to the actual data. The processing method of missing data and abnormal value is proved be effective. The random forest model is used to predict coal and gas outburst with high performance. The experiment shows that it can complete the task of real-time prediction of coal and gas outburst with high performance of sensitivity 100%, accuracy 97.5%, and specificity 84.6%. It can be used for safety production of coal mine in practical application.

Data Availability

The data used to support the findings of this study are available from the corresponding author upon request.

Conflicts of Interest

The authors declare that they have no conflicts of interest.

Acknowledgments

This work was supported by Fundamental Research Funds for the Education Department of Heilongjiang Province Universities (Grant no. Hkdqg201909).

References

[1] L. Yuan and S. Xue, *Theory and Technology of Coal and Gas Outburst Prediction by Coal Seam Gas Content Method*, Science Press, Beijing, China, 2014.

[2] X. Zhao, H. Sun, J. Cao, X. Ning, and Y. Liu, "Applications of online integrated system for coal and gas outburst prediction: A case study of Xinjing mine in Shanxi, China," *Energy Science and Engineering*, vol. 8, no. 2, pp. 1980–1996, 2020.

[3] D. J. Black, "Review of coal and gas outburst in Australian underground coal mines," *International Journal of Mining Ence and Technology*, vol. 29, no. 6, pp. 4–13, 2019.

[4] W. Zhang and Y. Hou, "Study on coal mine gas data denoising based on Ga-LSSVR," *Mining Safety and Environmental Protection*, vol. 44, no. 1, pp. 45–48, 2017.

[5] B. Nie, X. He, and E. Wang, "Research status and development trend of coal and gas outburst prediction technology," *China Safety Science Report*, vol. 13, no. 6, pp. 40–44, 2003.

[6] L. Xinling, Y. Mei, and Y. He, "Prediction of coal and gas outburst grade based on factor analysis and SVM model," in *Proceedings of the 2019 International Conference*, Moscow, Russia, 2019.

[7] Ministry of Coal Industry of the People's Republic of China, *Provisions on Prevention and Control of Coal and Gas Outburst*, Coal Industry Press, Beijing, China, 2009.

[8] Z. Xusheng, M. A. Guolong, and Q. Wei, "Early-warning index system of coal and gas outburst based on fault tree analysis," *Mining Safety & Environmental Protection*, vol. 46, no. 3, 2019.

[9] H. Peng, *Research on Gas Disaster Prediction Method Based on Data Mining and Information fusion*, China University of mining and Technology, Beijing, China, 2013.

[10] Z. Zhao and Y. Tan, "Study on prediction of coal and gas outburst precursor time series based on chaos theory," *Geotechnical Mechanics*, vol. 30, no. 7, pp. 2186–2190, 2009.

[11] Y. Y. Zhang, J. L. Cui, and X. D. Jiao, "Study of the multi-index coupling forecasting model of coal and gas outburst and its application," *Chinese Journal of Engineering*, vol. 11, pp. 45–52, 2018.

[12] Li Sheng, *Study on Pattern Recognition Method for Regional Prediction of Coal and Gas Outburst*, Liaoning University of Engineering and Technology, Liaoning, China, 2004.

[13] J. Mou, H. Liu, Y. Zou, and Q. Li., "A new method to determine the sensitivity of coal and gas outburst prediction index," *Arabian Journal of Geoences*, vol. 13, no. 12, pp. 1–9, 2020.

Hindawi
Mathematical Problems in Engineering
Volume 2020, Article ID 3753417, 10 pages
https://doi.org/10.1155/2020/3753417

Research Article

Linear Regression Estimation Methods for Inferring Standard Values of Snow Load in Small Sample Situations

Xudong Wang [1] **and Jitao Yao** [2]

[1]*School of Science, Xi'an University of Architecture and Technology, Xi'an 710055, China*
[2]*School of Civil Engineering, Xi'an University of Architecture and Technology, Xi'an 710055, China*

Correspondence should be addressed to Jitao Yao; 32782472@qq.com

Received 21 May 2020; Revised 24 June 2020; Accepted 25 June 2020; Published 27 July 2020

Academic Editor: Zeshui Xu

The aim of this paper is to establish a new method for inferring standard values of snow load in small sample situations. Due to the incomplete meteorological data in some areas, it is often necessary to infer the standard values of snow load in the conditions of small samples in engineering, but the point estimation methods of classical statistics adopted till now do not take into account the influences of statistical uncertainty, and the inference results are always aggressive. In order to overcome the above shortcomings, according to the basic principle of optimal linear unbiased estimation and invariant estimation of the minimum type I distribution parameters and the tantile, using the least square method, the linear regression estimation methods for inferring standard values of snow load in small sample situations are proposed, which can take into account two cases such as parameter-free and known coefficient of variation, and the predicted formulas of snow load standard values are given, respectively. Through numerical integration and Monte Carlo numerical simulation, the numerical table of correlation coefficients is established, which is more convenient for the direct application of inferential formulas. According to the results of theoretical analysis and examples, when using the indirect point estimation methods to infer the standard values of snow load in the conditions of small samples, the inference results are always small. The linear regression estimation method is suitable for inferring standard values of snow load in the conditions of small samples, which can give more reasonable results. When using the linear regression estimation to infer standard values of snow load in practical application, even if the coefficient of variation is unknown, it can set the upper limit value of the coefficient of variation according to the experience; meanwhile, according to the parameter-free and known coefficient of variation, the estimation is carried out, respectively, and the smaller value of the two is taken as the final estimate. The method can be extended to the statistical inference of variable load standard values such as wind load and floor load.

1. Introduction

Snow load is one of the main loads of buildings, and the inference of its standard value is the basis for the establishment of structural design and evaluation methods. At present, the inference of the standard values of snow load is generally fitting with the maximum type I distribution for the maximum annual snow pressure [1]; then, using the relation between the representative values and the distribution parameters, an estimate of the distribution parameters is given under a certain guaranteed rate. Among them, the estimation method of distribution parameters includes the moment method and the maximum likelihood method [2–13]. These are point estimation methods. They are mainly suitable for large samples. They require sufficient meteorological data as statistical samples. It is generally believed that at least 30 years of data are required [14, 15]. However, in engineering practice, it is sometimes necessary to infer the standard values of snow load under the condition that the test data are insufficient, and the actual sample capacity is often very limited. Statistical analysis is done mostly in the case of small sample capacity. This results in a significant reduction in parameter estimation accuracy when the sample capacity is small. In the case of such a small sample, if the current point estimation method is still used for inference, the result of inference is often reduced due to the

influence of statistical uncertainty. A more reasonable choice is to use a small sample inference method [16–19].

For dead loads, the standard for appraisal of reliability of civil buildings has proposed a small sample method for inferring its standard value [20]; however, the snow load usually obeys the maximum type I distribution, which is different from the probability distribution form of the dead load. Therefore, the same method cannot be used to infer the standard values of snow load. A method for estimating the maximum type I distribution parameters and tantile is proposed in the paper [21], which lays a theoretical foundation for the small sample inference of the standard values of snow load without parameter information. Therefore, the inference formula of the standard values of snow load without parameter information can be established. However, in some cases, the variable coefficients of the probability distribution of snow loads are known, or their upper limit values can be set based on experience. Using the additional information, the uncertainty of the statistics in the estimation process can be significantly reduced, and more favorable extrapolation results can be obtained under the same conditions. Therefore, it is necessary to study the inference method of the standard values of snow load when the coefficient of variation is known under the condition of small samples, to provide a better choice for the small sample inference of the standard values of snow load.

Based on the above analysis, the probability distribution model of snow load is established first in this paper because the standard values of snow load usually are expressed as a tantile of the distribution, type I maximum distribution, and type I minimum distribution which belong to the same extreme value distribution families and can be converted with each other; therefore, by using the least square method based on the best linear unbiased estimation and the invariant estimation principle of the current minimum type I distribution parameters, a linear regression estimation method for standard snow load under small sample conditions is proposed [22–31].

The inference formula of standard values of snow load is given in this paper, and no parameter information and the known coefficient of variation are both considered. Through numerical integration and Monte Carlo numerical simulation, a numerical table of correlation coefficient is established to tantile the application of the inference formula, and the conclusions and suggestions are given by comparing the results with the traditional large sample method. The method can be extended to the statistical inference of variable load standard values such as wind load and floor load.

2. Probability Distribution Model of Snow Load

A probability distribution model of snow load is established by using a stationary binomial random process [32].

It is assumed that the design reference period of the building structure is T, and it can be divided into r equal period of time in $[0, T]$; the average time for the snow load to change once is $\tau = T/r$; the probability of action at each time is p; the probability distribution function appearing on different time segments is $F_Q(x)$, and the random variables x on different time segments are independent of each other. The establishment of the snow load model requires the identification of the above three key parameters. The Unified Standard for Reliability Design of Building Structures uses a limit state design method based on probability theory, that is, a first-order second-moment method that considers the probability distribution type of basic variables. Since the basic variables are considered as random variables, the random process of the load must be converted into a random variable [33]. If random variables at any point time are used instead of random processes, it will be unsafe, so the maximum load random variables Q_T ($Q_T = \max Q_t, 0 \le t \le T$) appearing in the design reference period should be used instead of random processes for statistical analysis. The basic steps to convert the random process to the maximum load within T years are as follows:

Step 1: establish the load probability distribution function at any period time τ:

$$F_t(x) = P[Q(t) \le x, t \in T] = p \cdot F_i(x) + 1 - p = 1 - p[1 - F_i(x)], \tag{1}$$

where $F_i(x)$ is the load distribution function at i time point.

Step 2: establish the probability distribution function Q_T:

$$\begin{aligned} F_T(x) &= P[Q_T \le x] = P\left[\max_{0 \le t \le T} Q(t) \le x, t \in T\right] \\ &= \prod_{j=1}^{r} P\left[Q(t_j) \le x, t_j \in t\right] \\ &= \prod_{j=1}^{r} \{1 - p[1 - F_i(x)]\} = \{1 - p[1 - F_i(x)]\}^r. \end{aligned} \tag{2}$$

Assuming that the average number m is the snow load which occurs in T years, then

$$m = pr. \tag{3}$$

Obviously, when $p = 1$ and $m = r$, then,

$$F_T(x) = [F_i(x)]^m. \tag{4}$$

When $p < 1$, using the approximate relationship,

$$e^{-x} = 1 - x. \tag{5}$$

If $p[1 - F_i(x)]$ is sufficiently small in (2), then

$$F_T(x) \approx \left\{e^{-p[1-F_i(x)]}\right\}^r = \left\{e^{-[1-F_i(x)]}\right\}^{pr} \approx \{1 - [1 - F_i(x)]\}^{pr}. \tag{6}$$

Hence,

$$F_T(x) \approx [F_i(x)]^m. \tag{7}$$

It can be seen from the above equation that the probability distribution function $F_T(x)$ of the maximum load Q_T in the design reference period is equal to

the m-power of the probability distribution function $F_i(x)$ of the load at any time, and $F_i(x)$ can be obtained according to statistics [34].

Step 3: the probability distribution of snow load is fitting with the maximum type I distribution. The distribution function and probability density functions are, respectively, as follows:

$$F(x) = e^{-e^{-((x-\mu)/\alpha)}},$$
$$f_X(x) = \frac{1}{\alpha} e^{-((x-\mu)/\alpha)} \exp\left\{-e^{-((x-\mu)/\alpha)}\right\}, \tag{8}$$

where α and μ are the scale parameters and position parameters of the distribution.

3. Linear Regression Estimation Method for Standard Values of Snow Load

3.1. In the Condition of Unknown Parameter Information. The value at any time point of snow load obeys the maximum type I distribution, and the probability density function is

$$f_X(x) = \frac{1}{\alpha} e^{-((x-\mu)/\alpha)} \exp\left\{-e^{-((x-\mu)/\alpha)}\right\}, \tag{9}$$

where μ and α are distributed parameters, $-\infty < \mu < \infty$ and $0 < \alpha < \infty$. The standard values of snow load usually are expressed as down tantiles with p calibration of the random variable X, and they can be written as x_k; it meets that

$$P\{X \le x_k\} = \exp\left\{-e^{-((x_k-\mu)/\alpha)}\right\} = p,$$
$$x_k = \mu - \alpha \ln(-\ln p) = \mu + k\alpha, \tag{10}$$

where p is a guaranteed rate of the standard value x_k.

It is assumed that n samples of X are arranged from a small to large order: $X_{(1)}, X_{(2)}, \ldots, X_{(n)}$, and the test values are $x_{(1)}, x_{(2)}, \ldots, x_{(n)}$, respectively.

Let

$$Y' = -X. \tag{11}$$

Then, Y' obeys the minimum type I distribution with two parameters $-\mu$ and α, and the order statistic and up tantiles with p calibration are

$$Y'_{(j)} = -X_{(n-j+1)}, \quad j = 1, 2, \ldots, n,$$
$$y'_p = -\mu - k\alpha = -x_k. \tag{12}$$

For obtaining x_k which is the characteristic value of variable actions, we usually select the upper limit estimated value as the inferring results; when the load effect is favorable for the structure, the lower limit estimated value should be selected, but it has been rarely found in the most unfavorable combinations of the action effect [35]. We can use the upper and lower limit estimated values of y'_p to infer the upper and lower limit estimated values of x_k because the estimate values

$$-\tilde{\mu} = \sum_{j=1}^{n} D_I(n, n, j)\left[-x_{(n-j+1)}\right], \tag{13}$$

$$\tilde{\alpha} = \sum_{j=1}^{n} C_I(n, n, j)\left[-x_{(n-j+1)}\right], \tag{14}$$

$$y_{p,U}' = -\tilde{\mu} - v_{p,1-C}\tilde{\alpha}, \tag{15}$$

$$y_{p,L}' = -\tilde{\mu} - v_{p,C}\tilde{\alpha}. \tag{16}$$

And, for the random variables $-\tilde{\mu}$ and $\tilde{\alpha}$, we have,

$$P\left\{\frac{-\tilde{\mu} - y_p}{\tilde{\alpha}} \le v_{p,C}\right\} = P\left\{y_p \ge -\left(\tilde{\mu} + v_{p,C}\tilde{\alpha}\right)\right\} = P\left\{-y_p \le \tilde{\mu} + v_{p,C}\tilde{\alpha}\right\} = P\left\{x_k \le \tilde{\mu} + v_{p,C}\tilde{\alpha}\right\},$$
$$P\left\{\frac{-\tilde{\mu} - y_p}{\tilde{\alpha}} \ge v_{p,1-C}\right\} = P\left\{y_p \le -\left(\tilde{\mu} + v_{p,1-C}\tilde{\alpha}\right)\right\} = P\left\{-y_p \ge \tilde{\mu} + v_{p,1-C}\tilde{\alpha}\right\} = P\left\{x_k \ge \tilde{\mu} + v_{p,1-C}\tilde{\alpha}\right\}. \tag{17}$$

Thus, the upper and lower limit estimated values of x_k, which are the characteristic values of the variable actions, are

$$x_{k,U} = -y_{p,L}' = \tilde{\mu} + v_{p,C}\tilde{\alpha} = \sum_{j=1}^{n} D_I(n, n, j) x_{(n-j+1)} + v_{p,C} \sum_{j=1}^{n}\left[-C_I(n, n, j) x_{(n-j+1)}\right], \tag{18}$$

$$x_{k,L} = -y_{p,U}' = \tilde{\mu} + v_{p,1-C}\tilde{\alpha} = \sum_{j=1}^{n} D_I(n, n, j) x_{(n-j+1)} + v_{p,1-C} \sum_{j=1}^{n}\left[-C_I(n, n, j) x_{(n-j+1)}\right], \tag{19}$$

where $D_I(n, n, j)$ and $C_I(n, n, j)$ can be directly determined from the numerical table. Because $v_{p,C}$ and $v_{p,1-C}$ are present, numerical tables only give the numerical values when $p = 0.90, 0.95$, and 0.99, so the values of $v_{p,C}$ and $v_{p,1-C}$ usually cannot be directly determined from the numerical table [36]. Therefore, we propose a new approximate method which uses the present numerical table to infer the values of $v_{p,C}$ and $v_{p,1-C}$ in this paper.

We use p_0 to denote the guarantee rate when the present numerical tables are adopted, and down tantiles with p_0 calibration of the random variable X are expressed as x_{k0}, so we have

$$x_{k0} = \mu - \alpha \ln(-\ln p_0),$$
$$x_k = \mu + \frac{\ln(-\ln p)}{\ln(-\ln p_0)}(x_{k0} - \mu). \tag{20}$$

It is approximate let that

$$x_{k0,U} - \mu \approx x_{k0,U} - \widetilde{\mu} = v_{p_0,C}\widetilde{\alpha},$$
$$x_{k0,L} - \mu \approx x_{k0,L} - \widetilde{\mu} = v_{p_0,1-C}\widetilde{\alpha}. \tag{21}$$

Because of the corresponding relationships between $x_{k,U}$ and $x_{k0,U}$, $x_{k,L}$, and $x_{k0,L}$, we can obtain that

$$v_{p,C} = \frac{\ln(-\ln p)}{\ln(-\ln p_0)} v_{p_0,C},$$
$$v_{p,1-C} = \frac{\ln(-\ln p)}{\ln(-\ln p_0)} v_{p_0,1-C}. \tag{22}$$

In practical applications, we should select p_0 which is approximate to p. It is proved by calculation that when $n = 5 - 25$, $p \geq 0.90$, and $C = 0.6 - 0.95$, the margins of errors of $v_{p,C}$ and $v_{p,1-C}$ are -0.017 to 0.017 and -0.031 to 0.036, respectively. This method is more convenient and accurate than the interpolation method.

3.2. In the Condition of Known Coefficient of Variation

3.2.1. Linear Unbiased Estimation of Distribution Parameters. It is assumed that the value at any time point of snow load is X and the coefficient of variation δ_X of X is known, and the distribution parameters are

$$\alpha = \frac{\sqrt{6}}{\pi}\sigma_X,$$
$$\mu = \mu_X - C_E\alpha = \mu_X\left(1 - \frac{C_E\sqrt{6}}{\pi}\delta_X\right), \tag{23}$$

where μ_X, σ_X, and δ_X are the mean, standard deviation, and coefficient of variation of X, respectively, and C_E is the Euler constant. It is assumed that the samples of X are arranged from the small to large order: $X_{(1)}, X_{(2)}, \ldots, X_{(n)}$, that is, $X_{(1)} \leq X_{(2)} \leq \cdots \leq X_{(n)}$. At this time, the probability density function of $X_{(i)}$ and the joint probability density function of $X_{(i)}$ and $X_{(j)}$ $(1 \leq i < j \leq n)$ are

$$f_{X_{(i)}}(x) = \frac{n!}{(i-1)!(n-i)!}F_X(x)^{i-1}$$
$$[1 - F_X(x)]^{n-i} f_X(x), \quad i = 1, 2, \ldots, n,$$
$$f_{X_{(i)},X_{(j)}}(x, y) = \frac{n!}{(i-1)!(j-i-1)!(n-j)!}F_X(x)^{i-1}$$
$$[F_X(y) - F_X(x)]^{j-i-1}[1 - F_X(y)]^{n-j}$$
$$f_X(x) f_X(y), \quad 1 \leq i < j \leq n, x \leq y. \tag{24}$$

Let

$$Z = \frac{X - \mu}{\alpha}. \tag{25}$$

Then, Z obeys the standard maximum type I distribution, and its order statistic is

$$Z_{(i)} = \frac{X_{(i)} - \mu}{\alpha}, \quad i = 1, 2, \ldots, n, \tag{26}$$

the probability density function of $Z_{(i)}$ and the joint probability density function of $Z_{(i)}$ and $Z_{(j)}$ $(1 \leq i < j \leq n)$ are

$$f_{Z_{(i)}}(x) = \frac{n!}{(i-1)!(n-i)!}\left(e^{-e^{-x}}\right)^{i-1}$$
$$\left(1 - e^{-e^{-x}}\right)^{n-i} e^{-x} e^{-e^{-x}}, \quad i = 1, 2, \ldots, n,$$
$$f_{Z_{(i)},Z_{(j)}}(x, y) = \frac{n!}{(i-1)!(j-i-1)!(n-j)!}\left(e^{-e^{-x}}\right)^{i-1}$$
$$\left(e^{-e^{-y}} - e^{-e^{-x}}\right)^{j-i-1}\left(1 - e^{-e^{-y}}\right)^{n-j} e^{-x} e^{-e^{-x}}$$
$$e^{-y} e^{-e^{-y}}, \quad 1 \leq i < j \leq n, x \leq y. \tag{27}$$

The mean, the variance of $Z_{(i)}$, and the covariance of the $Z_{(i)}$ and $Z_{(j)}$ are

$$\mu_i = \int_{-\infty}^{\infty} x f_{Z_{(i)}}(x)\mathrm{d}x = \frac{n!}{(i-1)!(n-i)!}\int_0^1 [-\ln(-\ln u)]u^{i-1}(1-u)^{n-i}\mathrm{d}u, \quad i = 1, 2, \ldots, n, \tag{28}$$

$$v_{ii} = \int_{-\infty}^{\infty} x^2 f_{Z_{(i)}}(x)\mathrm{d}x - \mu_i^2 = \frac{n!}{(i-1)!(n-i)!}\int_0^1 [-\ln(-\ln u)]^2 u^{i-1}(1-u)^{n-i}\mathrm{d}u - \mu_i^2, \quad i = 1, 2, \ldots, n, \tag{29}$$

$$v_{ij} = \int_{-\infty}^{\infty}\int_x^{\infty} xy f_{Z_{(i)},Z_{(j)}}(x, y)\mathrm{d}y\mathrm{d}x - \mu_i\mu_j = \frac{n!}{(i-1)!(j-i-1)!(n-j)!}\int_0^1\int_u^1 [-\ln(-\ln u)][-\ln(-\ln v)]u^{i-1}(v-u)^{j-i-1}(1-v)^{n-j}\mathrm{d}v\mathrm{d}u - \mu_i\mu_j, \quad i = 1, 2, \ldots, n. \tag{30}$$

Then, the mean of $X_{(i)}$ is

$$\mu_{X_{(i)}} = \mu + \alpha\mu_i = \mu(1 + c\mu_i), \quad i = 1, 2, \ldots, n,$$
$$c = \frac{(\sqrt{6}/\pi)\delta_X}{1 - (C_E\sqrt{6}/\pi)\delta_X}. \tag{31}$$

The covariance matrix and its inverse matrix of $Z_{(1)}, Z_{(2)}, \ldots, Z_{(n)}$ are, respectively, denoted as

$$V = \begin{pmatrix} v_{11} & v_{12} & \cdots & v_{1n} \\ v_{21} & v_{22} & \cdots & v_{2n} \\ \vdots & \vdots & \ddots & \vdots \\ v_{n1} & v_{n2} & \cdots & v_{nn} \end{pmatrix},$$
$$V^{-1} = \begin{pmatrix} v^{11} & v^{12} & \cdots & v^{1n} \\ v^{21} & v^{22} & \cdots & v^{2n} \\ \vdots & \vdots & \ddots & \vdots \\ v^{n1} & v^{n2} & \cdots & v^{nn} \end{pmatrix}. \tag{32}$$

According to the least square method of parameter estimation [36], take the weighted average sum as

$$Q = \sum_{i=1}^{n}\sum_{j=1}^{n}\left[\left(X_{(i)} - \mu_{X_{(i)}}\right)v^{ij}\left(X_{(j)} - \mu_{X_{(j)}}\right)\right]. \tag{33}$$

When the coefficient of variation δ_X is known, let

$$\frac{dQ}{d\mu} = 0. \tag{34}$$

When the coefficient of variation δ_X is known, the least square estimate of the unknown parameter μ is

$$\mu^* = \sum_{j=1}^{n} D(n, n, j, \delta_X)X_{(j)}, \tag{35}$$

$$D(n, n, j, \delta_X) = \frac{\sum_{i=1}^{n}\left[(1 + c\mu_i)v^{ij}\right.}{\sum_{i=1}^{n}\sum_{j=1}^{n}\left[(1 + c\mu_i)v^{ij}\left(1 + c\mu_j\right)\right]}, \quad j = 1, 2, \ldots, n. \tag{36}$$

Since

$$X_{(j)} = \mu + \alpha Z_{(j)} = \mu\left(1 + cZ_{(j)}\right), \quad j = 1, 2, \ldots, n. \tag{37}$$

Hence, the mean of μ^* is

$$E(\mu^*) = \sum_{j=1}^{n}\frac{\sum_{i=1}^{n}(1 + c\mu_i)v^{ij}}{\sum_{i=1}^{n}\sum_{j=1}^{n}\left[(1 + c\mu_i)v^{ij}\left(1 + c\mu_j\right)\right]}\mu\left(1 + c\mu_j\right) = \mu, \tag{38}$$

that is, the linear unbiased estimator of μ [37]. If $x_{(1)}, x_{(2)}, \ldots, x_{(n)}$ are the test values of $X_{(1)}, X_{(2)}, \ldots, X_{(n)}$, then the linear unbiased estimate is

$$\mu^* = \sum_{j=1}^{n} D(n, n, j, \delta_X)x_{(j)}. \tag{39}$$

Compared to the corresponding coefficient in the current linear unbiased estimate $D(n, n, j)$ [37], the influence of the coefficient of variation δ_X is considered in the coefficient $D(n, n, j, \delta_X)$. Since it is difficult to obtain the analytical expressions of equations (28)–(30), the values of v_{ij}, μ_i, and v_{ii} must be determined by numerical integration, the value of $D(n, n, j, \delta_X)$ can be determined from (36), the values when $n = 10$ are listed in Table 1, and others are omitted.

3.2.2. Interval Estimation of Tantile. For the standard values of snow load, a relatively large tantile is usually selected under the condition of a small sample, and the upper limit value in the interval estimate should be used as its estimate value.

Table 1: Numerical of $D(n, n, j, \delta)$.

n	j	δ						
		0.2	0.3	0.4	0.5	0.6	0.7	0.8
10	1	0.2379	0.1713	0.0952	0.0173	−0.0529	−0.1076	−0.1434
10	2	0.1670	0.1454	0.1173	0.0852	0.0528	0.0239	0.0009
10	3	0.1355	0.1268	0.1131	0.0952	0.0749	0.0547	0.0369
10	4	0.1127	0.1118	0.1067	0.0974	0.0847	0.0702	0.0559
10	5	0.0944	0.0985	0.0992	0.0959	0.0885	0.0783	0.0667
10	6	0.0786	0.0862	0.0910	0.0920	0.0887	0.0817	0.0725
10	7	0.0644	0.0744	0.0822	0.0863	0.0861	0.0818	0.0745
10	8	0.0513	0.0628	0.0725	0.0790	0.0811	0.0790	0.0736
10	9	0.0386	0.0506	0.0614	0.0693	0.0733	0.0730	0.0691
10	10	0.0263	0.0380	0.0490	0.0576	0.0627	0.0638	0.0615

Let

$$x_p = \mu + k\alpha = \mu(1 + ck),$$
$$k = -\ln(-\ln p), \tag{40}$$

where p is the guaranteed probability when $\{X \le x_p\}$, and the value is relatively large. When the coefficient of variation δ_X is known, it can be known from (35) and (37) that

$$\frac{\mu}{\mu^*} = \frac{1}{\sum_{j=1}^{n} D(n, n, j, \delta_X)\left(1 + cZ_{(j)}\right)}. \tag{41}$$

Let $U = \mu/\mu^*$, then U is a statistic that is independent of the distribution parameters μ and α. Based on the probability distribution of U, the estimate available of μ by the upper limit in the interval estimate is

$$\tilde{\mu} = u(n, n, \delta_X, C)\mu^*, \tag{42}$$

where $u(n, n, \delta_X, C)$ is the down tantile of U, C is the confidence degree, and the value is relatively large. The value of x_p estimated from the upper limit is

$$\tilde{x}_p = \tilde{\mu}(1 + ck) = u(n, n, \delta_X, C)\mu^*(1 + ck). \tag{43}$$

It is almost impossible to determine $u(n, n, \delta_X, C)$ by the analytical method, so we need to use Monte Carlo numerical simulation to determine the value. The random numbers that obey the standard maximum type I distribution which are first generated in each simulation, a set of sample values $Z_{(1)}, Z_{(2)}, \ldots, Z_{(n)}$, can be obtained after sorting, and the sample value of U is obtained from equation (41). When the number of simulations is sufficient, any tantile $u(n, n, \delta_X, C)$ can be obtained by statistics. Here, the number of simulations is 50,000. Table 2 lists the partial numerical tables when $n = 10, 15, 20$.

4. How to Choose the Confidence Degree in Engineering Practice

The confidence degree C is a representative of the trust level for the inferring results, and it has a direct impact on the inferring results; the higher the confidence degree, the higher the upper limit estimated value and the lower the lower limit

Table 2: Numerical of $u(n, n, \delta, C)$.

n	C	δ						
		0.2	0.3	0.4	0.5	0.6	0.7	0.8
10	0.50	1.0030	1.0046	1.0066	1.0095	1.0130	1.0164	1.0183
10	0.75	1.0417	1.0678	1.0960	1.1238	1.1518	1.1760	1.1962
10	0.90	1.0770	1.1266	1.1818	1.2409	1.2976	1.3490	1.3923
15	0.50	1.0020	1.0032	1.0047	1.0061	1.0086	1.0107	1.0123
15	0.75	1.0336	1.0537	1.0754	1.0974	1.1186	1.1365	1.1511
15	0.90	1.0626	1.1023	1.1466	1.1908	1.2332	1.2698	1.3001
20	0.50	1.0013	1.0023	1.0035	1.0047	1.0061	1.0069	1.0079
20	0.75	1.0284	1.0456	1.0640	1.0827	1.1002	1.1148	1.1266
20	0.90	1.0537	1.0870	1.1229	1.1595	1.1942	1.2233	1.2483

estimated value, and vice versa. At present, there is no suggestion about how to choose the confidence degree for inferring representative values and design values of variable actions in the literature.

Generally speaking, the larger the variability of the random variable X, the larger the value range of the distributed parameter and tantiles in the inference; moreover, the changes of C have great influences on the upper and lower limit estimated values when the confidence degree C gets larger and larger; that is, along with the C becoming larger, the upper limit estimated value is increased relatively quickly and the lower limit estimated value is reduced relatively quickly. When the variability of the random variable X is larger, and if we select the higher confidence degree in this case, the inferring results are too conservative, so we should select the relatively lower confidence degree. On the contrary, we should select the relatively higher confidence degree when the variability of the random variable X is smaller; it can avoid too aggressive inferring results.

The National Standard of the People's Republic of China (standard for appraiser of reliability of civil buildings) (GB50292-1999) throws out some suggestion about how to select the confidence degree to infer the standard value of the material strength: for steel, select $C = 0.90$; for concrete, select $C = 0.75$; for masonry, select $C = 0.60$; and it is suggested that $C = 0.95$ to infer the standard value of permanent action. The variation coefficients of material strength of the permanent action, steel, concrete, and masonry are in the order as 0.07, 0.06–0.10, 0.16–0.23, and 0.20–0.24 [20]. It can be seen that the value of the confidence degree in the National Standard of the People's Republic of China conforms to the above rules. The variation coefficient of snow load is more variable [38]; according to the above rules, we should select the relatively lower confidence degree, but the value should not be less than 0.5; otherwise, the lower limit estimated value will be higher than the upper limit estimated value. When the confidence degree $C = 0.5$ and all other conditions are equal, we contrast the inferring results of the moment method and the liner regression estimation method. It shows that the inferring result of the liner regression estimation method is slightly higher than the moment method, which is close to the result without considering the influence of statistical uncertainty. When the confidence degree C is not great, the changes of C have no great influence on the inferring results [39], so we can select the slightly higher confidence degree, which can take into account the influences of statistical uncertainty more fully and avoid the too aggressive inferring results. In this article, we suggest to select the confidence degree $C = 0.75$ to infer the standard values of snow load. We will illustrate the correctness by an example in Section 5.

5. Examples

In this section, we use the established linear regression estimation method to estimate the standard values of snow load. The data used in this article are the actual snowfall data from 1989 to 2008 in the Shuyang county [40], and the specific values are shown in Table 3.

To compare and analyze the differences in the extrapolation results under different sample sizes, the above sample values are divided into three groups: 2008–1999 (10 sample data), 2008–1994 (15 sample data), and 2008–1989 (20 sample data) [41–45]. The results are calculated according to different inference methods.

We select the guarantee rate $p = 1 - 1/50 = 0.98$, and the confidence degree C in the interval estimate is 0.75.

By using the moment method, we can obtain the estimate of the standard values of snow load through calculation as follows:

$$\begin{aligned} \alpha &= \frac{\sqrt{6}}{\pi} s = 0.042, \\ \mu &= \overline{x} - C_{\mathrm{E}}\alpha = 0.121, \\ x_p &= \mu + k\alpha = 0.285. \end{aligned} \tag{44}$$

According to the maximum likelihood estimation method, by introducing the likelihood function, we can derive the parameter estimation formula as follows:

$$\begin{aligned} \mu &= -\alpha \ln\left(\frac{1}{n}\sum_{i=1}^{n} e^{-(x_i/\alpha)}\right), \\ \alpha &= \overline{x} - \frac{\sum_{i=1}^{n}\left(x_i e^{-(x_i/\alpha)}\right)}{\sum_{i=1}^{n} e^{-(x_i/\alpha)}}. \end{aligned} \tag{45}$$

We can obtain the estimated values of the parameters, respectively, by the iterative method, and finally obtain the standard values of snow load through calculation as follows:

$$\begin{aligned} \widehat{\alpha} &= 0.041, \\ \widehat{\mu} &= 0.122, \\ \widehat{x}_p &= 0.282. \end{aligned} \tag{46}$$

By using the linear regression estimation method of the standard value of snow load in the condition of unknown parameter information (equations (13), (14), and (18)), we can obtain the estimate through calculation as follows:

$$\begin{aligned} \widetilde{\alpha} &= -\sum_{j=1}^{n} C_I(n, n, j) x_{(n-j+1)} = 0.042, \\ \widetilde{\mu} &= \sum_{j=1}^{n} D_I(n, n, j) x_{(n-j+1)} = 0.119, \\ \widetilde{x}_p &= \widetilde{\mu} + \nu_{p,C}\widetilde{\alpha} = 0.339. \end{aligned} \tag{47}$$

Table 3: Statistics of the maximum snow depth and pressure every year in the Shuyang county.

Year	Snow depth (m)	Snow pressure ($kN \cdot m^{-2}$)
2008	0.18	0.265
2007	0.05	0.074
2006	0.11	0.162
2005	0.09	0.132
2004	0.09	0.132
2003	0.1	0.147
2002	0.08	0.118
2001	0.10	0.147
2000	0.06	0.088
1999	0.13	0.191
1998	0.11	0.162
1997	0.08	0.118
1996	0.08	0.118
1995	0.06	0.088
1994	0.13	0.191
1993	0.14	0.206
1992	0.08	0.118
1991	0.21	0.309
1990	0.11	0.162
1989	0.11	0.162

Table 4: Numerical table and calculation process.

j	$x_{(10-j+1)}$	$D_I(10, 10, j)$	$C_I(10, 10, j)$	$xD_I(10, 10, j)$	$-xC_I(10, 10, j)$
1	0.265	0.0273	−0.0727	0.0072	−0.0192
2	0.191	0.0400	−0.0780	0.0076	−0.0149
3	0.162	0.0525	−0.0772	0.0085	−0.0125
4	0.147	0.0654	−0.0719	0.0096	−0.0106
5	0.147	0.0793	−0.0617	0.0117	−0.0091
6	0.132	0.0946	−0.0454	0.0125	−0.0060
7	0.132	0.1124	−0.0207	0.0149	−0.0027
8	0.118	0.1342	0.0179	0.0158	0.0021
9	0.088	0.1642	0.0851	0.0145	0.0075
10	0.074	0.2300	0.3246	0.0169	0.0239
Sum		1	0	0.119	0.042

The values of $D_I(10, 10, j)$ and $C_I(10, 10, j)$ are listed in Table 4, and $v_{0.99,0.75} = 6.23$.

In the condition of the known coefficient of variation, to facilitate comparison under the same conditions, we select $\delta_X = 0.4$, by using the moment method, then

$$\mu' = \overline{x}\left(1 - \frac{C_E\sqrt{6}}{\pi}\delta_X\right) = 0.120,$$
$$x_p' = \mu'(1 + ck) = 0.297. \tag{48}$$

By using the maximum likelihood estimation method, we can obtain the estimated values of the parameters, respectively, by the iterative method, and finally obtain the standard values of snow load:

$$\breve{x}_p = 0.286. \tag{49}$$

By using the linear regression estimation method that the coefficient of variation is known (equations (39) and (42)), then

$$\mu^* = \sum_{j=1}^{n} D(n, n, j, \delta_X)x_{(j)} = 0.120,$$
$$\widetilde{x}_p = u(n, n, \delta_X, C)\mu^*(1 + ck) = 0.327, \tag{50}$$

where $u(10, 10, 0.4, 0.75) = 1.096$ and the value of $D(10, 10, j, 0.4)$ is shown in Table 1; Table 5 shows the calculation process.

To facilitate comparative analysis, Table 6 lists the statistical extrapolation results of different estimation methods and different sample sizes in two cases where the coefficient of variation is known and the parameter information is unknown.

A comparative analysis of the calculations presented in Table 6 shows that

(1) Regardless of whether the coefficient of variation is unknown or known, the results estimated by the maximum likelihood method are the smallest, followed by the moment method, because these two

Table 5: Numerical table and calculation process.

j	x_j	$D(10, 10, j, 0.4)$	$xD(10, 10, j, 0.4)$
1	0.074	0.0952	0.013
2	0.088	0.1173	0.012
3	0.118	0.1131	0.012
4	0.132	0.1067	0.012
5	0.132	0.0992	0.013
6	0.147	0.091	0.013
7	0.147	0.0822	0.014
8	0.162	0.0725	0.013
9	0.191	0.0614	0.010
10	0.265	0.0490	0.007
Sum			0.120

Table 6: Comparison of inference results of different inference methods.

Parameter information	Inference method	Inference results ($kN{\cdot}m^{-2}$)			Relative error (%)		
		$n = 10$	$n = 15$	$n = 20$	$n = 10$	$n = 15$	$n = 20$
Unknown information	Moment	0.285	0.268	0.304	18.9	17.9	16.8
	Likelihood	0.282	0.265	0.295	20.2	19.2	20.3
	Regression	0.339	0.316	0.355			
Known coefficient of variation	Moment	0.297	0.289	0.314	10.1	9.0	7.0
	Likelihood	0.286	0.268	0.304	12.9	14.9	9.6
	Regression	0.327	0.315	0.336			

classical statistical methods do not take into account the influences of statistical uncertainty, and the inferred results are always on the aggressive side.

(2) Regardless of whether the coefficient of variation is unknown or known, with the gradual increase in the sample capacity, the relative errors of the results of the linear regression method and the classical statistical methods (the moment method and the maximum likelihood method) are gradually reduced, which is due to the gradual reduction of the influence of statistical uncertainty when the sample capacity increases.

(3) According to the linear regression method, at different sample sizes, the estimated results when the coefficient of variation is known are smaller, which is due to the significant reduction in the uncertainty of the statistic U in the estimation process.

Due to space limitation, this paper only compares the extrapolation values of different inference methods in three groups of sample sizes. By calculating and comparing the extrapolation of the standard values of snow loads in other sample sizes, the same results can be obtained.

6. Conclusions

(1) When we use the current statistical inference method to infer the standard value of snow load in the conditions of small samples, the inferring results are always on the aggressive side because it does not take into account the influences of statistical uncertainty.

(2) The linear regression estimation method presented in this paper can reduce the influence of statistical uncertainty when the sample is small, and it is applicable to the statistical inference of the standard values of snow load in small sample conditions; considering the two cases where no parameter information and the coefficient of variation are known, more reasonable inference results can be given.

(3) We suggest to select the confidence degree $C = 0.75$ to infer the standard value of snow load.

(4) In the practical application, even if the coefficient of variation is unknown, the upper limit of the coefficient of variation can be set based on experience, the estimation can be made according to the no parameter information, the coefficients of variation are known, and the smaller value of the two is taken as the final estimate. The research in this paper can provide a theoretical basis for adjusting snow load.

Data Availability

The authors solemnly inform that the key data in the calculation process have been listed in the data list of the article, and other nonkey detailed data can be obtained by contacting the corresponding author if necessary.

Conflicts of Interest

The authors declare that they have no conflicts of interest.

Acknowledgments

This project was supported by the National Natural Science Foundation of China (nos. 50678143 and 51278401) and the Education Department of Shaanxi (no. 17JK0440).

References

[1] GB50009-2012, *Load Code for the Design of Building Structure*, China Architecture & Building Press, Beijing, China, 2012.

[2] J. Aitchison and S. D. Silvey, "Maximum-likelihood estimation of parameters subject to restraints," *The Annals of Mathematical Statistics*, vol. 29, no. 3, pp. 813–828, 1958.

[3] D. D. Dorfman and E. Alf, "Maximum-likelihood estimation of parameters of signal-detection theory and determination of confidence intervals-rating-method data," *Journal of Mathematical Psychology*, vol. 6, no. 3, pp. 487–496, 1969.

[4] S. I. Aihara, "Regularized maximum likelihood estimate for an infinite-dimensional parameter in stochastic parabolic systems," *SIAM Journal on Control and Optimization*, vol. 30, no. 4, pp. 745–764, 1992.

[5] S. S. Li, "Estimation method for parameters of extreme value I distribution," *Journal of Fuzhou University*, vol. 16, no. 1, pp. 79–84, 1998.

[6] Z. D. Duan and D. C. Zhou, "A comparative study on parameter estimate method for extremal value distribution," *Journal of Harbin Institute of Technology*, vol. 36, no. 12, pp. 1605–1609, 2004.

[7] G. Aneiros-Pérez and P. Vieu, "Semi-functional partial linear regression," *Statistics & Probability Letters*, vol. 76, no. 11, pp. 1102–1110, 2006.

[8] P. Hall and J. L. Horowitz, "Methodology and convergence rates for functional linear regression," *The Annals of Statistics*, vol. 35, no. 1, pp. 70–91, 2007.

[9] I. Naseem, R. Togneri, and M. Bennamoun, "Linear regression for face recognition," *IEEE Transactions on Pattern Analysis and Machine Intelligence*, vol. 32, no. 11, pp. 2106–2112, 2010.

[10] F. Cribari-Neto and W. B. da Silva, "A new heteroskedasticity-consistent covariance matrix estimator for the linear regression model," *AStA Advances in Statistical Analysis*, vol. 95, no. 2, pp. 129–146, 2011.

[11] Y. Zhao, X. Meng, and H. Yang, "Jackknife empirical likelihood inference for the mean absolute deviation," *Computational Statistics & Data Analysis*, vol. 91, pp. 92–101, 2015.

[12] G. C. Manjunath Patel, P. Krishna, and M. B. Parappagoudar, "Squeeze casting process modeling by a conventional statistical regression analysis approach," *Applied Mathematical Modeling*, vol. 40, no. 15-16, pp. 6869–6888, 2016.

[13] T. Sun, L. Cheng, and H. Jiang, "Greedy method for robust linear regression," *Neurocomputing*, vol. 243, pp. 125–132, 2017.

[14] M. O'Rourke, A. DeGaetano, and J. Tokarczyk, "Analytical simulation of snow drift loading," *Journal of Structural Engineering*, vol. 131, no. 4, pp. 660–667, 2005.

[15] Y. N. Zhang, Y. Zhang, Y. Q. Wang, and Y. J. Shi, "Calculation and analysis of basic snow pressure in Liaoning province," *Journal of South China University of Technology (Natural Science Edition)*, vol. 38, no. 9, pp. 108–112, 2010.

[16] S. Basu, "Improved small sample inference procedures for epidemiological parameters under cross-sectional sampling," *Journal of the Royal Statistical Society: Series D (The Statistician)*, vol. 50, no. 3, pp. 309–319, 2001.

[17] S. Paul and X. Zhang, "Small sample GEE estimation of regression parameters for longitudinal data," *Statistics in Medicine*, vol. 33, no. 22, pp. 3869–3881, 2014.

[18] T. P. Talafuse and E. A. Pohl, "Small sample discrete reliability growth modeling using a grey systems model," *Grey Systems: Theory and Application*, vol. 8, no. 3, pp. 246–271, 2018.

[19] S.-K. Fan, C.-H. Jen, and J.-X. Lee, "Profile monitoring for autocorrelated reflow processes with small samples," *Processes*, vol. 7, no. 2, p. 104, 2019.

[20] GB50292-1999, *Standard for Appraiser of Reliability of Civil Buildings*, China Architecture & Building Press, Beijing, China, 1999.

[21] J. T. Yao and X. D. Wang, "Minor sample estimation of the parameters and fractile of largest extreme value distribution type I," *Statistics and Decision*, vol. 19, pp. 11–14, 2014.

[22] S. Emilio and B. Sen, "Nonparametric least squares estimation of a multivariate convex regression function," *The Annals of Statistics*, vol. 39, no. 3, pp. 1633–1657, 2011.

[23] S. Aihara, "Consistency property of extended least-squares parameter estimation for stochastic diffusion equation," *Systems & Control Letters*, vol. 34, no. 5, pp. 249–256, 1998.

[24] D. Kumar, S. F. Ali, and A. Arockiarajan, "Structural and aerodynamics studies on various wing configurations for morphing," *IFAC-PapersOnLine*, vol. 51, no. 1, pp. 498–503, 2018.

[25] B. Keshtegar and P. Hao, "A hybrid self-adjusted mean value method for reliability-based design optimization using sufficient descent condition," *Applied Mathematical Modelling*, vol. 41, pp. 257–270, 2017.

[26] Y.-G. Zhao and T. Ono, "Moment methods for structural reliability," *Structural Safety*, vol. 23, no. 1, pp. 47–75, 2001.

[27] X. Shi, A. P. Teixeira, J. Zhang, and C. Guedes Soares, "Structural reliability analysis based on probabilistic response modelling using the maximum entropy method," *Engineering Structures*, vol. 70, pp. 106–116, 2014.

[28] X. Zhang and M. D. Pandey, "Structural reliability analysis based on the concepts of entropy, fractional moment and dimensional reduction method," *Structural Safety*, vol. 43, pp. 28–40, 2013.

[29] M. Koliou and A. Filiatrault, "Development of wood and steel diaphragm hysteretic connector database for performance-based earthquake engineering," *Bulletin of Earthquake Engineering*, vol. 15, no. 10, pp. 4319–4347, 2017.

[30] Z. Xi, C. Hu, and B. D. Youn, "A comparative study of probability estimation methods for reliability analysis," *Structural and Multidisciplinary Optimization*, vol. 45, no. 1, pp. 33–52, 2012.

[31] S. S. Mao, *Statistics Handbook*, Science Press, Beijing, China, 2003.

[32] SJ/T11099-1996, *Tables for Best Linear Unbiased Estimate (BLUE) (Extreme-Value Distribution, Weibull Distribution)*, China Architecture & Building Press, Beijing, China, 1996.

[33] GB50068-2001, *Unified Standard for Reliability Design of Building Structures*, China Architecture & Building Press, Beijing, China, 2001.

[34] GB50153-2008, *Unified Standard for Reliability Design of Engineering Structures*, China Architecture & Building Press, Beijing, China, 2009.

[35] S. S. Dai and H. L. Fei, *Reliability Test and Statistical Analysis (First Book)*, National Defence Industry Press, Beijing, China, 1983.

[36] Research Department of Machinery Industry Standard Fourth, *Table for Reliability Test*, National Defence Industry Press, Beijing, China, 1979.

[37] GB12282 1-90, *Tables for Life Testing Tables for Best Linear Unbiased Estimate (BLUE) (Extreme-Value Distribution, Weibull Distribution)*, Publishing House of Electronics Industry, Beijing, China, 1996.

[38] Z. Chang and X. M. Xie, "Research and suggestions on wind and snow live load value of buildings," *Building Science*, vol. 27, no. 1, pp. 83–85, 2011.

[39] J. T. Yao and X. D. Wang, "Linear regression estimation of representative values of variable actions," *Journal of Building Structures*, vol. 35, no. 10, pp. 98–103, 2014.

[40] C. J. Kang, W. F. Du, X. Yang, and Z. Zhu, "Calculation and analysis of snow loads based on the maximum likelihood method," *Journal of Henan University (Natural Science)*, vol. 46, no. 2, pp. 220–225, 2016.

[41] A. Q. Baig, M. Naeem, and W. Gao, "Revan and hyper-Revan indices of octahedral and icosahedral networks," *Applied Mathematics and Nonlinear Sciences*, vol. 3, no. 1, pp. 33–40, 2018.

[42] M. Dewasurendra and K. Vajravelu, "On the method of inverse mapping for solutions of coupled systems of nonlinear differential equations arising in nanofluid flow, heat and mass transfer," *Applied Mathematics and Nonlinear Sciences*, vol. 3, no. 1, pp. 1–14, 2018.

[43] Y. Qin, Y. Luo, Y. Zhao, and J. Zhang, "Research on relationship between tourism income and economic growth based on meta-analysis," *Applied Mathematics and Nonlinear Sciences*, vol. 3, no. 1, pp. 105–114, 2018.

[44] J. F. Gómez-Aguilar and A. Atangana, "Time-fractional variable-order telegraph equation involving operators with Mittag-Leffler kernel," *Journal of Electromagnetic Waves and Applications*, vol. 33, no. 2, pp. 165–177, 2019.

[45] D. P. Ahokpossi, A. Atangana, and P. D. Vermeulen, "Hydrogeochemical characterizations of a platinum group element groundwater system in Africa," *Journal of African Earth Sciences*, vol. 138, pp. 348–366, 2018.

Hindawi
Mathematical Problems in Engineering
Volume 2020, Article ID 6328176, 13 pages
https://doi.org/10.1155/2020/6328176

Research Article

Evaluation of Resilience of Battle Damage Equipment Based on BN-Cloud Model

Mingchang Song, Quan Shi, Qiwei Hu, Zhifeng You, and Yadong Wang

Equipment Support Department, Army Engineering University, Shijiazhuang, China

Correspondence should be addressed to Quan Shi; 3141454967@qq.com

Received 31 March 2020; Revised 26 April 2020; Accepted 11 May 2020; Published 4 July 2020

Guest Editor: Huchang Liao

In order to solve the problem of a lack of supportive means for evaluating the resilience of battle damage equipment, a Bayesian network cloud model is proposed to evaluate the resilience of battle damage equipment. The equipment functional features are analyzed to establish the equipment functional state evaluation model. Moreover, the samples of Bayesian network parameters training are obtained by inserting the results of battle damage simulation into the functional evaluation model. The simulation flow of parts state recovery probability is designed to determine the relationship between parts' functional state and time. Based on the cloud model, the transformation model of functional state level probability to functional index is established. Hence, the equipment functional state level probability obtained by Bayesian network reasoning is transformed into a functional index and the transformation from uncertainty to certainty is realized. Considering self-propelled artillery as the object of resilience evaluation, the results of numerical examples show that by this method, the problem of equipment resilience evaluation can be effectively solved, and more information can be obtained by the accurate representation method compared to the traditional Bayesian network probabilistic evaluation results. This is greatly significant to the wartime maintenance support decision.

1. Introduction

The evaluation of the resilience of battle damage equipment refers to evaluating the capability of the equipment to recover the specified functions after being damaged by a specific threat under specific battlefield conditions. The key to assess the resilience of battle damage equipment is to determine the relationship between recovery status and recovery time. In the previous researches on equipment damage assessment, the damage degree of equipment after hitting is assessed mainly reflecting the state of equipment not recovered after hitting. At present, the recovery time evaluation research is mainly the equipment state classified into two intact and damaged discrete states determining the recovery time probability curve of the equipment form damage to good condition. However, this does not reflect the function of the equipment characteristics of diversity. Therefore, it is necessary to study the relationship between the functional state of the equipment and the recovery time.

In the assessment of equipment resilience, it is essential to consider the effects of equipment damage, support resources, environment, combat mission, and human subjective. Compared with the assessment of equipment damage status and recovery time, the randomness is stronger with a more complex assessment. Regarding the evaluation of functional status and recovery time, the studies [1–5] used cloud model to evaluate the status of equipment considering the fuzziness and randomness of data. In the literature [6–9], the status of equipment was evaluated by combining fuzzy theory with analytic hierarchy process and other methods. Although these two methods can take into account the fuzziness and uncertainty of the functional state of damaged equipment, it is difficult to take into account the changing relationship of the functional state of equipment with time. In the studies [10–12], the damage state of equipment is determined by damage mode effect analysis (DMEA) and damage tree analysis. The assessment result is accurate and can be closely related to the reality; however, it cannot be

accurately quantified; hence, it is difficult to judge the state change with time. In other studies [13–17], based on Markov model, the discrete states of components are analyzed and then mapped to the system level, so as to obtain the state evaluation results of the system. This model has a great advantage in showing the correlation between time and state; however, when existing more parts, there is the problem of state space explosion [18]. The study in [19–22] obtained the maintenance time distribution of equipment by collecting the maintenance time data of equipment through mathematical statistics. This method needs a large amount of equipment repair time data to support; however, at present, our team encounters the problem of lacking the recovery time data of war-wounded equipment. The study in [23–27] uses Bayesian network to determine the state of the system, which can deal with uncertainty and timing problems. Simultaneously, the obtained information is the evidence to update the model in real time. Although the assessment results are more accurate and reliable, the time-invariant hypothesis and the Markov hypothesis must be satisfied. In addition, the evaluation results are expressed as the probability with great uncertainty and insufficient accuracy.

According to the above analysis, it is found that Bayesian network does not have the problem of state space explosion, and the model can be updated in real time, with strong operability. Therefore, it has more obvious advantages compared with other assessment methods to solve the problem of resilience assessment of complex equipment. Cloud model is a qualitative and quantitative uncertainty transformation model, which has certain advantages in dealing with the problems of randomness and fuzziness. Through this model, the state probabilistic uncertainty results obtained by Bayesian network can be accurately expressed to compensate the lack of accuracy of Bayesian network evaluation results. For this reason, this paper proposes a resilience evaluation method for battle damage equipment based on Bayesian network cloud model. Firstly, the functional states of parts and functional states of equipment are linked probabilistically by establishing Bayesian network. Then, the change process of the parts state probability with time is used as the prior information to update the functional state of the equipment, and the relationship between the functional state of the equipment and time is obtained. Finally, on the basis of the Bayesian network evaluation results, the transformation model from the probability to the function index of the equipment's functional status level is established using the cloud model theory to achieve the accuracy of the evaluation results.

The main contribution of this paper is embodied in the following three aspects. First, in previous studies, the dynamic change process of equipment function state with recovery time was not included, while it was studied in this paper. Secondly, a recovery capability assessment method of Bayesian network cloud model is proposed. Compared with Markov, DMEA, and damage tree methods, this combination method does not have the problem of state space explosion, and the model can be updated in real time. In comparison to the mathematical statistics method, this method requires less data and the evaluation result is more accurate. The proposed method has few assumptions and overcomes the problem of large uncertainty of Bayesian network evaluation results. Third, in the traditional Bayesian network state evaluation research, the conditional probability is often determined according to experience; this method has a large error. The simulation method proposed in this paper makes up for this defect and makes the evaluation result more accurate.

In the first section, the research status of equipment damage status assessment and recovery time are introduced. In the second section, the basic theories of Bayesian network and cloud model are described. In the third section, a combination of Bayesian network and cloud model is used to define the assessment steps of the resilience of battle damage equipment, and three key problems are analyzed in detail. In the fourth section, self-propelled artillery is used as the recovery capability evaluation object, and the method proposed in this paper is applied. The result shows that this method is reasonable. The fifth section deals with the research conclusion.

2. Basic Theory of Bayesian Network and Cloud Model

2.1. Bayesian Network Model. Bayesian network is an uncertain knowledge representation and inference model as a graphical network based on probabilistic inference. The Bayesian network model can be expressed as $B(G, P)$. As shown in Figure 1, G represents a directed acyclic graph structure composed of multiple nodes. Each node X in the graph represents a variable, and the directed arcs between nodes reflect the dependencies between variables. P represents the conditional probability associated with each node and represents the probabilistic dependence among variables in a quantitative way.

Based on the direction of reasoning, the Bayesian network is classified into three main inference modes of causal reasoning, diagnostic reasoning, and explanatory reasoning [28]. The causal reasoning also known as top-down reasoning is a positive reasoning process starting from prior probability. Diagnostic reasoning is bottom-up reasoning probably leading to the conclusion on the premise of a known conclusion. Explanatory reasoning can be summarized as the use of causal reasoning in diagnostic reasoning. However, regardless of the type of reasoning mode, its reasoning is oriented by the Bayes formula. One has

$$p(x|l) = \frac{p(l|x)p(x)}{\sum_x p(l|x)p(x)}, \tag{1}$$

where $p(x|l)$ is the posterior probability of the variable x after obtaining the evidence information l, $p(l|x)$ shows the likelihood function, and $p(x)$ represents the prior probability of the variable.

To establish a complete Bayesian network, two kinds of parameters need to be determined, namely, the distribution of initial state $P(X_0)$ and the distribution of observation conditions $P(X_i \mid \pi(X_i))$. $\pi(X_i)$ represents the parent of X_i.

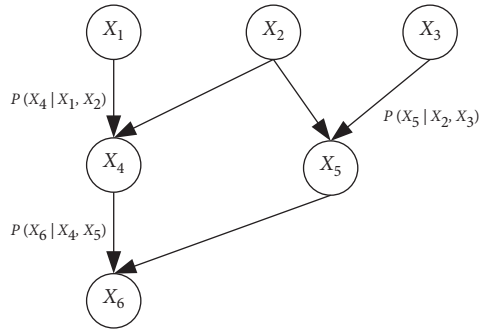

Figure 1: Bayesian network.

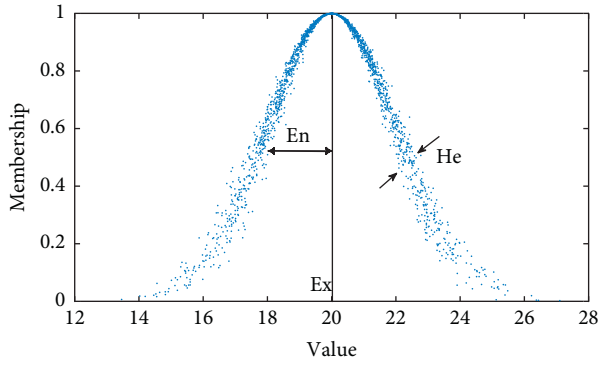

Figure 2: Normal cloud model.

After determining the parameters, the Bayesian update can be carried out according to the evidence information.

2.2. Cloud Model. The cloud model is a qualitative and quantitative uncertainty transformation model proposed based on the traditional fuzzy set theory and probability statistics. Its definition can be expressed as follows. Let U be a quantitative domain expressed numerically. C is the qualitative concept in this quantitative domain U. Let the quantitative value $x \in U$ be a random implementation of the qualitative concept C, and the certainty degree $\mu(x) \in [0, 1]$ of x to C is a random number with stable tendency: μ: $U \longrightarrow [0, 1]$, $\forall x \in U, x \longrightarrow \mu(x)$; then the distribution of x in the concept U is called the cloud, denoted as the cloud $C(x)$. Each x is called a cloud drop and is represented as drop$(x, \mu(x))$. A cloud is composed of numerous cloud droplets. A cloud droplet is a transformation from a qualitative concept to a quantitative value.

Cloud $C(x)$ is represented by expectation Ex, entropy En, and hypertrophy He. The expectation Ex represents the point where cloud droplets represent qualitative concepts in the domain space. It is a typical sample of concept quantification and the most representative numerical feature. On the one hand, the randomness of the qualitative concept is measured by entropy En and the degree of cloud drop dispersion of the qualitative concept is reflected. On the other hand, the fuzziness of qualitative concepts is measured and the value range of cloud drop accepted by the concept can be reflected. Hypertrophy He is the uncertainty measure of entropy, which is determined by the uncertainty and fuzziness of entropy En. A normal cloud model of expectation Ex = 20, entropy En = 2, and hyperentropy He = 0.4 is represented in Figure 2. The universality of normal distribution and normal membership function jointly lays the foundation for the universality of the normal cloud mode [4].

2.3. Cloud Generator Algorithm Implementation. Two key algorithms in the cloud model are forward cloud generator and reverse cloud generator. Through the forward cloud generator, the range and distribution law of the quantitative data can be obtained from the qualitative information, which is the forward mapping from qualitative to quantitative. A certain number of precise values can be converted by the reverse cloud generator effectively into proper qualitative language values as a reverse mapping from quantitative to qualitative values. The qualitative concept is mainly transformed by this appropriate mode into quantitative value. Algorithm 1 is described as follows [3].

3. Description of the Equipment Resilience Evaluation Method

Regarding the strong reasoning ability of the Bayesian network model in processing uncertain information and the transformation ability of the cloud model between qualitative concept and quantitative value, a Bayesian network cloud (BN-cloud) model is proposed in this paper to solve the problem of evaluating the resilience of battle damage equipment. The basic steps are as follows [7]:

Step 1: according to the equipment functional structure model, the corresponding network node variables and the Bayesian network topology diagram are determined.

Step 2: based on the battlefield environment, equipment characteristics and sources of threat and other pieces of information are obtained through the battle damage simulation platform to damage simulation of equipment, function state, and damage probability of the equipment parts. To attain the equipment discrete state training samples, the parts functional state data obtained from each simulation are inserted into the equipment functional state evaluation model. Then, it is trained by the parameter learning algorithm of the Bayesian network to obtain the conditional probability distribution of each node.

Step 3: based on the probability density function of parts' emergency repair time and the damage probability of parts, the state probability information of parts at each moment is predicted. Then, they are inserted into the Bayesian network model as evidence information to obtain the state probability of equipment at each moment.

Step 4: the transformation model of function state level probability is established to function index based on the cloud model and obtain the relationship of function

index of equipment with time to solve the problem of insufficient accuracy of Bayesian network.

Step 5: if the available information is obtained during the actual repair process, the parts state probability can be updated by adjusting the parts emergency repair parameters, and then it can be reentered into the Bayesian network model as evidence information for reasoning to obtain the updated equipment functional state evaluation result.

Figure 3 represents the overall process. Generally, three problems exist in evaluating the resilience: first, the conditional probability determination of Bayesian network nodes, second, determination of part state recovery probability, and third, establishing the transition model from the probability of functional state level to the functional index based on the cloud model.

3.1. Determination of Conditional Probability of Bayesian Network Nodes. The parameter learning of Bayesian network requires numerous samples, and through random experiment and simulation, a large number of relatively accurate battle damage data can be obtained using Monte Carlo simulation method. Since numerous discrete state samples are required for parameter learning in this paper, the damage data is processed within this work by establishing a functional state evaluation model, to obtain a complete and reliable parameter learning sample of the Bayesian network. The methods to determine the conditional probability of Bayesian network nodes are as follows:

(1) The equipment function block diagram is drawn according to the equipment structure. Then, in combination with the current task, the importance ranking of each element in the equipment functional block diagram is determined according to the expert opinion. Table 1 represents the judging standard. p_{ij} represents the relationship of importance between elements, and a_i shows the elements in the block diagram.

(2) The index judgment matrix $R_w = (r_{ij})_{q\times p}$ is obtained according to the importance degree of elements and the criterion of judgment scale, where

$$\begin{cases} r_{ij} = \dfrac{(r_i - r_j)}{[2(n-1)]} + 0.5, \\ r_i \displaystyle\sum_{t=1}^{q} p_{it}, \\ r_j \displaystyle\sum_{t=1}^{q} p_{jt}. \end{cases} \tag{2}$$

(3) Normalize the column vectors of the matrix R_w, and then calculate the average of the sum of the rows to obtain the combined weight value $\omega = \{\omega_{F_1}, \ldots, \omega_{F_k}, \omega_{m_1}, \ldots, \omega_{m_d}\}$ of each element relative to the target.

(4) Obtain the damage probability λ_k of each part and the function index of the damaged part v_k based on the battlefield information to simulate the equipment in the battle damage simulation system. One has

$$\lambda_k = \frac{N_k}{Ns}, \tag{3}$$

where Ns shows the simulation times; N_k is the number of times the hit kth part.

The function index of parts is calculated as follows:

$$b_f = \begin{cases} 0, & h_{f_i} < h_1, \\ \dfrac{h_{f_i} - h_1}{N(h_c - h_1)}, & h_1 \le h_{f_i} < h_c, \\ 1, & h_f \ge h_c, \end{cases} \tag{4}$$

$$v_k = \prod_{i}^{s} (1 - b_{fi}),$$

where b_{f_i} shows the damage probability of a single fragment f to the part. h_f is the penetration depth of the fragment to the part. When the penetration depth h_f is less than a certain threshold h_1, the function of the part is basically unaffected. When the penetration depth is greater than h_1 and less than the thickness of the part h_c, the damage degree of the part is a linear function of the penetration depth. When the penetration depth is greater than h_c, the impact of fragments on the function of parts reaches the maximum. v_k represents the functional index of the damaged part. s shows the number of fragments hit on the part.

(5) The functional damage information of each part obtained in each simulation is inserted into the functional evaluation model, and the equipment is evaluated based on the weight value obtained in step (3). When solving the functional exponential for the parts in parallel relation, the weighted summation method is used, and the power exponential method is utilized when solving the functional exponential for the parts in series relation [29]. The function index of each level element $(v_W, v_{F_1}, \ldots, v_{M_d})$ is calculated, and the function state level of each element of equipment is determined according to the function level classification standard; therefore, the state vector of elements $(S_W, S_{F_1}, \ldots, S_{M_d})$ is obtained.

(6) The obtained state vectors of each element are taken as training samples, and the parameter learning algorithm in the Bayesian network is used to train the samples and obtain the conditional probability of each node.

3.2. Recovery Probability Determination of Parts State. The recovery probability of parts state is determined as the probability that the part is in good or lost state at any time. The recovery probability of parts at any time is affected by

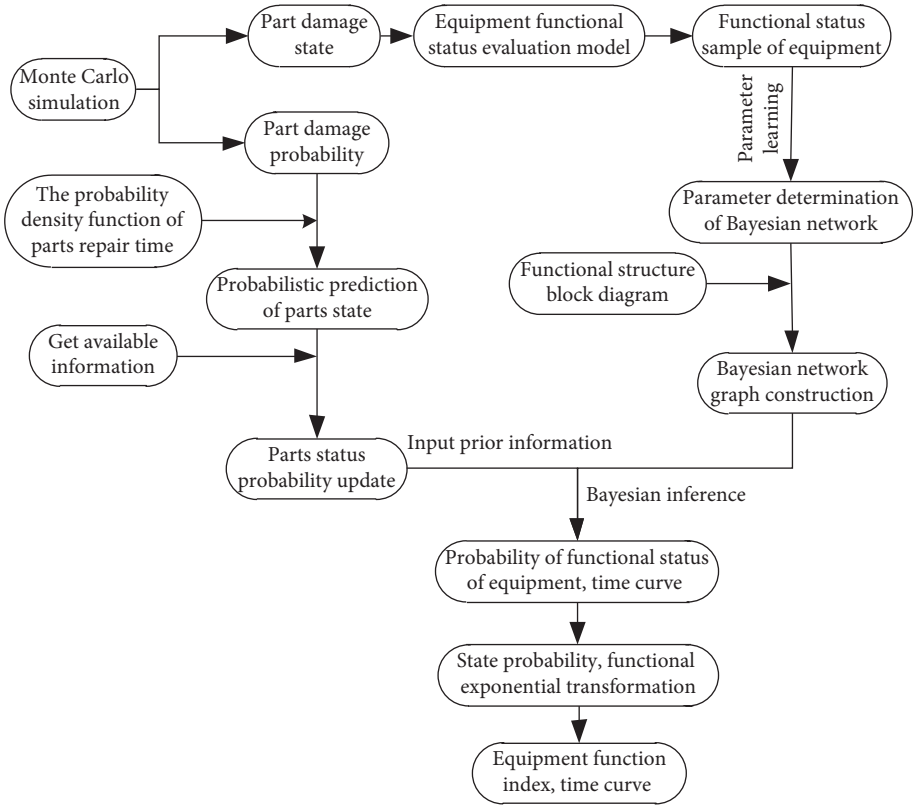

Figure 3: Procedure for evaluating the resilience of battle damage equipment.

Input: three numerical characteristics representing qualitative concept Q expectation Ex, entropy En, hyperentropy He, and cloud drop number N
Output: the quantitative value x of N cloud droplets and the certainty degree y that the qualitative concept Q represented by each cloud droplet
(1) Generate a normal random number En1 with En as expectation and He as a standard deviation
(2) Generate a normal random number x with expectation En1 and standard deviation Ex
(3) Calculate the certainty degree $y = \exp(-(x - \mathrm{Ex})^2/2(\mathrm{En1})^2)$ corresponding to x
(4) Repeat steps (1)~(3) N times to obtain the normal cloud model composed of N random cloud droplets (x, y)

Algorithm 1: Forward cloud generator.

resources, personnel, equipment damage result, equipment structure, and mission requirements. When determining the probability, it is necessary to take the distribution function of the parts' emergency repair time as the basis, take the waiting time before the parts' emergency repair and the repair time of the parts into comprehensive consideration, and judge the change process of the probability of the parts' intact or lost state with time. The time consumed by damage assessment and resource preparation before the emergency repair is t_d. Then, the probability that the part i function is intact at the time of t can be expressed as

$$\begin{aligned} T_i &= t_d + \sum_{j \in \Omega_i} t_j \\ P_i(t); &= P_i\left(T_i + t_i \le t, \text{repairable parts damage}\right) \\ &\quad + P_i(\text{parts not damaged}) \\ &= 1 - \lambda_i + \lambda_i \eta_i P_i\left(T_i + t_i \le t\right), \end{aligned} \tag{5}$$

where Ω_i represents the set of parts with higher priority than i. t_j represents the repair time of the part j. T_i represents the time from the start of equipment repair to the start of the part i repair. $P_i(t)$ represents the probability that the part i is in good condition at the time t. t_i represents the time of

emergency repair of the part i. η_i is the probability that parts i can be repaired after being damaged. λ_i is the part i damage probability. $P_i(T_i + t_i \le t)$ represents the probability that the repair time of the part i is less than t, when the part i is damaged and repairable.

Considering the complexity of the analytical calculation of $P_i(t)$, the simulation method is adopted for calculation, for which the recovery probability simulation process of the part state is shown in Figure 4.

The specific implementation steps are as follows:

(1) The probability density function of part repair time $f_k(t)$, part repairable probability λ_k, number of parts m, and priority of parts repair are obtained. The total number of simulation runs is Ns, and the serial number of simulation runs is j, so $j = 1, 2, \ldots Ns$.

(2) Sort the parts from high priority to low priority and get the new parts sort label.

(3) According to the probability density function of parts emergency repair time, parts emergency repair time data group $T_m = (t_1, t_2, \ldots, t_m)$ is generated.

(4) Generate random numbers x and h that are uniformly distributed [0, 1].

(5) For each part in Ω_i, judge whether it is $x \le \lambda_k$ or not. If it is not true, it is considered that the part k is not damaged; then let $t_k = 0$. Rather, the part k is considered damaged, and the continued damaged parts are judged. If $h \le \eta_k$ is established, the part is considered repairable. If not, the part is considered unrepairable; then let $t_k = 0$, which is ordered to prevent the impact of the repair time of the estimated parts. Update the data group T_m.

(6) Calculate the recovery time $Z(j)$ under the repairable condition, when the ith part is damaged in the jth simulation. One has

$$Z(j) = \text{sum}(T(1{:}\ i-1)) + t_i + t_d. \tag{6}$$

(7) To see whether $0 < Z(j) \le t$ is true, it is believed that, in the jth simulation, the part i can be repaired at the time t under the damaged and repairable condition; then, let $n_i = n_i + 1$. If it is not true, it is believed that the damaged part i in this simulation cannot be repaired within time t; let $n_i = n_i$.

(8) Repeat steps (3~7) for a total of Ns times, and calculate the probability $p_i(t)$ that the part i is in good condition at the time t. One has

$$p_i(t) = \lambda_i \eta_i \frac{n_i}{Ns} + 1 - \lambda_i. \tag{7}$$

Obtaining some available information in practical application, such as the complete recovery of communication function or basic recovery of motor function at t_0 moment, it is used as evidence to conduct Bayesian diagnostic reasoning to obtain the $P_{ip}(t_0)$ of part recovery probability after reasoning. Then, based on the recovery probability $P_{ip}(t_0)$ of the part, the recovery parameters of the part are modified to meet the condition, where the recovery probability of the part is $P_{ip}(t_0)$ at t_0 moment.

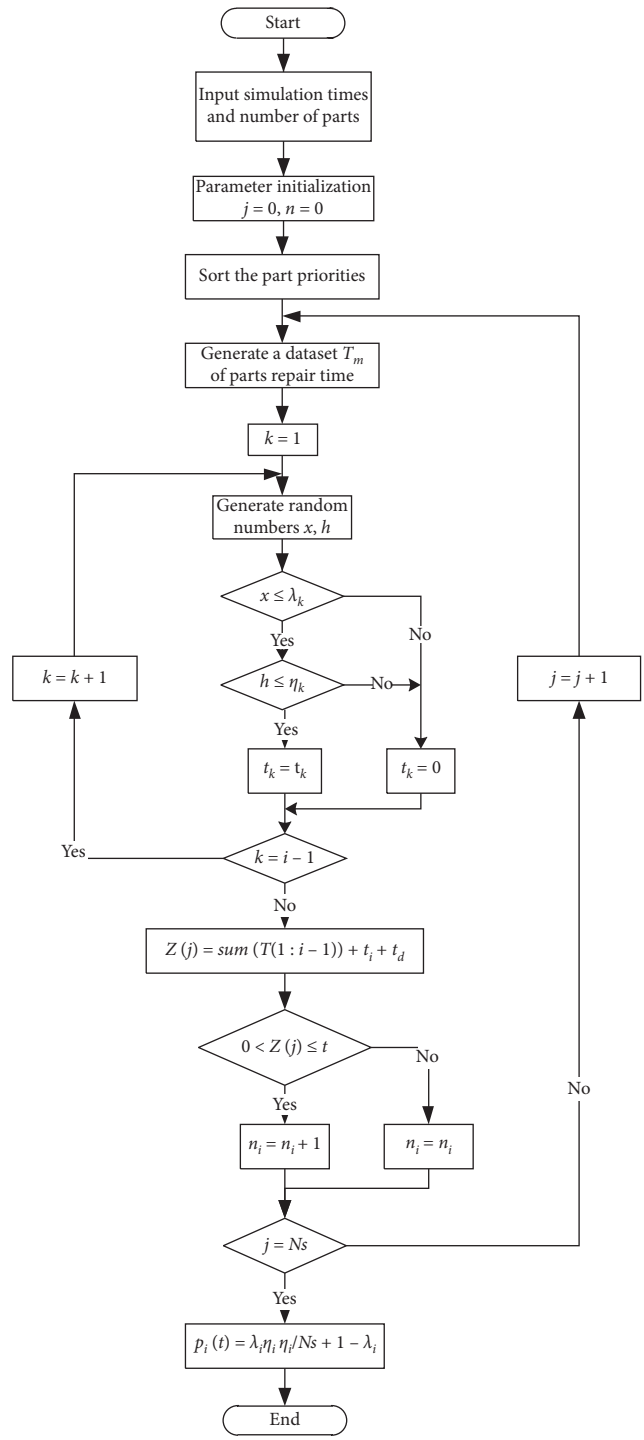

Figure 4: The recovery probability simulation flowchart of parts state.

Changing the parameters such as the repairable probability, the probability density function of the repair time and the damage probability of the part will result in changing the part state recovery probability. When updating the part

parameters, the parameter with the greatest possibility of change can be rationally adjusted according to the changes before and after the probability. If the adjustment of this parameter cannot support the result, the next probably changing parameter can be selected for analysis until the part probability meets the requirements. After obtaining the changed parameters, the state probability of the part at each moment is simulated again accordingly, and the probability information is inserted into the Bayesian network model; finally, the updated evaluation result of the equipment's functional state is obtained.

3.3. Establishment of the Transition Model from Functional State Level Probability to Functional Index Based on the Cloud Model. The transformation from the functional state level probability to the functional index mainly includes the transformation from the functional state level to the cloud model and the transformation from the state level probability to the functional index. The transformation from the functional state level to the cloud model aims at quantifying the qualitative language of the equipment functional state by using the three digital features $(\mathrm{Ex}, \mathrm{En}, \mathrm{He})$ of the cloud model, which is the foundation of the transformation model of the equipment functional state level probability to functional index. Let U be the theory domain of equipment function state, and $U = [0,1]$, $U_1, U_2, \ldots, U_k$ is the division of the theory domain U, which shall meet the following requirements: (1) $\cup_{i=1}^{k} U_i = U$; (2) $\cap_{i=1}^{k} U_i = \varnothing$; (3) $\forall u_i \in U_i, \forall u_j \in U_j$. If $i < j$, $u_i < u_j$. Let $W_1, W_2, \ldots, W_k$ be the qualitative language of equipment's functional state level, $\forall W_i, u_{W_i}(w)$ represent the degree of certainty of w with respect to W_i, and $u_{W_i}(w) \in [0,1]$. The distribution of w over W_i is called state level cloud C_{W_i}, each w is a cloud droplet, represented by drop $(w, \mu_{W_i}(w))$, and the value of w represents the equipment function index in this article.

According to the classification criteria of functional damage in [30] as well as expert opinions, this paper divides the overall functional status of equipment into three grades: functional intact (FI), functional weakened (FW), and functional lost (FL). The evaluation criteria are shown in Table 2. For parts, the evaluation method of equipment resilience is based on the probability density function of parts' emergency repair time. In this paper, the functional status of parts is divided into two grades of functional intact (FI) and functional loss (FL). Due to the great differences in the structure and tasks undertaken by the parts, the functional classification criteria of the parts are different. In practical application, the specific analysis should be made according to the characteristics of parts and the undertaken tasks.

By using the transformation relation between interval number and cloud model, the interval of equipment function state is transformed into the cloud model. If a function index interval is $[a_i, a_j] 0 < a_i < a_j < 1$, then the characteristic parameters of the cloud model can be determined according to the index approximation method:

$$\begin{cases} \mathrm{Ex} = \dfrac{\left(a_i + a_j\right)}{2}, \\ \mathrm{En} = \dfrac{\left(a_j - a_i\right)}{6}, \\ \mathrm{He} = 0.15\mathrm{En}. \end{cases} \tag{8}$$

When the function index interval is $[0, a_i)$, since the ideal function index is 0, Ex = 0 and En = $a_i/3$ are taken. When the function index interval is $(a_j, 1]$, since the ideal function index is 1, Ex = 1 and En = $(1 - a_j)/3$ are taken. Then, the three clouds in the functional state domain in this paper, respectively, represent the functional intact cloud $C_{FI}(1, 0.05, 0.0075)$, the functional weakened cloud $C_{FW}(0.4, 0.1, 0.015)$, and the functional lost cloud $C_{FL}(0, 0.0333, 0.005)$ (Figure 5). The blue image represents functional loss cloud C_{FL}, the red image represents functional weakening cloud C_{FW}, and the yellow image represents a functional intact cloud C_{FL}.

The purpose of this model is to convert the probabilistic value of the equipment function state obtained by Bayesian network reasoning into the accurate description value of the function state. In the cloud model, the closer the membership degree to 1, the higher the degree that the functional index x belongs to C_W; the closer the membership degree to 0, the lower the degree that the functional index x belongs to C_W. The established transformation model is as follows:

$$\begin{cases} u_i = \sum_{i=1}^{k} p_{W_i} w_i, \\ w_i = Ex(i) + \sqrt{-2\left(\mathrm{En1}(i)\right)^2 ln\left(p_{W_i}\right)}, \quad \text{if } p_{W_1} \geq p_{W_3} \text{ or } i = 3, \\ w_i = Ex(i) - \sqrt{-2\left(\mathrm{En1}(i)\right)^2 ln\left(p_{W_i}\right)}, \quad \text{if } p_{W_1} < p_{W_3} \text{ or } i = 1, \end{cases} \tag{9}$$

where u_i represents the equipment function index, p_{W_i} represents the probability that the device is in the ith functional state class, and w_i represents the function index of an item at the ith functional status level.

4. Analysis of Examples

A type of self-propelled artillery is taken for the resilience evaluation. Figure 6 illustrates the functional state diagram of this self-propelled artillery [6]. The equipment functional state diagram should contain all the functions of the equipment and all the key parts related to the equipment functions. However, considering the complexity of the self-propelled artillery equipment system, this paper simplifies the description of self-propelled artillery equipment system, divides the function of self-propelled artillery into firepower function, maneuvering function, protection function, and communication function, and takes the key part of the function as the three-level indicator.

Table 1: Criteria for judging the importance.

p_{ij}	Criteria instructions
0.5	The element a_i has the same importance as a_j
0.6	Element a_i is one level higher than the element a_j
0.7	Element a_i is two levels higher than the element a_j
0.8	Element a_i is three levels higher than the element a_j
0.9	Element a_i is four levels higher than the element a_j
0.1, 0.2, 0.3, 0.4	The results of the reverse comparison and positive comparison are complementary

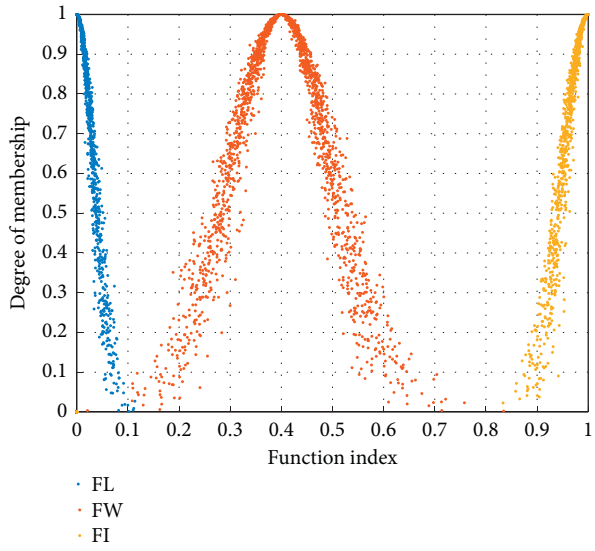

Figure 5: The cloud model of equipment functional state level.

In the battle damage simulation platform, the equipment and threat model are inserted, Monte Carlo simulation is conducted, each simulation result is inserted into the functional state evaluation model, and the functional index of the equipment is calculated. In the evaluation model, according to the functional characteristics of self-propelled artillery, the functional index relationship of each node can be described by the following formula:

$$\begin{cases} F_W = \omega_{F_1} F_{F_1} \times \omega_{F_2} F_{F_2} \times \omega_{F_3} F_{F_3} \times \omega_{F_4} F_{F_4}, \\ F_{F_1} = F_{M_1}^{\omega_{M_1}} \times F_{M_2}^{\omega_{M_2}} \times F_{M_3}^{\omega_{M_3}}, \\ F_{F_2} = F_{M_4}^{\omega_{M_4}} \times F_{M_5}^{\omega_{M_5}} \times F_{M_6}^{\omega_{M_6}}, \\ F_{F_3} = \omega_{M_7} F_{M_7} + \omega_{M_8} F_{M_8} + \omega_{M_9} F_{M_9} + \omega_{M_{10}} F_{M_{10}}, \\ F_{F_4} = \omega_{M_{11}} F_{M_{11}} + \omega_{M_{12}} F_{M_{12}} + \omega_{M_{13}} F_{M_{13}}, \end{cases} \tag{10}$$

where F_G represents the function index of the node $G \in \{W, F_1, F_2, \ldots, M_{12}, M_{13}\}$ and ω_G represents the weight of the node G.

The elements in the functional state diagram of this type of self-propelled artillery are set as the nodes in the Bayesian network, and the discrete state of each node is given at the same time. The part layer is divided into two status grades of functional integrity (FI) and functional loss (FL), and the equipment's integrated function and subfunction are divided into three status grades of functional integrity (FI), functional weakened (FW), and functional loss (FL). Then, according to the interlayer relationship of each element and the upper and lower relationships, Netica software is used to establish the directed acyclic graph of the static Bayesian network, as shown in Figure 7.

Based on the establishment of the Bayesian network topology, the state information of each node of the equipment obtained through the functional evaluation model is taken as the sample of parameter learning, and the EM algorithm in the parameter learning of Bayesian network is adopted to train it. The obtained conditional probability of each node is inserted into the Bayesian network topology diagram to obtain the complete Bayesian network structure diagram.

According to the previous emergency repair data and expert experience, the consumption time before the emergency repair of this type of self-propelled artillery is $t_d \approx 5$. The probability density function of emergency repair time and the repairable probability of each part under the current maintenance supportive condition are shown in Table 3. According to the probability calculation method of part state in Section 2.2, the probability value of the functional state of the part at t time can be calculated and input it as a prior probability into the Bayesian network model for Bayesian reasoning to obtain the probability value of some functional state of the equipment at t time. Let $\Delta t = 5$, with Δt being the time interval; list the variation trend of the probability value of each functional state rating of the equipment in $t = [0, 100]$, as shown in Figure 8.

To verify the usability of Bayesian model, three axioms proposed in literature [31] should be satisfied. At this point, the initial integrity probability of node M_1 is set from 0.553 to 0.653. The integrity probability of the system increased from 0.296 to 0.315. Continue to set the initial integrity probability of node M_2 from 0.761 to 0.861; then the system's integrity probability increases to 0.334. Continue to set the initial integrity probability of node M_3 from 0.833 to 0.933; then the system's integrity probability increases to 0.353. Then, improve the integrity probability of M_4, M_5, and M_6 by 0.1 and the system integrity probability to 0.353. It can be seen that the Bayesian model in this paper satisfies the three axioms of literature [31], and the usability of the model is verified.

If the moment $t = 20$, then the self-propelled artillery firepower function is in good condition; at this time through the Bayesian diagnosis reasoning, the state probability of M_1, M_2, and M_3 parts is changed. By the information on various aspects to analyze the data, the experts consider the

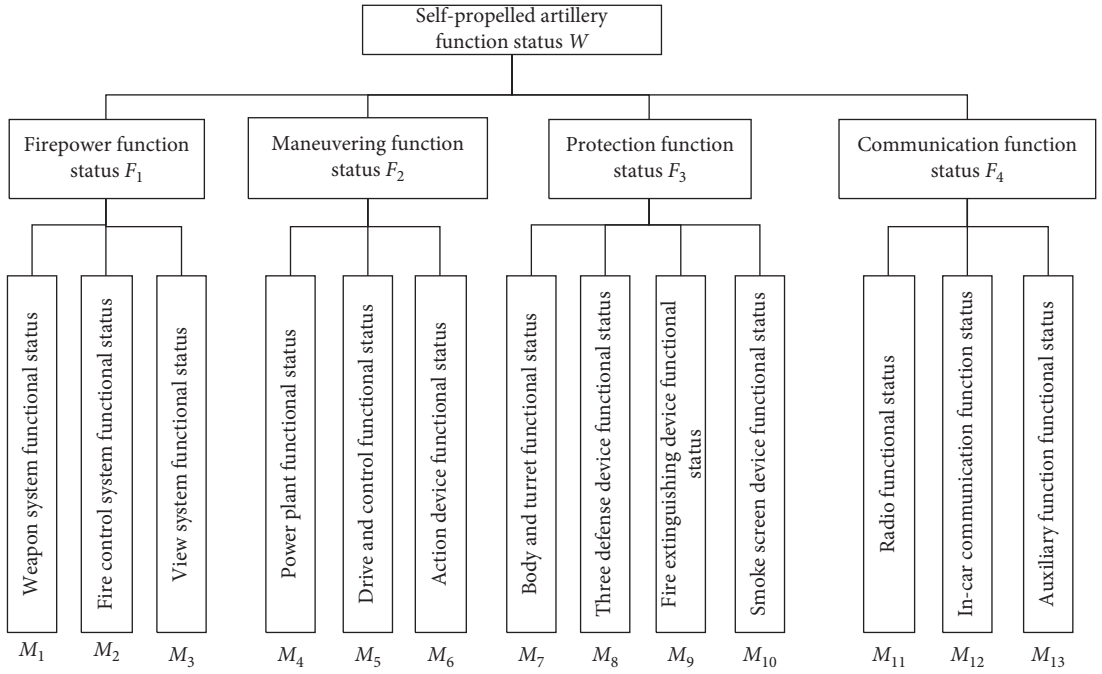

Figure 6: Functional state diagram of self-propelled artillery.

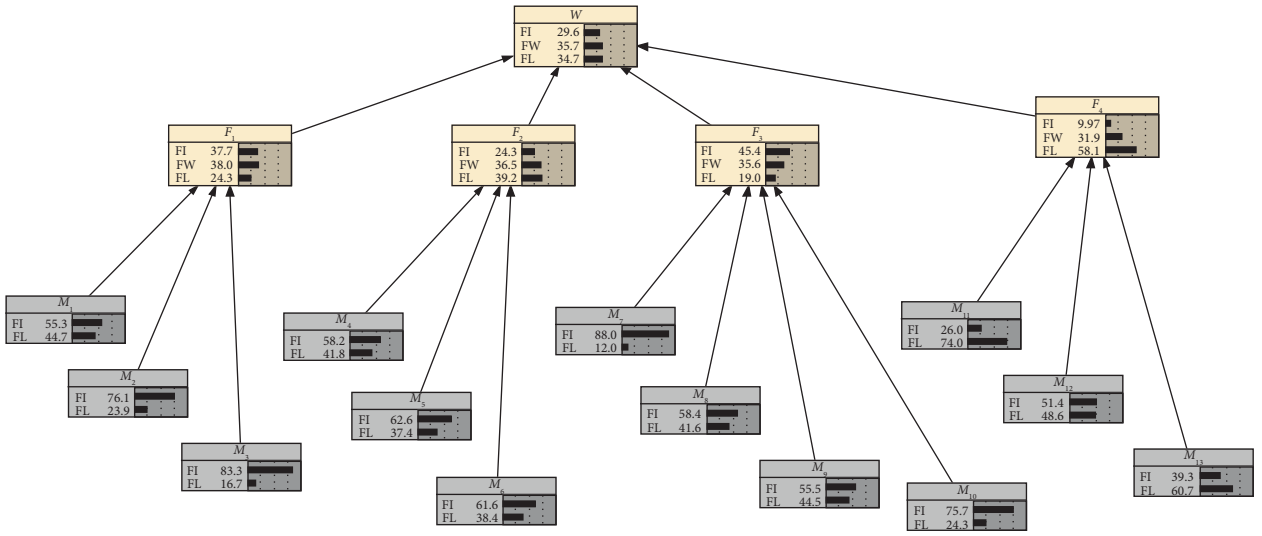

Figure 7: Bayesian network structure of self-propelled artillery.

Table 2: Classification criteria of equipment functional status.

State level	Functional exponential interval	Functional description
Functional intact	0.7~1.0	The completion of the intended function is barely affected
Functional weakened	0.1~0.7	The completion of the intended function is affected
Functional lost	0~0.1	The completion of the intended function cannot be completed

three-part repairable probability as most likely changed and the possibility of damage probability change as minimal. Then, the part parameter information is adjusted, and the updated state level probability information of each part is shown in Table 4. The updated probability change curve of the equipment's functional state rating is shown in Figure 9.

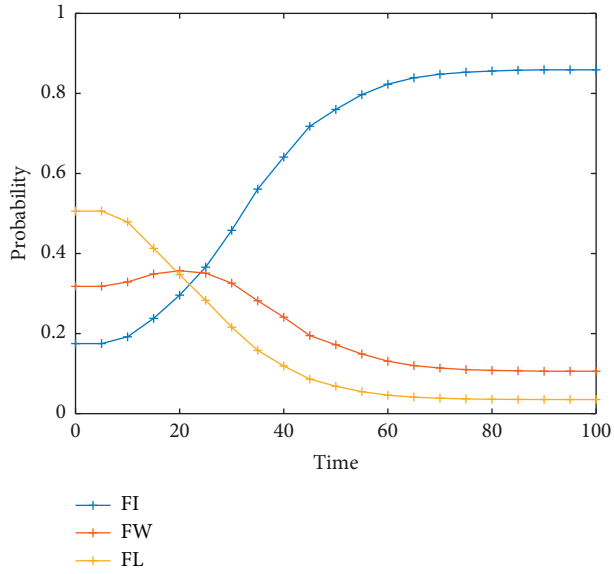

Figure 8: Probability change curve of functional state level.

Table 3: Emergency repair information table for each node element.

Functional level	Variable G	Damage probability λ	Weight value ω_G	Repairable probability η_G	Probability density function of emergency repair time $f_i(u)$
Self-propelled artillery W	F_1	—	0.3012		—
	F_2	—	0.2671		—
	F_3	—	0.1988		—
	F_4	—	0.2329		—
Firepower function F_1	M_1	0.559	0.4038	0.8	$U(10, 30)$
	M_2	0.464	0.2276	1	$N(8, 0.26)$
	M_3	0.359	0.3686	1	$E(6.5)$
Maneuvering function F_2	M_4	0.532	0.3668	0.56	$LN(1.8, 0.46)$
	M_5	0.458	0.3166	1	$U(6, 16)$
	M_6	0.502	0.3166	1	$E(5.5)$
Protection function F_3	M_7	0.128	0.3012	0.6	$N(2, 0.34)$
	M_8	0.436	0.1988	0.95	$LN(1.32, 0.25)$
	M_9	0.487	0.2671	1	$E(4)$
	M_{10}	0.251	0.2329	0.95	$U(4, 10)$
Communications functions F_4	M_{11}	0.889	0.3841	0.76	$N(3, 0.52)$
	M_{12}	0.557	0.3333	1	$N(5, 0.24)$
	M_{13}	0.648	0.2826	0.68	$LN(1.58, 0.43)$

According to Figures 8 and 9, it is indicated that, over a longer duration of the repair, the probability of equipment in functions integrity state (FI) decreases gradually in a state of function weakened (FW) state and function loss (FL) state probability. After obtaining the information of intact firepower function, the probability of the whole equipment in the intact function state increases, while the time of approaching steady state is shortened, and the evaluation result is reasonable. However, it is found that, within the period of 0–20 before and 0–30 after the update, the probability of the equipment in each functional state is making problems for evaluation decisions. Therefore, according to the transformation model of equipment function state rating probability to function index in Section 2.3, the obtained result is converted into quantitative form, and the curve shown in Figure 10 can be obtained. The initial point of the function recovery curve represents the function index of the equipment after being hit reflecting the damage degree of the equipment. The slope of the curve represents the recovery rate of the function. Since the equipment adopts the strategy of repairing important parts before repairing minor parts in rush repair, the recovery rate of equipment function is large at the initial moment and gradually decreases with the extension of time. Moreover, it gradually decreases with the extension of time. The ultimate steady-state value reached by the curve represents the maximum function index that can be restored under the current guarantee conditions after the equipment is damaged.

As can be seen from Figure 10, with the extension of time, the function of the equipment gradually recovers the function weakened state (FW) to the function intact state

Table 4: Update information of component state probability.

Part number M_i	$P_i(20)$	$P_{ih}(20)$	Repairable probability η_i	Probability density function $f_i(t)$	Damage probability λ_i
1	0.5529	0.9494	1.00	$U(8, 16)$	0.406
2	0.7611	0.9953	1.00	$N(1, 0.14)$	0.046
3	0.8334	0.9945	1.00	$E(1.5)$	0.042
4	0.5821	0.6614	0.56	$LN(1.8, 0.46)$	0.532
5	0.6259	0.7378	1.00	$U(6, 16)$	0.458
6	0.6158	0.7139	1.00	$E(5.5)$	0.502
7	0.8800	0.8897	0.60	$N(2, 0.34)$	0.128
8	0.5836	0.6095	0.95	$LN(1.32, 0.25)$	0.436
9	0.5550	0.6029	1.00	$E(4)$	0.487
10	0.7568	0.7673	0.95	$U(4, 10)$	0.251
11	0.2598	0.3908	0.76	$N(3, 0.52)$	0.889
12	0.5136	0.5914	1.00	$N(5, 0.24)$	0.557
13	0.3929	0.4374	0.68	$LN(1.58, 0.43)$	0.648

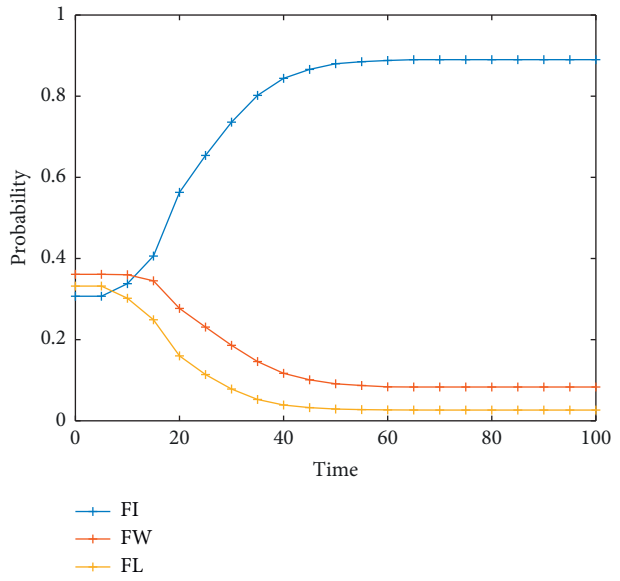

Figure 9: Probability change curve of the functional status level after updating.

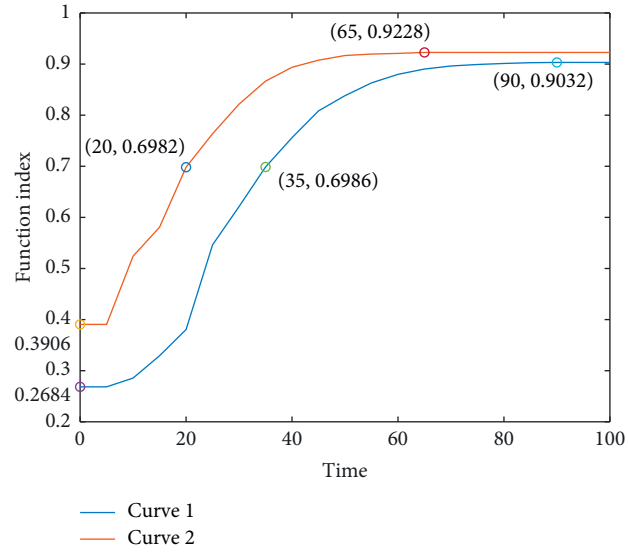

Figure 10: Functional index recovery curve. Curve 1 represents the functional recovery curve before the update, and curve 2 shows the functional recovery curve after the update.

(FI). Before obtaining the information of intact firepower function, the function index of the equipment is 0.2684 after being damaged, and the equipment function is seriously damaged; nevertheless, it is still in the state of function weakening (FW). Before $t = 5$, since the equipment is not officially started to repair, therefore, its function index is not changed. After $t = 35$, the functional state of the equipment changes from the function weakened state (FW) to the function intact state (FI), and at $t = 90$, the function index tends to be stable. However, due to the equipment damage, some parts are difficult to be repaired under the current supporting conditions; hence, the function cannot be fully restored and only be restored to 0.9032.

After updating the equipment function status, the initial function index of the equipment is 0.3906, which increased by 0.1222. At $t = 20$, the equipment functions are gradually recovered from the weakened state (FW) to the intact state (FI). It is about 15 min earlier than previously. The ultimate functional index limit for the device recovering is 0.9228, which is 0.0196 higher than the original one, and the time of equipment recovering to a stable state is 25 min less than the original one.

Since the calculation of part state recovery probability is not an independent process, parts with a high priority will have a certain impact on the part state probability with low priority; therefore, when the obtained firepower function information is inserted as evidence, it will influence the part state recovery probability of maneuvering function, communication function, and protection function. For the convenience of analysis, the recovery curve of the equipment maneuvering function index is drawn as shown in Figure 11. As it is observed in Figure 11, after obtaining the intact information of the firepower function, the recovery time of the maneuvering function of the equipment is shortened, and the time to reach the steady state is shortened by about 25 min. Based on the evidence information observed before and after the input simultaneously, there is no translational change in the recovery curve of

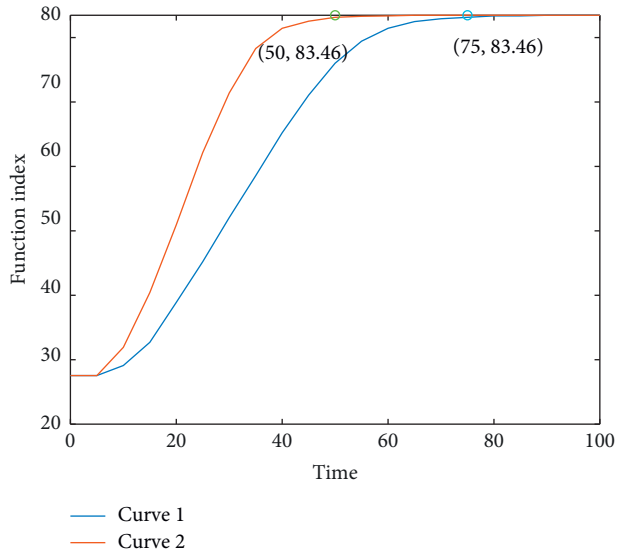

Figure 11: Recovery curve of maneuvering function. Curve 1 represents the maneuvering function index recovery before the update. Curve 2 represents the maneuvering function index recovery after the update.

equipment function index; nonetheless, the recovery curve still starts from $t = 5$ and gradually tends to the steady state since the function index in this paper is transformed based on the probability. Therefore, the changing process must be a continuous process from the beginning of equipment repair to a steady state.

5. Conclusion

This paper proposed a resilience evaluation method for battle damage equipment based on the BN-cloud model. The model completely represented the strong reasoning ability of the Bayesian network model in dealing with uncertain information. It also made use of the transformation ability of the cloud model between qualitative concepts and quantitative values to compensate for the nonaccuracy of Bayesian network reasoning results. The assessment results expressed more information and were more valuable for decision-making.

This paper proposed a method to generate training samples using battle damage simulation and equipment functional state modeling compensating the lack of data support in the parameter learning of Bayesian network for battle damage equipment.

The proposed simulation method for calculating the recovery probability of parts could be used as the input of prior information of the Bayesian network; in addition, it could update the probability information of functional states of parts after obtaining the available information. Finally, an example was given to verify the effectiveness and practicability of the method.

Data Availability

No data were used to support this study.

Conflicts of Interest

The authors declare that they have no conflicts of interest.

References

[1] S. X. Zhang, X. Zan, and H. Li, "Technical condition evaluation of equipment based on cloud gravity center evaluation method and entropy method," *Computer Measurement & Control*, vol. 22, no. 12, pp. 4015–4018, 2014.

[2] J. C. Gu, H. W. Zhang, and L. Qi, "Evaluation of efficiency of the phased array radar system based on the theory of center of gravity of cloud," *Electronic Science and Technology*, vol. 3, no. 24, pp. 73–75, 2011.

[3] C. Lu, T. X. Xu, and J. Zhao, "Equipment condition assessment method based on cloud matter-element model of DSm evidence," *Systems Engineering and Electronics*, vol. 7, no. 39, pp. 1549–1554, 2017.

[4] Y. Xu and X. Chen, "Transformer status assessment based on cooperative game and cloud model," *Electric Power Automation Equipment*, vol. 3, no. 35, pp. 88–93, 2015.

[5] Y. Song and J. M. Zhang, "Condition assessment of wind turbine based on cloud model," *Applied Mechanics & Materials*, vol. 448-453, no. 28, pp. 3327–3330, 2013.

[6] Z. Y. Sun, J. Zheng, and C. Xiong, "Health status assessment of equipment based on variable weight theory and TFN-AHP," *Journal of Gun Launch & Control*, vol. 4, no. 37, pp. 29–34, 2016.

[7] Y. L. Sun, R. Q. Lu, and L. Tian, "Function damage condition evaluation of power truck based on FAHP and grey clustering," *Equipment Environment Engineering*, vol. 10, no. 14, pp. 110–114, 2017.

[8] A. V. Agunov, A. V. Grishchenko, and V. A. Kruchek, "A method of using neural fuzzy models to determine the technical state of a diesel locomotive's electrical equipment," *Russian Electrical Engineering*, vol. 10, no. 88, pp. 634–638, 2017.

[9] H. Ge and S. Asgarpoor, "Reliability evaluation of equipment and substations with fuzzy markov processes," *IEEE Transactions on Power Systems*, vol. 3, no. 25, pp. 1319–1328, 2010.

[10] Y. H. Zeng, J. Yan, and K. Feng, "Analysis and design of assessment system for damage degree of equipment on battlefield," *Acta Armamentarii*, vol. 4, no. 26, pp. 531–534, 2005.

[11] R. S. Wang and X. S. Jia, "Battlefield damage assessment based on damage tree model," *Acta Armamentarii*, vol. 1, no. 26, pp. 72–76, 2005.

[12] H. Y. Ma, F. Gao, and Z. F. Zhang, "Notice of retraction: process and application of equipment battlefield damage assessment based on damage tree," in *Proceedings of the 2013 International Conference on Quality, Reliability, Risk, Maintenance, and Safety Engineering (QR2MSE)*, pp. 1068–1072, IEEE, Chengdu, China, July 2013.

[13] G. S. Nie, "A study of aviation weapon equipment maintenance based on the semi-markov model," *International Journal of Plant Engineering and Management*, vol. 2, no. 12, pp. 101–106, 2007.

[14] M. A. Chun, S. Yan, H. X. Pan, and Y. J. Liu, "TBF prediction of equipment based on the gray markov model," *Acta Armamentarii*, vol. 9, no. 34, pp. 1193–1196, 2013.

[15] G. Kumar, V. Jain, and O. P. Gandhi, "Availability analysis of mechanical systems with condition-based maintenance using Semi-markov and evaluation of optimal condition monitoring interval," *Journal of Industrial Engineering International*, vol. 14, no. 1, pp. 119–131, 2018.

[16] W. J. LU, Y. Y. Chen, and J. M. Liu, "Research of RSS in power equipment reliability evaluation," *Journal of Hunan University*, vol. 4, no. 38, pp. 47–50, 2011.
[17] S. J. Du, *Maintainability Modeling and Analysis of Polymerization Stochastic Process*, Beijing Institute of Technology, Beijing, China, 2015.
[18] W. Si, Z. Cai, S. Sun, and S. Si, "Integration of failure prediction Bayesian networks for complex equipment system," in *Proceedings of the IEEE International Conference on Industrial Engineering and Engineering Management*, pp. 1161–1165, IEEE, Bandar Sunway, Malaysia, 2014.
[19] X. H. Han, Y. H. Zhang, and S. H. Wang, "Research on the maintenance evaluation method of repairable unit combination task," *Acta Armamentarii*, vol. 11, no. 37, pp. 2058–2065, 2016.
[20] Q. Miao, L. Liu, and Y. Feng, "Complex system maintainability verification with limited samples," *Microelectronics Reliability*, vol. 2, no. 51, pp. 294–299, 2011.
[21] P. S. Rajpal, K. S. Shishodia, and G. S. Sekhon, "An artificial neural network for modeling reliability, availability and maintainability of a repairable system," *Reliability Engineering & System Safety*, vol. 91, no. 7, pp. 809–819, 2006.
[22] M. Zhang, H. J. Su, and L. Yuan, "Research on problems and basal theory of engineering equipment's maintainability test," *Advanced Materials Research*, vol. 328-330, no. 84, pp. 2446–2449, 2011.
[23] B. Y. Jia, X. L. Yu, and Q. S. Yan, "Method of bridge condition assessment based on discrete dynamic bayesian networks," *Bridge Construction*, vol. 3, no. 46, pp. 74–79, 2016.
[24] A. David, V. John, and G. Michael, "Bayesian networks for combat equipment diagnostics," *Interfaces*, vol. 47, no. 1, pp. 85–105, 2017.
[25] Q. Liao, Z. Qiu, and J. Zeng, "Retracted article: fuzzy Bayesian Networks and its application in pressure equipment's security alerts," in *Proceedings of the International Conference on Natural Computation*, IEEE, Shanghai, China, pp. 211–227, 2011.
[26] L. Lu, "Bayesian evaluation of system structure for reliability assessment," *Quality Engineering*, vol. 31, no. 4, pp. 581–595, 2019.
[27] J. Li and X. L. Wang, "Reliability and availability analysis of pumping system using modeling based on decomposition approach," *Chinese Journal of Engineering Design*, vol. 1, no. 22, pp. 18–25, 2015.
[28] J. Rasa and J. F. Peter, "Exploiting causal independence in large Bayesian networks," *Knowledge-Based Systems*, vol. 4, no. 18, pp. 153–162, 2004.
[29] X. A. Zhao, Z. P. Jiang, and X. S. Huang, "The framework of comprehensive analysis for the combat capability of weapon system of systems," *Fire Control & Command Control*, vol. 7, no. 36, pp. 7–10, 2011.
[30] W. B. Yang, Y. Liu, and J. Liu, "Damage effect evaluation of system target based on weighted network," *Fire Control & Command Control*, vol. 2, no. 38, pp. 145–148, 2013.
[31] B. Jones, I. Jenkinson, and Z. Yang, "The use of Bayesian network modelling for maintenance planning in a manufacturing industry," *Reliability Engineering and System Safety*, vol. 95, no. 3, pp. 267–277, 2010.